Functional characterization of wheat Fusarium head blight resistance QTL (*Fhb1*) based on non-targeted metabolomics and proteomics

Raghavendra Gunnaiah
Doctor of Philosophy
Department of Plant Science
McGill University
Montreal, Quebec, Canada

April 2013

A thesis submitted to the McGill University in partial fulfillment of the requirements of the degree of Doctor of Philosophy

This thesis is dedicated to my beloved parents

TABLE OF CONTENTS

LIST OF TABLES

LIST OF FIGURES

LIST OF APPENDICES

LIST OF ABBREVIATIONS

15ADON	15-acetyl-deoxynivalenol
3ADON	3-acetyl-deoxynivalenol
AME	Accurate mass error
AUDPC	area under disease progress curve
BLAST	Basic local alignment search tool
Ca^{2+}	Divalenet calcium ion
CAD	Cinnamoyl alcohol dehydrogenase
CCoAMT	Caffeoyl-CoA O-methyltransferase
CDA	Canonical discriminant analysis
COMT	Caffeic acid O-methyltransferase
D3G	DON-3-O-glucoside
Da	Dalton
DON	Deoxynivalenol
dpi	Days post inoculation
ESI	Electrospray ionization
ET	Ethylene
FC	Fold change
FHB	Fusarium Head Blight
FMT	Flavonoid O-methyltransferase
GC-MS	Gas chromatography mass spectrometry
GS	Growth stages
hai	Hours after inoculation
HCAA	Hydroxycinnamic acid amides
HCT	Hydroxycinnamoyl transferase
hpi	Hours post inoculation
HRC	Histidine rich Ca2+ binding protein
JA	Jasmonic acid
LC-MS	Liquid chromatography mass spectrometry
m/z ratio	Mass to charge ratio
MetSyn	Methionine synthase

MS	Mass spectrometry
MTHFR	5,10-methylene-tetrahydrofolate reductase
NIL	Near isogenic line
NIV	Nivalenol
PAL	Phenylalanine ammonia lyase
PCR	Polymerase chain reaction
PDC	Proportion of DON conversion
PR-Protein	Pathogenesis related protein
PRr	Pathogenesis related in resistant genotype
PRs	Pathogenesis related in susceptible genotype
PSD	Proportion of spikelets diseased
QTL	Quantitative trait loci
RM	Mock inoculated resistant genotype
ROS	Reactive oxygen species
RP	Pathogen inoculated resistant genotype
RR	Resistance related
RRC	Resistance related constitutive metabolite
RRI	Resistance related induced metabolite
RT	Retention time
S/G	Syringyl/Guacoyl lignin ratio
SA	Salicylic acid
SAHH	S-adenosylhomocysteine hydrolase
SAMS 2	S-adenosylmethionine synthase 3
SAMS1	S-adenosylmethionine synthase 1
SM	Mock inoculated susceptible genotype
SP	Pathogen inoculated susceptible genotype
TaACT	Triticum aestivum Agmatine Coumaroyltransferase
TDP	Total DON produced
Tri5	Trichodiene synthase
UDP	Uridine diphosphate
UGT	UDP-glycosyltransferase

ABSTRACT

Fusarium head blight (FHB) caused by *Fusarium graminearum* is a dreadful disease of wheat (*Triticum aestivum* L.). Host resistance to FHB in wheat is quantitatively inherited. Though more than 100 QTLs have been identified, only a few have been validated. However, the resistance mechanisms governed by these QTLs are poorly understood. A type II FHB resistance QTL *Fhb1* is the most consistent and largest effect QTL in wheat against FHB spread in wheat. Non-targeted metabolic and proteomic profiling of wheat near isogenic lines (NILs) with resistant and susceptible *Fhb1* alleles was used to functionally characterize *Fhb1* using a high resolution LC-MS. The *Fhb1* from a moderately resistant cultivar Nyubai was associated with cell wall thickening, mainly at the rachis, due to deposition of hydroxycinnamic acid amides (HCAAs), phenolic glucosides and flavonoids. A hypothetical protein coding gene (GenBank: CBH32656.1) near *Fhb1* locus was putatively identified as hydroxycinnamoyl transferase, which catalyzes the biosynthesis of HCAAs. Deoxynivalenol (DON) accumulation was high in both the NILs, eliminating DON detoxification as a mechanism associated with *Fhb1* (Chapter III). For additional confirmation, the *Fhb1* resistant allele, from a highly FHB resistant cultivar Sumai-3 was profiled. Even though the DON accumulation was low in resistant NIL, the detoxification of DON by host UDP-glycosyltransferase was moderately high in both the NILs, with no significant difference. Interestingly, unlike in the resistant NIL, constitutively present glycerophospholipids were absent in the susceptible NIL following pathogen inoculation due to degradation of membrane. Membrane degradation was caused due to programmed cell death as evidenced by DNA laddering in the susceptible NIL. A locus *TAA_ctg0954b.00390.1* was identified as an *Fhb1* candidate gene that contains a calmodulin binding motif and two nucleolar localization signal motifs and hence re-annotated as calmodulin binding protein (TaCaMBP_*Fhb1*). The *TaCaMBP_Fhb1* is induced following pathogen infection, binds to Ca^{2+} bound calmodulin, and triggers Ca^{2+} signalling cascade including transcriptional activation of endonucleases that cleaves the genomics DNA and cause

programmed cell death. The resistant allele of *TaCaMBP_Fhb1* lacks part of the promoter region and is non-functional in triggering Ca^{2+} signalling. While the susceptible allele of *TaCaMBP_Fhb1,* with functional promoter region is capable of triggering Ca^{2+} signalling and programmed cell death. The necrotrophic pathogen *F. graminearum* feeds on the dead tissue, multiply in the host and produce more DON, following a repeated cycle in the susceptible genotype (Chapter IV). The wheat resistance mechanisms against FHB were further confirmed, based on metabolic profiling of rachis, from a resistant cultivar Sumai-3 and a susceptible cultivar Roblin, for resistance against spread of a trichothecene producing (Wild: *FgTri5*$^{+}$) and a trichothecene non- producing (mutant: *FgTri5*$^{-}$) isolates of *F. graminearum*. The wild isolate repressed several host resistance mechanisms in both the cultivars due to production of DON. The FHB resistance to spread in Sumai-3 was mainly because of increased cell wall thickening, especially at rachis, due to deposition of lignin, HCAAs and flavonoids, and partially, due to induced RR metabolites which in turn reduced the fungal biomass and toxin biosynthesis. The resistance was not attributed to DON detoxification by UDP-glycosyltransferase, as it was not significant in both the cultivars confirming our previous studies (Chapter V). The resistant alleles of two *Fhb1* candidate genes, identified in this study, can be suitably stacked into genome of elite cultivars to enhance FHB resistance in wheat.

RÉSUMÉ

La fusariose de l'épi est une maladie fongique attaquant le blé (*Triticum aestivum*) induite par *Fusarium graminearum*. La fusariose cause de sévères pertes économiques dues à la réduction de la qualité et des rendements suite à la contamination par les mycotoxines trichothecene. La résistance du blé face à la fusariose est un trait quantitatif. Plus de 100 LCQ on été identifiés et un petit nombre a été validé. Cependant, les mécanismes de résistance gouvernés par ces LCQ sont peu connus. *Fhb1* est le LCQ le plus consistent qui produit le plus grand effet face à la fusariose du blé. Une caractérisation fonctionnelle à l'aide d'un LC-MS à haute résolution de lignées isogéniques avec ou sans l'allèle susceptible Fhb1 a générée des profils de métabolites non ciblés ainsi que protéomique. Le *Fhb1* d'un cultivar modérément résistant, Nyubai, a été associé avec le développement de la paroi cellulaire plus épaisse, surtout au niveau du rachis due à la déposition d'acides amides hydroxycinnamic (HCAAs), de glucosides phénolique ainsi que de flavonoïdes. Le gène codant pour une protéine hypothétique (GenBank: CBH32656.1) située près du locus Fhb1 a été identifiée comme étant possiblement une hydroxycinnamoyle transférase. Cette protéine déclencherait la biosynthèse de HCAAs. L'accumulation de DON a été plus élevée dans les deux lignes isogéniques. La détoxification de DON est un mécanisme associé avec *Fhb1* (Chapitre III). Pour confirmer, l'allèle *Fhb1* la résistance du cultivar Sumai-3 a été profilé. Contrairement aux lignes iso géniques, aucune présence constitutive de glycérophospholipides, n'a été détectée chez les lignées susceptibles en raison de la dégradation des membranes. La dégradation de membrane s'est avérée être causée par la mort cellulaire programmée comme le démontre le patron de dégradation de l'ADN de la variété susceptible NIL. Le locus TAA_ctg0954b.00390.1 fut identifié comme candidat pour le gène *Fhb1* qui contient un domaine de liaison à la calmoduline et deux signaux de localisation nucléaire. Ce dernier fut donc annoté en tant que protéine de liaison à la calmoduline (*TaCaMBP_Fhb1*). *TaCaMBP_Fhb1* est induit suite à l'infection du pathogène pour ensuite se lier à la calmoduline liée au Ca^{2+} pour

ensuite initier une cascade de signaux qui inclut l'activation transcriptionnelle d'endonucléases qui clivent l'ADN génomique causant ainsi la mort cellulaire programmée. L'allèle résistante de *TaCaMBP_Fhb1* présente une délétion au niveau du promoteur ce qui la rend non fonctionnel pour l'activation du signalement Ca^{2+} impliqué dans la mort cellulaire programmée. Le pathogène nécrotrophe *F. graminearum* se nourrit des tissus morts, se multiplie et produit plus de DON pour faciliter l'infection; perpétuant ainsi un cercle vicieux chez le génotype susceptible (Chapitre IV). C'est résultats on été confirmés à l'aide d'un profilage métabolique des rachis de la lignée résistante Sumai-3 et la lignée susceptible Roblin lors de l'infection avec (Wild : *FgTri5*$^{+}$) trichothécène producteur et (Mutant :*FgTri5*$^{-}$) trichothécène non producteur qui sont deux isolats de *F. graminearum*. L'isolat producteur est parveu à inhiber plusieurs mécanismes de résistance de l'hôte dans les deux cultivars grâce à la production de DON. La résistance FHB à l'infection dans Sumai-3 était principalement lié à l'augmentation des parois cellulaires particulièrement au niveau des rachis à cause de la déposition de lignine, HCAAs et de flavonoïdes et partiellement due à l'augmentation des métabolite RR qui réduisent la biomasses des champignons ainsi que la synthèse des toxines. La résistance n'a pas été attribuée à détoxification de DON par l'UDP-glycosyltransferase, puisque les résultats étaient similaires dans les deux cultivars (Chapitre V). Les allèles résistants, des deux gènes candidats *Fhb1* identifiés dans cette étude, pourraient-être ajoutés au génome de cultivars élites de blé pour augmenter leur résistance au FHB.

ACKNOWLEDGMENTS

It is my pleasure to convey my gratitude and acknowledge the contribution of all, who have contributed to my Ph. D. thesis research and writing this dissertation. First of all, I owe sincere appreciation to my research advisor Dr. Ajjamada C. Kushalappa for his supervision, patience, motivation, immense knowledge and guidance from the very early stage of this research. He has molded me into an independent researcher by giving me all the intellectual freedom to put my own thoughts in designing and conducting the experiments. I am grateful to him for holding me to a high research standards and enforcing strict validation for each study. He has been my oasis, whenever I was lost in the dessert of confusions. His interests in complex aspects of plant biology, commitment towards the science and society has motivated me to step forward in the same path. Without his guidance and persistent help, this dissertation would not have been possible. I am indebted to him more than he owes. I would like to convey my sincere gratitude to my research advisory committee members, Dr. Jean-Benoit Charron, Dr. Jaswinder Singh and Dr. Jean-Francois Laliberthe, for their constructive criticism and suggestions which helped me to focus my research objectives. My special thanks to Dr. Jean-Benoit Charron for his un-conditional support with long discussions and insightful suggestions that helped me to troubleshoot technical difficulties in my research.

I am thankful to our research collaborator, Dr. Raj Duggavathi, for his scientific advice and knowledge and many insightful discussions and suggestions in spite of our differed research areas, and also for providing lab space and equipment. My thanks are also due to our other collaborators, Dr. Somers D. J. and Dr. Fox S., from AAFC, Winnipeg, Canada for providing us with the seeds of wheat near isogenic lines and Dr. Yves Dion from CEROM for providing us with the seeds of wheat cultivars Sumai-3 and Roblin to test our hypothesis. Profound thanks are due to Dr. Denis Faubert and his team members Mrs. Boulos Marguerite and Dr. Sylvian from IRCM, Montreal for the timely analysis of metabolites and proteins based on LC-MS and responding to our technical needs by changing the columns

and machine set up. Many thanks go in particular to Dr Danielle J. Donnelly, Dept. of Plant Science for helping me out with getting good sections of rachis, that were hard to take out and Mr. Serge Dernovici, technician, school of parasitology for teaching me to use confocal microscope, together, which added more histological proofs in my first study. I would like to thank Dr. Sylvie De Blois for editing my thesis format. My thanks are also due to the graduate co-ordinators of Dept. of plant science, Dr. Martina Stromvik and Dr. Dr Pierre R. L. Dutilleul for recommending to in-house scholarships.

I would be remiss if I didn't thank Mr. Guy Rimmer and Mr. Simon Hebert who deserve credit for much needed assistance in green house experiments and Miss Carolyn Bowes and Miss. Lynn Bachand for assistance with administrative tasks and reminding me of impending deadlines and keeping my work running smoothly.

I gratefully acknowledge Dr. Kumaraswamy G. K. and Dr. Venkatesh Bollina for teaching me the basics of metabolomics and software for metabolomics data processing. My special thanks to my childhood friend, Dr. Kumaraswamy G. K., who kept confidence in me and recommended to join Dr. Kushalappa's lab. He has unconditionally supported me in all my endeavours of life. I gratefully thank my fellow lab mates, Mr. Shivappa Hukkeri and Dr. K. Yogendra for helping me in greenhouse and lab experiments and sample collections at odd times. Along, I also thank Mr. Shailesh Karre, Dr. Kundan Kumar, Dr. Siva Chamarthi and Dr. Kareem Mosa for the stimulating discussions and sending relevant research articles. My appreciation is also due to my fellow Ph.D scholars, Mrs. Sowmya Subramanian and Mr. Rony Chamoun for their valuable suggestions in research and needful assistance in cracking down the comprehensive exam. I am also thankful Mr. Dayanand Siddappa, Dept. of Animal Science for his co-operation and help during qRT-PCR and histo-chemical studies. My special thanks to Mr. François Gagné-Bourque, for translating my thesis abstract to French language. I would like to thank all other friends in the Department of Plant science, for keeping me cheerful throughout my student tenure.

I have no words to express my gratitude to my parents and all family members for their constant love, encouragement and understanding all over the years. My heartfelt thanks and love are due to my wife and also a fellow lab mate, Mrs. Pushpa Doddaraju for helping me with greenhouse and lab experiments and data analysis. She has provided me an unflinching encouragement and support and has un-conditionally loved me during my good and bad times.

I am grateful to Indian Council of Agricultural Research, New Delhi for awarding me the "ICAR-International fellowship", without which I would never have started my Ph. D. I sincerely thank Dr. B.S. Bisht, Dr. R. K. Mittal, and Mr. Bhagawath Singh from ICAR for processing of my fellowship from time to time. I would like to extend my gratitude to NSERC, Canada for granting the research funds. I would also like extend my acknowledgements to the McGill University for awarding the Schulich graduate fellowship and graduate research excellence awards in the department of plant science. I also thank Network Innovagrains, Quebec, and Canada for recognition of our research work and awarding me the graduate research excellence award in the Agricultural and Environmental Sciences, for the year 2012.

PREFACE AND CONTRIBUTION OF THE AUTHORS

Preface

Fhb1 is the most consistent and largest effect Fusarium head blight (FHB) quantitative trait loci (QTL) in wheat. Non-targeted metabolomics and proteomics were applied to elucidate the biochemical mechanisms governed by *Fhb1* and identify the FHB resistance related genes at this locus. The following research findings are original scholarship and distinct contribution to the scientific knowledge:

- Biochemical mechanism associated with the most consistent and largest effect wheat FHB resistance QTL, *Fhb1* is revealed. *Fhb1* codes for a non-functional calmodulin binding protein (*TaCaMBP_Fhb1)* that rescues host cells from programmed cell death induced by *F. graminearum* produced deoxynivalenol.
- In response to FHB in wheat, hydroxycinnamic acids (HCAAs) and flavonoids are deposited at the cell walls of rachis to strengthen the cell wall for pathogen penetration. The gene hydroxycinnamoyl transferase (*HCT*) catalyzing the synthesis of HCAAs can be used as a candidate gene for marker assisted breeding, following its validation.
- *Fhb1* does not contain deoxynivalenol (DON) detoxifying UDP-glycosyltransferase and does not regulate the expression of DON detoxifying UDP-glycosyltransferase as hypothesised before.
- Proportion of DON conversion to less toxic D3G by UDP-glycosyltransferase decreases with an increase in total DON concentration.
- Metabolomics and proteomics can be used to discover plant biotic stress related genes (forward functional genomics)
- Phenylpropanoid pathway plays a major role in FHB resistance. Total phenylpropanoids and flavonoids or key phenylpropanoids/flavonoids can be used as potential biomarkers for FHB resistance.

- Deoxynivalenol represses several host resistance genes or RR metabolite synthesis. The resistance in wheat to FHB can be improved either by reducing DON accumulation or by increasing DON detoxification.
- Plant defense signalling molecule jasmonic acid (JA) is common to both resistant and susceptible genotypes. Downstream of JA signalling pathway determines the resistance.

Contribution of the authors

This thesis comprises of three studies leading to three manuscripts in chapters III, IV and V. The first manuscript published in PLoS One is authored by Raghavendra Gunnaiah, Kushalappa A.C., Duggavathi R., Fox S. and Somers D.J. Raghavendra Gunnaiah designed and conducted the greenhouse and laboratory experiments, analysed the data and wrote the manuscript. Dr. Kushalappa guided in designing the experiments, supervised the experiments, and provided research funds to carry out the experiments, guided in writing and thoroughly edited the manuscript. Dr. Raj Duggavathi guided and supervised qRT-PCR experiments, provided lab space and equipment to conduct qRT-PCR experiments and edited the manuscript. Dr. Somers D.J and Dr. Fox S. developed the wheat genotypes used in the study and edited the manuscript.

The second and the third manuscripts are authored by Raghavendra Gunnaiah and Kushalappa A.C. Raghavendra Gunnaiah designed and conducted the greenhouse and laboratory experiments, analysed the data and wrote the manuscripts. Dr. Kushalappa guided in designing the experiments, supervised the experiments, and provided research funds to carry out the experiments and guided in writing and thoroughly edited the manuscripts.

CHAPTER I: GENERAL INTRODUCTION

Bread wheat (*Triticum aestivum* L.) is an economically important food crop grown around the world. It is the second largest produced food crop after maize, with global production of 704 million tons (MT) and the second most consumed food crop (66 kg/capita/year) after rice (FAO, 2012). Wheat provides 21% of the food calories and 20% of the protein to more than 4.5 billion people in 94 developing countries (Braun et al., 2010). Canada is the seventh largest producer in the world with 25.6 MT in 2011 (FAO 2012). Wheat grown areas and productivity are consistently increasing over years due to genetic improvements in yield potential, resistance to diseases, adaptation to abiotic stresses and better agronomic practices. Nevertheless, further improvements in productivity are anticipated to meet global challenges of food security to balance the increasing demand from an expanding human population and preference for wheat-based food and the loss of agricultural land caused by urbanization, scarcity of resources and unpredictable global climate changes (Chakraborty and Newton, 2011).

Fusarium head blight (FHB), also called 'scab' has re-emerged as a disease of global significance, which cause economic losses due to reduction in grain yield and contamination of grains with trichothecene mycotoxins. Eighteen *Fusarium* species are reported to cause head blight in wheat and barley throughout the world (Stępień and Chełkowski, 2010). *Fusarium graminearum* Schwabe (teleomorph *Gibberella zeae* (Schweinitz) Petch), is the principal species in most parts of the world affected by FHB (Xu and Nicholson, 2009). The fungus over-winters saphrophytically in the crop residues and infects wheat inflorescence during favorable, warm and humid conditions at anthesis and grain development. Once established within the floret, the fungal hyphae can spread from spikelet to spikelet through the vascular bundles of the rachis (Kang and Buchenauer, 2000, Parry et al., 1995). A trichothecene mycotoxin, deoxynivalenol (DON), produced by *F. graminearum*, promotes the pathogen colonization and spread in the host tissue (Bai et al., 2002, Jansen et al., 2005).

Management of FHB is classically dominated with the development of resistant genotypes. Other management practices such as decomposing the crop residues through tillage, fungicide application and biological control are effective only when used along with resistant cultivars (Bai and Shaner, 1994). Host resistance to FHB is quantitatively inherited, governed by oligo/polygenes (Bai and Shaner, 1994, Eeuwijk et al., 1995). Development of resistant genotypes through conventional breeding is often hindered by linkage drag of undesirable agronomic traits. Host resistance to FHB in wheat has been classified into five types: type I resistance, resistance to initial infection; type II resistance, resistance to spread of the disease within spike; type III resistance, ability to degrade DON; type IV, tolerance to high DON concentration; type V, resistance to kernel infection. However, only three types type I, type II and type III resistance are commonly followed in wheat breeding (Schroeder and Christensen, 1963, Wang and Miller, 1988). With the advancements in molecular biology tools, more than 100 FHB resistant quantitative trait loci (QTLs) have been identified in wheat (Buerstmayr et al., 2009). Major QTLs on chromosomes 3B (*Fhb1*), 6B (*Fhb2*) and 2D for type II resistance and on 5A (*Fhb5*) and 4B (*Fhb4*) mainly for type I resistance are reported in multiple studies and validated under field conditions (Buerstmayr et al., 2009). However, the resistance mechanisms governed by these QTLs are inadequately studied.

Fhb1 is the most consistent and the largest effect QTL for FHB spread, identified in Sumai-3 and its derivatives (Anderson et al., 2001, Bai et al., 1999, Buerstmayr et al., 2002, Waldron et al., 1999), Wangshuibai (Lin et al., 2004, Zhang et al., 2004) and Nyubai (Somers et al., 2003). *Fhb1* has been fine mapped as a Mendelian gene, within 1.2 cM between STS142 and STS18 (Cuthbert et al., 2006). However, the gene responsible for FHB resistance was unidentified. It was previously reported that *Fhb1* might co-localize with a gene coding for UDP glycosyl transferase which detoxifies DON into less toxic DON-O-glucoside (D3G) or regulate its expression (Lemmens et al., 2005). However, a recent publication of wheat chromosome 3B sequence confirmed that no UDP-

glycosyltransferase genes are present in the *Fhb1* region (Choulet et al., 2010). Regulation of UDP-glycosyltransferase by *Fhb1* is to be investigated. Further, *Fhb1* was narrowed down to a 261 Kb region with seven putative *Fhb1*candidate genes. None of the seven genes showed resistance on transferring to a susceptible wheat cultivar (Liu et al., 2008). A few comparative transcript analysis studies have revealed up-regulation of host cell death related transcripts in genotypes with susceptible *Fhb1* alleles (Jia et al., 2009, Xiao et al., 2013) and up-regulation of a transcript associated with reduced susceptibility to FHB in resistant genotypes (Zhuang et al., 2013). Nevertheless, *Fhb1* candidate genes responsible for resistance/susceptibility or reduction in DON accumulation are unknown.

Comparative "Omics" technologies have proven to be potential tools in identification of genes and deciphering gene functions. Differentially accumulating transcripts, proteins and metabolites can be linked back to the genome to identify genes responsible for their differential accumulation. The integration of transcriptomics, proteomics and metabolomics through bioinformatics tools, and the identification of the function of un-annotated genes in the published genomes are the future challenges of the post genomics era (Tohge and Fernie, 2010). Non-targeted metabolic profiling of barley and wheat genotypes with varied levels of FHB resistance has revealed the role of phenylpropanoid, flavonoid, fatty acid and jasmonic acid (JA) signalling pathways and DON detoxification in host defense against FHB (Bollina et al., 2010, Bollina et al., 2011, Hamzehzarghani et al., 2005, Kumaraswamy et al., 2011, Kumaraswamy et al., 2011). In parallel, transcript profiling of wheat and barley cultivars identified several other host resistance mechanisms due to PR-proteins, DON sequestration by multidrug resistance proteins and oxidative stress resistance, which were not identified at the metabolome level. In addition, up-regulated transcripts of a UDP-glycosyltransferase responsible for DON detoxification, phenylpropanoid and JA signalling pathway confirmed the host defense responses identified using metabolomics (Foroud et al., 2011, Gardiner et al., 2010, Jia et al., 2009). Following the clues from metabolomics and

transcriptomics, a gene coding for DON detoxifying UDP-glycosyltransferase was identified in barley (Schweiger et al., 2010). In parallel, up-regulated enzymes of phenylpropanoid pathway and JA signalling in proteome profiling, provided a direct link between gene and metabolome through the enzymes catalyzing resistance related metabolites (Geddes et al., 2008, Zhou et al., 2005). Consequently, this study was aimed to identify the genes localizing at the major wheat FHB resistant QTL, *Fhb1*, by non-targeted profiling of metabolites and proteins, which are closer to the phenotype. The genes present between *Fhb1* flanking markers on the *Fhb1* localizing contig, *ctg0954* (GENBANK: FN564434) were studied for the metabolite/protein perturbation. Further, a targeted gene expression analysis at the transcript level was used to confirm the findings of non-targeted metabolite/protein analyses.

General hypothesis

Wheat near isogenic lines (NILs) with resistant and susceptible *Fhb1* alleles, also differentially accumulate constitutive and/or *F. graminearum* induced resistance related metabolites and proteins. The differential accumulation is governed by genes localized at *Fhb1* locus.

General objectives

1. To determine the host biochemical resistance mechanisms governed by FHB QTL *Fhb1*, derived from a wheat cultivar Nyubai, against spread of *F. graminearum* by non-targeted metabolomic and proteomic profiling and confirm the candidate genes by transcript expression analysis of NILs with resistant and susceptible *Fhb1* alleles.
2. To confirm the function of *Fhb1* candidate genes derived from wheat cultivar Nyubai with those derived from wheat cultivar Sumai-3, based on differentially accumulating metabolites and/or proteins and validating the candidate genes by transcript expression analysis.
3. To confirm host resistance mechanisms in the FHB resistant cultivar Sumai-3 in comparison to the susceptible cultivar Roblin.

CHAPTER II: REVIEW OF THE LITERATURE

2.1 Fusarium head blight of wheat

Fusarium head blight (FHB) caused by an Ascomycota fungus *Fusarium* spp. is a devastating disease of wheat, barley, oats, corn and other cereals. Eighteen *Fusarium* species infecting wheat have been reported all over the world (Stępień and Chełkowski, 2010). *F. graminearum,* Schwabe (teleomorph=*Gibberella zeae* (Schweinitz.) Petch) is more prominent in causing FHB of wheat all over the world (Xu and Nicholson, 2009). The fungus survives saprotrophycally on crop debris in the absence of host. Sexual ascospores, and asexual macroconidia, chlamydospores and hyphal fragments surviving on crop residues are the major source of inoculum (Parry et al., 1995, Sutton, 1982). FHB inoculum is dispersed through wind, rain and some insect vectors such as mites and thrips (Parry et al., 1995). Wheat plants are more vulnerable to FHB infection at the anthesis stage and remain susceptible until soft dough stage and infection occurs under favorable conditions such as continuous wetness at 25^0C (Bushnell et al., 2003). Betaine and choline present in the extruding anthers also stimulate the growth of fungal hyphae (Strange et al., 1974). First visible symptoms as brown colored necrotic patches appear within 2-4 days of infection under favourable conditions (Bushnell et al., 2003). *Fusarium* can enter wheat florets either passively through natural openings, such as crevices, openings between lemma and palea and stomata or occasionally by active direct penetration through the cuticle and sub cuticle using infection hyphae (Kang and Buchenauer, 2000, Pritsch et al., 2000). The pathogen spreads intra-cellularly and inter-cellularly all along the ovary, lemma, palea and reaches the rachilla node (Kang and Buchenauer, 2000). It also enters the vasculature of the rachis and spreads to the upper and lower un-inoculated spikelets by colonizing the vasculature bundles (Brown et al., 2010, Kang and Buchenauer, 2000). The pathogen initially establishes itself in the host tissue as a biotroph during initial infection period of 48-72 hours after inoculation (hai) and shifts to necrotrophic phase at a later stage of colonization (Brown et al., 2010, Kang and Buchenauer, 1999). By 5 days post inoculation (dpi), the colonized spikelets bleach due to loss of host cellular contents and bleaching symptoms expand to rachis by 12 dpi (Brown et al., 2010). A shift from biotrophic to necrotrophic phase of *F. graminearum*

might be promoted by the trichothecene mycotoxins produced by the pathogen (Ilgen et al., 2009, Jansen et al., 2005).

2.2 Impact of *Fusarium* and the trichothecene mycotoxins

2.2.1 Reduction in grain yield

Fusarium infection of developing caryopsis leads to the development of shrivelled, pinkish deformed kernels known as 'tombstone' kernels (Bushnell et al., 2003). FHB infection reduces both kernel size and number of kernels, ultimately leading to drastic reduction in grain yield (Bushnell et al., 2003). Up to 70 % yield losses have been reported in Paraguay in 1972-75, and the USA and Canada have experienced severe yield losses during 1991-1995 due to warm humid climate and large growing areas (Dubin, 1997).

2.2.2 Toxicity of trichothecenes

The major impact of FHB is on the quality of grains, which contaminates grains with trichothecene mycotoxins. Trichothecenes are sesquiterpenoid toxins produced by most *Fusarium* spp. (Mirocha et al., 2003). Deoxynivalenol (DON) and its derivatives, 3-acetylated DON, 15-acetylated DON, nivalenol (NIV), fusarenon and zearelanone (ZON) are the most commonly found trichothecenes in *F. graminearum* infected wheat (Mirocha et al., 2003, O'Donnell et al., 2000). A type B trichothecene DON is often found in high concentration in FHB infected kernels and causes severe acute and chronic toxic effects in animals. Acute toxicity involves vomiting, hemorrhage/necrosis of the intestinal tract, necrosis in bone marrow and lymphoid tissues. Chronic toxic effects of DON are decreased weight gain, anorexia, and altered nutritional efficiency (Pestka, 2007). Severe gastrointestinal disorders, alimentary toxic aleukia and other fusariotoxosis associated diseases have been reported all over the world (Bhat et al., 1989).

2.2.3 Role of deoxynivalenol in FHB spread within spike

Deoxynivalenol is the most commonly detected trichothecene in cereal grains at high concentrations (Trucksess et al., 1995). Deoxynivalenol is not only phytotoxic but also a pathogen aggressiveness factor that facilitates the spread of FHB, and thus determining

the aggressiveness of the pathogen in wheat (Bai et al., 2002, Mesterházy, 2002). Role of DON in FHB spread was demonstrated by inoculating wheat spikes with trichothecene non-producing and trichodiene synthase disrupted mutant (*FgTri5*$^{-}$) mutant of *F. graminearum* (Proctor et al., 1995). Trichodiene synthase (*Tri5*) is a key enzyme of type-B trichothecenes biosynthesis in *F. graminearum*. A *Tri5* gene knock out mutant (*FgTri5*$^{-}$) could infect the spikelets but the colonization was limited to the rachilla and rachis node and it failed to infect the adjacent un-inoculated spikelets (Bai et al., 2002, Jansen et al., 2005).

Phytotoxic effects of DON were identified in a series of histological, biochemical and molecular experiments. DON was found in cytoplasm, chloroplasts, plasmalemma, cell wall, vacuoles, and endoplasmic reticulum, moving ahead of the intruding fungal hyphae (Kang and Buchenauer, 1999). DON kills the host cells by disrupting the cell membrane causing cellular electrolyte leakage and an increase in cytoplasmic Ca^{2+} ions leading to its imbalance in cellular homeostasis (Bushnell et al., 2010, Cossette and Miller, 1995). Damaged host cells systematically transduce defense signals in the host to produce reactive oxygen species (ROS), such as H_2O_2, which, in turn trigger cell death (Desmond et al., 2008). Unlike in biotrophs, ROS induced cell death facilitates the pathogen colonization in necrotrophs, causing bleaching symptoms, instead of stopping the pathogen spread. Thus, DON plays a key role as pathogen aggressiveness factor by inducing cell death. Host resistance to DON accumulation and cell death are key components in breeding for FHB resistant wheat cultivars.

2.3 Wheat breeding for FHB resistance

Management of FHB through cultural practices and fungicide sprays is challenging. Concepts of no tillage/minimum tillage, unavailability of specific fungicides, residual chemical toxicity and limitation in determination of optimum timing of spray application challenge the management of FHB (Bai and Shaner, 2004). Biological control of FHB through use of microbial antagonists has been successful, only when used along with some foliar fungicides and at least partially resistant cultivars (Luz et al., 2003). Hence, breeding for FHB resistant cultivars is considered as the more viable and environment friendly approach for management of FHB. Host resistance to FHB in wheat is generally

classified into five components but only three are commonly employed. Type I (resistance to initial infection), type II (resistance to spread) and type III (ability to degrade DON) are commonly followed in wheat breeding (Miller and Arnison, 1986, Schroeder and Christensen, 1963). In addition, type IV (tolerance to high DON concentration) (Wang and Miller, 1988) and type V (resistance to kernel infection) (Mesterhazy, 1995) were postulated but used to a lesser extent in wheat breeding.

Ample genetic resources for FHB resistance are available from all over the world, prominently from China (Wangshibai, Sumai-3 and its derivatives), Japan (Shinchunaga, Nobeokabouzu and Nyu Bai), Brazil (Frontana and Encruzilhada), USA (Ernie and Freedom) and several others including some alien sources maintained at CIMMYT (Bai and Shaner, 2004). However, many such FHB sources are associated with undesirable agronomic traits. Moreover, resistance to FHB in wheat is quantitatively inherited (Bai and Shaner, 1994, Eeuwijk et al., 1995, Snijders and Eeuwijk, 1991) and transfer of quantitative traits to elite cultivars is a time consuming and challenging task due to linkage drag of other undesirable traits.

2.4 Wheat FHB resistance QTLs

With the advancement in the development of DNA based markers such as RFLP, AFLP, SSR and SNP, it became feasible to generate linkage maps and map the QTLs conferring FHB resistance. More than one hundred QTLs have been identified, governing type I, type II and type III resistance on all the wheat chromosomes, except on 7D (Buerstmayr et al., 2009). The QTLs on chromosomes 3B, 6B, 5A, 4B and 2D were repeatedly identified in different mapping populations and were also validated (Buerstmayr et al., 2009).

The first major FHB resistance QTL for type II resistance was identified from Sumai-3 on chromosome 3B in the cross Sumai-3 X Stoa, designated as *Qfhs.ndsu-3BS* (Anderson et al., 2001, Waldron et al., 1999). The major QTL on 3BS (*Qfhs.ndsu-3BS*) was repeatedly identified in Ning-7840 X Clark populations (Bai et al., 1999, Zhou et al., 2002) and was validated in a doubled haploid population of CM-82036 X Remus (Buerstmayr et al., 2002, Buerstmayr et al., 2003). The largest effect QTL region for type

II resistance was precisely fine mapped as a single Mendelian gene within a 1.2 cM interval and renamed as *Fhb1* (Cuthbert et al., 2006). In addition to the Sumai-3 derived genotypes, *Fhb1* was also identified from another highly FHB resistant Chinese landrace Wangshibai (Lin et al., 2004, Zhang et al., 2004, Zhou et al., 2004) and a Japanese cultivar Nyuabai (Somers et al., 2003). Till now, *Fhb1* has been found in 26 QTL mapping studies and considered to be the best validated FHB resistance QTL (Buerstmayr et al., 2012). Another major QTL for type II resistance was identified on chromosome 6 from Sumai-3 (Anderson et al., 2001, Waldron et al., 1999) and Wangshibai (Lin et al., 2004) and was fine mapped as single Mendelian factor and renamed as *Fhb2* (Cuthbert et al., 2007).

Apart from these two major type II FHB resistance QTLs, two QTLs, *Qfhs.ifa-5A* and *Qfhi.nau-4B* on chromosome 5A and 4B, respectively, contribute significantly to type I resistance. *Qfhs.ifa-5A* was identified from Sumai-3 with major effect (Buerstmayr et al., 2002, Buerstmayr et al., 2003) and was also reported to contribute to type II resistance with small effect (Somers et al., 2003). *Qfhs.ifa-5A* was also frequently identified and validated in independent populations (Buerstmayr et al., 2009). Recently, it was fine mapped to a 0.3 cM region flanked between Xgwm304 and Xgwm415 and renamed as *Fhb5* (Xue et al., 2011).

Qfhi.nau-4B, another frequently reported QTL for resistance to initial infection with high phenotypic variance was identified from Wanghsuibai (Lin et al., 2004, Lin et al., 2006), Wuhan (Somers et al., 2003), Chokwang (Yang et al., 2005) and Ernie (Liu et al., 2007). Considering its major effect, the QTL region was saturated with microsatellite markers and fine mapped to 1.7-cM interval flanked by *Xhbg226* and *Xgwm149* in Wangshuibai (Xue et al., 2010).

Interestingly, the resistant alleles of some of the FHB QTLs were identified from the susceptible parents. FHB QTLs for type II resistance on chromosome 2AL and 4B were derived from the susceptible parent Stoa in the cross Sumai-3 X Stoa. Sumai-3 alleles contributed negatively on this region (Anderson et al., 2001, Waldron et al., 1999). Similarly, a major QTL on 2D for FHB spread was identified from the populations of Sumai 3 X Gamenya, Nobeokabouzu-komugi X Sumai 3 and Ning894037 X Alondra,

in which resistant 2D alleles were derived from the susceptible parents Gramenya, Nobeokabouzu-komugi and Alondra (Shen et al., 2003, Xu et al., 2001). Coincidentally, a QTL for DON resistance was also mapped to the same region on 2D derived from the resistant cultivars Wuhan (Somers et al., 2003) and Wangshuibai (Jia et al., 2005). Close locations of two QTLs on 2D was hypothesized to play a pleiotropic effect on FHB resistance (Yang et al., 2005). However, Sumai-3 possesses a susceptible allele at the QTL, 2D, coding for a multidrug resistance-associated protein, which is reported to be involved in DON sequestration (Handa et al., 2008).

All the above major QTLs were consistently detected during the meta-analysis of FHB QTLs identified in different mapping populations (Liu et al., 2009, Löffler et al., 2009). In addition, several other QTLs with minor effects are well documented in a review by Buerstmayr et al., (2009) and can be used to enhance FHB resistance through QTL pyramiding or gene stacking following fine mapping.

2.5 Functional characterization of *Fhb1*

Fhb1 (*Qfhs.ndsu-3BS*) is the most consistent and the largest effect FHB resistance QTL, explaining up to 60 % of the phenotypic variance for resistance to disease spread (type II) (Cuthbert et al., 2006, Liu et al., 2006, Pumphrey et al., 2007, Waldron et al., 1999). *Fhb1* was reduced to a 261 Kb region that contain seven candidate genes through positional cloning. However, the candidate genes exhibited susceptibility on expression in a susceptible wheat cultivar (Liu et al., 2008). The locus for DON resistance (type III) was mapped to the same locus as *Fhb1* and hypothesized to co-localize gene(s) that encode either UDP-glycosyltransferase, which catalyzes the conjugation of glucose to DON to produce less toxic DON-3-glucoside (D3G) (Lemmens et al., 2005, Poppenberger et al., 2003). However, *Fhb1* located on a mega base contig, *ctg0954* (GenBank: *FN564434.1*) doesn't localize any genes that encode UDP-glycosyltransferase (Choulet et al., 2010). Regulation of UDP-glycosyltransferase by *Fhb1* is to be investigated. Multiple transcriptomics studies have been conducted to investigate possible biochemical mechanisms associated with *Fhb1*. Transcriptomics of resistant genotypes (Sumai-3, CM82036 and DH1) revealed up-regulation of transcripts of pathogenesis-related (PR) proteins, such as β-1, 3-glucanase (PR-2), wheatwins (PR-4), and thaumatin-

like proteins (PR-5), phenylalanine ammonia lyase (PAL), Dna-J like protein in resistant genotypes that possess resistant *Fhb1* allele compared to their susceptible counterparts (Golkari et al., 2009, Steiner et al., 2009). However, *Fhb1* specific mechanisms could not be explained as none of the up-regulated transcripts was mapped to the *Fhb1* region.

In other studies, a few transcripts localizing to *Fhb1* region were identified along with the general pathogen resistance mechanisms, such as up-regulation of transcripts related to JA signalling pathway, phenylpropanoid pathway and PR-proteins as previously identified (Jia et al., 2009, Zhuang et al., 2013). Up-regulated *Fhb1* specific transcripts were related to cell wall biogenesis, while down-regulated transcripts were associated with cell death, suggesting association of *Fhb1* with reduced susceptibility to cell death due to DON (Jia et al., 2009). Association of *Fhb1* with susceptibility was also evidenced with the identification of a putative *Fhb1* candidate gene, *WFhb1_c1* (GenBank: CA640991-weakly similar to Arabidopsis pectin methyl esterase inhibitor), which contributes to FHB resistance by reducing susceptibility (Zhuang et al., 2013). Similarly, Ca^{2+} signalling pathway genes that contribute to the necrotrophic phase during *F. graminearum* infection through programmed cell death (PCD), were significantly up-regulated in the *Fhb1* deleted susceptible mutant genotype as compared to the another type II FHB resistant cultivar Wangshuibai (Xiao et al., 2013). However, the candidate genes for DON reduction and/or genes contributing to susceptibility in *Fhb1* are yet to be explored.

2.6 Functional genomics of FHB resistance

2.6.1 Transcriptomics of FHB resistance

Comprehensive and high-throughput analysis of gene expression, termed as transcriptomics, is an informative technology to screen candidate genes and predict gene function. Genome wide analysis of host response to biotic and abiotic cues provides information regarding genes that are induced and/or repressed during stress. With the advancements in development of genome arrays such as Affymetrix chips and custom oiligo-DNA arrays, multiple transcriptomics studies have been conducted in wheat and barley against *F. graminearum* or DON inoculations.

Microarray analysis of transcripts from spikes of FHB resistant, Sumai-3 derived cultivar Ning-7840 and a susceptible cultivar Clark identified 44 genes significantly, differentially expressed between the cultivars. Host defense related genes such as chitinase II precursor, PR-1, PR-10 and a P450 were up-regulated in resistant cultivar Ning-7840 at early stage of infection and down-regulated at later stages (24 hpi) compared to a susceptible cultivar. In this study, more genes were up-regulated in a susceptible cultivar than in resistant cultivar and it was hypothesised that such genes were related to susceptibility, and the resistant cultivar Ning-7840 might have lost those genes during evolution (Bernardo et al., 2007). However, many such susceptibility genes were not annotated. Analysis of transcripts from glume, lemma, palea, anther, ovary and rachis dissected from *F. graminearum* infected spikes of a wheat FHB resistant line '93FHB37' using a wheat cDNA microarray with 5739 ESTs revealed accumulation of organ specific transcripts at 24 hpi. Highest numbers of transcripts (36 % of total induced transcripts) were induced in the glumes compared to the water inoculated samples, followed by rachis with 30 %. Positive correlation of transcripts induced in the bract tissues, glume, lemma and palea, which were also positively correlated with the rachis indicated similar host responses to pathogen infection in these organs. In accordance with previous studies, induced defense genes included PR-proteins, oxidative burst, phenylpropanoid pathway and ribosomal proteins (Golkari et al., 2007). In a simultaneous study, RNA profiling of spikes of Ning-7840 showed differential expression of 125 genes, following water and *F. graminearum* inoculation. However, qRT-PCR expression of 51 differentially expressed genes showed differential expression of only 19 genes with a fold change greater >2, which cautions about the false positives in "omics". Highly up-regulated genes in the resistant cultivars were P450, P450 reductase and a multidrug resistance gene that were hypothesised to play a major role in DON detoxification similar to their annotated function of detoxification of xenobiotics (Kong et al., 2007). A more comprehensive profiling of perturbed genes was conducted using an Affymetrix GeneChip wheat genome array that contained 61,127 probe sets representing 55,052 wheat transcripts following *F. pseudograminearum* or water inoculations of stem base of susceptible cultivar Kennedy. 1248 unique genes were induced and 1497 unique genes were

repressed that belonged to primary metabolism, secondary metabolism and plant defense such as oxidative stress, defense signalling and antimicrobial proteins. In comparison to the genes induced by a biotrophic rust pathogen *Puccinina triticina*, genes involved in oxidative stress were exclusively induced in *F. pseudograminearum* indicative of oxidative stress caused by the necrotrophic pathogen. Oxidative stress related genes were also induced by DON along with UDP-glycosyltransferase that detoxifies DON. However, overexpression of DON induced UDP-glycosyltransferase in *Arabidopsis* failed to confer DON resistance (Desmond et al., 2008). This comprehensive study, with more genes revealed several other host resistance mechanisms including involvement of jasmonic acid and salicylic acid signalling that were unaddressed in previous studies.

The next stage transcriptomics studies were focused on revealing the host resistance mechanisms to pathogen aggressiveness factor, DON. Inoculation of barley and wheat spikes with DON led to increased abundance of transcripts related to DON detoxification and sequestration, such as UDP-glycosyltransferase, and ABC transporters and also related to oxidative stress and host cell death. In addition, DON repressed many host defense related transcripts (Foroud et al., 2011, Gardiner et al., 2010). Similar to DON treatment, inoculation with *FgTri5*$^{+}$ up-regulated transcripts related to DON detoxification and sequestration, and cell death, but not in the *FgTri5*$^{-}$ mutant strain in barley (Boddu et al., 2007). In addition, *FgTri5*$^{+}$suppressed the expression of 18 host defense related transcripts in contrast to just one transcript by the *FgTri5*$^{-}$ mutant. In wheat, more DON resistance related transcripts were up-regulated in the FHB resistant wheat near isogenic lines (NILs), GS1-EM0040 and GS1- GS-1-EM0168 compared to the susceptible cultivar, Superb following *FgTri5*$^{+}$ inoculation, in all time points tested, but not with *FgTri5*$^{-}$ inoculated samples. In contrast, more transcripts of ribosomal proteins were down regulated in Superb compared to the resistant NILs (Foroud et al., 2011).

A few transcriptomics studies were conducted to functionally characterize the genes localized at FHB QTL regions. Many efforts were made to characterize a major and the most consistent wheat QTL, *Fhb1 f*or type II FHB resistance. Initially, two transcriptomics studies associated *Fhb1* with general host defense mechanisms such as

induction of PR-proteins and phenylpropanoid pathway genes (Golkari et al., 2009, Steiner et al., 2009). Although, none of the differentially accumulated genes were mapped to the *Fhb1* locus, those genes might be regulated by other genes localized on *Fhb1*. Transcriptomics of NILs with resistant and susceptible *Fhb1* allele identified host cell death related genes and cell wall biogenesis genes that map to *Fhb1*. (Jia et al., 2009). Similarly, genes that reduce susceptibility to FHB were mapped to chromosome 3 BS region (Zhuang et al., 2013). Recently, RNA sequencing of the FHB resistant landrace Wangshuibai that contains resistant *Fhb1* allele and mutants of Wangshuibai deleted in the *Fhb1* region, explained association of *Fhb1* with resistance to cell death. The study revealed that genes involved in Ca^{2+} signalling and cell death were highly up-regulated in susceptible mutant. However, none of the *Fhb1* candidate genes could explain the mechanisms of low DON accumulation and resistance to FHB spread.

2.6.2 Proteomics of plant disease resistance

Plant defense mechanisms, either innate or induced, involve various kinds of proteins such as pathogen/pattern recognition receptors, proteins produced by the R genes, enzymes mediating oxidative burst, hypersensitive response, PR proteins, signaling pathways and enzymes catalyzing the biosynthesis of secondary metabolites. Characterization of proteins will help in understanding the host pathogen interaction and host defense responses. Proteomic changes in the host plant due to pathogen attack can be traced back to their molecular level of defense mechanism and annotated to the genome sequence. The resulting biochemical changes may give insight into critical 'switch points' in defense-related pathways that could be manipulated to engineer host plants with improved resistance or immunity to the pathogen (Bhadauria et al., 2010).

Proteomics is the global study and characterization of a complete set of proteins of an organism, individually or collectively of an organ or organelle or cell under a given condition (Wilkins et al., 1995). Proteomics provides the complete outlay of cellular responses at various stages of growth and development and environment. It also provides information on various post translational modifications and their biological relevance, sub cellular location of a biochemical reaction, epigenetic DNA modification and

alternate splicing of mRNA leading to more than one protein which are otherwise not provided by the genome sequencing and transcriptomics (Quirino et al., 2009).

Irrespective of significant developments in shotgun proteomics, most of the proteomic analyses of FHB resistance in wheat and barley have been based on two-dimensional gel electrophoresis (2-DE). A temporal protein expression of a wheat FHB resistant cultivar Wangshibai at 6, 12 and 24 h after inoculation with *F. graminearum* were analysed in 2DE. Thirty protein spots that were expressed at greater than 3 fold change were identified using MALDI-TOF MS. Based on their temporal expression; identified proteins were classified into different categories. Plant defense related proteins were both increased at the initial time point and decreased later or were highly expressed at all points (Wang et al., 2005). However, because of early sampling, many of the defense proteins identified were of general host response to stress such as heat shock proteins and β-glucosidase. In contrast, many host defense proteins were significantly induced at advanced stages of infection (5 dpi) in response to *F. graminearum* inoculation compared to water in the spikes of Sumai-3 derived cultivar, Ning-7840. Induced defense proteins were ROS neutralizing antioxidant proteins such as superoxide dismutase, dehydro-ascorbate reductase, and glutathione S-transferase (GSTs) and a PR-2 (β-1, 3-glucanase) protein (Zhou et al., 2005). Induction of antioxidant proteins in the resistant cultivar indicated defense responses to DON induced H_2O_2. *F. graminearum* down-regulated many proteins involved in photosynthesis and primary metabolism in the susceptible cultivar Sypro Ruby. In contrast, only a few proteins of anti-oxidative stress, JA signalling and PR proteins were up-regulated. Nine of the differentially regulated proteins were localized to chloroplast (Zhou et al., 2006). A comprehensive analysis of differentially expressing proteins in barley genotypes with varied levels of resistance showed up-regulation of defense related PR-proteins (PR3 and PR-5) in the resistant genotypes, CI4196, Svansota, Harbin, and an intermediate resistant genotype CDC Bold. On the contrary, oxidative stress response proteins were up-regulated in the susceptible genotype, Stander and in an intermediate resistant genotype CDC Bold. The study revealed contrasting protein profiles in resistant and susceptible genotypes and showed that *F. graminearum* induced oxidative stress by saprophytic feeding in mainly

susceptible genotypes (Geddes et al., 2008). A comparative proteomics analysis of resistant and susceptible genotypes can give a functional view of resistance that can be targeted for utilization in crop breeding.

2.6.3 Metabolomics of plant disease resistance

It has been estimated that plants produce over 200,000 metabolites which are involved in both primary and secondary metabolism (Wink, 1988). A metabolome is the complete set of small molecules in an organism and represents the ultimate phenotype of cells encoded by the genome and the modulation of protein functions, which are caused by mutations or the environment including biotic and abiotic stress. 'Metabolomics' is the analysis of the full set of small molecules (metabolites) in a biological sample to reveal the current state of metabolism (Fernie and Schauer, 2009). The metabolome include both primary metabolites that are necessary for normal growth and development and secondary metabolites that are produced in response to environmental or genetic manipulation (Dixon, 2001). The secondary metabolite biosynthesis pathway evolved during plant evolution as a defense against microorganisms (viruses, bacteria, fungi), herbivores (molluscs, arthropods, vertebrates), and competing plants (allelopathy) (Wink, 1988). Analysis of biochemical changes during biotic stress helps to illustrate host defense responses and elucidate the causes of such perturbations at genome, transcriptome and proteome levels and/or consequences of such changes (Kushalappa and Gunnaiah, 2013).

The principle advantages of metabolomics over other 'omics' approaches in functional genomics are: it doesn't require prior information about the genome sequence, it provides information on the end product of a gene, thus providing the exact functional information of a gene surpassing all the post transcriptional and post translational modifications and is the cheapest (Fernie and Schauer, 2009). Metabolomics has wide applications in identifying chemical signatures for discovering bioactive compounds (metabolotyping), elucidating physiological functions (Hegeman, 2010), evaluation of genetically modified crops (Garcia-Canas et al., 2011), elucidating host defense responses to biotic and abiotic stresses (Arbona et al., 2013, Bollina et al., 2010, Kumaraswamy et al., 2011, Kusano et al., 2011), understanding plant-pathogen interactions (Allwood et al., 2010) and many

more. With the availability of several crop genome sequences, metabolomics is used as a potential tool in functional genomics to identify gene functions (Gunnaiah et al., 2012, Lloyd et al., 2011, Watanabe et al., 2008). Like any other quantitative traits that are governed by poly or oligo genes, several physiological traits are controlled by quantitative variation in the metabolites. Identifying metabolomic QTLs (mQTLs) and mQTLs hotspots have led to identification of small regions on the genome responsible for the metabolome variation and further gene functions were elucidated (Keurentjes et al., 2006, Lisec et al., 2009, Matsuda et al., 2012) .

With significant developments in the field of metabolomics, FHB resistance was not left behind in elucidating host defense responses in wheat and barley. Metabolic profiling of spikelets of the FHB resistant cultivar Sumai-3 and the susceptible cultivar Roblin using GC-MS showed perturbation of volatile metabolites following *F. graminearum* inoculation. Factor analysis grouped metabolites specific to resistant and susceptible cultivars and also discriminated pathogen and mock treatments. Metabolites associated with resistant cultivar Sumai-3 were hypothesised to be involved in plant defense such as cell signalling (myo-inositol), plant defense signalling (fatty acids) and antimicrobial compounds (cinnamic acids and coumaric acids) (Hamzehzarghani et al., 2005). Further, metabolotyping of six wheat cultivars with GC-MS with varied levels of FHB resistance identified potential biomarkers (RR metabolites) that were either constitutively present or induced following *F. graminearum* infection with higher abundance in resistant cultivars. Consistent with their previous study, potential biomarker metabolites identified were from the phenylpropanoid and fatty acid pathway and cell wall polysaccharides, which play a significant role in plant defense against pathogens (Hamzehzarghani et al., 2008). GC-MS based metabolic profiling was also extended to characterize one of the major wheat FHB resistance QTL 2DL comparing NILs with resistance and susceptible alleles. The study identified 27 resistance related (RR) metabolites that were higher in resistant NIL, belonging to phenylpropanoid and fatty acid pathways (Hamzehzarghani et al., 2008). However, resistance mechanism specific to QTL 2DL, was not identified. In another study, the effect of DON on host resistance mechanisms in FHB resistant (Sumai-3) and susceptible (Roblin) cultivars were revealed using GC-MS. The Fusarium toxin

DON repressed host resistance mechanisms in both resistant and susceptible cultivars and induced polyamines in Roblin with higher abundance, that play major role in the growth of *F. graminearum* (Paranidharan et al., 2008). However, GC-MS could detect only volatile metabolites and hence only partial resistance mechanisms based on the detected volatiles were identified using GC-MS.

More comprehensive analysis of perturbed metabolome was done in barley cultivars with varied levels of resistance using high resolution LC-MS. Metabolites with higher abundance in resistance cultivars were portrayed as resistance related constitutive (RRC) metabolites (higher abundance in mock treated samples) and resistance related induced (RRI) metabolites (induced following *F. graminearum* inoculation). In addition, pathogen toxin, DON and its derivatives, which are present in susceptible genotypes with higher abundance and their detoxified products, were classified as resistance indicator (RI) metabolites (Bollina et al., 2010, Kumaraswamy et al., 2011). Independent studies with six row barley (Bollina et al., 2010) and yellow barley (Kumaraswamy et al., 2011), comprising of a resistant (Chevron, H106-4) and susceptible cultivars (Stander and H106-371) revealed common resistance mechanisms conferred by antimicrobial metabolites belonging to phenylpropanoid, flavonoid, fatty acid and terpenoid pathways. Antifungal activity of some of the significant RR metabolites was confirmed by *in vitro* bioassays. Capric acid and *p*-coumaric acid from six row barley cultivar Chevron, exhibited high resistance equivalence. Even though, capric acid was present at lower abundance compared to other RR metabolites, it showed the highest resistance equivalence with lowest LD-50 values, indicating it was highly toxic even at lower concentrations (Bollina et al., 2010). In yellow barley cultivar H106-4, the plant defense signalling molecule methyl jasmonate showed the highest resistance equivalence (Kumaraswamy et al., 2011).

Identification of diverse chemical groups of metabolites using LC-MS led to the identification of biomarker metabolites in different two row and six row barley cultivars, with varied levels of resistance. Comparative metabolotyping of two row barley resistant cultivars (CIho 4196, Zhedar-1, Zhedar-2, Fredrickson, and Harbin-2r) with a susceptible cultivar CH 9520–30 identified five biomarker metabolites, phenylalanine, *p*-coumaric

acid, kaempferol 3-isorhamninoside, jasmonic acid and linolenic acid as biomarker metabolites that were consistently detected in higher abundance in 3 or more resistant genotypes compared to susceptible genotype (Kumaraswamy et al., 2011). In six row FHB resistant barley cultivars (Chevron, H5277-44, H5277-164, M92-513 and M122), nine metabolites were identified as biomarker metabolites in comparison to the susceptible cultivar, Stander (Bollina et al., 2011). *P-coumaric* acid and linolenic acid were common biomarkers for six row and two row barley cultivars. Six row barley cultivars exhibited more number of flavonoids compared to two row barley (Bollina et al., 2011). Comparatively, two row barley cultivars were more resistant to FHB than six row barley. Nevertheless, DON detoxification was very high in all the barley cultivars tested, with no significant difference among them including the susceptible cultivar. Metabolic profiling was also used to assess the effect of DON on host resistance mechanisms by inoculating barley cultivars with trichothecene-producing (*FgTri5*$^{+}$) and -nonproducing (*FgTri5*$^{-}$) isolates of *F. graminearum*. The necrotrophic plant signalling molecule jasmonic acid was significantly induced in response to *FgTri5*$^{+}$ but not to *FgTri5*$^{-}$ strain. Plant defense compounds belonging to the phenylpropanoid pathway were either highly induced or induced only in response to *FgTri5*$^{-}$ strain inoculation, indicating defense suppression action of DON (Kumaraswamy et al., 2011).

The studies suggested that non-targeted metabolic profiling using high resolution LC-MS can be used as a tool to decipher host resistance mechanisms against pathogen attack. Integrated analysis of transcriptome, proteome and metabolome can lead to the elucidation of novel gene functions (Tohge et al., 2005).

2.7 Metabolomic and proteomic analysis platforms

Metabolomics deals with large number of diverse chemical compounds differing in their biochemical properties. The large variations in the relative concentrations of metabolites also add to the complications of metabolite analysis. Therefore, comprehensive coverage of metabolites of an organism can be achieved by using multi-parallel complementary extraction and detection technologies with careful experimental design. Metabolic profile data are obtained using biochemical analytical platforms such as GC-MS, LC-MS, and NMR, each having its own advantages and limitations.

NMR spectroscopy is a high throughput technology which can provide global view of metabolites and capable of structure elucidation. It is a non-destructive technique which requires minimal sample preparation and hundreds of samples can be analysed in a day. It is based on the principle that nuclei with odd atomic or mass act like magnets and can interact with an external magnetic field by a process termed nuclear spin (Hatada and Kitayama 2004). H-NMR has proven to be an appropriate tool for untargeted plant metabolomics, especially where studies focus upon samples that contain highly abundant bulk metabolite species (Biais *et al*., 2009). It has the advantage of producing signals that correlate directly and linearly with compound abundance (Lewis *et al*., 2007). However, the sensitivity of NMR is comparatively low and most of the secondary metabolites in plants cannot be detected.

Chromatography combined with mass spectrometry (MS) is widely used in plant metabolic profiling. In this technique, ions are generated and extracted into the analyser region of the MS where they are separated by their mass-to charge (m/z) ratios. The separated ions are detected and the signal sent to a data system, where the m/z ratios are stored together with their relative abundance for presentation as a mass spectrum. The GC-MS method is one of the most popular metabolomics techniques since the beginning of metabolomics study and continues to be the choice for target analysis of volatile compounds. It can be used to determine the levels of primary metabolites such as amino acids, organic acids, and sugars by employing a chemical derivatization of these metabolites. The GC-MS method also has good reproducibility in terms of the sharp separation of metabolites by GC combined with the stable ionization achieved by electron impact (EI). This method is preferable for analyzing complex plant extracts. Multiple fragmentations of ions by EI are well suited for metabolite identification. However, GC-MS is biased more towards volatile polar compounds and does not detect the heat labile compounds. Hence, it profiles limited number of compounds (Vorst et al., 2005).

Liquid Chromatography (LC-MS) can detect a wide range of metabolites based on the polarity of the column and is best suited for non-targeted plant metabolomics as the plants are rich in diverse metabolites (Allwood and Goodacre, 2010). Liquid chromatography (LC) is the separation of components of a mixture based upon the rates

at which they elute from a stationary phase over a mobile phase gradient and is dependent on the differing affinities of the components for the stationary and mobile phase. The advantages of LC-MS include production of accurate masses and high resolution, which adds another dimension of separation of ions. Resolution of MS detectors varies from 10^3 in ion trap/quadruple to 10^6 in FTMS. However, quantitation through LC-MS is not accurate as co-eluting compounds may cause ion suppression and signal to concentration varies in such situations (Hegeman, 2010). Ion suppression can be significantly reduced through nano-electro spray ionization (nESI) and use of high resolution MS. Absolute quantification can be obtained in LC-MS by using calibration curves and standard curves but it is limited to few known compounds (Kiefer et al., 2008). Relative quantification based on changes in abundance is useful in biological experiments (Huang and Regnier, 2008).

A novel MS platform, orbitrap, provides a higher mass resolution and mass accuracy over a wider dynamic range. It has higher potential to detect greater number of metabolites of similar accurate mass with a high level of confidence of metabolite identification. The combination of orbitrap with a linear ion trap, in the hybrid LTQ-orbitrap analytical platform, offers the advantage of acquiring two different scan types. The two scan types are the collection of an 'accurate mass' spectrum in the orbitrap in parallel to the collection of single or multiple MS/MS mass spectra using data-dependent analysis (DDA) in the linear ion trap. A limited number of metabolomics studies have been reported using LTQ-orbitrap instruments (Bollina et al., 2010). A latest introduction of LTQ-orbitrap-Velos enables hierarchical fragmentation allowing separation of several isomers which are common in plant metabolomics.

2.8 Bioinformatics tools for non-targeted metabolomics and proteomics

2.8.1 Software for LC-MS data processing

Liquid chromatography mass spectrometry data processing to extract true signals is the key step in non-targeted biochemical analysis. Several bioinformatics tools are available for LC-MS data processing. Most of the spectral data processing software, such as XCMS (Smith et al., 2006), involve four basic steps: deconvolution, grouping, alignment

across samples and gap filling. The peaks (*m/z*) and their intensities in different samples are used in statistical analysis. Alternatively, user interactive tools such as MZmine2 (Pluskal et al., 2010) and web based tools, MetaboAnalyst (Xia and Wishart, 2011) are more suited for biologists, with limited knowledge on mass spectrometry. The processed outputs from these tools generally contain multiple peaks of the same compound, including isotopes, adducts, neutral loss, and dimers. Thus, the direct use of these peaks in multivariate analysis can lead to erroneous conclusions (Evans et al., 2009). The processed output in matrix is imported to MS-EXCEL spreadsheet and the peaks inconsistent among replicates, isotopes and adducts can be sieved for further statistical analysis.

2.8.2 Metabolite identification

Several web based tools are available for metabolite annotation, with links to mass spectral libraries. A peak or metabolite can be putatively identified based on three criteria: *i) Accurate mass match with reference compound libraries*: Each accurate mass from LC-MS is matched with previously identified compounds using various libraries. A metabolite match with an accurate mass error of AME > 5 ppm can be considered un-annotated; *ii) Number of carbons based on isotope ratio*: the isotope ratios of carbon (also others) can be used to calculate the number of carbons in the molecular formula (Iijima et al., 2008); *iii) Fragmentation patterns of peak*: the fragmentation patterns can be either matched with those published in several databases, such as MASSBANK, METLIN and ReSpecT or with that of in-house spiked compound library. The fragmentation patterns also can be manually checked using *in silico* fragmentation tools, such as ChemSketch in IntelliXtract. A complete identification requires satisfaction of remaining of the seven golden rules (Kind and Fiehn, 2007). Reverse stable isotope labelling, using labelled carbon and nitrogen sources during plant growth, and then, spiking with non-labelled metabolites can facilitate large scale identification of metabolites (Hegeman et al., 2007).

2.8.3 Protein identification

LC-MS/MS data output from peptide analysis is very complex, as each protein is proteolyzed into more than one peptide before analysis, and each peptide ion produces multiply charged ions. High resolution MS^n can be used to sequence the amino acids in peptides. Generally, tandem mass spectra are matched to an inventory of mass values generated by *in silico* fragmented peptides for peptide identification using search engines: MASCOT, SEQUEST, XiTandem and InSpeCT. These search engines are linked to various proteome and genome databases like GenBank at NCBI, SWISSPROT, UNIPROT, PPDB, and ProMEX which can lead to the identification of corresponding genes.

2.8.4 Quantification of metabolites and proteins

Generally relative quantification of metabolites and proteins, based on the individual peak abundance, is used in treatment comparisons. Absolute quantification can be done by stable isotope labeling (Hegeman et al., 2007) or a separate standard curve can be established (Bollina et al., 2011). Label free absolute quantification of proteins can be accomplished based on spectral counts, protein abundance index and absolute protein expression (Matros et al., 2011).

CONNECTING STATEMENT FOR CHAPTER III

The following chapter III entitled "Integrated Metabolo-Proteomic Approach to Decipher the Mechanisms by which Wheat QTL (*Fhb1*) Contributes to Resistance against *Fusarium graminearum*" is published in *PLoS One* journal (PLoS One 7(7): e40695).The manuscript is co-authored by Raghavendra Gunnaiah, Ajjamada C. Kushalappa1, Raj Duggavathi, Stephen Fox and Daryl J. Somers.

The mechanisms of resistance governed by the most consistent and the largest effect wheat FHB QTL, *Fhb1*, were poorly understood. *Fhb1* has been identified from multiple resistant sources: Sumai-3 and its derivatives, Wangshuibai and Nyubai. Multiple studies have been conducted to decipher the function of *Fhb1* from Sumai-3 (Golkari et al., 2009, Jia et al., 2009). The *Fhb1* from Nyubai also significantly contributes to type II resistance, and also for DON reduction along with *Fhb5*, and it was fine mapped to 6.05 cM (Cuthbert et al., 2006, Somers et al., 2003). But Nyubai is not efficiently used in breeding as the resistance mechanisms are not known. The pathogen *F. graminearum* spreads through rachis, and the host defense responses are specific to organs, but host biochemical mechanisms in the rachis are not well studied (Golkari et al., 2007). An understanding of the host defense responses at rachis that blocks the pathogen spread within spike is crucial. Proteins and metabolites are closer to the phenotype, and accordingly the metabolic profiling has been used to decipher the host defense mechanisms and identify biomarkers (Bollina et al., 2010, Kumaraswamy et al., 2011). However, the metabolic and protein profiling of wheat for FHB resistance, using high resolution LC-MS, have not been attempted. Consequently, it was hypothesised that, *Fhb1* derived from Nyubai exhibits novel resistance mechanisms at the rachis for resistance to spread, and the near isogenic lines (NILs) with resistance and susceptible *Fhb1* alleles would differentially accumulate metabolites and proteins. The metabolites and proteins higher in abundance in resistant NIL than in susceptible NIL were used to identify candidate genes for resistance to FHB.

CHAPTER III

Integrated metabolo-proteomics approach to decipher the mechanisms by which wheat QTL (*Fhb1*) contributes to resistance against *Fusarium graminearum*

Raghavendra G.[1], Kushalappa A.C.[1*], Duggavathi R.[2], Fox S.[3] and Somers D.J.[4]

[1]Plant Science Department, and [2]Animal Science Department, McGill University, Ste. Anne-de-Bellevue, Quebec, Canada H9X3V9; [3]Agriculture and Agri-Food Canada, Winnipeg, Manitoba, Canada R3T2M9 and [4]Vineland Research and Innovation Center, Vineland, Ontario, Canada L0R 2E0.

3.1 ABSTRACT

Resistance in plants to pathogen attack can be qualitative or quantitative. For the latter, hundreds of quantitative trait loci (QTLs) have been identified, but the mechanisms of resistance are largely unknown. Integrated non-target metabolomics and proteomics using high resolution hybrid mass spectrometry were applied to identify the mechanisms of resistance governed by the Fusarium head blight resistance locus, *Fhb1,* in the near isogenic lines derived from wheat genotype Nyubai. The metabolic and proteomic profiles were compared between the near isogenic lines with resistant and susceptible alleles of *Fhb1* upon *F. graminearum* or mock-inoculation. The resistance-related metabolites and proteins identified were mapped to metabolic pathways. Metabolites of the shunt phenylpropanoid pathway such as hydroxycinnamic acid amides, phenolic glucosides and flavonoids were significantly increased in the resistant NIL following pathogen inoculation. The identities of these metabolites were confirmed with fragmentation patterns using the high resolution LC-LTQ-orbitrap. Concurrently, the enzymes of phenylpropanoid biosynthesis such as cinnamoyl alcohol dehydrogenase, caffeoyl-CoA *O*-methyltransferase, caffeic acid *O*-methyltransferase, flavonoid *O*-methyltransferase, agmatine coumaroyltransferase and peroxidase were also up-

regulated. Increased cell wall thickening due to deposition of hydroxycinnamic acid amides and flavonoids was confirmed by histo-chemical localization of the metabolites using confocal microscopy. The present study demonstrate that the resistance in *Fhb1* derived from the wheat genotype Nyubai is mainly associated with cell wall thickening due to deposition of hydroxycinnamic acid amides, phenolic glucosides and flavonoids, but not with the conversion of deoxynivalenol to less toxic deoxynivalenol 3-*O*-glucoside.

3.2 INTRODUCTION

Disease resistance in plants can be broadly classified as qualitative or quantitative. Qualitative resistance is generally governed by mono/oligo-genes and imparts complete resistance. Significant advances have been made in the past few decades in understanding the defense mechanisms associated with qualitative resistance, and many genes governing resistance have been identified and used for plant improvement. On the other hand, quantitative resistance is mostly governed by polygenes and imparts partial but durable resistance. Due to its genetic complexity, progress in the characterization of quantitative defense mechanisms has been slower. The use of DNA markers has led to the identification of quantitative trait loci (QTL) governing partial resistance (Young, 1996). Biotic stress resistance QTLs have been identified in several crop diseases such as late blight of potato (*Phytophthora infestans)* (Danan et al., 2011), rice blast (*Magnporthegrisea*) (Ballini et al., 2008), fusarium head blight (*Fusarium graminearum*) (Buerstmayr et al., 2009) and cereal rusts (*Puccinia* spp.) (Qi et al., 1998). These QTLs generally co-localize several genes, but cloning of QTL to identify all the co-localizing genes is a difficult task. Hence, the biochemical mechanisms by which QTLs drive disease resistance are largely unknown. Identification of specific defense mechanisms and genes associated with QTLs can lead to the pyramiding of suitable alleles to enhance resistance in elite cultivars.

Fusarium head blight (FHB) caused by *Fusarium graminearum* Schwabe (Teleomorph: *Gibberella zeae* (Schwein.) Petch) is a devastating disease of wheat and barley. The disease FHB causes severe economic damage by reducing grain yield and also deteriorates the grain quality by contamination with trichothecene mycotoxins.

Deoxynivalenol (DON), a type B trichothecene produced by *F. graminearum*, is highly toxic to animals at very low concentrations (Pestka and Smolinski, 2005) and is also a pathogen aggressiveness factor (Proctor et al., 1995). The use of resistant genotypes is considered to be the best practical approach to manage FHB. Resistance to FHB in wheat is quantitative and is governed by polygenes (Bai and Shaner, 2004). The resistance has been classified into five types (Mesterhazy, 1995), however, only three types- type I (resistance to initial infection of spikelets), type II (resistance to spread of pathogen within spike) (Schroeder and Christensen, 1963) and type III (resistance to DON) (Miller et al., 1985) have been extensively used. More than one hundred FHB resistance associated QTLs have been identified in wheat (Buerstmayr et al., 2009). The major QTLs mapped on chromosomes 3BS, 4B, 5A, and 6B have been validated and used in marker-assisted selections. However, the resistance mechanisms governed by these QTLs are unknown, except partially for the QTL on chromosome 3BS.

The major QTL on 3BS, referred as *Fhb1*, explains up to 60% of the phenotypic variation for type II FHB resistance (Bai et al., 1999, Cuthbert et al., 2006). It has been speculated that *Fhb1* derived from Sumai-3 either encodes or regulates the expression of a UDP glycosyltransferase that converts DON to DON-3-*O*-glucoside (D3G) (Lemmens et al., 2005, Poppenberger et al., 2003). QTL specific transcriptome analysis of the *Fhb1* locus derived from genotype Sumai-3 showed greater accumulation of ten transcripts, including two cell wall biogenesis and two of general defense mechanisms (Jia et al., 2009). However, several other constitutive and induced chemical and structural host defense mechanisms have been documented against *Fusarium* infection (Walter et al., 2010).

Non-target metabolomics has been applied to study mechanisms of resistance in wheat (Hamzehzarghani et al., 2005, Hamzehzarghani et al., 2008) and barley (Bollina et al., 2010, Bollina et al., 2011, Kumaraswamy et al., 2011, Kumaraswamy et al., 2011) against *F. graminearum*. The quantitative resistance in barley and wheat was associated with the activation of phenylpropanoid, terpenoid and fatty acid metabolic pathways, in addition to the detoxification of DON to D3G in barley. The metabolites of these pathways are involved in plant defense signaling, antimicrobial and cell wall strengthening properties. Non-target proteomics, based on 2D gel electrophoresis

combined with LC-MS/MS, has also been applied to explain the resistance mechanisms against *F. graminearum* in barley (Geddes et al., 2008, Yang et al., 2010) and wheat (Wang et al., 2005, Zhou et al., 2005). Proteomics revealed diverse mechanisms of resistance such as oxidative stress response, induction of PR proteins and activation of phenylpropanoid pathway. Non-target metabolomics combined with proteomics could enable the identification of key metabolites and proteins that are the end products of gene expression, associated with *Fhb1* explaining specific mechanisms of resistance.

Nyubai is a moderately resistant Japanese cultivar that explained up to 30% phenotypic variance for type II resistance, and is also a potential alternative source to widely used Sumai-3 for FHB resistance (McCartney et al., 2007, Somers et al., 2005). *Fhb1,* from Nyubai was mapped to the same locus as that of *Fhb1* derived from Sumai-3 but with different allele sizes (Cuthbert et al., 2006). The objective of the present study was to investigate the resistance mechanisms in wheat to the spread of FHB within spike governed by the QTL, *Fhb1* based on non-target metabolomics and proteomics tools. Use of NILs minimizes the background effect and better explains the resistance mechanism governed by a specific locus for which NILs are differing. Hence two NILs, with resistant (NIL-R) and susceptible (NIL-S) alleles of *Fhb1,* derived from Nyubai were used to investigate the mechanism of resistance governed by a QTL.

3.3 MATERIALS AND METHODS

3.3.1 Development of wheat NILs with contrasting alleles of *Fhb1*

Resistant and susceptible NILs of wheat were derived from the mapping population HC374 (resistant)/98B69*L47 (susceptible) by backcross breeding (Somers et al., 2005). The FHB resistant parent HC374 was derived from the cross Wuhan/Nyubai which carried FHB resistance QTLs on 3BS, 2DL, 3BSc, 4B and 5AS (Somers et al., 2003). The FHB susceptible parent 98B69*L47 was an elite hard red spring wheat accession. BC2F1 plants with 89% recurrent genome and heterozygous between the markers gwm533 and wmc808 which flank *Fhb1* were used in the study. Since Wuhan is a genetic source of other QTLs, plants were selected for homozygous susceptible alleles at other known FHB resistance loci on chromosomes 2DL, 3BSc, 4B and 5AS.

Microsatellite alleles across the genome of 98B69*L47 were used for recurrent parent genome selection to derive the resistant NIL (NIL-R) and the susceptible NIL (NIL-S). The NILs carried either resistant or susceptible alleles at the *Fhb 1* locus on chromosome 3BS.

3.3.2 Plant production, *F. graminearum* inoculum production and inoculation

Wheat NIL-R and NIL-S were grown in greenhouse at 25 ± 3^0C with 70±10% relative humidity and 16 h light and 8 h darkness. *F. graminearum* (Schwabe) isolate 15-35 (obtained from Dr. S. Rioux, CEROM, Quebec) was maintained on PDA media. For spore production, cultures were grown on rye B agar media, under UV light and darkness, for 16 h and 8 h, respectively, at 25^0C. Macroconidia were harvested and the spore count was adjusted to $1x10^5$ macroconidia ml^{-1}. Wheat spikelets were point inoculated with 10 µl of spore suspension (approx. 1000 macroconidia per spikelet) at 50% anthesis, using a syringe with an auto dispenser (GASTIGHT 1750DAD W/S, Hamilton, Reno, NV, USA). For disease severity assessment, a pair of alternative spikelets, approximately at middle of the spike was inoculated. For metabolic/protein profiling, three alternate pairs of spikelets (six spikelets per spike), around the middle of spike, were inoculated. Ten spikes from 6 plants were inoculated for each treatment (pathogen or mock) per replication. The inoculated plants were covered with moistened plastic bags to maintain a saturated atmosphere to facilitate infection, and the bags were removed 48 h post inoculation (hpi).

3.3.3 Disease severity assessment

The number of spikelets diseased was recorded at 3 day intervals until 21 days. From these data, the proportion of spikelets diseased (PSD = number of spikelets diseased/ total number of spikelets in a spike and area under the disease progress curve (AUDPC) were calculated (Hamzehzarghani et al., 2005). A student's *t*-test was used to compare the AUDPC variation between NILs (SAS v 9.2, 2004).

3.3.4 Sample collection, metabolites extraction and LC-hybrid MS analysis

Inoculated spikes were harvested at 72 hpi. The spike was trimmed on both ends; six inoculated spikelets and rachis harvested separately were immediately frozen in liquid

nitrogen and stored at -80^{0}C until use. The rachis and spikelet samples were ground in liquid nitrogen. Metabolites were extracted in 60% ice-cold aqueous methanol as standardized in our lab and analysed using liquid chromatography coupled with hybrid mass spectrometers (LC-nESI-LTQ-Orbitrap, Thermo Fisher, Waltham, MA), fitted with a relatively polar reverse phase C18 Kinetex column (Phenomenex, CA, USA) (Bollina et al., 2010). Mass resolution was set to 60 000 (FWHM) at 400 *m/z*. MS1 data were recorded in centroid mode. For compound identification, one sample each from a treatment was rerun to obtain MS/MS fragmentation at normalized collision energy of 35 eV.

3.3.5 LC-hybrid MS data processing using XCMS

The output from the LC-hybrid MS was imported to XCMS bioinformatics tool on R platform for peak detection, matching, grouping and retention time alignment of peaks across the samples. For feature (*m/z* and retention time) detection, *centWave* alogorithm with mass deviation (μ) = 3 ppm, peak width (range wmin - wmax) of 10-30, and signal to noise (*S/N*) ratio of 5 was employed (Tautenhahn et al., 2008). XCMS processing was carried out independently for rachis and spikelets, in pair-wise treatment combinations (RP versus RM, RM versus SM, SP versus SM and RP versus SP). The adducts, isotopes and neutral losses were identified using CAMERA algorithm based on peak annotation (Kuhl et al., 2009). Following this, the data from all four treatment combinations were combined using MetaXCMS (Tautenhahn et al., 2011), separately for rachis and spikelets. The accurate masses and their abundance (relative intensity) were imported to MS Excel; peaks that were not consistent among replicates and those annotated as isotopes, adducts, dimers and neutral losses were excluded from further analyses.

3.3.6 Experimental design, statistical analysis and identification of resistance related (RR) metabolites

The experiment was conducted in a greenhouse as a randomized complete block design with two NILs (NIL-R & NIL-S) and two inoculations (pathogen and mock) making four treatment combinations; RP, RM, SP and SM. Treatments were independently replicated

five times, at three day intervals. Each sample or the experimental unit consisted of about 60 spikelets or ten rachises that were collected from ten spikes per replication.

Data on intensity of peaks (*m/z* mass/charge ratio) equivalent to mono-isotopic masses subtracted with a proton mass was subjected to pair-wise student's *t*-test analysis, using SAS (SAS v 9.2, 2004). The treatment combinations tested were RM versus. SM, RP versus RM and SP versus SM and the peaks with $P<0.05$ were considered as treatment significant. A data dimension reduction technique, canonical discriminant analysis, was applied to classify the treatment effects based on metabolites (Hamzehzarghani et al., 2008). The abundances of 672 and 693 metabolites common to all treatments from rachises and spikelets, respectively, were subjected to canonical discriminant analysis to classify the observations. The Can vectors were used to identify the resistance functions, by correlating the observed clusters to resistance phenotypes. The treatment significant metabolites were also used to identify resistance related (RR) metabolites. Metabolites with significantly higher abundances in NIL-R than in NIL-S were considered as RR metabolites. These were further grouped into RR constitutive (RRC = RM > SM) and RR induced metabolites (RRI = (RP > RM) > (SP>SM)). For these RR metabolites, the fold change (FC) in abundance relative to susceptible (NIL-R/NIL-S) was calculated. When a metabolite was induced only in the NIL-R (PRr = pathogenesis related) and not in the NIL-S (PRs), then the fold change was considered infinity. For such metabolites, only the fold change in PRr metabolite (RP/RM) was reported. The RR metabolites were putatively identified based on three criteria: i) accurate mass match (accurate mass error (AME) of < 5ppm) with metabolites reported in different databases: METLIN, KNApSAcK, Plant Metabolic Network (PMN), LIPIDMAPS, KEGG and McGill-MD (Tohge and Fernie, 2010); ii) fragmentation pattern match with those in databases and also those from in-house spiked standards (Kushalappa, 2011); iii) *in silico* fragmentation verification using Massspec scissors in Chemsketch (ACD labs, Toronto) (Matsuda et al., 2009). The metabolites were mapped on metabolic pathways using pathway tool omics viewer (PMN, 2011) searched against *Arabidopsis thaliana* and *Populus trichocarpa* metabolites. Concentration of DON, 3ADON and D3G were calculated based on standard curves previously developed (Bollina et al., 2011). Total DON produced (TDP) was

calculated by summing the quantity of DON and D3G, and the proportion of TDP converted to D3G based on the ratio, PDC = D3G/TDP.

3.3.7 Histo-chemical staining of hydroxycinnamic acid amides (HCAAs) and flavonoids

Rachis tissue, ten each from pathogen and mock inoculated spikes of wheat NILs was harvested at 72 hpi. Rachis nodes of inoculated spikelet along with one internode above were cut using a scalpel and immediately frozen at -20^0 C. For cryo-sectioning, tissues were embedded in Shandon CRYOMATRIX (Richard-Allan Scientific, Kalamazoo, MI) just prior to sectioning at -25^0 C. Thin, 10 µm cross sections were cut using a cryotome (Leica, CM1850, Concord, Ontario) and collected on glass slides. Sections were washed with distilled water for 2 min, stained with Neu's reagent (1% 2-amino ethyl diphenyl borinate (Sigma Aldrich) in absolute methanol) for 5 min and mounted in 15% glycerol (Alemanno et al., 2003). The cross sections of ten rachis for each treatment with at least five sections from each rachis were observed under confocal microscope (Nikon, Eclipse E800, USA) for chemi-fluorescence. Fluorescence of HCAAs was observed with blue laser diode excitation at 405 nm fitted with emission filter HQ442/45. Fluorescence of flavonoids was observed with Argon excitation filter (488 nm) and emission filter HQ 515/30.

3.3.8 Protein extraction and shotgun proteomic analysis

The residual tissue after metabolite extraction from pathogen and mock inoculated rachises was used for protein extraction. Total protein was extracted using plant total protein extraction kit (PE0330, Sigma Aldrich, USA) supplied with protease inhibitor. Two milligrams of protein was digested in trypsin solution (6 ng/µl) (Promega, QC, Canada) at 58^0C for 1 h and peptides were extracted using the extraction buffer (1% formic acid/50% ACN) and dried using vacuum centrifuge.

3.3.9 LC-hybrid MS analysis of tryptic peptides

Peptide extracts were re-solubilized in 0.2% formic acid and analysed using LC-nESI-LTQ-Orbitrap (Thermo Fisher, Waltham, MA) fitted with a C18 Jupiter column (Phenomenex, CA, USA) installed on the nanoLC-2D system (Eksigent, Florida, USA)

(Cloutier et al., 2009). LC-hybrid MS data acquisition was accomplished using a four scan event cycle comprised of a full scan MS for scan event 1 acquired in the Orbitrap. The mass resolution for MS was set to 30,000 (at *m/z* 400) and used to trigger the three additional MS/MS events acquired in parallel in the linear ion trap for the top three most intense ions. The full MS scan range was divided into 2 smaller scan ranges (300–700 and 700-2000 Da) to improve dynamic range. The data dependent scan events used a maximum ion fill time of 100 ms and 1 microscan to increase the duty cycle for ion detection. Target ions already selected for MS/MS were dynamically excluded for 15 s.

3.3.10 Protein identification and quantification

Shotgun proteome profiling data were analyzed using MASCOT (Matrix Science, London, UK; version 2.2.04). MASCOT was set to search the nr_20101214 database (selected for Viridiplantae, 848476 entries as of 12 March 2012). Trypsin was used as the enzyme allowing for up to 2 missed cleavages. The mass tolerances for precursor ion and fragment ions were set to 15 ppm and 0.6 Da, respectively. Carbamidomethyl and oxidation of methionine were allowed as variable modifications. Scaffold (version Scaffold 3.3.1, Proteome Software Inc., Portland, OR) was used to validate MS/MS based peptide and protein identifications. Peptide identifications were accepted if they exceeded MASCOT threshold level of 20. Proteins that contained similar peptides and could not be differentiated based on MS/MS analysis alone were grouped to satisfy the principles of parsimony. Peptide and proteins were identified with >95.0% probability and proteins identified with at least 2 identified peptides were retained.

Normalized spectral abundance factor (NSAF) (Paoletti et al., 2006) was used for the relative quantification and identification of resistance related induced (RRI= (RP>RM)> (SP>SM)) proteins, using student's *t* test. Three biological replicates were used for the analysis and each biological replicate consisted of 10 spikes collected from 5 different plants. Blast2GO was used to assign gene ontology (GO) terms and mapping on KEGG pathways. Proteins were also searched in AgBase (Mississippi State University) and Plant protein database (PPDB, http://ppdb.tc.cornell.edu/) for GO association.

3.3.11 Quantitative real-time PCR of hydroxycinnamoyl transferase

Total RNA was extracted from five biological replicates (10 rachis collected from 5 plants for each replicate) using RNeasy Plant mini kit (Quiagen) and treated with DNase I (Quiagen). Purified RNA (500 ng from each sample) was reverse transcribed using iScript cDNA synthesis kit (BioRad, ON, Canada). Two microliters of 40x-diluted cDNA was used in a quantitative real-time PCR (qPCR) reaction using iQ SYBR Green Supermix (BioRad) in an CFX384TM Real-Time System (BioRad, ON, Canada). Dilution series were used for relative quantification, normalized to the mRNA abundance of housekeeping gene, actin. Primers used for actin and agmatine coumaroyl transferase were as below:

GENBANK ID	Gene name	Forward primer	Reverse primer
AY234333.1	*TaACT*	CATCCTGCTACCGTCCTTC	GGAGCTAGTCGAGGGTGTAG
AB181991.1	*Actin*	CCGGCATTGTCCACATGAA	CCAAAAGGAAAAGCTGAACCG

3.4 RESULTS

3.4.1 FHB disease severity of NILs

FHB disease severity on NILs with resistant and susceptible alleles of *Fhb1* was assessed following point inoculation of a pair of middle spikelets with spores of *F. graminearum*. Dark brown discoloration of inoculated spikelets was observed at 3 days post inoculation (dpi) in both resistant and susceptible NILs. By 9 dpi, the non-inoculated spikelets above and below the point of inoculation were bleached and started drying up (Fig. 3.1). Both dark brown and bleached spikelets were considered diseased. Discoloration of spikelets was more rapid towards the tip than towards the base of the spikelets. Area under disease progress curve (AUDPC) calculated based on the proportion of spikelets diseased was highest in NIL-S (AUDPC= 10.45) significantly (P<0.001) differing from NIL-R (AUDPC = 6.08).

3.4.2 Differential metabolic profiles of wheat NILs with resistant and susceptible *Fhb1* alleles

Non-target metabolic profiling of rachis and spikelets of two NILs with resistant and susceptible alleles of *Fhb1* inoculated with *F. graminearum* and water (mock) produced several significant metabolites. Initially, we examined constitutive metabolites, using only the mock inoculated NIL-R and NIL-S. In rachises, 271 metabolites were differentially accumulated between NILs and 235 had higher abundance in NIL-R. The latter were designated as the resistance related constitutive (RRC) metabolites (Table 3.1, 3.2 & Appendix 3.1). In spikelets, only 123 metabolites were differentially accumulated between NILs, of these 71 metabolites were classified as RRC metabolites (Table 3.1, 3.2 & Appendix 3.2).

Following *F. graminearum* inoculation, 1309 metabolites were differentially accumulated in rachises of either NIL-R or NIL-S (Fig.3.2). The metabolites either induced only in NIL-R (qualitative) or induced at greater abundance in NIL-R were designated as RRI metabolites. In rachises, 473 metabolites were classified as RRI, including 314 induced only in NIL-R. In spikelets, 2412 metabolites were differentially accumulated in either of the NILs, of which 340 were classified as RRI metabolites, including 109 induced only in NIL-R (Fig. 3.2). Comparatively, more resistance related (RR) metabolites were detected in rachises than in spikelets.

A data dimension reduction technique, canonical discriminant analysis, was applied to classify the treatment effects based on metabolites (Hamzehzarghani et al., 2008). In rachises, 672 differentially accumulated metabolites, present in all the four treatments (excluding qualitative metabolites), were subjected to canonical discriminant analysis. The CAN1 vector explained 78.5 % variance and identified the constitutive resistance function, discriminating the NIL-R from NIL-S. The CAN2 vector explained 18.8 % variance, and it identified the pathogenesis function, discriminating the pathogen inoculation from mock inoculation (Fig. 3.3a). In spikelets, 693 metabolites were subjected to canonical discriminant analysis. The CAN1 vector failed to explain any resistance function, whereas the CAN2 explained 37.87% variance, and it partially

identified the resistance function by discriminating the resistant NIL from the susceptible NIL (Fig. 3.3b).

3.4.3 Resistance related constitutive (RRC) metabolites associated with *Fhb1*

Out of 235 RRC metabolites in rachises, 19 metabolites were putatively identified by accurate mass match (Table 3.1, 3.2 & Appendix 3.1). The identified metabolites were sinapic acid, 11 flavonoids, and two lignans of phenylpropanoid pathway, three fatty acids and one terpenoid. In spikelets, 10 of the 109 RRC metabolites were putatively identified. Of that, seven belonged to phenylpropanoid pathway (Table 3.1, 3.2 & Appendix 3.1 and 3.2).

3.4.4 Resistance related induced (RRI) metabolites associated with *Fhb1*

Among 473 metabolites classified as RRI in rachises, 68 were putatively identified and the identities of the most significant metabolites were confirmed based on fragmentation patterns using LC-LTQ-Orbitrap (Table 3.1, 3.2 & Appendix 3.1). Thirty three of the identified metabolites belonged to phenylpropanoid pathway, including 9 hydroxycinnamic acid amides (HCAAs), seven flavonoids and four phenolic glycosides that are known to be involved in cell wall strengthening. The HCAAs, especially *p*-coumaroylputrescine, feruloylputrescine, cis-p-coumaroylagmatine, cinnamoylserotonin, feruloylagmatine, *p*-coumaroylserotonin and feruloylserotonin, were induced only in NIL-R (qualitative). Similarly, among the seven identified flavonoids five (5,6-dimethoxyflavone, 2-hydroxyisoflavanone naringenin, naringenin 7-O-β-D-glucoside, 5-hydroxy-7,8-dimethoxyflavanone 5-rhamnoside and kaempferol 3-rhamnoside-7-xylosyl-(1->2)-rhamnoside) were induced only in NIL-R. In addition, glycosides of caffeic acid, ferulic acid, sinapic acid and coniferyl alcohol were induced in NIL-R. Other significant RRI metabolites detected in rachises were S-adenosylmethionine and homocysteine of cysteine and methionine metabolism, fatty acids, terpenoids and alkaloids. The several fold increase of HCAAs, flavonoids and glycosides of phenolic compounds led to the hypothesis that *Fhb1* might mainly regulate phenylpropanoid pathway.

In spikelets, 346 metabolites were classified as RRI metabolites, of which 47 were putatively identified (Table 3.1, 3.2 & Appendix 3.2). Twenty five of these RRI

metabolites belonged to the phenylpropanoid pathway, including 11 flavonoids, 4 HACAAs, and 3 lignans. Hydroxycinnamic acid amides, *cis*-*p*-coumaroylagmatine, caffeoylserotonin and feruloylserotonin were detected only in NIL-R. Six glycerophospholipids involved in wax biosynthesis and deposited at the cuticle were detected only in spikelets and might play a significant role in type I resistance.

The necrotropic plant signaling molecule jasmonic acid was detected as a RRI metabolite in both rachises and spikelets. However, the amino acid conjugates of jasmonic acid: (+)-7-iso-jasmonoyl-L-isoleucine and jasmonoyl valine were detected only in rachises. Biotrophic plant defense signaling molecule, salicylic acid and its glucoside were detected only in rachises.

3.4.5 Resistance indicator (RI) metabolites induced following pathogen stress

F. graminearum produces DON during infection and host detoxifies DON by glycosylating DON to D3G. These two metabolites were defined as resistance indicator (RI) metabolites (Bollina et al., 2011). Both DON and D3G were quantified using standard curves. The total amount of DON produced (TDP=DON + D3G) was lower (1.57 mg kg^{-1}) in rachises than in spikelets (23.84 mg kg^{-1}) (Table 3.3, Fig. 3.4a). Conversely, the proportion of DON converted to D3G was higher in rachises (PDC = 0.39) than in spikelets (Table 3.3), meaning the proportion of DON conversion was higher at lower concentrations of TDP (Fig. 3.4b). However, the amount of DON, TDP, D3G or proportion of DON converted to D3G (PDC) were not significantly different between the NIL-R and NIL-S (Table 3.3).

3.4.6 Histo-chemical localization of HCAAs and flavonoids

Following pathogen inoculation, several HCAAs and flavonoids were either induced only in the rachis of NIL-R (qualitative) or the fold change in induction was much greater than in rachis of NIL-S. To confirm the deposition of HCAA and flavonoids at cell walls, a histo-chemical staining technique was used to visualize the location of these metabolites. Thickening of xylem and surrounding sclerified cell walls, especially of the meta-xylem cells was observed following *F. graminearum* inoculation. Deposition of HCAAs (blue fluorescence) and flavonoids (yellow fluorescence) were greater in pathogen treated NIL-

R cells than in mock treated NIL-R and pathogen or mock treated NIL-S (Fig. 3.5). Blue and yellow fluorescence due to accumulation of HCAAs and flavonoids was detected in phloem cells also. However, significant variation in the fluorescence at phloem cells was not observed between NILs. This further confirmed that the mechanism of resistance in rachis of NIL-R is mainly due to deposition of HCAAs and flavonoids.

3.4.7 *Fhb1* specific differential expression of proteins

Metabolomics of rachises revealed qualitative and quantitative accumulation of several metabolites following pathogen inoculation. Hence, a shotgun proteomic profiling of proteins isolated from rachises was done to further characterize the resistance mechanisms governed by *Fhb1*. 512 non-redundant proteins were identified, with 0.1 % protein false discovery rate (FDR) and1.1 % peptide FDR, from 30193 spectra in *F. graminearum* or mock inoculated two wheat NILs with alternative alleles of *Fhb1*. Thw very low FDR suggests that sufficient stringency was allowed for protein identification with at least 2 peptides/protein, >95% peptide accuracy and >99% protein accuracy. 172 proteins induced upon *F. graminearum* inoculation were identified in either of the NILs. Among these, 104 proteins were identified as RRI proteins, including 13 proteins induced only in NIL-R (Appendix 3.3).

3.4.6.1 Resistance related induced (RRI) proteins

The 104 proteins classified here as RRI proteins in rachises were characterized according to their role in biological process in plant system (Fig. 3.6). More than 50 % of the RRI proteins identified here were known to be induced in response to biotic or abiotic stresses, endogenous stimulus and signal transduction, including four pathogenesis related (PR) proteins: PR-1, β-1,3- glucanases (PR-2), chitinases (PR-3) and PR-10. Thirteen proteins were related to cell death that might have been induced as an early response to necrotrophs. A total of 61 RRI proteins were mapped onto different metabolic pathways, based on KEGG (Appendix 3.3). Consistent with our metabolomics data, enzymes of cysteine and methionine metabolism: MetSyn, SAMS, MTHFR and SAHH that increase the metabolic flux towards ethylene and phenylpropanoid biosynthesis were up regulated in NIL-R. In parallel, a few phenylpropanoid pathway

enzymes, such as COMT, CCoAMT, CAD, peroxidases and FMT that are involved in lignin and flavonoid biosynthesis pathway were also significantly induced higher in Nil-R than NIL-S (Table 3.4). Hydroxycinnamoyl transferases (*HCT*) that are involved in HCAA biosynthesis were detected at low stringency of 80 % protein identification probability and one peptide per protein. Hence, differential gene expression of *HCT* was studies by quantitative RT-PCR of one othe *HCT*s, *T. aestivum* agmatine counaroyl transferase (*TaACT*), was conducted. The gene expression of *TaACT* was significantly higher in the rachis of pathogen treated NIL-R than in NIL-S (Fig. 3.7).

3.5 DISCUSSION

Molecular marker based technology has been used to identify and introgress disease resistance QTLs to improve resistance against biotic stresses in elite cultivars. More than 100 FHB resistant QTLs have been identified in wheat, but the host defense mechanisms associated with them is largely unknown, except partially for the *Fhb1*. An integrated metabolomics and proteomics approach was used to explain the mechanisms of resistance associated with *Fhb1*, using NILs with minimum background effect derived from wheat genotype Nyubai. This study reports several RR metabolites in wheat, with confirmative identification, including *in-planta* metabolite MS/MS fragmentation based on a high resolution LC-MS, LTQ-Orbitrap (Appendix 3.1 and 3.2). The RR metabolites and proteins were mapped to metabolic pathways (Fig. 3.8, 3.9 and 3.10). Based on the identified metabolites and proteins, the plausible biochemical mechanisms of resistance against FHB, specific to the QTL *Fhb1* derived from Nyubai are discussed below.

3.5.1 *Fhb1* is associated with secondary cell wall thickening

After initial colonization of a spikelet, *F. graminearum* spreads to other spikelets through the cortical cells and vasculature of the rachis (Brown et al., 2010). Wheat resists the spread of *F. graminearum* by induced chemical defenses such as cell wall thickening and biotransformation of DON to less toxic D3G (Walter et al., 2010). Here, we provide compelling evidence that reduced spread of the pathogen through rachis in NIL with resistant *Fhb1* allele is mainly due to strengthening of rachis cell walls through deposition of HCAAs, flavonoids and phenolic glycosides that are synthesized via a

shunt phenylpropanoid metabolism. Activation of phenylpropanoid pathway following *F. graminearum* inoculation was evident with up regulation of enzymes of methionine metabolism (Table 3.4) that increase metabolic flux towards phenylpropanoid biosynthesis and also enzymes of phenylpropanoid pathway. Methionine is a precursor for SAM biosynthesized by SAM synthase. SAM as a methylgroup donor is needed for the biosynthesis of phenylpropanoids, leading to increased cell wall appositions in wheat leaves following infection by powdery mildew pathogen, *Blumeria graminis* (Bhuiyan et al., 2007). In our study, key phenylpropanoid enzymes such as COMT, CCoAMT, CAD, peroxidases and FMT were up-regulated in NIL-R. The biochemical pathways of cell wall thickening are complex and are discussed below.

3.5.1.1 Cell wall thickening due to deposition of HCAAs and flavonoids

Most strikingly, HCAAs of putrescine, tyramine, agmatine and serotonin were highly induced following pathogen inoculation in the resistant but not in the susceptible NIL. These HCAAs act as phytoalexins and also deposited to strengthen cell walls. They are synthesized in a shunt phenylpropanoid pathway (Fig. 3.8) by the condensation of hydroxycinnamoyl-CoA thioesters of the phenylpropanoid pathway with aromatic amines such as serotonin, agmatine, putrescine, spermine, spermidine and tyramine, by amine specific hydroxycinnamoyltransferases (Bassard et al., 2010, Edreva et al., 2007, Facchini et al., 2002). Hydroxycinnamoyl moieties of HCAAs cross link with polysaccharides, lignin and suberin of the cell wall by etheric linkage and are deposited as cell wall appositions at the inner side of plant cell walls (Buanafina de O, 2009). Thickening of the xylem and surrounding cells rachis of NIL-R was confirmed in our study based on HCAA specific fluorescence using confocal microscopy (Fig.3.5a). Furthermore, the up regulation of transcript expression of agmatine coumaroyltransferase, involved in the biosynthesis of *p*-coumaroyl agmatine, was also proved based on quantitative real time PCR (Fig. 3.7). The QTL *Fhb1* is physically mapped on the contig *ctg0954* which carries 41 genes (Choulet et al., 2010). One of the hypothetical proteins on *ctg0954* (GenBank: *CBH32656.1*) has a functional domain of N-hydroxycinnamoyl/benzoyltransferase (searched using PSI-BLAST). It is possible that *Fhb1* mainly codes for the hydroxycinnamoyl transferases (*HCT*) involved in HCAA

biosynthesis. Cross linkage of different polymers at the cell wall increases its rigidity and confers resistance to physical, chemical and enzymatic breakdown by pathogens (Grabber et al., 1998, Matern et al., 1995). In previous reports, HCAAs: feruloyl-3'-methoxytyramine, feruloyltyramine, and *p*-coumaroyltyramine were detected in cell walls of epidermal onion cells at the sites of *Botrytis allii* penetration (McLusky et al., 1999). Similarly, serotonin and its hydroxycinnamic acid amides, *p*-coumarylserotonin and feruloylserotonin accumulated in *Bipolaris oryzae* infected leaves of rice (Ishihara et al., 2008). It is possible that cell wall thickening also occurs in spikelets, as three hydroxycinnamic acid amides (*cis*-*p*-coumaroylagmatine, caffeoylserotonin and feruloylserotonin) were detected in spikelets of only in NIL-R but not in NIL-S. However, *HCT* as *Fhb1* candidate gene is ambiguous as more than one *HCT* is involved in HCAA biosynthesis.

Deposition of glycosylated isoflavonoids in rachises was also higher in the resistant than in the susceptible NIL. Flavonoids were also localized to the cell walls of xylem cells and their surrounding cells in NIL-R (Fig.3.5b). Seven genes encoding different classes of glycosyltransferases were identified in *ctg0954* (Choulet et al., 2010). These glycosyltransferases might catalyze the biosynthesis of glycosides including flavonoid glucosides. Isoflavonoids confer durability, longevity, and resistance to the heartwoods of many tree species against wood-rotting fungi (Gang et al., 1999).

3.5.1.2 Accumulation of phenolic glucosides and altered lignin biosynthesis pathway in wheat

Following pathogen inoculation, phenolic acid glucosides such as β-D-glucopyranosyl-caffeic acid, β -D-glucopyranosyl-sinapic acid and ferulic acid 7-*O*-glucoside were induced in the resistant but not in the susceptible NIL. In transgenic *Populus tremuloides*, down regulation of 4-coumaroyl ligase increased accumulation of phenolic acid glucosides of *p*-coumaric, ferulic, and sinapic acids and decreased total lignin content, but the syringyl/guaiacyl lignin ratio remained unchanged in the xylem tissue (Suzuki et al., 2010). Likewise, we detected high fold changes in abundance of the sinapyl alcohol precursor, sinapaldehyde (RRI, FC= 2.2) and sinapyl alcohol glucoside, syringin (RRI, FC=1.9) in rachises of resistant NIL with no significant change in coniferyl alcohol

related metabolites that may lead to increased syringyl/guaiacyl lignin ratio. The monolignols syringin and coniferin are stored and transported as phenolic glucosides in plant tissues (Boerjan et al., 2003). A class of UDP-glycosyltransferases (Lim et al., 2005), along with β-glucosidase, regulate the storage and mobilization of monolignols for lignin biosynthesis (Dharmawardhana et al., 1995). High syringyl/guaiacyl lignin ratio enhanced the resistance to wheat powdery mildew (Menden et al., 2007). However, a specific role of glycosyltransferases present on *ctg0954* and their substrate specificity in catalyzing formation of phenolic and flavonoid glucosides need to be studied.

3.5.2 DON resistance is not a major mechanism of FHB resistance associated with Nyubai alleles of *Fhb1*

In the present study, neither total DON produced (TDP) nor did the proportion of DON conversion to D3G (PDC) significantly varied between the resistant and susceptible NILs at 72 hpi, in both spikelets and rachises. Hence, the resistance governed by *Fhb1*, derived from Nyubai, is not due to DON detoxification by DON-3-*O*-glucosyltransferase. Similarly, no significant difference in DON accumulation was observed between resistant and susceptible NILs of wheat with *Fhb1* derived from Sumai-3 X Stoa (Jia et al., 2009). However, the conversion of DON to D3G was associated with recombinant inbred populations containing *Fhb1* of the wheat double haploid lines, originating from the cross Sumai-3 and Thornbird (Lemmens et al., 2005). An average PDC of 0.39 in rachis of NIL-R were observed here but it was not significantly different from NIL-S (PDC=0.32). In barley, the resistant genotypes had up to PDC=0.6 at 72 hpi, and these were significantly higher than in a susceptible genotype (Kumaraswamy et al., 2011). Other mechanisms reported *in vitro* for DON detoxification is DON-glutathione conjugation (Gardiner et al., 2010). Although two glutathione S-transferases were significantly induced in NIL-R (Appendix 3.3), we did not detect DON-glutathione conjugates in the metabolites.

3.5.3 Plant defense signaling and oxidative stress response

For the first time we report, the possible role of jasmonic acid signaling in type II FHB resistance in rachises. Along with jasmonic acid, a biologically active form of

jasmonates, (+)-7-iso-jasmonoyl-L-isoleucine, was accumulated in greater abundance in NIL-R. (+)-7-iso-jasmonoyl-L-isoleucine is considered to be the bioactive jasmonate biosynthesized by amino acid synthetase (*JAR1*) (Staswick and Tiryaki, 2004). Jasmonic acid elicits several disease resistance related genes involved in biosynthesis of systemin (Li et al., 2002), defensin (Penninckx et al., 1996), and lignin (Xue et al., 2008) and the terpenoid indole alkaloid biosynthesis pathway (Wei, 2010). We detected monoterpenoids: iridotrial glucoside and loganin, and indole alkaloids: 16-epivellosimine and vomilenine which have antimicrobial properties. In wheat, plant defense signaling occurs in a sequential cascade, with Ca^{2+} and salicylic acid signaling active during early infection, followed by ethylene signaling and jasmonic acid signaling (Ding et al., 2011). Jasmonic acid signaling was also reported in barley inoculated with trichothecene producing but not with non-producing mutant *Fusarium* isolates (Kumaraswamy et al., 2011). It is possible that in our study in the *Fusarium* inoculated NIL-R, DON induces ethylene and jasmonic acid signaling, which in turn activates the biosynthesis of HCAAs. Ethylene non-producing mutants of *Arabidopsis* were unable to produce hydroxycinnamic acid amides following inoculation with *Botrytis cinerea* (Lloyd et al., 2011). SAM, synthesized by SAMS and a precursor of ethylene, is a methylgroup donor for the phenylpropanoid pathway; the expression of SAMS was greater in NIL-R than in NIL-S. It is possible that cell wall thickening we observed may be mainly due to ethylene and jasmonic acid signaling leading to the production of HCAAs. Necrotrophs induce hydrogen peroxide production and kill host tissue. In response, plants neutralize the reactive oxygen species by counteracting them. Manganese superoxide dismutase, ascorbate peroxidase and glutathione transferase were significantly induced in NIL-R as a general response to pathogen invasion (Table 3.4). Superoxide dismutase neutralizes the free radicals and further the hydrogen peroxide generated by neutralization will be removed by catalase or ascorbate peroxidase (Chen et al., 1997).

In this study, based on non-target metabolomics using LC-hybrid MS, we have provided evidence that the resistance in *Fhb1* derived from Nyubai is not due to the detoxification of the aggressiveness factor DON by glucosyltransferase to D3G. Instead, we provide strong evidence for involvement of hydroxycinnamic acid amides and lignin monomers

in the formation of cell wall appositions, which play a significant role in restricting the movement of *F. graminearum* in the rachises of NIL with FHB resistance at *Fhb1*. However, *HCT* as an *Fhb1* candidate gene has to be validated in different FHB resistant sources. Integrated non-target metabolomics and proteomics technologies using LC-hybrid MS can be applied to elucidate the mechanisms of resistance in more than 100 FHB resistance QTLs identified in wheat and barley. This technology can be adapted to prove the mechanisms of resistance in plants to other biotic stresses. High throughput protocols such as high performance LC (HPLC) (Aldini et al., 2011), Fourier transform infrared spectroscopy (FTIR) (Cerretani et al., 2010) and near infrared spectroscopy (NIRS) (Zhang et al., 2008) can be developed to screen for several of the resistance related metabolites as biomarkers for resistance to FHB. Alternatively, specific RRI enzymes identified here can be further explored to enhance plant resistance to FHB.

Table 3.1: FHB resistance related metabolites contributing towards cell wall strengthening in rachis and spikelets of wheat NIL with resistant *Fhb1* allele upon *F. graminearum* or mock inoculation.

Observed mass (Da)	**Putative name[£]**	**Fold change[@]**	
		Rachis	**Spikelets**
Phenylpropanoids: Phenolics and Lignans			
148.0527	*trans*-Cinnamic acid	1.27*(RRI)	2.0* (RRI)
165.0797	L-Phenylalanine		1.56* (RRI)
208.0722	Sinapaldehyde	2.22*(RRI)	3.36* (RRI)
224.0700	Sinapic acid	2.6*(RRC)	
320.0888	4-Coumaroylshikimate	85.1*(PRr;***RRI***)	
338.0993	4-Coumaroylquinate	43.1*(PRr;***RRI***)	
342.1002	β-D-glucopyranosyl-caffeic acid	2.6*(RRI), 4.0*(PRr)	
342.1308	Coniferin	1.58*(RRI)	1.41* (RRI)
344.1458	Dihydroconiferyl alcohol glucoside	10**(PRr;***RRI***)	
356.1101	Ferulic acid 7-O-glucoside	28.7* (PRr;***RRI***)	
370.1265	Sinapaldehyde glucoside	93.1*(PRr;***RRI***)	1.14* (RRI)
372.1425	Syringin	1.92 *(RRI)	2.09* (RRI)
386.1210	β -D-glucopyranosyl-sinapic acid	2.8 * (RRI)	
398.1356	Deoxypodophyllotoxin	1.4*(RRI), 1.4*(RRC)	
550.2036	Medioresinol 4'-O-beta-D-glucopyranoside	1.6*(PRr;***RRI***)	
674.1447	Phyllanthusmin B	1.5*(RRC)	
686.2743	Secoisolariciresinol di-O-glucoside	1.46*(RRI)	

Phenylpropanoids: Hydroxycinnamic acid amides			
234.1367	*p*-Coumaroylputrescine	24.6** (PRr;***RRI***)	1.93* (RRI)
264.1473	Feruloylputrescine	407.8*(PRr;***RRI***)	
267.1268	Cinnamoyltyramine	262.8*(PRr;***RRI***)	
276.1584	*cis*-*p*-Coumaroylagmatine	44.3*(PRr;***RRI***)	41** (PRr;***RRI***)
306.1688	Feruloylagmatine	104.2 *(PRr;***RRI***)	
322.1321	p-Coumaroylserotonin	99.1*(PRr;***RRI***)	
338.1258	Caffeoylserotonin	2.45*(RRI)	16.1 *(PRr;***RRI***)
352.1421	Feruloylserotonin	1194.8*(PRr;***RRI***)	30.7* (PRr;***RRI***)
Phenylpropanoids: Flavonoids			
282.0887	5,6-Dimethoxyflavone	126.6*(PRr;***RRI***)	
288.0622	2-hydroxyisoflavanone naringenin	16.3*(PRr;***RRI***)	
434.1219	Naringenin 7-O-β-D-glucoside	23.7*(PRr;***RRI***)	1.83* (RRI)
446.1567	5-Hydroxy-7,8-dimethoxyflavanone 5-rhamnoside	74.4*(PRr;***RRI***)	
710.2085	Kaempferol 3-rhamnoside-7-xylosyl-(1->2)-rhamnoside	34.9*(PRr;***RRI***)	

£ Detailed compound identification is presented in Appendix 3.1 and 3.2

@ Fold change calculation: were based on relative intensity of metabolites, RRC= RM/SM, PRr= RP/RM, RRI= (RP/RM)/(SP/SM); PRr;***RRI*** = RP/RM, PRr fold change is reported for the metabolites detected only in NIL-R (qualitative) as the RRI fold change would be infinity;

***** *t* test significance at $P<0.05$, ****** *t* test significance at $P<0.01$, *** *t* test significance at $P<0.001$

NIL is Near isogenic line, Da: Daltons, RRC is Resistance related constitutive, RRI is Resistance related induced, PRr is Pathogenesis related metabolite detected in resistant NIL; RP is resistant NIL with pathogen inoculation, RM is resistant NIL with mock inoculation, SP is susceptible NIL with pathogen inoculation, SM is susceptible NIL with mock inoculation

Table 3.2: Putatively identified FHB resistance related metabolites, other than phenylpropanoids, in rachis and spikelets of resistant wheat NIL with *Fhb1* QTL upon *F. graminearum* or mock inoculation.

Observed mass (Da)	**Putative name[£]**	**Fold change[@]**	
		Rachis	**Spikelets**
Plant signaling molecules (Jasmonic acid biosynthesis)			
210.1255	Jasmonic acid	1.14**(RRI)	1.52* (RRI)
278.2257	α-Linolenate		2.79** (RRI)
280.2403	Linoleic acid	1.5*(RRC)	2.61* (RRI)
296.2351	9S-hydroxy-10E,12Z-octadecadienoic acid (9(S)-HODE)	1.6*(RRC)	
309.1935	Jasmonoyl-valine	79.1*(PRr;***RRI***)	
310.2138	13(S)-Hydroperoxylinolenic acid	1.5*(RRC)	
323.2093	(+)-7-iso-Jasmonoyl-L-isoleucine	1.76*(RRI)	1.82*(RRI)
Plant signaling molecules (Salicylic acid biosynthesis)			
138.0320	Salicylic acid	3.2*(PRr;***RRI***)	
300.0841	Salicylic acid 2-O-β-D-glucoside	1.03*(RRI)	
Terpenoids			
248.1419	Abscisic aldehyde	163.1*(PRr;***RRI***)	1.22* (RRI)
250.1568	Xanthoxin	2.68*(RRI)	
250.1568	Abscisic alcohol	2.67*(RRI)	
280.1309	8'-Hydroxyabscisate	529.4*(PRr;***RRI***)	
344.1471	Iridotrial glucoside		12.3* (PRr;***RRI***)
346.1260	Aucubin	2.6*(PRr;***RRI***)	

346.1261	Deutzioside	1.56*(RRI)	
360.1416	7-Deoxyloganate	1.4*(RRC)	1.30** (RRI)
390.1508	Loganin	1.70*(RRI)	
406.1467	10-Hydroxyloganin	1.01*(RRI)	
426.1881	Abscisic acid glucose ester	189.1*(PRr;***RRI***)	
Indole alkaloids			
292.1560	16-epivellosimine	35.3*(PRr;***RRI***)	
350.1636	Vomilenine	1054.4**(PRr;***RRI***)	8.21** (RRI)
Methionine biosynthesis			
384.1209	2-S-adenosyl-L-homocysteine	132.6*(PRr;***RRI***)	
399.1437	S-adenosyl-L-methionine	Inf*(***RRI***)	

£ Detailed compound identification is presented in Appendix 3.1 and 3.2

@ Fold change calculation: were based on relative intensity of metabolites, RRC= RM/SM, PRr= RP/RM, RRI= (RP/RM)/(SP/SM); PRr;***RRI*** = RP/RM, PRr fold change is reported for the metabolites detected only in NIL-R;

***** *t* test significance at $P<0.05$, ****** *t* test significance at $P<0.01$, *** *t* test significance at $P<0.001$

NIL= Near isogenic line, Da: Daltons, RRC = Resistance related constitutive, RRI = Resistance related induced, PRr=Pathogenesis related metabolite detected in resistant NIL; RP= resistant NIL with pathogen inoculation, RM= resistant NIL with mock inoculation, SP= susceptible NIL with pathogen inoculation, SM= susceptible NIL with mock inoculation

Table 3.3: DON & 3ADON accumulation and DON detoxification in wheat NILs[a] with contrasting alleles of *Fhb1,* inoculated with *F. graminearum*.

Metabolite	NIL-R			NIL-S		
	Rachis	**Spikelets**	***P* value[b]**	**Rachis**	**Spikelets**	***P* value[b]**
DON (mg kg $^{-1}$)	1.05	13.35	0.001	0.92	15.42	0.002
D3G (mg kg $^{-1}$)	0.84	6.15	0.01	0.66	8.42	0.009
TDP (mg kg $^{-1}$)	1.89	19.51	0.01	1.57	23.84	0.004
PDC (D3G/ TDP)	0.39	0.32	0.57	0.32	0.34	0.871

[a]There was no significant difference between NIL-R and NIL-S for any of the metabolites, but the spikelet metabolites were significantly different from rachis.

[b]*P* values were derived based on two way ANOVA

NIL-R=near isogenic line- resistant, NIL-S=near isogenic line- susceptible, DON = Deoxynivalenol, D3G = Deoxynivalenol-3-*O*-glucoside, TDP = Total DON produced (DON + D3G), PDC = Proportion of DON converted, 3ADON = 3 Acetyl

Table 3.4: Resistance related induced (RRI) proteins identified in wheat NIL with resistant and susceptible Fhb1 alleles derived from Nyubai inoculated with *F. graminearum*

gi number	Identified Proteins (512)	RRI fold change ($P<0.05$)
Cysteine and methionine metabolism		
585032	Cysteine synthase	1.90
162458737	Cysteine synthase precursor	14.67
50897038	Methionine synthase (MetSyn)	1.13
68655500	Methionine synthase 2 enzyme (MetSyn2)	1.14
115470493	Os07g0134800 (homologous to L-serine ammonia-lyase)	6.01
115589742	5,10-methylene-tetrahydrofolate reductase (MTHFR)	1.20
115589748	S-adenosylhomocysteine hydrolase (SAHH)	1.18
223635282	S-adenosylmethionine synthase 1 (SAMS1)	2.60
122220777	S-adenosylmethionine synthase 3 (SAMS 2)	1.99
Phenylpropanoid biosynthesis		
194268461	Chorismate synthase	1.67
298162735	Cinnamyl alcohol dehydrogenase (CAD)	1.26
126723796	Caffeoyl-CoA O-methyltransferase (CCoAMT)	7.00
30385246	Caffeic acid O-methyltransferase (COMT)	1.3
129806	Peroxidase 1	3.00
2759999	Peroxidase	1.86
57635161	Peroxidase 8	1.92
77818928	Flavonoid O-methyltransferase (FMT)	1.34

[@]RRI= (RP/RM)/(SP/SM). RP: resistant NIL with pathogen inoculation, RM: resistant NIL with mock inoculation, SP: susceptible NIL with pathogen inoculation, SM: susceptible NIL with mock inoculation.

Fig. 3.1: *Fusarium graminearum* infected spikes of wheat NILs with resistant and susceptible alleles of *Fhb1*, at 9 dpi and 21 dpi. Arrows indicate the sites of point inoculations, NIL-R=NIL with resistant allele of *Fhb1*, NIL-S= NIL with susceptible allele of *Fhb1*.

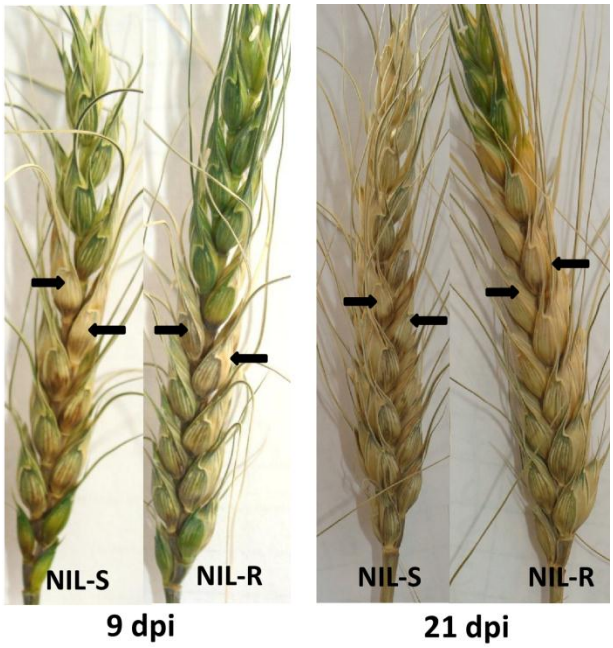

Fig. 3.2: Venn diagram of differentially accumulated metabolites (P<0.05) detected in wheat NILs with resistant and susceptible alleles of *Fhb1* upon *F. graminearum* or mock inoculation. Numbers in dotted circle= number of resistance related induced metabolites (RRI).

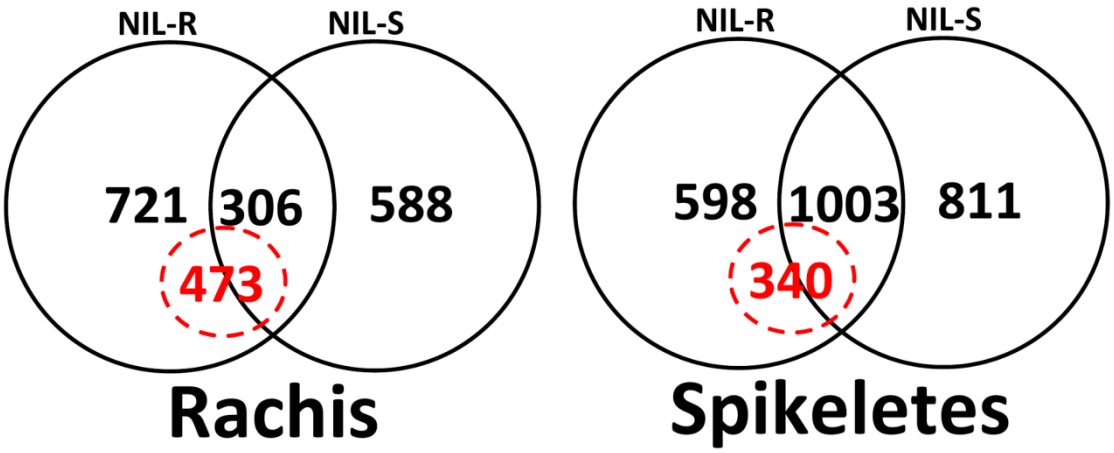

Fig. 3.3: Canonical discriminant analysis of significant (P <0.05) metabolites in: (a) rachises and (b) spikelets of wheat NILs with resistant and susceptible alleles of *Fhb1* upon *F. graminearum* or mock inoculation. Where, RP is *F. graminearum* inoculated NIL-R, RM is mock-inoculated NIL-R, SP is *F. graminearum* inoculated NIL-S, SM is mock-inoculated NIL-S.

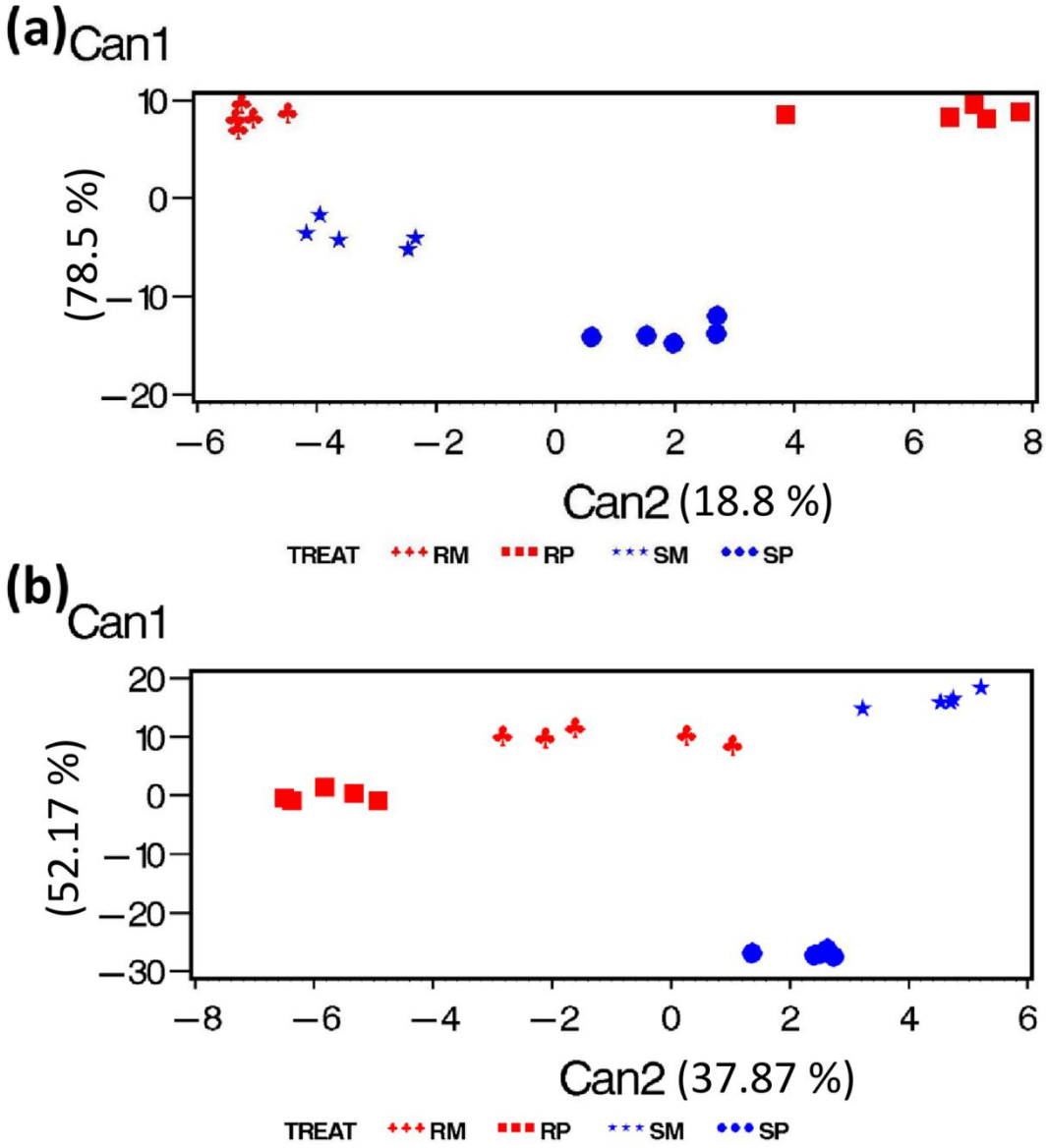

Fig. 3.4: Accumulation of resistance indicator (RI) metabolites in wheat NILs with resistant and susceptible alleles of *Fhb1* inoculated with *F. graminearum* (a) Accumulation of DON, 3ADON and D3G; (b) Regression models to predict proportion of total DON converted to D3G (PDC) as a function of total DON produced (TDP). Where, DON = deoxynivalenol, 3ADON = 3-acetyl-deoxynivalenol, D3G = DON-3-*O*-glucoside, TDP = total DON produced, PDC = proportion of DON converted to D3G.

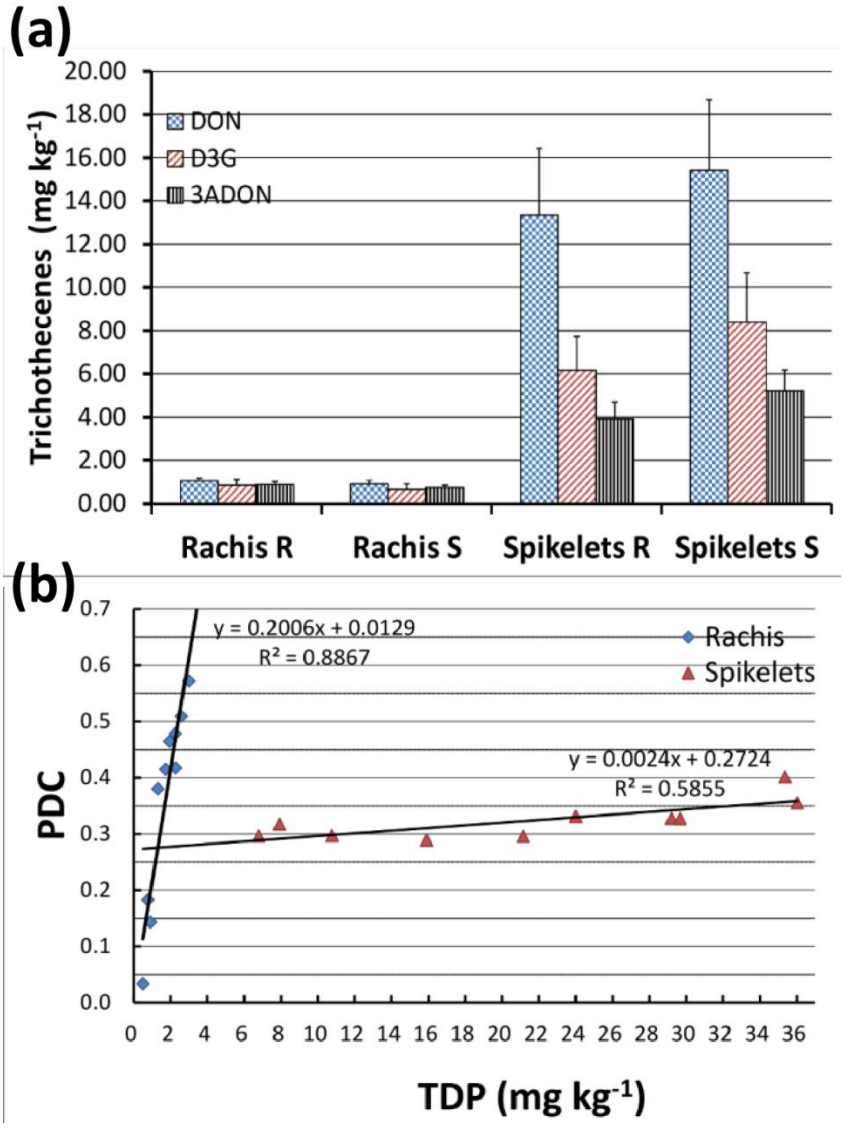

Fig. 3.5: Laser scanning confocal micrographs of rachis sections, exhibiting secondary cell wall thickening, due to: a) HCAAs (blue fluorescence) and b) flavonoids (yellow fluorescence). RP is resistant NIL with *F. graminearum* (pathogen) inoculation, RM is resistant NIL with mock inoculation, SP is susceptible NIL with *F. graminearum* inoculation, SM is susceptible NIL with mock inoculation, mx is meta xylem, px is protoxylem, ph is phloem, c is cortical cells.

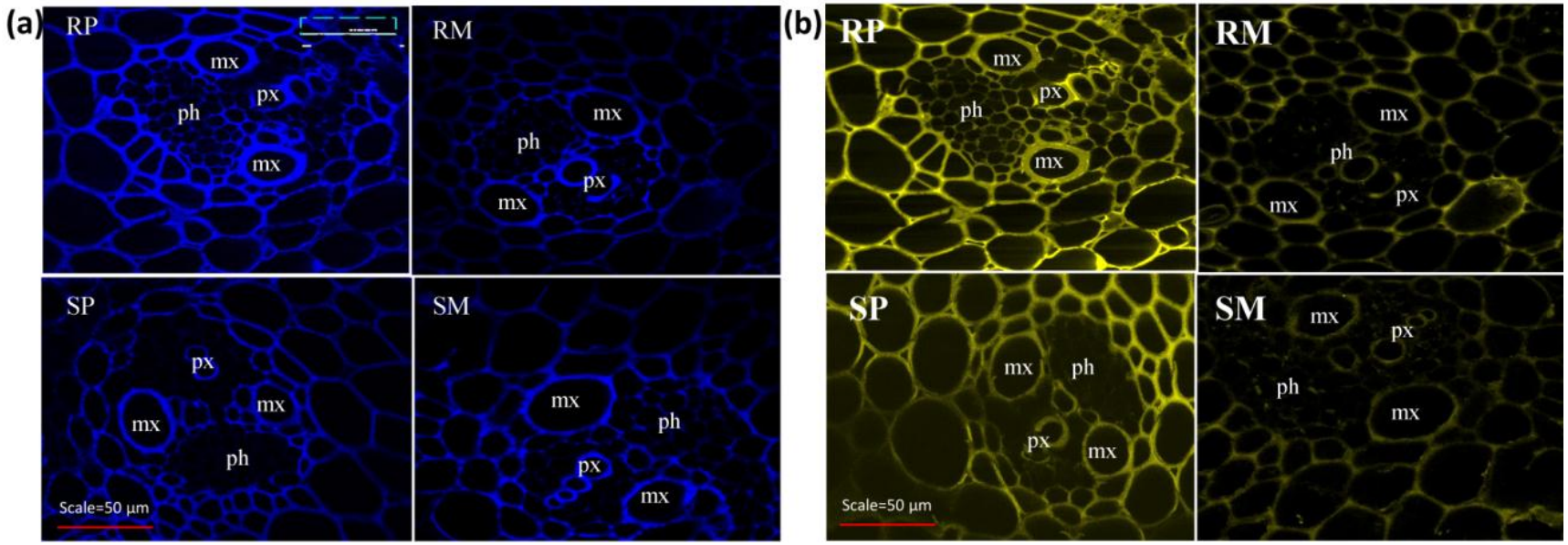

Fig. 3.6: Resistant related induced (RRI) proteins in wheat NIL with resistant *Fhb1*allele following *F. graminearum* inoculation.

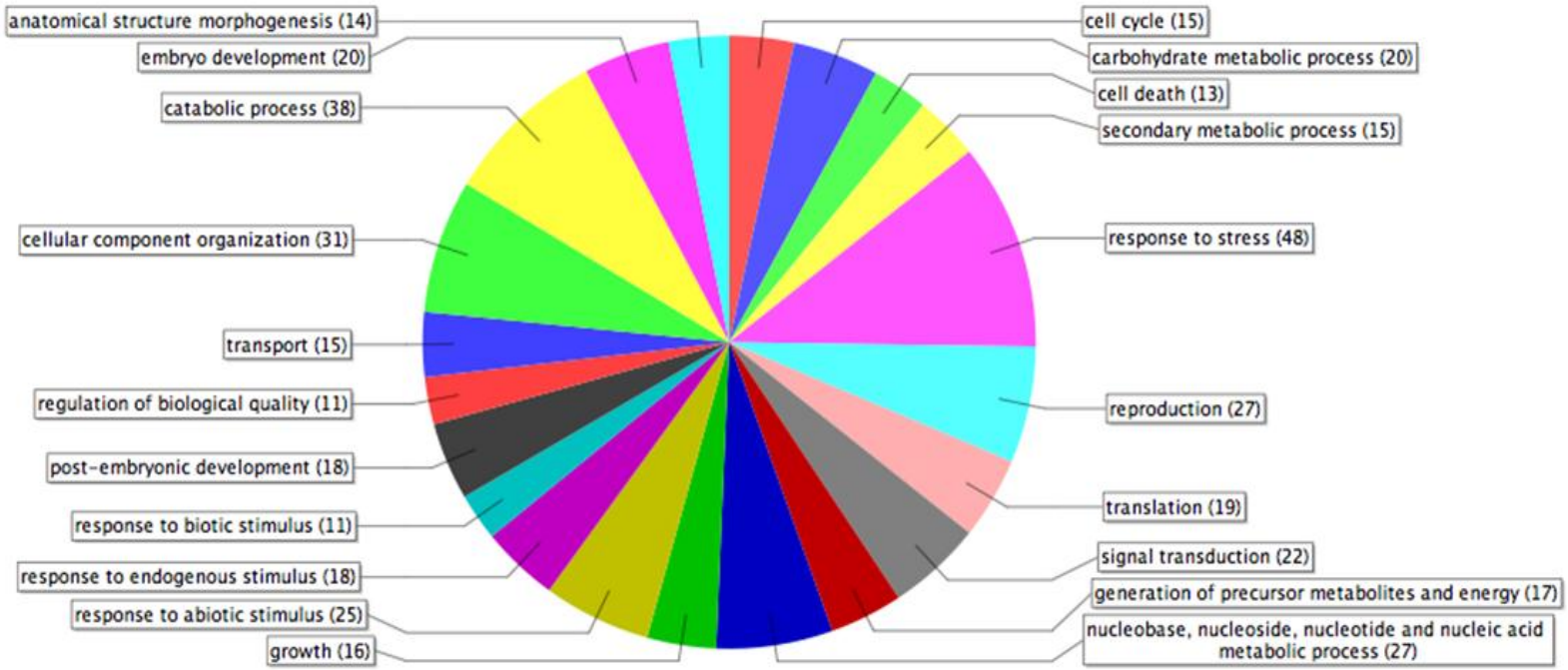

Figure 3.7: Relative transcript expression of *Triticum aestivum* agmatine coumaroyl transferase (*TaACT*) at 72 hpi in wheat NILs with resistant and susceptible alleles of *Fhb1* upon *F. graminearum* and mock inoculation. RP is resistant NIL with *F. graminearum* inoculation, RM is resistant NIL with mock inoculation, SP is susceptible NIL with *F. graminearum* inoculation, SM is susceptible NIL with mock inoculation.

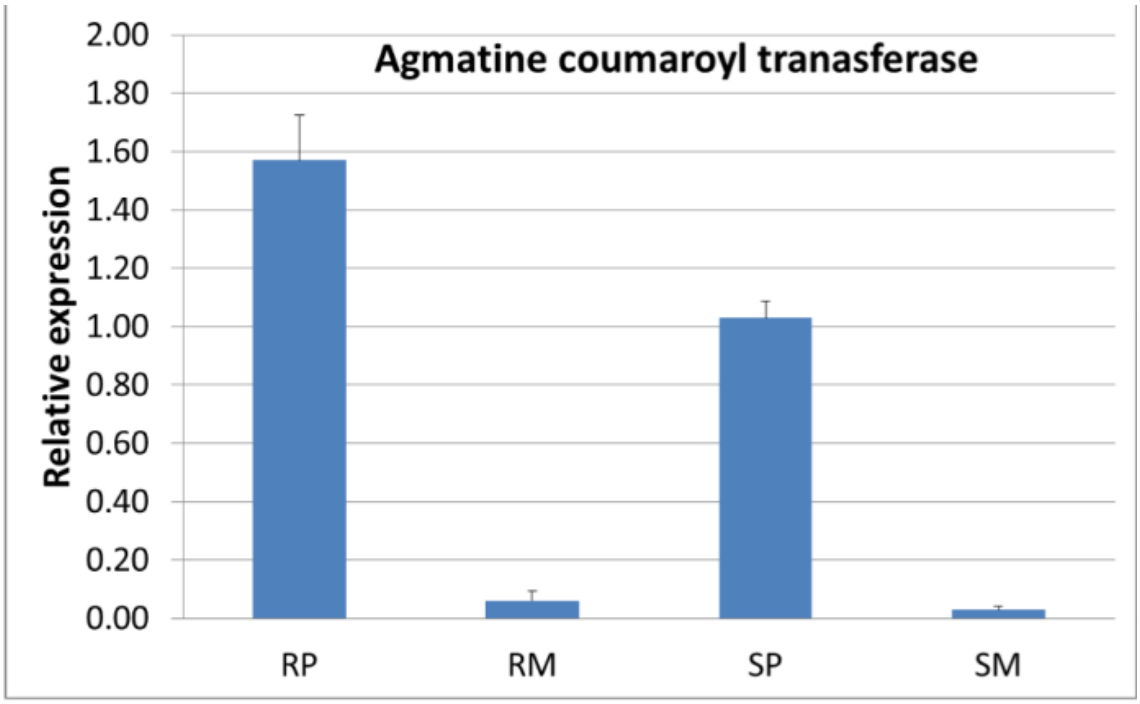

Fig. 3.8: *F. graminearum* induced phenylpropanoid pathway leading to secondary cell wall thickening in rachises of wheat NIL with resistant *Fhb1* allele (Compounds and enzymes in bold/red letters are detected in the study). Where, HCAA is hydroxycinnamic acid amides; PAL is phenylalanine ammonia lyase, 4CL is 4 coumaryl ligase, C4H is trans-cinnamate 4-monooxygenase, COMT is caffeic acid 3-*O*-methyltransferase, *HCT* is hydroxycinnamoyltransferase, C3H is coumaroylquinate(coumaroylshikimate) 3'-monooxygenase, CCR is cinnamoyl-CoA reductase, GT is glycosymethyl transferase.

Pathway adapted fromhttp://www.genome.jp/kegg-bin/show_pathway?ko00940+C00482

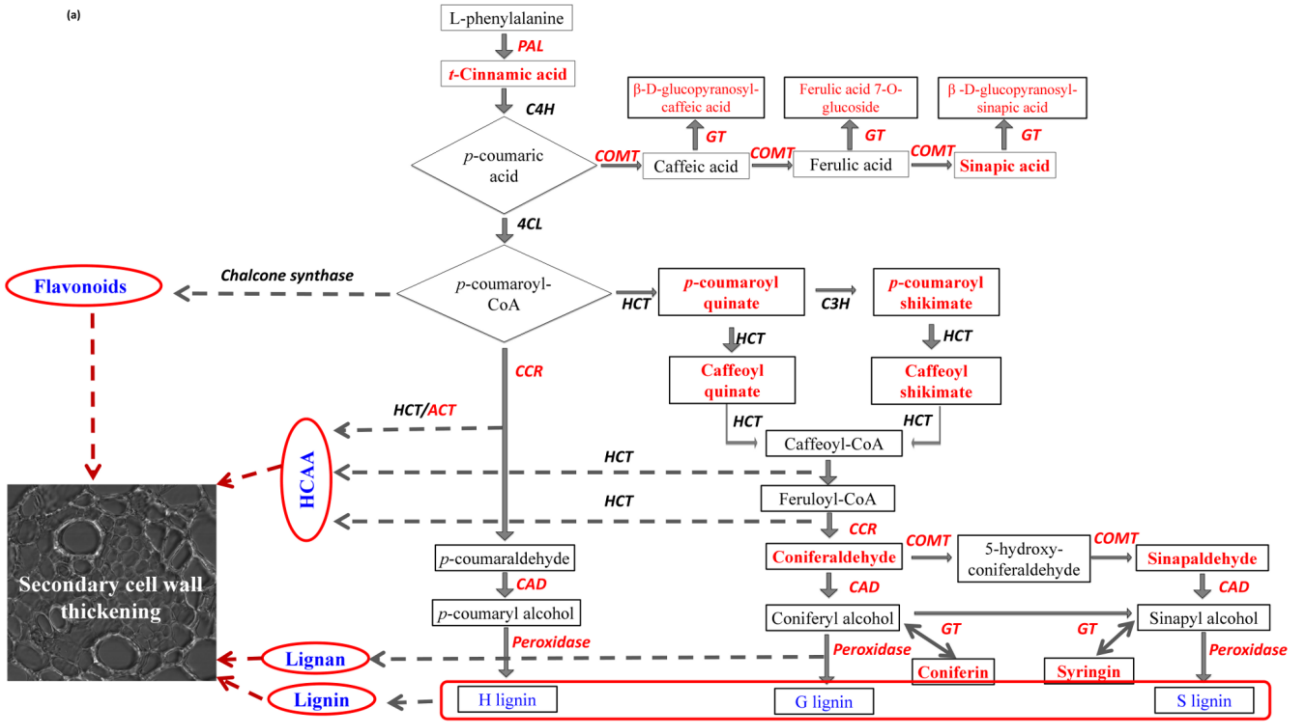

Fig. 3.9: *F. graminearum* induced shunt phenylpropanoid pathway showing the synthesis of hydroxycinnamic acid amides following the conjugation of amides synthesized from amino acids with hydroxycinnamic acid CoA thioesters (Compounds in bold/red letters are detected in the study). Pathway adapted from http://pmn.plantcyc.org/ARA/NEW-IMAGE?type=PATHWAY&object=PWY-5473, 5474, 40.

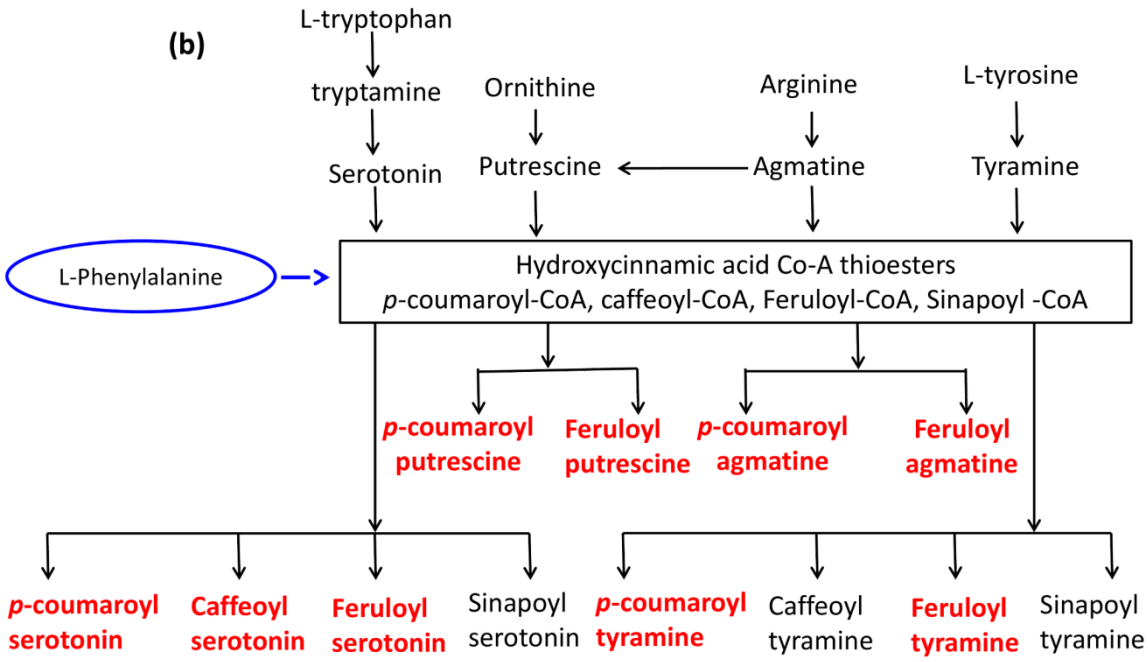

Fig. 3.10: Satellite metabolic pathways of wheat-*Fusarium* interaction

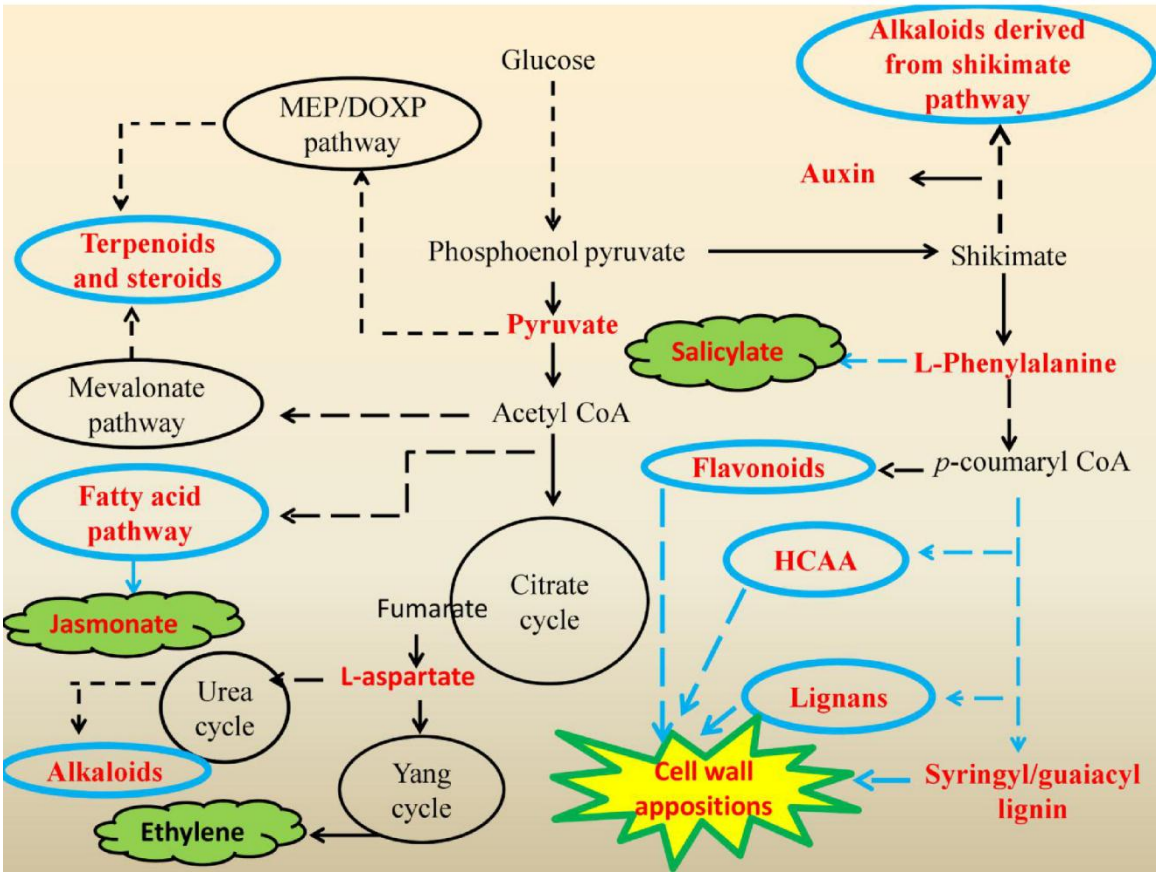

CONNECTING STATEMENT FOR CHAPTER IV

Chapter IV, is a manuscript entitled "Functional characterization of wheat Fusarium head blight QTL, *Fhb1* based on non-targeted metabolomics and targeted genomics" prepared by Raghavendra Gunnaiah and Kushalappa AC. The manuscript will be submitted to a peer reviewed scientific journal for publication.

In chapter III, non-targeted metabolome and proteome profiling of wheat NILs with resistant and susceptible *Fhb1* alleles, derived from a moderately resistant cultivar, revealed novel resistance mechanisms, at the rachis that were unknown before. *Fhb1* was associated with cell wall strengthening due to deposition of HCAAs, flavonoids and other phenylpropanoids. Cell wall strengthening can block the pathogen penetration into cells and provide partial resistance. However, a high DON accumulation bleached the un-infected spikelets even in NIL with resistant *Fhb1* alleles, leading to drying up of the entire spike. No significant difference in DON accumulation and DON detoxification were observed between the NILs (Gunnaiah et al., 2012). Contrastingly, *Fhb1* derived from CM8-2306 (a derivative of Sumai-3) was hypothesised to regulate DON detoxification by regulating the expression of DON detoxifying UDP-glycosyltransferase (Lemmens et al., 2005). It is also reported that, *Fhb1* behaves differently in different genetic backgrounds (Zhou et al., 2002). Apparently, in our previous study, *Fhb1* was under susceptible genome background, in which pathogen may have produced high DON, as there were less antioxidants to limit pathogen growth, which in turn may have reduced DON detoxification. Hence, the present study was planned to decipher the resistance mechanisms governed by *Fhb1* derived from Simai-3, under resistance genome background and validate deposition of HCAAs at the rachis in response to FHB incriminating *HCT* as *Fhb1* candidate gene. It was also hypothesized that, the efficient DON detoxification takes place at later stages of infection. So, rachis was also collected at both 3dpi and 7dpi to assess DON detoxification and host defense responses to spread.

CHAPTER IV

Functional characterization of wheat fusarium head blight QTL *Fhb1* based on non-targeted metabolomics and targeted genomics

Raghavendra Gunnaiah, Kushalappa A. C.,

Plant Science Department, McGill University, Ste. Anne de Bellevue, Quebec, Canada H9X3V9

4.1 ABSTRACT

Fusarium head blight (FHB) caused *Fusarium* spp. is a devastating disease of wheat and other cereal grains around the globe. The disease FHB causes severe economic damage through yield loss and contaminates grains with trichothecene mycotoxins. Deoxynivalenol (DON), a type B trichothecene, is a pathogen aggressiveness factor that facilitates lesion expansion within spikes of wheat. Breeding for FHB resistant cultivars is a viable and environmentally friendly option for FHB management. Host resistance to FHB is quantitatively inherited; more than 100 quantitative trait loci (QTL), governing resistance against initial infection, lesion expansion and DON have been identified. *Fhb1* is the largest effect and stably inherited QTL for resistance to lesion expansion, fine mapped as a single major gene. A non-targeted metabolic profiling of wheat near isogenic lines (NILs) with resistant and susceptible *Fhb1* alleles revealed the absence of glycerophospholipids in the susceptible NIL, due to degradation of membrane caused by programmed cell death (PCD). A non-functional *Fhb1* candidate gene calmodulin binding protein (*TaCaMBP_Fhb1*) rescues host cells from PCD in the resistant NIL. While a functional *TaCaMBP_Fhb1* in the susceptible NIL is induced by *F. graminearum*, trigger Ca^{2+} signalling by binding to Ca^{2+} bound calmodulin, and transcriptionally activate host endonucleases that cleave the host DNA, causing PCD. The necrotrophic pathogen *F. graminearum* feeds on the dead cells and facilitates pathogen progress in NIL-S. The proportion of DON detoxification, by the host UDP-glycosyltransferase, was moderately high in both the NILs, with no significant difference. The resistant *Fhb1* candidate gene *TaCaMBP_Fhb1* can be stacked into elite wheat cultivars to enhance FHB resistance.

4.2 INTRODUCTION

Fusarium head blight (FHB) of wheat, caused by *Fusarium* spp., reduces grain yield and contaminates grains with trichothecene mycotoxins leading to severe economic losses. Deoxynivalenol (DON), a type B trichothecene is acutely toxic to animals at low concentrations of less than 1 ppm (Pestka, 2007), and is also a pathogen aggressiveness factor for lesion expansion within spikes (Bai et al., 2002). Breeding for FHB resistance is considered a reliable and environmentally friendly approach to manage FHB. Host resistance to FHB is quantitatively inherited and more than 100 quantitative trait loci (QTL) have been mapped for FHB resistance to initial infection (type I), resistance to lesion expansion (pathogen colonization or spread within spike = type II) and resistance to DON (type III) on all of the wheat chromosomes, except 7D (Buerstmayr et al., 2009). Due to the complexity of the wheat genome and lack of complete genome sequence, host resistance mechanisms associated with these QTLs are largely unknown. Accordingly, they have not been effectively utilized in wheat breeding to enhance resistance through QTL pyramiding or gene stacking.

Fhb1 (*Qfhs.ndsu-3BS*), the most consistent and the largest effect FHB resistance QTL, is mapped to the short arm of chromosome 3B and can explain up to 60 % the phenotypic variance for resistance to disease spread, commonly referred as type II resistance (Cuthbert et al., 2006, Liu et al., 2006, Pumphrey et al., 2007, Waldron et al., 1999). Because of its substantial contribution to FHB resistance, significant efforts have been made to functionally characterise *Fhb1*. The locus for DON resistance (DON/ DON-*3-o*-glucoside (D3G)) was mapped to the same locus as *Fhb1* in doubled haploid mapping populations derived from the cross CM-82036 X Remus (Lemmens et al., 2005). The trichothecene DON is converted to less toxic D3G by host UDP-glycosyltransferase (UGT) (Poppenberger et al., 2003). Hence, *Fhb1* was hypothesized to co-localize gene(s) that encode either *UGT* or regulate its expression. However, the recent publication of the wheat chromosome 3B genome sequence has revealed that *Fhb1* on the megabase contig *ctg0954* (GenBank: *FN564434.1*) does not include genes that encode *UGT* (Choulet et al., 2010). Co-localization of UGT regulating elements in *Fhb1* loci remains to be investigated.

A few 'omics' studies have been conducted to investigate possible biochemical mechanisms associated with *Fhb1* using isogenic lines with resistant and susceptible *Fhb1* alleles. Transcripts of pathogenesis-related (PR) proteins, such as β-1, 3-glucanase (PR-2), wheatwins (PR-4), thaumatin-like proteins (PR-5) and phenylalanine ammonia lyase (PAL) were significantly up-regulated in Sumai-3, which contains resistant *Fhb1* allele, as opposed to the susceptible near isogenic lines (NILs) that lacked a resistant *Fhb1* allele (Golkari et al., 2009). In another study with the Sumai-3 derived cultivar CM82036, transcripts of UGT, PAL, Dna-J like protein and a PR-protein family protein were up-regulated in a *Fhb1* resistant allele containing CM82036 and a doubled haploid line DH1, compared to the susceptible genotypes Remus and DH-2 (Steiner et al., 2009). However, none of the up-regulated transcripts was mapped to the *Fhb1* region in these studies.

Seven transcripts that map to the *Fhb1* containing chromosome 3BS were differentially regulated in the transcriptomics analysis of wheat NILs derived from Sumai-3 with resistant and susceptible *Fhb1* alleles. Up-regulated transcripts in NIL carrying a resistant *Fhb1* allele were related to cell wall biogenesis, while up-regulated transcripts in NIL-S were associated with cell death (Jia et al., 2009). A putative *Fhb1* candidate gene, *WFhb1_c1* (GenBank: CA640991-weakly similar to *Arabidopsis* pectin methyl esterase inhibitor), which contributes to FHB resistance by reducing susceptibility, was identified by expression QTL (eQTL) analysis of *Fhb1*-containing NILs (Zhuang et al., 2013). However, *WFhb1_c1* is not co-localized in the *ctg0954* region with *Fhb1*. However, both the transcriptomics studies hinted an association of *Fhb1* with reduced susceptibility. Similarly, Ca^{2+} signalling pathway genes that contribute to the necrotrophic phase during *F. graminearum* infection through programmed cell death (PCD) were significantly up-regulated in the *Fhb1* deleted susceptible mutant genotype compared to the another type II FHB resistant cultivar (Wangshuibai) and a few candidate genes were proposed to govern general disease resistance (Xiao et al., 2013). Nevertheless, candidate genes localized at *Fhb1* which explain either resistance or susceptibility remain unidentified.

Non-targeted metabolomics and proteomics of NILs with resistant and susceptible *Fhb1*alleles have indicated that *Fhb1* encodes more than one gene governing FHB

resistance mechanisms. *Fhb1* from the moderately resistant cultivar Nyubai is associated with cell wall thickening, more evident at the rachis than in spikelets, due to deposition of hydroxycinnamic acid amides (HCAAs), phenolic glucosides and flavonoids. A hypothetical protein coding gene (GenBank: CBH32656.1) near the *Fhb1* locus was putatively identified as hydroxycinnamoyl transferase, and was considered to be involved in the biosynthesis of HCAAs (Gunnaiah et al., 2012). However, a high accumulation of DON was observed in both resistant and susceptible NILs that caused bleaching of the spikelets, with similar proportion of DON detoxification. Hence, resistance mechanisms against DON accumulation were unexplained.

Evaluation of several wheat genotypes suggested that the levels of FHB resistance vary with different sources of resistance (Bernardo et al., 2012). The cultivar Sumai-3 and its derivatives have shown the highest levels of resistance to disease spread and DON detoxification. Yet, the level of DON resistance (type III resistance) varied among different Sumai-3 derived resistant cultivars (Bai et al., 2001), and also among the genome background into which *Fhb1* from Sumai-3 was introgressed (Jia et al., 2009, Lemmens et al., 2005). Apparently, the resistance level drastically decreased when chromosome 3B from Sumai-3 was substituted into the genome background of the moderately susceptible cultivar Chinese Spring, compared to Sumai3 background (Zhou et al., 2002).

With advancements in genome sequencing and physical mapping of chromosome 3B, the physical location of *Fhb1* has been variedly mapped to a 2.2-2.8 Mb region on the contig ctg0954 (Genbank: FN564434) (Hao et al., 2010). The *Fhb1* region co-localizes 16-22 protein coding genes. In the present study, using the information on genes co-localized at *Fhb1* region as a guide, mechanisms of resistance to disease spread or lesion expansion associated with *Fhb1* locus were explored by non-targeted metabolic profiling of wheat NILs with resistant and susceptible *Fhb1* alleles derived from Sumai-3. A *Fhb1* candidate gene *TaCamB_Fhb1* coding for calmodulin binding protein was identified. A non-functional *TaCamB_Fhb1* in the FHB resistant genotype rescues host cells from PCD, limiting the proliferation of necrotrophic *F. graminearum* only to the inoculated spikelet.

4.3 MATERIALS AND METHODS

4.3.1 Plant material

Near isogenic lines with resistant and susceptible *Fhb1* alleles (seeds provided by Dr. S. Fox, AAFC, Winnipeg) were developed by marker assisted backcross breeding using highly FHB resistant cultivar, Sumai-3 as a recipient parent and a susceptible cultivar, Thatcher, as a donor parent (Cuthbert et al., 2006). The NILs used in this study were polymorphic for the fine mapped *Fhb1* flanking markers STS-80 and STS-142. The NIL with the *Fhb1* resistant allele (NIL-R) showed disease severity of 0-5 % with homozygous resistant alleles and the NIL with the *Fhb1* susceptible allele (NIL-S) showed disease severity of 100 % with homozygous susceptible alleles for the *Fhb1* flanking markers, STS-80 and STS-142. Both NIL-R and NIL-S were homozygous resistant for the other reported type II FHB resistance QTLs on chromosomes 5A (*Fhb5*) and 6B (*Fhb2*) from Sumai-3.

4.3.2 Pathogen and spore production and inoculation

F. graminearum Schwabe, strain GZ3639, was maintained on potato dextrose agar. For spore production, the culture was grown on rye B agar with half the concentration of sucrose under 16 h of white light and 8 hrs of dark for three days and under 16 hrs of UV light and 8 hrs. of dark for the next four days at 23 $\pm 2^0$C. Spore suspension was prepared from a seven day old culture by extracting macroconidia in sterile water and the concentration of the spores was adjusted to 10^5 spores mL^{-1}.

Wheat plants at growth stage 65 (50 % anthesis) were selected for inoculation. For metabolic profiling and transcript expression studies, three alternate pairs of spikelets at the middle of the spike were point inoculated with 10 µl spore suspension per spikelet using a syringe with an auto dispenser (GASTIGHT 1750DAD W/S, Hamilton, Reno, NV, USA). For disease severity analysis, a single pair of spikelets at the middle of the spike was inoculated.

4.3.3 Disease Severity Assessment

The number of spikelets diseased was recorded at 3 day intervals for15 days. From these data, the proportion of spikelets diseased (PSD = number of spikelets diseased/total number of spikelets in a spike and area under the disease progress curve (AUDPC) were calculated. A student's *t*-test was used to compare the AUDPC variation between NILs.

4.3.4 Sample collection, metabolite extraction and LC/MS analysis

For metabolite and RNA extraction, *F. graminearum* or mock inoculated spikes were harvested at 3 and 7 dpi. Three pairs of inoculated spikelets and alternating three pairs of un-inoculated spikelets, above the inoculated spikelets, and rachis in between the top and bottom inoculated spikelets were separately collected, immediately frozen in liquid nitrogen and stored at -80^0C until use. Inoculated and un-inoculated spikelets were mixed and ground together; rachis was separately ground in liquid nitrogen, using pre-cooled mortar and pestle. Metabolites were extracted with pre cooled 60% aqueous methanol as described previously (Bollina et al., 2010). The metabolites were analyzed using liquid chromatography coupled with high resolution hybrid mass spectrometers (LC-ESI-LTQ-Orbitrap, Thermo Fisher, Waltham, MA) as described previously (Bollina et al., 2010, Gunnaiah et al., 2012)

4.3.5 LC/MS data processing

Thermo Scientific, Xcalibur RAW files were converted to mzXML files using ReAdW version 4.3.1. Data were processed using an user interactive LC/MS data processing software, mzMine2 with high sensitive peak detection algorithm, XCMS *centwave* (Pluskal et al., 2010). Metabolites were identified by searching matching *m/z* values in PlantCyc, KEGG, LIPIDMAPS, METLIN and in house McGill-MD databases with < 5 ppm accurate mass error and were confirmed with MS/MS fragmentation pattern in MASSBANK, METLIN, in house spiked MS/MS library and *in silico* fragmentation as described previously (Gunnaiah et al., 2012).

4.3.6 Identification of RR metabolites

Peaks from adduct and complex ions were removed from the data matrix and subjected to pair wise student *t*-test in RP versus RM, SP versus SM, RM versus SM and RP versus SP combinations, separately for the data from spikelets at 3 dpi, rachis at 3 dpi and rachis at 7 dpi. Resistance related (RR) metabolites, resistance related constitutive (RRC) and resistance related induced (RRI) metabolites were identified as previously described (Gunnaiah et al., 2012)

4.3.7 RNA extraction and Quantitative Real-time PCR

Total RNA extracted from both spikelets and rachis of NILs derived from Sumai-3 and from the rachis of NILs derived from Nyubai (chapter III) was used to study differential gene expression of putative *Fhb1* candidate genes; UDP-glycosyltransferase (UGT), hydroxycinnamoyl transferase (*HCT*), UDP-glucose dehydrogenase (UGDH) and sarcoplasmic histidine rich Ca^{2+} binding protein, which has a calmodulin binding motif and henceforth referred as *T. aestivum* calmodulin binding protein (*TaCaMBP_Fhb1*). Total RNA was extracted using an RNeasy Plant mini kit (Quiagen) with DNase I treatment. 500 ng of total RNA from each sample was reverse transcribed to cDNA using iScript cDNA synthesis kit (BioRad, ON, Canada). Two microliters of 40x-diluted cDNA in 10 µl reaction volume was used in a quantitative real-time PCR (qRT-PCR) reaction using iQ SYBR Green Supermix (BioRad) in an CFX384TM Real-Time System (BioRad, ON, Canada). 5X dilution series prepared by mixing equal amounts of concentrated cDNA from each sample were used to plot standard curve and determine PCR efficiency. The starting quantity of the transcript generated by plotting C_t values along standard curves, normalized with the reference gene, *Ta2291* was used for relative quantification. Relative transcript abundance between treatments was compared by one-way ANOVA using SigmaPlot 12.5. Primer sequences used for target genes and reference gene and their PCR efficiencies are given in Table 4.1. Primer sequences for the wheat reference gene *Ta2291* encoding ADP-ribosylation factor were used from Paolacci et al, (2009).

4.3.8 DNA cleavage analysis and charecterization of *Fhb1* candidate gene *TaCaMBP_Fhb1*

Genomic DNA (gDNA) extracted from the *F. graminearum* infected rachis at 7 dpi of wheat NILs derived from Sumai-3 was extracted using DNeasy Plant Mini Kit (Qiagen GmbH, Hilden, Germany). For assessing DNA degradation due to PCD, 25 µg of DNA from NIL-R and NIL-S, 1 µg each of 100 bp and 1 Kb (Invitrogen, Carlsbad, CA, USA) were resolved on 2% agarose gel made with TAE buffer and stained with ethidium bromide. Gel images were captured using Molecular Imager ChemiDoc XRS System (Bio-Rad Laboratories). The *Fhb1* candidate gene *TaCaMBP_Fhb1* from NIL-R and NIL-S was amplified with forward primer (*TaCaMBP_Fhb1*-F $5^{!}$-TCAGGTTCTGAGGCATTTTAACAAC-$3^{!}$) and reverse primer *TaCaMBP_Fhb1*-R- $5^{!-}$GAGGAACGACTTTTCGCTGGT-$3^{!}$). Amplicons were resolved in resolved on 2% agarose gel made with TAE buffer and stained with ethidium bromide.

4.4 RESULTS

4.4.1 FHB disease severity

Disease severity in NILs with either the resistant or susceptible *Fhb1* allele was assessed based on necrotic and bleaching symptoms on spikelets from 3 to 15 dpi, following *F. graminearum* inoculation. Necrotic symptoms were observed on the spikelets of both NILs at 3 dpi. Symptoms were restricted to the point inoculated spikelet in NIL-R for the entire period of study. In NIL-S, the necrotic symptoms expanded equally to top and bottom spikelets from the point of inoculation. The disease severity was significantly (P<0.0001) higher in NIL-S (AUDPC = 5.58) than in NIL-R (AUDPC =1.5). Spikelet bleaching (drying of spikelets without necrosis) was not observed in NIL-R during the entire period. In NIL-S, the top 3-5 spikelets were bleached after 12 dpi and the entire spike was dried by 15 dpi.

4.4.2 Trichothecenes and their conjugates

Deoxynivalenol is a pathogen aggressiveness factor aiding in the expansion of *Fusarium* colonization. Since resistance in *Fhb1* was hypothesized to be associated with DON detoxification, DON and other trichothecenes along with their glucose conjugates were

analyzed through targeted peak search. In this study, three trichothecenes: DON, 3-ADON and fusarenone, and their respective glucose conjugates: DON-glucoside (D3G), 3ADON-glucoside, and fusarenone- glucoside were detected. Apart from the previously reported DON conjugates, novel DON conjugates: DON-xyloside and DON-glucuronidine were also detected (Table 4.2, Fig.4.1).

None of the trichothecenes or their conjugates was detected in rachis of either of NILs at 3 dpi. In spikelets at 3 dpi, the amount of DON accumulated in NIL-S (2.32 ppm) was almost double the amount accumulated in NIL-R (1.2 ppm). A small amount of D3G was observed only in NIL-R (D3G = 0.93 ppm), with moderate PDC of 0.43. Apart from the frequently detected *Fusarium* toxins and their glucose conjugates, novel fusarenon and fusarenone-glucoside were also detected in spikelets at 3 dpi, but with no significant difference between the NILs.

In rachis at 7 dpi, a very low amount of DON accumulated in NIL-R (0.5 ppm) compared to NIL-S (1.36 ppm). In parallel, D3G accumulation was high in both NILs, but the PDC was similar (0.76 and 0.66 respectively in NIL-R and NIL-S) with no significant difference between them, implicating high DON detoxification in both NILs. At 7 dpi, two novel DON sugar conjugates, DON-xylose and DON-glucuronidine, were also detected. However, there was no significant difference in the abundances of conjugates between the NILs. Acetylated DON, 3ADON and 4, 15 diacetyl-DON were detected in NIL-S only, while, 3ADON-glucoside was detected in both NILs. Even though fusarenon was not detected in rachis of either NILs at 7 dpi, the fusarenone-glucoside was detected with no significant difference between NILs.

4.4.3 Metabolic profiles of wheat NIL pair with resistant or susceptible *Fhb1* alleles

Rachis at 3 dpi

Compared to spikelets, fewer RR metabolites were identified in rachis at 3 dpi. Among the 108 RR metabolites, 21 were classified as RRC and 87 were classified as RRI. However, only 22 were putatively identified (Appendix 4.1) and belonged to primary metabolism such as shikimate, glycolate, sugars (glucose, fructose, xylobiose), one

flavonoid (apigenin 7-(2"-acetyl-6"-methylglucuronide) and an antimicrobial compound, anthraquinine (aurantio-obtusin beta-D-glucoside).

Spikelets at 3 dpi: 262 metabolites were identified as RR and further classified into 51 RRC and 211 RRI metabolites. Seventy nine RR metabolites belonging to different chemical groups were putatively identified in spikelets (Table 4.3, Appendix 4.1). The majority of RR metabolites were from the phenylpropanoid pathway, belonging to free phenylpropanoids, phenolic glucosides, lignans and flavonoids. Among these, sinapoyl alcohol, *p*-coumaroyldiketide, sinapic acid methyl ester and a lignan, clesitanthin A, accumulated with more than two fold changes. The next largest group of RR metabolites were of the lipid biosynthesis pathway, including fatty acids with anti-oxidative properties, fatty acyls, sterol lipids, prenol lipids and glycerophospholipids with plant defense signalling properties. Five terpenoids and two alkaloids induced upon jasmonic acid signalling were also induced with high fold change in the spikelets of resistant NIL. Apart from the major groups, some of the precursor metabolites of primary metabolism such as sugars, sugar alcohols, chlorophyll biosynthesis and precursors of secondary metabolism such as succinate (FC=6.27), lauric acid, anthranilic acid, vanillin, L-tryptophan, phenylpyruvic acid and glutathione were also identified as RR metabolites.

Rachis at 7 dpi: Since *Fhb1* was mainly associated with resistance to expansion of pathogen colonization through rachis, metabolites accumulated in rachis at a later stage of infection (7 dpi), when lesion expansion to other spikelets was observed, were profiled. 73 RR metabolites were identified, among these 30 classified as RRC and 43 as RRI metabolites. Seven of the RRC metabolites identified were: one glycerophosphate and six related to primary metabolism. Among the 43 RRI metabolites, 13 were identified, of which four belonged to lipid biosynthesis pathway two glycerophosphoglycerols (PG), one glycerophosphate (PA), one prenol lipid, four terpenoids and two metabolites involved in chlorophyll metabolism (Appendix 4.1).

At 7 dpi, a very high number (420) of metabolites was detected in the pathogen treated rachis. Among these, 307 were significantly higher in NIL-S (PRs), and five were higher in NIL-R (PRr). Of the 307 PRs metabolites, many were belonged to phenylpropanoids,

including flavonoids and other antimicrobial compounds which were also identified as RR metabolites in spikelets of NIL-R at 3 dpi (data not shown).

Interestingly, 78 metabolites were detected only in the pathogen treated NIL-R. Even though these were present in both the mock treated NILs, their abundances were not significantly different. Of these, 25 were identified and 18 belonged to five classes of glycerophospholipids (Table 4.4): (PC: glycerophosphocholines [GP01], PE: glycerophosphoethanolamines [GP02], glycerophosphoserines [GP03], PG: glycerophosphoglycerols [GP04] and PA: glycerophosphates [GP10]). The identity of these metabolites were confirmed by matching observed MS/MS fragments with *in silico* identified fragments using a 'Product ion calculation tool for Glycerophospholipids (negative ion mode)' and Glycerolipid MS/MS Prediction at Lipidomics Gateway (http://www.lipidmaps.org/tools/structuredrawing/GP_p_form.php). The others were p-coumarate and coniferin of the phenylpropanoid pathway, one each of a terpenoid, alkaloid, polyketide, and phosphatidylglycerol chemical groups (Appendix 4.1).

4.4.4 Putative *Fhb1* candidate genes expression

UDP-glycosyltransferase (UGT): *Fhb1* is reported to be associated with detoxification of DON through glucose conjugation by UGTs. To study the expression of probable DON detoxifying UGTs, primers were designed to amplify different regions of wheat UGT sequences, homologous to barley DON detoxifying UGT (*HvUGT13248*) and their expression was analysed using qRT-PCR in spikelets at 3 dpi and rachis at 7 dpi, which had differential accumulation of DON and D3G. Expression of UGT1 (929-1094) and UGT2 (1204-1338) was up-regulated following pathogen inoculation, in both the NILs, but not in the mock inoculated samples. UGT1 and UGT2 showed similar expression patterns in both NILs (Fig. 4.2). There was no significant difference in the expression of UGT1 and UGT2 between NIL-R and NIL-S in spikelets at 3 dpi (Fig. 4.2a). Differential expression of UGT1 and UGT2 was observed in rachis at 7 dpi with higher expression of both UGTs with a fold change (with respect to reference gene) of 3.6 and 2.7, respectively, for UGT1 and UGT2 in NIL-S, compared to 0.5 and 0.3, respectively, for UGT1 and UGT2 in NIL-R (Fig. 4.2b). Since significant amounts of DON and D3G accumulated in the rachis of NILs derived from Nyubai at 3dpi (Gunnaiah et al., 2012),

the expression of UGT1 and UGT2 in the NILs derived from Nyubai were also checked. Similar to Sumai-3 derived NILs, the expression of UGTs in mock samples was insignificant, but was highly expressed in pathogen treated samples. However, there was no significant difference in the expression of UGTs between NILs. The fold change expression of UGT1 was 2.1 and 3.9 and UGT2 expression was 1.9 and 1.8, respectively, in NIL-R and NIL-S.

UDP-glucose dehydrogenase (UGDH): A pesudogene of UDP-glucose dehydrogenase on the *Fhb1* region was hypothesized to be *Fhb1* candidate gene, which acts as positive regulator of DON detoxification by negatively regulating its parent gene, UDP-glucose dehydrogenase. To test this hypothesis, the expression of wheat UGDH (GENBANK: BT009444.1), which is 92 % identical to *PsUGDH*, was analyzed by designing primers at the region where UGDH is not identical to *PsUGDH*. UDP-glucose dehydrogenase was expressed in both pathogen and mock treated samples. However, there was no significant difference in its expression, either between pathogen and mock treated spikelets, or between NILs at 3 dpi (Fig. 4.2c). In rachis at 7 dpi, its expression was significantly (P<0.001) increased two fold in pathogen treated NIL-S, while no significant difference was observed between pathogen and mock treated samples in NIL-R. Also, there was no significant difference in the expression of UDP-glucose dehydrogenase between NIL-R and NIL-S in rachis at 7 dpi.

Sarcoplasmic/endoplasmic histidine rich Ca^{2+} binding protein / calmodulin binding protein (*TaCaMBP_Fhb1*): *In-silico* analysis revealed a gene encoding putative Sarcoplasmic/endoplasmic histidine rich Ca^{2+} binding protein at *Fhb1* locus. The protein contains a calmodulin binding motif and henceforth referred as calmodulin binding protein (*TaCaMBP_Fhb1*) was explored as possible candidate gene for FHB resistance. The gene expression of *TaCaMBP_Fhb1* in spikelets at 3dpi was similar in all the treatments with no significant difference. In rachis at 7 dpi, its expression significantly (P<0.001) increased in NIL-S by 1.9 fold following pathogen inoculation, from its constitutive expression of 1.1 in mock, while no significant difference was observed in NIL-R. The expression of *TaCaMBP_Fhb1* in in the pathogen treated NIL-S was also significantly higher than both the pathogen and mock-inoculated NIL-R (Fig. 4.3).

Agmatine coumaroyltransferase (AgCT): *AgCT* is one of the many hydroxycinnamoyl transferases involved in the biosynthesis of HCAAs. Consistent with the high accumulation of HCAAs in both NIL-R and NIL-S, the gene coding *AgCT* was also highly expressed in both the pathogen treated NILs, with no significant difference between NILs, in spikelets at 3 dpi. Its expression in mock samples was not significant. The expression of *AgCT* increased significantly ($P<0.001$) following pathogen inoculation, in NIL-S by 2.73 fold in the rachis at 7 dpi (Fig. 4.4).

4.4.5 DNA laddering in NIL-S and variation in the length of *TaCaMBP_Fhb1* in NILs

A distinct DNA laddering due to DNA cleavage, a characteristic feature of PCD was observed only NIL-S and DNA was intact in NIL-R (Fig. 4.6). Amplified gene length including coding region and *in-silico* predicted promoter region of the *Fhb1* candidate gene *TaCaMBP_Fhb1* in NIL-S was approximately 2.0 Kb as in another susceptible cultivar Chinese Spring. While in NIL-R, the gene length was approximately 1.5 Kb, probably due to deletion in the promoter region (Fig. 4.7). The coding region was 782 bp in both the NILs, as in Chinese spring. However, the length of the promoter region of *TaCaMBP_Fhb1* was short in NIL-R compared to NIL-S, which was similar to the region in Chinese spring (data not shown).

4.5 DISCUSSION

The wheat QTL *Fhb1* is the largest effect FHB resistance QTL among more than 100 QTLs identified. *Fhb1* is physically located on contig *ctg0954* (GENBANK: FN564434.1), on the short arm of chromosome 3B, bin 0.78-0.87 (Choulet et al., 2010). In this study, a consensus map of genes localized in the *Fhb1* region, based on flanking markers reported in different studies and the protein coding genes located between the flanking markers on the *Fhb1* region along with their biological functions, was reconstructed (Appendix 4.2). Three genes that may explain resistance to FHB: TAA_ctg0954b.00350.1 a pseudogene of UDP-glucose 6-dehydrogenase (*PsUGDH*), TAA_ctg0954b.00390.1 coding for a calmodulin binding protein (*TaCaMBP_Fhb1*) and TAA_ctg0954b.00400.1 putatively annotated as hydroxycinnamoyl transferase (*HCT*) were selected as putative *Fhb1* candidate genes for further study. In this study, metabolic

profiles of two NILs with resistant and susceptible alleles of *Fhb1*, flanked by the fine mapped STS markers STS-80 and STS-142 were compared following pathogen or water inoculation. Differentially accumulated metabolites between resistant and susceptible *Fhb1* NILs were linked to the genes co-localized at *Fhb1* region. Genes with suspected links were tested for their differential expression to identify potential *Fhb1* candidate genes.

4.5.1 No difference in DON detoxification, by UDP-glycosyltransferase, between NILs

In this study, FHB severity and accumulation of DON varied significantly between NIL-R and NIL-S, with high disease and high DON accumulation in NIL-S, but not the proportion of DON converted (PDC) to the detoxified conjugate, D3G. Recently, a barley gene encoding UGT (*HvUGT13248*) has been cloned and proved to possess DON detoxification function through heterologous expression in yeast (Schweiger, et al., 2010) and validated through overexpression in *Arabidopsis* (Shin, et al., 2012). Wheat UGTs homologous to barley UGT (HvUGT13248) coding sequence were retrieved from the wheat chromosome survey sequences using BLAST analysis at http://urgi.versailles.inra.fr:80 (IWGSC). Contig sequences longer than 200 Kb with significant hits (>80% identity) to the HvUGT13248 sequence from each of the chromosome were downloaded. Homologous sequences for HvUGT13248 were found on 8 wheat chromosome segments: 2AS, 2BL, 2BS, 2DS, 5AL, 5BL, 5BS, 5DL and 5DS (Table 4.6). Transcript expression of wheat UDP-glycosyltransferase homologous to *HvUGT13248* was higher in NIL-S compared to NIL-R, and correlated with total DON produced (Fig. 4.5). The expression of host UDP-glycosyltransferase was dependent on the amount of DON produced irrespective of the NIL. Collectively, the DON detoxification efficacy by UDP-glycosyltransferase didn't vary between NILs that contained resistant and susceptible *Fhb1* alleles. Low DON accumulation in NIL-R is due to other host resistance factors, such as inhibition of growth of the pathogen, inhibition of trichothecene biosynthesis or avoidance of cell death (Bollina and Kushalappa, 2011, Boutigny et al., 2010). Similarly, no significant DON detoxification was observed between NILs with resistant and susceptible *Fhb1* alleles derived from a

moderately resistant cultivar, Nyubai, with susceptible genome background. In similar way, no significant difference in DON accumulation was reported between NILs with resistant and susceptible *Fhb1* alleles derived from the cross: Sumai-3 X Stoa (Jia et al., 2009). In contrary, DON resistance (D3G/DON) was mapped to the same locus as *Fhb1* in a doubled haploid mapping population from the cross "CM-82036 X Remus", with resistant lines showing significantly higher D3G/DON ratios. Accordingly, *Fhb1* was hypothesized to include gene(s) that code for UDP-glycosyltransferase or regulate its expression. Nevertheless, from the genome sequence information of 3BS it is evident that genes encoding UDP-glycosyltransferase are not present in the *Fhb1* region. Regulation of UDP-glycosyltransferase by *Fhb1* is also debatable as transcript expression of UDP-glycosyltransferase correlated with TDP, irrespective of the genotype. Further validation studies are needed to prove the relation of DON resistance to resistance controlled by *Fhb1*.

An alternative candidate gene in *Fhb1* region that might play a role in DON resistance is a pseudogene (*PsUGDH*, *TAA_ctg0954b.00350.1*) processed from the gene coding for UDP-glucose dehydrogenase (UGDH). UGDH is a key enzyme in the biosynthesis of a nucleotide sugar, UDP-glucuronic acid, from which other cell wall building nucleotide sugars such as UDP-xylose and UDP-arabinose are synthesised (Reboul et al., 2011). UDP-glucose is a common substrate for UGDH and several other glycosylation reactions in the plant cell, including DON detoxifying UGTs (Kleczkowski et al., 2010). It was hypothesised that higher expression of UGDH might deplete the availability of UDP-glucose for DON detoxification. The processed pseudogene on *Fhb1* region might silence the parent UGDH and make available more UDP-glucose for DON detoxification. However, its expression was neither correlated with the expression of UGTs nor with the PDC. Moreover, its expression was not down regulated in NIL-R as hypothesised. Indeed, several other trichothecene glucosides, phenolic and flavonoid glucosides were accumulated in both spikelets and rachis that also utilize UDP-glucose as substrate for glucose conjugation. Consequently, the expression of UGDH influenced by its pseudogene counterpart might not have a role in DON detoxification.

4.5.2 Reduction of growth *F. graminearum* and trichothecene biosynthesis due to RR metabolites in spikelets

In spite of similar resistant genome background of both NILs, many RR metabolites were significantly accumulated the spikelets of NIL-R, with greater fold change compared to NIL-S. Even though the NILs were developed by backcrossing to a resistant genome, they were verified for homozygous resistant alleles for only *Fhb2* and *Fhb5* (Cuthbert et al., 2006). Variation in the residual genome of the susceptible cultivar Thatcher might have accounted for greater accumulation of RR metabolites in NIL-R. In addition, the *Fhb1* region flanked by STS-80 and STS-142 co-localizes three putative glycosyltransferase domain containing protein coding genes and a terpene synthase that may play a significant role in the biosynthesis of some of the glucoside conjugates and terpenoids, respectively (Degenhardt et al., 2009, Wang and Hou, 2009).

Consistent with previous studies in barley and wheat infected with *F. graminearum*, most RR metabolites reported here also belong to the class of phenylpropanoids, lipid biosynthesis, terpenoids, alkaloids and few organic acids and sugars, implying their association with broad host defense mechanisms (Bollina et al., 2010, Gunnaiah et al., 2012, Kumaraswamy et al., 2011). Several of phenylpropanoids detected as RR metabolites can be used as biomarker metabolites for *Fusarium* resistance in wheat and barley (Kumaraswamy et al., 2011). Cinnamic acids detected in this study, including *trans*-cinnamic acid, 4-coumaric acid and sinapic acid methyl ester, are precursors of many downstream metabolites, such as HCAAs, flavonoids, lignin and lignans, which enhance host resistance to pathogen attack as phytoalexins and/or secondary cell wall thickening compounds (Naoumkina et al., 2010). Host produced phenolic acids and antioxidant molecules inhibit the growth of *F. graminearum* as well as the biosynthesis of trichothecenes by *F. graminearum* (Bollina and Kushalappa, 2011, Ponts et al., 2011). In our previous study with NILs derived from Nyubai, HCAAs and flavonoids were significantly induced with very high fold changes in NIL-R and were demonstrated to be localized at the cell wall, resisting pathogen colonization, especially through rachis (Gunnaiah et al., 2012). In the present study, HCAAs were induced with very high abundance in both resistant and susceptible NILs (Table 4.5, Fig.4.4), as both had high

FHB resistant Sumai-3 background genome. Hence, *HCT* near the *Fhb1* region catalyzing the biosynthesis of HCAAs was ruled out as *Fhb1* candidate gene, and accordingly should be considered as a novel RR gene. Similarly, very few flavonoid glucosides were identified as RR metabolites compared to several with very high fold change in our previous study. Lignans such as (+)- pinoresinol, podophyllotxin and their derivatives isolated from different plants have been proved *in vitro* to have antifungal activities (Anil Kumar et al., 2007, Carpinella et al., 2003) and are also involved in cell wall thickening (Umezawa, 2010).

A few metabolites of lipid biosynthesis were also detected as RR metabolites, including two fatty acids. L-threonate and caprate are involved in β-oxidation of fatty acids in the cutin and lipid biosynthesis pathway (Imaishi and Petkova-Andonova, 2007). Glycerophospholipids play a key role in membrane integrity, defense signalling and cell homeostasis (Farooqui, 2009). Sugars, amino acids and other organic acids are key components of primary and secondary metabolism. Overall, these RR metabolites play key role in resisting initial infection (type I resistance) in spikelets and augment resistance to pathogen colonization in rachis encoded by *Fhb1*.

4.5.3 *Fhb1* rescues host cell from programmed cell death, regulated by a calmodulin binding protein (*TaCaMBP_Fhb1*)

At 7 dpi, the rachis was completely colonized by *F. graminearum* in NIL-S but not in NIL-R, albeit the NIL-S had detoxified a higher amount of DON (high D3G). Metabolic profiling of rachis at 7 dpi revealed that several glycerophospholipids were constitutively present in the mock treated rachis of both NILs, and also in the pathogen treated NIL-R, but were not in the rachis of pathogen treated NIL-S (Table 4.4). The glycerophospholipids are the structural components of cellular membranes that play key roles in maintaining cell membrane integrity, cell fluidity and ion permeability (Farooqui, 2009) and the rupture of plasma membrane and sequestration of membrane bound glycerophospholipids is a characteristic feature of programmed cell death (PCD) in plants (Van Doorn, et al., 2011), suggesting PCD in the NIL-S. In confirmation, genomic DNA (gDNA) laddering, a characteristic of programmed cell death, was observed only in the NIL-S and the gDNA was intact in the NIL-R (Fig. 4.6). Coincidentally, the expression

of a gene localized on *Fhb1* locus, which encodes HRC was significantly up-regulated in NIL-S following pathogen inoculation (Fig. 4.3). HRC possess a motif x**W**xxx (**I/L**) xxxx commonly referred as NSCaTE (N-terminal spatial Ca^{2+} transforming element) to which another Ca^{2+} sensor and signalling protein, calmodulin (CaM) binds (Taiakina et al., 2013). Henceforth HRC will be referred as CaM binding protein (*TaCaMBP_Fhb1*). The calmodulin binding motif NSCaTE is a highly conserved in many Ca^{2+} sensor proteins in plants that regulate Ca^{2+} signalling in host cells by binding to CaM (Du et al., 2011). Following Ca^{2+} influx into the cytoplasm, CaM senses increase in cytoplasmic Ca^{2+} and binds to *TaCaMBP_Fhb1* at NSCaTE motif. The CaM bound *TaCaMBP_Fhb1* triggers transcriptional activation of endonuclease that cleaves the chromosomal DNA, leading to PCD, as hypersensitive response against biotrophs, which restricts pathogen to the infected site (Reddy et al., 2003). In contrast, hypersensitive response facilitates necrotrophic pathogen infection as the necrotrophs feed on dead tissue and exploit a host defense mechanism for their pathogenicity (Govrin and Levine, 2000). Disruption of NSCaTE motif in a Cam binding protein failed to bind to CaM, thus blocking Ca^{2+} signalling (Hwang et al., 2000). We hypothesize that the resistant *Fhb1* allele contains a non-functional *TaCaMBP_Fhb1* (Fig. 4.7), either not produced due to deletion in the promoter region or does not bind to CaM and thus does not induce Ca^{2+} signalling and PCD. Hence, pathogen starves and its multiplication in the host tissue is restricted (Fig.4.8a). Low DON accumulated at the beginning of infection is detoxified by host UDP-glycosyltransferases and H_2O_2 is neutralized by RR metabolites and induced proteins such as peroxidases and superoxide dismutases that act as antioxidants (Bollina et al., 2011, Geddes et al., 2008, Gunnaiah et al., 2012, Kumaraswamy et al., 2011). While in genotypes with *Fhb1* susceptible alleles, Ca^{2+} activated CaM binds to functional *TaCaMBP_Fhb1* with intact promoter region (Fig. 4.7), and induces Ca^{2+} signalling that further triggers endonucleases, which cleaves the chromosomes, causing PCD and cell membrane disruption (Fig. 4.8b). Necrotrophic F. *graminearum* feeds on dead tissue and continue to progress in the host tissue producing more DON that further induce more H_2O_2 and Ca^{2+} influx and the vicious cycle continues leading to complete death of spikes. Similarly, a high concentration of DON induced the production of H_2O_2 triggering the

disruption of cell membranes and leading to host cell death in susceptible genotypes of wheat and barley (Bushnell et al., 2010, Desmond et al., 2008, Miller and Ewen, 1997). In parallel, glycerophospholipids were not detected in cell cultures of *Taxus cuspidate* inoculated with Celium (Ce^{4+}), which induces PCD. While glycerophospholipids were prominent in cell culture of *T. cuspidate,* inoculated with methyl jasmonate (Yang et al., 2008). Hence, the glycerophospholipids were detected only in NIL-R, which were extracted from the intact membrane even at seven days after *F. graminearum* inoculation, while they were degraded in NIL-S due to *TaCaMBP_Fhb1* mediated host cell death.

The host cell death associated *TaCaMBP_Fhb1* gene (TAA_ctg0954b.00390.1) was consistently mapped within all the reported *Fhb1* flanking markers (Appendix 4.2). Further, locus *cfb6059,* which is significantly associated with *Fhb1,* was mapped very close to the *TaCaMBP_Fhb1* gene (Hao, et al., 2012). A comparative *in silico* expression analysis using PLEXdb (Dash et al., 2012) also revealed that transcripts of *TaCaMBP_Fhb1* were often up-regulated in susceptible genotypes of wheat and barley under biotic and abiotic stresses. Similarly, a wheat transcript, *Ta.28185.1.S1_at*, annotated as a putative HRC or *TaCaMBP_Fhb1*, was also highly up-regulated in a NIL carrying the susceptible *Fhb1* allele (Jia et al., 2009, Schweiger et al., 2013). However, *TaCaMBP_Fhb1* is often overlooked in plants and further studies are required to understand the downstream and upstream Ca^{2+} signalling cascade. To better understand the molecular function, sequencing of *TaCaMBP_Fhb1* in NILs derived from Sumai-3 and Nyubai with resistant and susceptible *Fhb1* alleles is under progress. Other genes on *Fhb1* loci, *TAA_ctg0954b.00370.1* and *TAA_ctg0954b.00260.1* coding for oxido-reductase NAD-binding domain containing protein and sodium/hydrogen exchanger, respectively, might also be involved in maintaining Ca^{2+} homeostasis that was minimally altered by the *TaCaMBP_Fhb1* in the resistant genotypes (Arrizabalaga et al., 2004, Hayashi et al., 2005).

The role of *TaCaMBP_Fhb1* in FHB resistance has to be validated based on loss function and (or) gain of function studies. Suitably, DNA markers associated with resistant alleles can be used as biomarkers for FHB resistance following validation. Alternatively, susceptible alleles can be edited or knocked out in elite cultivars to enhance resistance.

Table 4.1: Primer sequences used for studying transcript expression in wheat near isogenic lines with resistant and susceptible alleles of *Fhb1* using quantitative real-time PCR

Gene	Name	Forward Primer (5^1 to 3^1)	Reverse primer (5^1 to 3^1)	Amplicon (bp)	Amplification efficiency (%)
UGT1	UDP-glycosyltransferase	AGCTTGGCAATGGACTGTGC	TCCACAGTGGGTAACAAAGC	185	98.20
UGT2	UDP-glycosyltransferase	GAGAGTGCATGGAGCATGGG	CCTTGGCCTTTTGCATCCAC	154	102.6
UGDH	UDP-glucose dehydrogenase	GTGGCCTAAGTTCACCTCGT	GGCGCAAACATGTATCGGAA	177	101.0
TaCaMBP_Fhb1	Calmodulin binding protein	TCATTCATCTTGTCTGGCTC	AGTGATGATGATGAGCGAAG	233	102.9
Ta2291	ADP-ribosylation factor	GCTCTCCAACAACATTGCCAAC	GCTTCTGCCTGTCACATACGC	165	99.98
TaACT	Agmatine coumaroyltansferase	CATCCTGCTACCGTCCTTC	GGAGCTAGTCGAGGGTGTAG	139	103.5

Table 4.2: Trichothecene mycotoxins and their conjugates detected in wheat near isogenic lines with resistant/susceptible alleles of Fusarium head blight QTL, *Fhb1*, inoculated with *F. graminearum*.

Metabolite	**Rachis_3dpi**			**Spikelets_3dpi**			**Rachis_7dpi**		
	RP	SP	RP/SP	RP	SP	RP/SP	RP	SP	RP/SP
Deoxynivalenol (ppm)	ND	ND	-	1.2	2.32	**0.52****	0.5	1.36	**0.37*****
Deoxynivalenol-*3-o*-glucoside (ppm)	ND	ND	-	0.93	ND	-	1.53	2.7	**0.57***
PDC	-	-	-	0.43	-	-	**0.76**	**0.66**	1.15 NS
Deoxynivalenol -Xylose#	ND	ND	-	ND	ND	-	4.12	4.36	0.94 NS
Deoxynivalenol -glucuronidine#	ND	ND	-	ND	ND	-	4.14	4.75	**0.87***
Other mycotoxins and their conjugates #									
3-acetyldeoxynivalenol#	ND	ND	-	4.46	4.77	0.93 NS	ND	4.12	-
4,15-diacetyldeoxynivalenol#	ND	ND	-	ND	ND	-	ND	3.92	-
3 Acetyldeoxynivalenol -glucoside#	ND	ND	-	4	4.04	0.99 NS	4.55	4.92	0.93
Fusarenon (4-Acetylnivalenol) #	ND	ND	-	4.2	4.31	0.98 NS	ND	ND	-
Fusarenon glucoside#	ND	ND	-	3.97	3.99	0.99 NS	3.43	3.67	0.93

Other than deoxynivalenol and deoxynivalenol-3-o-glucoside, values are log10 transformants of peak intensity in pathogen inoculated NIL-R (RP), pathogen inoculated NIL-S (SP) and RP/SP=Fold change

Student t-test P value: *** <0.001, ** <0.01, * <0.05, NS-Non significant

Table 4.3: Resistance related (RR) metabolites detected in spikelets of wheat near isogenic lines with resistant/susceptible *Fhb1*alleles after 72 hours of post inoculation with *F. graminearum*

Sl No.	Observed Mass (Da)	Metabolite[£]	Fold change	RR classification
A. Phenylpropanpoids : Free phenylpropanoids, Lignans, phenolic glucosides and flavonoids				
1	148.0525	*trans*-cinnamic acid	1.24*	RRI
2	164.0473	4-coumaric acid	1.45***	RRI
3	206.0579	*p*-coumaroyldiketide	2.09*	RRI
4	210.0891	Sinapyl-alcohol	4.4*	RRI
5	238.084	Sinapic acid methyl ester	2.99*	RRI
6	250.1346	N-Caffeoylputrescine	1.11*	RRI
7	342.097	Caffeic acid 3-glucoside	1.64*	RRI
8	356.1104	1-O-Feruloyl-β-D-glucose	1.49*	RRI
9	358.1411	(+)-pinoresinol	1.24**	RRI
10	372.1203	(+)-sesamolinol	1.81***	RRI
11	414.1277	(-)-Podophyllotoxin	1.5*	RRI
12	520.1936	(-)-Pinoresinol glucoside	1.53**	RRI
13	540.1623	Cleistanthin A	2.34	RRI
14	540.1658	2"-o-p-Coumaroylaloesin	1.35	RRI
15	550.204	Medioresinol 4'-O-β-D-glucopyranoside	1.39	RRI
16	328.1306	2,3,4,6-Tetramethoxychalocone	1.54*	RRI
17	340.1306	6-Prenylnaringenic	1.3**	RRI
18	402.1128	8-p-Coumaroyl-3,4-dihydro-5,7-dihydroxy-4-phenylcoumarin	1.55*	RRI
19	422.1714	Lupinisoflavone G	1.14*	RRI
20	446.1239	Biochanin A- β -D-glucoside	1.34*	RRI
21	478.2769	3-Geranyl-4-2',4',6'-tetrahydroxy-5prenyldihydrochalcone	1.38***	RRC
22	500.13	Epigallocatechin 5,3',5'-trimethyl ether 3-O-gallate	1.2*	RRI
23	564.1068	Isorhamnetin 3-(6"-malonylglucoside)	2.53	RRI
24	580.2147	(+)-Syringaresinol O- β -D-glucoside	1.75	RRI
25	602.2352	5,4'-Dihydroxy-6-C-prenylflavanone 4'-xylosyl-(1->2)-rhamnoside	1.11	RRI
26	654.1786	Iristectorigenin A 7-O-gentiobioside	1.94	RRI
27	680.2277	3-(3-Methylbutyl)tricetin 5-neohesperidoside	1.54	RRI
28	726.2354	Naringenin 7-O-(2",6"-di-O-alpha-rhamnopyranosyl)-beta-glucopyranoside	1.43	RRI
29	742.2666	Acanthoside D or (-)-Syringaresinol di-beta-D-glucoside	1.29	RRI
30	800.2357	Tricin 7-rutinoside-4'-glucoside	1.56	RRI

31	862.2141	Cyanidin 3-[6-(6-p-hydroxybenzoylglucosyl)-2-xylosylgalactoside]	1.75	RRI
B. Lipid biosynthesis				
32	136.0374	Threonate	1.24*	RRI
33	172.1464	Caprate	1.78*	RRI
34	436.2667	1alpha-hydroxy-24-methylsulfonyl-25,26,27-trinorvitamin D3 / 1alpha-hydroxy-24-methylsulfonyl-25,26,27-trinorcholecalciferol	1.33*	RRI
35	438.261	(-)-Fusicoplagin A	2.74*	RRI
36	440.2766	PA(17:1(9Z)/0:0);1-(9Z-heptadecenoyl)-sn-glycero-3-phosphate	3.11*	RRI
37	592.2638	PI(18:4(6Z,9Z,12Z,15Z)/0:0)	2.16*	RRC
38	600.231	12S-acetoxy-punaglandin 2	1.48	RRI
39	600.2312	12S-acetoxy-punaglandin 2	1.56	RRI
C. Terpenoids and alkaloids				
40	154.1359	(3S)-linalool	1.29*	RRI
41	240.0898	β-Carboline-1-propionic acid	1.3*	RRI
42	376.1361	Loganate	1.59*	RRI
43	376.1516	Euparotin	1.08***	RRI
44	376.1516	Ailanthone	1.54**	RRI
45	418.1623	Euparotin acetate	1.28**	RRI
46	522.2091	Isobrucein A	1.46*	RRI
D. Other metabolites (Sugars, sugar alcohols, Phenolic compounds, organic acids)				
47	116.0112	Maleate	1.14*	RRI
48	118.0239	Succinate	6.27**	RRC
49	134.0581	3-deazaadenine	1.42*	RRI
50	137.024	Anthranilic acid	2.16*	RRI
51	140.0462	3,5-dihydroxyanisole	1.89**	RRI
52	152.0474	Vanillin	2.34*	RRI
53	164.0474	Phenylpyruvic acid	1.55*	RRI
54	164.0571	1,5-Anhydro-D-glucitol	1.23*	RRI
55	180.0599	Mannose	1.13*	RRI
56	180.0634	B-D-fructofuranose	1.09***	RRI
57	185.9682	2-phosphoglycerate	Inf	RRC
58	200.1813	Lauric acid	1.84*	RRI
59	204.0899	L-tryptophan	1.14*	RRI
60	290.0399	D-sedoheptulose-7-phosphate	1.14*	RRI
61	297.0893	5'-Methylthioadenosine	1.9*	RRI
62	307.0835	Glutathione	1.47**	RRI
63	353.1104	2-oxindole-3-acetyl-beta-D-glucose	1.64*	RRI
64	365.1469	Indole-3-butyryl-glucose	1.44**	RRI
65	402.1519	Benzyl alcohol β-D-xylopyranosyl (1->6)-beta-D-	1.34**	RRI

		glucopyranoside		
66	540.1844	Oleuropein	1.96	RRI
67	584.2249	Mg-protoporphyrin	1.48***	RRI
68	632.2457	3-Hydroxyethylchlorophyllide a	1.57	RRI
69	642.1966	Haemocorin	1.47	RRI
70	862.2892	Sirohydrochlorin	1.63	RRI

£ Detailed compound identification is presented in Appendix 4.1

@ Fold change calculation: were based on relative intensity of metabolites, RRC= RM/SM, RRI= (RP/RM)/(SP/SM); Da: Daltons, RRC is Resistance related constitutive, RRI is Resistance related induced, RP is resistant NIL with pathogen inoculation, RM is resistant NIL with mock inoculation, SP is susceptible NIL with pathogen inoculation, SM is susceptible NIL with mock inoculation

Student t-test *P* value: *** <0.001, ** <0.01, * <0.05, NS-Non significant

Table 4.4: Glycerophospholipds detected in rachis of wheat near isogenic lines with resistant/susceptible *Fhb1*alleles, after 7 days of post inoculation with *F. graminearum*

Observed mass (Da)	Metabolite	RM/SM	RP/RM	Comment
432.2265	PA(18:3(6Z,9Z,12Z)/0:0)	1.01	0.94	Absent in SP
453.2846	PE(16:0/0:0)	1.05	1.04	Absent in SP
479.3001	PC(15:1(9Z)/0:0)	0.99	0.91	Absent in SP
503.3	PE(20:3(8Z,11Z,14Z)/0:0)/LysoPE(0:0/20:3(11Z,14Z,17Z))	0.97	1.00	Absent in SP
505.3154	PC(17:2(9Z,12Z)/0:0) or LysoPE(0:0/20:1(11Z))	1.07	0.93	Absent in SP
507.3315	PC(17:1(10Z)/0:0)	1.01	0.90	Absent in SP
508.3132	PG(19:0/0:0): 1-nonadecanoyl-glycero-3-phospho-(1'-sn-glycerol)	0.97	1.0	Absent in SP
519.2594	PS(18:3(6Z,9Z,12Z)/0:0)	0.97	0.97	Absent in SP
555.3524	PC(17:0/0:0);1-heptadecanoyl-sn-glycero-3-phosphocholine	0.96	1.12	Absent in SP
559.2872	PS(19:1(9Z)/0:0): 1-(9Z-nonadecenoyl)-glycero-3-phosphoserine	1.06	0.96	Absent in SP
567.3523	PS(21:0/0:0)	1.07	0.86	Absent in SP
578.4295	PA(O-16:0/12:0)	1.06	0.98	Absent in SP
581.368	PS(22:0/0:0)	1.07	0.89	Absent in SP
638.414	PG(14:0/12:0)	0.85	1.17	Absent in SP
662.4139	PG(14:1(9Z)/14:1(9Z))	0.92	1.12	Absent in SP
755.5054	PS(O-16:0/17:1(9Z)):1-hexadecyl-2-(9Z-heptadecenoyl)-glycero-3-phosphoserine	0.96	0.99	Absent in SP
976.5501	PI(20:2(11Z,14Z)/22:4(7Z,10Z,13Z,16Z)):1-(11Z,14Z-eicosadienoyl)-2-(7Z,10Z,13Z,16Z-docosatetraenoyl)-glycero-3-phospho-(1'-myo-inositol)	1.02	0.94	Absent in SP
990.5409	PIP(16:0/20:1(11Z)):Phosphatidylinositol Phosphate	1.0346	0.93	Absent in SP
738.448	PG(14:1(9Z)/20:5(5Z,8Z,11Z,14Z,17Z))			1.63*(RRI)
740.4609	PG(14:1(9Z)/20:4(5Z,8Z,11Z,14Z))			5.09*** (RRI)
772.5038	PA(20:2(11Z,14Z)/22:6(4Z,7Z,10Z,13Z,16Z,19Z))			4.39***(RRI)

RM: Mock inoculated NIL with resistant *Fhb1* allele, SM: Mock inoculated NIL with susceptible *Fhb1* allele, RP: pathogen inoculated NIL with resistant *Fhb1* allele, SP: pathogen inoculated NIL with susceptible *Fhb1* allele, RRC; resistance related constitutive, RRI: resistance related induced

Student t-test *P* value: *** <0.001, ** <0.01, * <0.05, NS-Non significant

Table 4.5: Hydroxycinnamic acid amides (HCAAs) detected in wheat near isogenic lines with resistant/susceptible *Fhb1*alleles, inoculated with *F. graminearum*

Observed mass (Da)	**Metabolite**	**Fold change (NIL-R/NIL-S)**		
		Rachis 3dpi	**Spikelets 3dpi**	**Rachis 7dpi**
234.1365	*p*-coumaroylputrescine	0.96^{NS}	0.97^{NS}	0.89***
264.1468	Feruloylputrescine	0.96^{NS}	ND	0.85**
276.1579	4-coumaroylagmatine	0.96^{NS}	0.97^{NS}	0.93**
293.1642	4-coumaroyl-3-hydroxyagmatine	ND	1.03^{NS}	ND
306.136	Cinnamoylserotonin	ND	ND	0.82***
306.1684	Feruloylagmatine	0.95^{NS}	0.98^{NS}	0.88**
322.1309	*p*-coumaroylserotonin	ND	0.95^{NS}	0.95^{NS}
352.1414	Feruloylserotonin	0.91*	0.97^{NS}	0.96^{NS}

ND: Not detected, Student t-test *P* value: *** <0.001, ** <0.01, * <0.05, NS-Non significant

Table 4.6: *Triticum aestivum* contigs longer than 200 Kb identical to barley UDP-glycosyltransferase gene *HvUGT13248*

Chromosome	Contig	Mtaching region	% identity	Amplicon
2AS	2AS_5280303	209-706, 1018-1313	88, 87	UGT2
	2AS_5285656	1088-1417	79	UGT2
	2AS_5304694	144-516	80	
2BL	2BL_7888162	1018-1498	81	UGT2
2BS	2BS_5169942	84-581, 1024-1406	85, 80	UGT2
	2BS_5174254	30-352	80	
	2BS_5221073	704-1079, 1096-1424	78, 83	UGT2
	2BS_5245364	722-1020	82	UGT2
2DS	2DS_5298154	396-706	83	
	2DS_5321770	30-419, 469-703	79	
	2DS_5336342	30-706	81	
	2DS_5356097	1086-1424	80	UGT2
	2DS_5369360	88-706	87	
5AL	5AL_2682437	13-96, 1092-1428	94, 91	UGT1
	5AL_2739316	13-115	97	
	5AL_2754211	13-115	97	
	5AL_2798550	644-1020, 1018-1490	97, 93	UGT1
5BL	5BL_9618500	644-1020, 1092-1428	98, 91	UGT1
	5BL_10835715	1-166, 13-208	91, 94	
5BS	5BS_2251770	30-352	83	
5DL	5DL_4606679	644-1020, 1018-1520	98, 99	UGT1
5DS	5DS_2722475	30-703	82	

Fig. 4.1: Differentially accumulated deoxynivalenol (DON), DON-3-O-glucoside (D3G) and proportion of DON converted to D3G (PDC) in spikelets at 3dpi (A) and rachis at 7dpi (B) of wheat near isogenic lines (NILs) with resistant and susceptible *Fhb1* alleles inoculated with *F. graminearum*. TDP: total DON produced (DON+D3G). Error bars indicate standard error of mean

4.1 A.

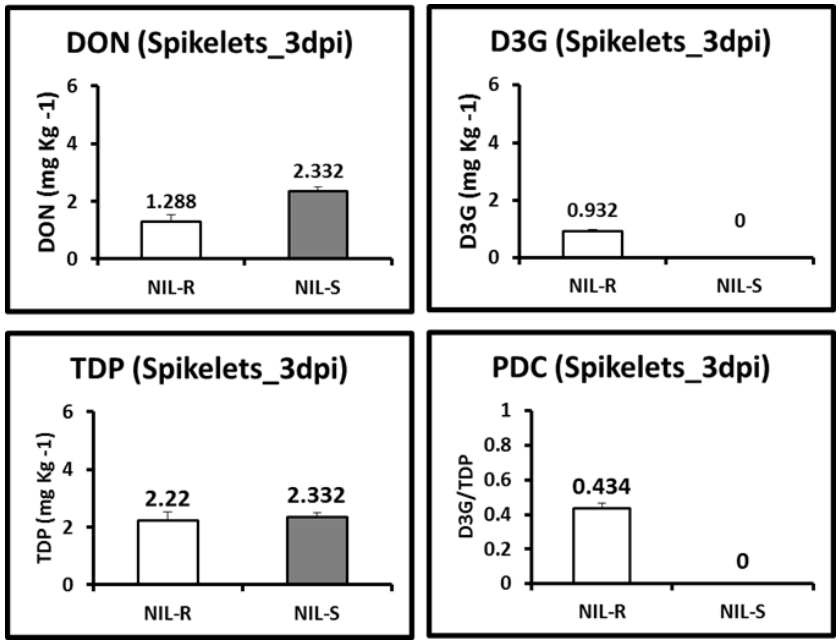

4.1 B.

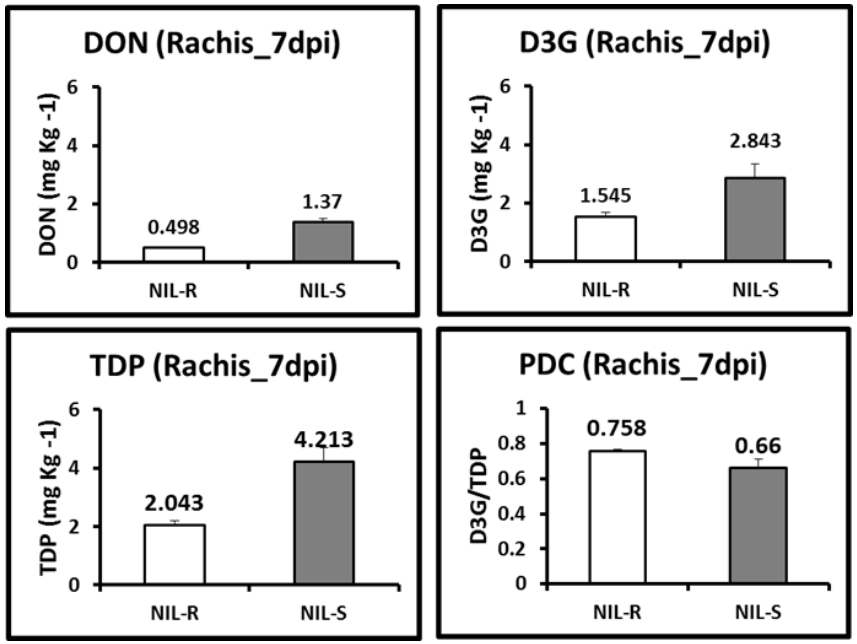

Fig. 4.2: Transcript expression of UDP-glycosyltransferase (UGT) and UDP-glucose dehydrogenase (UGDH) in wheat near isogenic lines (NILs) with resistant and susceptible *Fhb1* alleles inoculated with *F. graminearum*. UGT1: identical to barely UGT (HvUGT13248) at 929-1094, UGT2: 1204-1338, SXT: NILs derived from Sumai-3, Nyubai: NILs derived from Nyubai, dpi: days to post inoculation, NS: Non significant, significant at 0.05, ** significant at 0.01, error bars indicate standard error of mean.

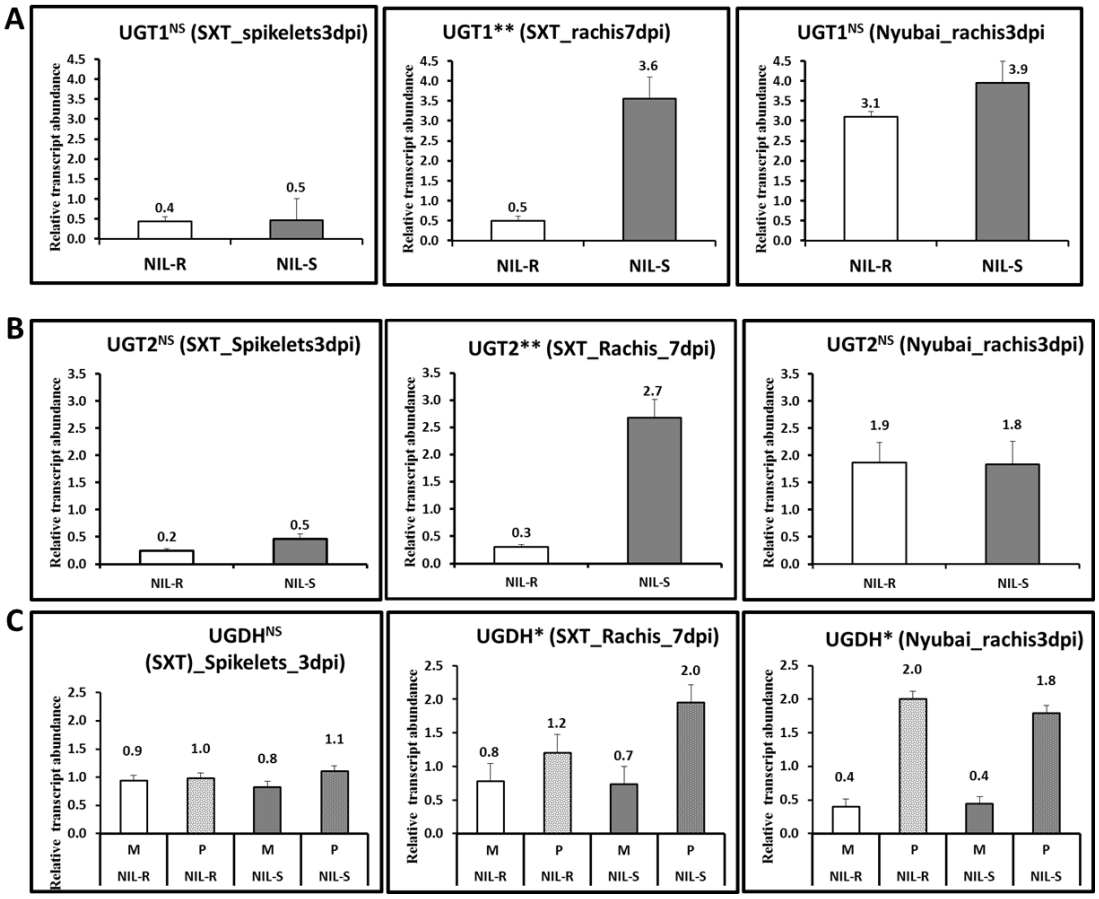

Fig. 4.3: Transcript expression of calmodulin binding protein (*TaCaMBP_Fhb1)* protein in wheat near isogenic lines (NILs) with resistant and susceptible *Fhb1* alleles inoculated with *F. graminearum*. SXT: NILs derived from Sumai-3, Nyubai: NILs derived from Nyubai, dpi: days to post inoculation. Error bars indicate standard error of mean

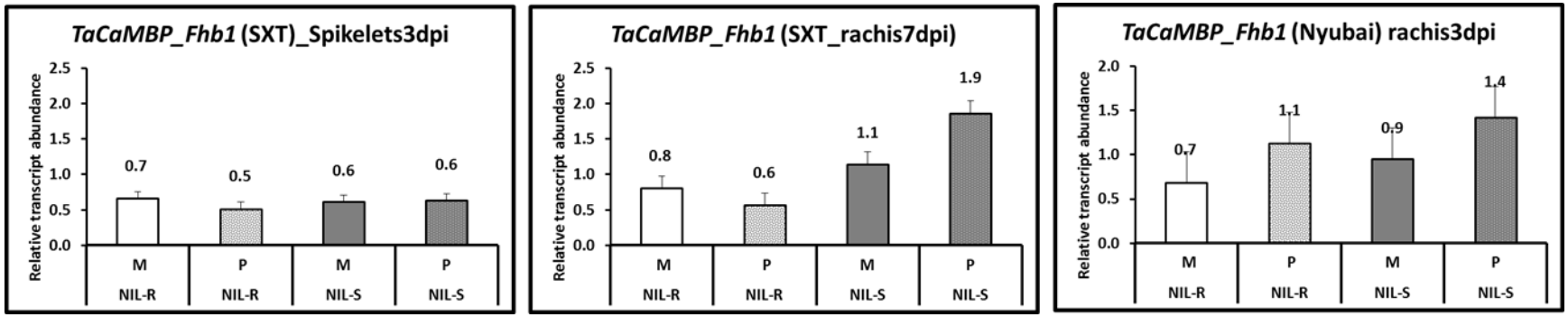

Fig. 4.4: Transcript expression of agmatine coumaroyltransferase (*AgCT*) in wheat near isogenic lines (NILs) with resistant and susceptible *Fhb1* alleles derived from Sumai-3, inoculated with *F. graminearum*. Error bars indicate standard error of mean

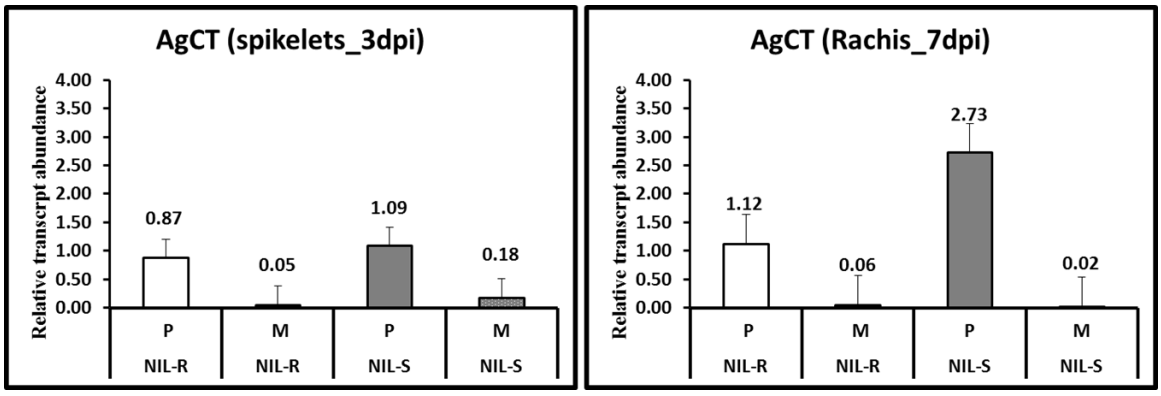

Fig. 4.5: Correlation of expression of UDP-glycosyltransferase (UGT) with total DON produced (TDP) wheat near isogenic lines (NILs) with resistant and susceptible *Fhb1* alleles derived from Sumai-3, inoculated with *F. graminearum*.

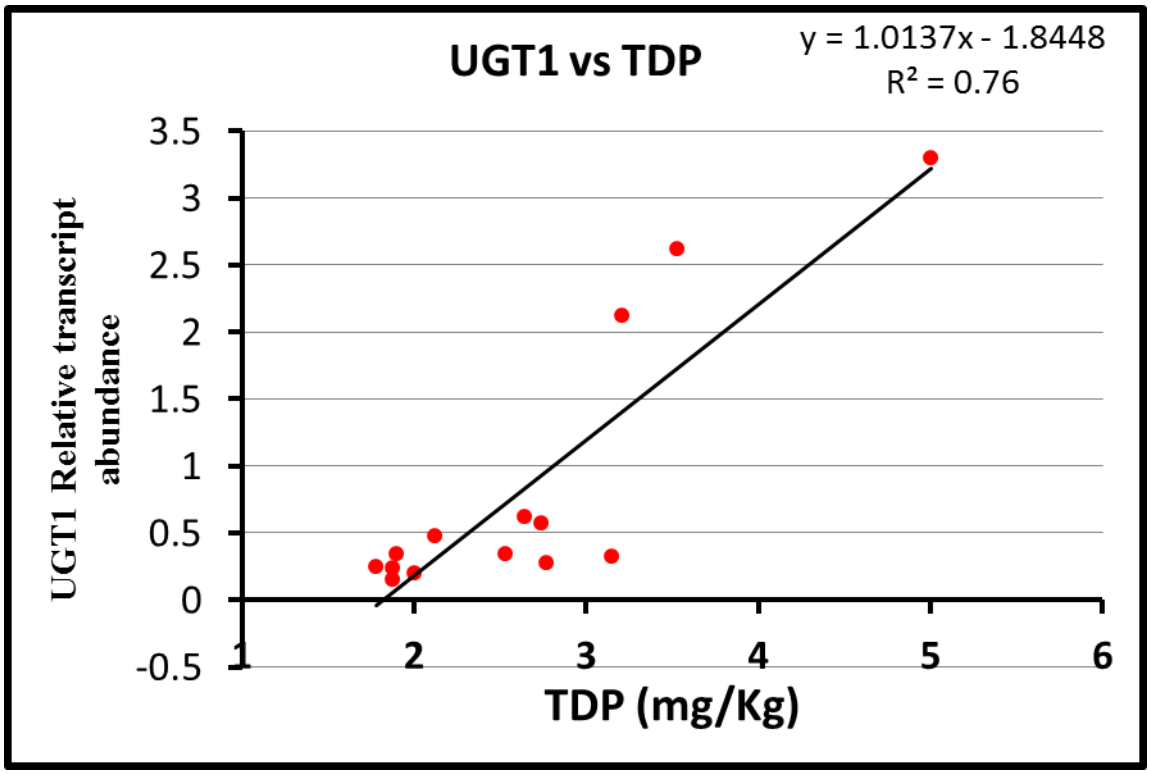

Fig. 4.6: Genomic DNA laddering in wheat near isogenic lines (NILs) with resistant and susceptible *Fhb1* alleles derived from Sumai-3 at 7dpi, inoculated with *F. graminearum*. 1: 100 bp DNA ladder, 2: NIL with susceptible *Fhb1* allele, 3: NIL with resistant *Fhb1* 4: 1 Kbp DNA ladder

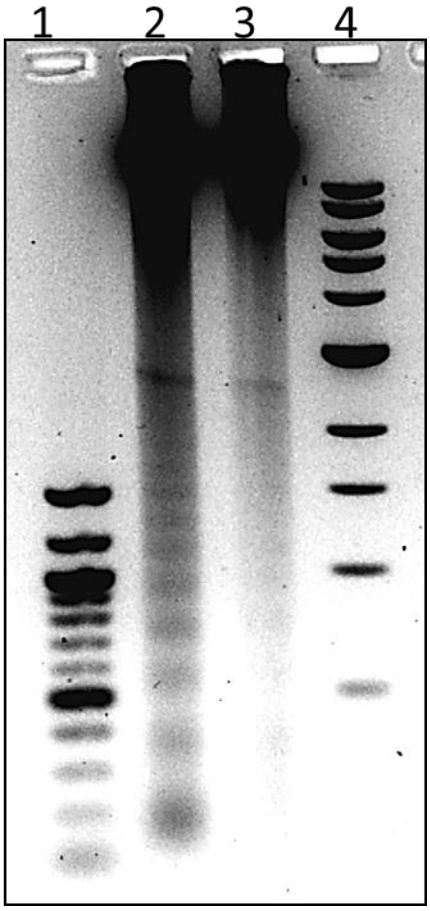

Fig. 4.7: Amplification of *Fhb1* candidate gene *TaCaMBP_Fhb1* in wheat near isogenic lines (NILs) with resistant (NIL-R) and susceptible (NIL-S) *Fhb1* alleles derived from Sumai-3

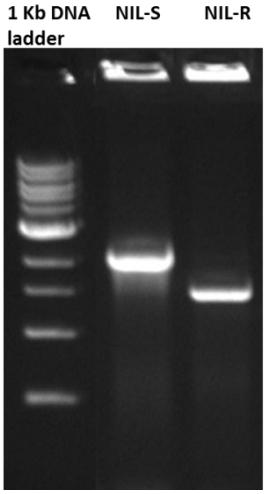

Fig. 4.7: Mechanism of FHB resistance (a): due to non-production of *TaCaMBP_Fhb1* coded calmodulin binding protein or lack of CaM binding domain and susceptibility (b) due to functional *TaCaMBP_Fhb1* induced PCD

a.

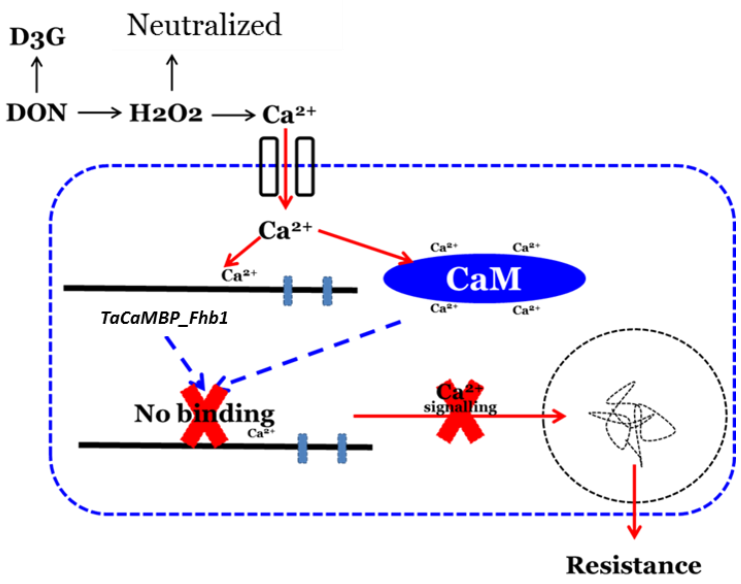

b.

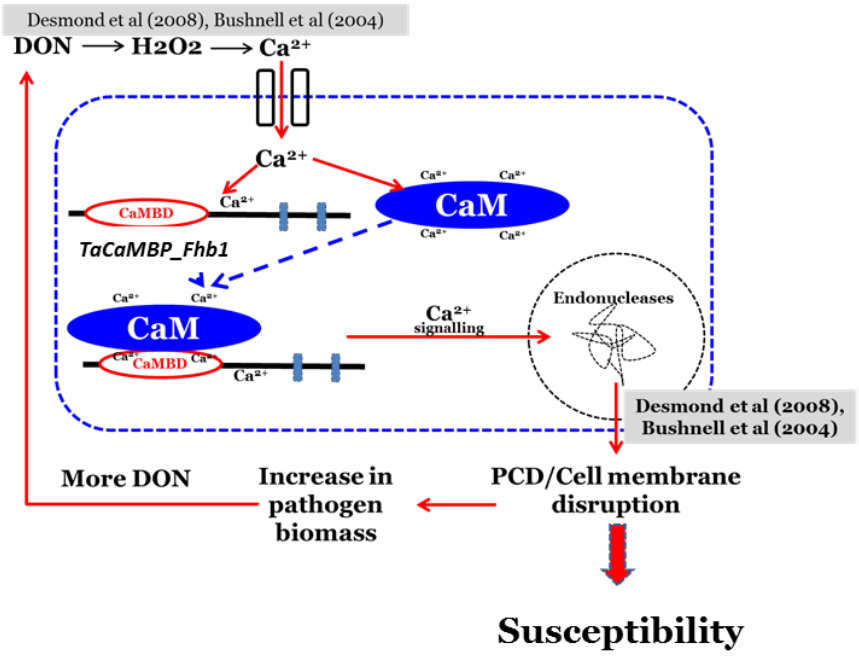

CONNECTING STATEMENT FOR CHAPTER V

Chapter V is a manuscript entitled "Metabolomics approach to decipher host resistance mechanisms in the wheat cultivar Sumai-3, against deoxynivalenol producing and non-producing *Fusarium graminearum"* authored by Raghavendra Gunnaiah and Dr. Kushalappa A.C. The manuscript will be submitted to a peer reviewed scientific journal.

In chapter III and IV, it was revealed that, over all resistance governed by a major type II FHB resistant QTL, *Fhb1* depends on the genotype from which it is derived and also the genotype into which it is introgressed. *Fhb1* from Nyubai, exhibited resistance to pathogen spread with increased cell wall thickening mainly at the rachis. Albeit, complete spike in NIL-R was bleached and dried up due to due to high DON accumulation. *Fhb1* from Sumai-3 exhibited resistance to both spread of the pathogen and also to DON accumulation. Both resistant and susceptible NILs derived from Sumai-3 accumulated many phenylpropanoid including HCAAs and flavonoids with high abundance indicating significant association with phenylpropanoid pathway. Sumai-3 is reported to possess inherent type II resistance in resisting the spread of pathogen through the rachis (Bai and Shaner, 2004). Confoundedly, Sumai-3 possesses a susceptible allele for DON detoxification, which is pathogen aggressiveness factor for resistance to spread (Handa et al., 2008). Hence, the following study was planned to understand the host resistance responses to disease spread at rachis against deoxynivalenol producing and non-producing *Fusarium graminearum.*

CHAPTER V

Metabolomics approach to decipher host resistance mechanisms in the wheat cultivar Sumai-3, against deoxynivalenol producing and non-producing *Fusarium graminearum*

Raghavendra Gunnaiah, Kushalappa A.C.

Plant Science Department, McGill University, Ste. Anne de Bellevue, Québec, Canada H9X3V9

5.1 ABSTRACT

Fusarium head blight (FHB) of wheat caused by *Fusarium* spp. is a global threat to wheat production. FHB causes severe economic damage by reducing grain yield and also by contaminating grain with trichothecene mycotoxins. Host resistance to FHB is quantitatively inherited and more than 100 QTLs have been mapped, but host resistance mechanisms are poorly understood. Non-targeted metabolic profiling was applied to elucidate host resistance mechanisms to disease spread in rachis of wheat cultivar Sumai-3, against trichothecene producing and non-producing isolates of *F. graminearum*. The accumulation of deoxynivalenol (DON) in Sumai-3 was low; however, the resistance to spread was not due to its detoxification into DON-3-O-gluciside (D3G), as the proportion of total DON converted to D3G was not significantly different from the susceptible cultivar Roblin. Instead, it was due to increased host cell wall thickening that limited pathogen spread by forming a rigid physical barrier, and also other antifungal or antioxidant metabolites that reduced both pathogen growth and trichothecene biosynthesis. Resistance in Sumai-3 to FHB was mainly associated with the phenylpropanoid pathway: preformed syringyl-rich monolignols and their glucosides that formed lignin; preformed flavonoids were antimicrobial; induced hydroxycinnamic acid amides enhanced cell wall thickening; cinnamic acids and iso-flavonoids were antimicrobial; lignans, induced by DON, that reduced reactive oxygen species that were induced by DON. Enhancement of resistance in wheat against FHB can be carried out through stacking of these candidate genes, along with DON-glycosyltransferases.

5.2 INTRODUCTION

Fusarium head blight (FHB) caused by *Fusarium graminearum* Schwabe (teleomorph *Gibberella zeae* (Schwein.) Petch) is one of the most destructive global diseases of wheat (*Triticum aestivum L.*). FHB causes significant reductions in grain yield and deteriorates grain quality by contamination them with trichothecene mycotoxins. The trichothecene deoxynivalenol (DON) is acutely toxic to eukaryotes, at relatively low concentration (< 1 ppm). DON inhibits protein synthesis by arresting host peptidyltransferase and pose serious health risks (Pestka, 2010). Breeding for FHB resistant cultivars is considered a viable and environmentally friendly approach to manage FHB. Host resistance to FHB is quantitatively inherited; more than 100 QTLs have been identified including a few with large effects: *Fhb1*, *Fhb2* and *Fhb5* are stably inherited (Buerstmayr et al., 2009). However, the pyramiding of these QTLs failed to significantly enhance FHB resistance (McCartney et al., 2007), due to limited knowledge of the genetic, molecular and biochemical mechanisms governed by these QTLs against *F. graminearum* and its aggressiveness factor DON.

Trichothecenes are phytotoxic and a type B trichothecene, deoxynivalenol (DON), is a pathogen aggressiveness factor which facilitates the movement of pathogen from the inoculated spikelet to the adjacent spikelets through rachis (Bai et al., 2002, Jansen et al., 2005). DON was found in cytoplasm, chloroplasts, plasma lemma, cell wall, vacuoles, and endoplasmic reticulum, moving ahead of the intruding fungal hyphae (Kang and Buchenauer, 1999). DON kills host cells by disrupting the cell membrane that causes cellular electrolyte leakage and an increase in cytoplasmic Ca^{2+} ions leading to its imbalance in cellular homeostasis (Bushnell et al., 2010, Cossette and Miller, 1995). Damaged host cells systematically transduce defense signals in the host, to produce reactive oxygen species (ROS) such as H_2O_2, which in turn trigger cell death (Desmond et al., 2008). Unlike in biotrophs, ROS induced cell death further facilitates the necrotrophic phase of *F. graminearum* colonization in necrotrophs, causing bleaching symptoms, instead of stopping the pathogen spread. Hence, aggressiveness of the pathogen depends on its DON-producing capacity, which in turn alters host defense mechanisms (Mesterházy, 2002).

The influence of DON on host resistance mechanisms has been studied at transcript and metabolite level by inoculating hosts with either different concentrations DON or *F. graminearum* mutant strains with loss of function of *Tri5* gene, which encodes trichodiene synthase, the first enzyme in the trichothecene biosynthetic pathway. Barley spikes treated with DON, expressed more transcripts related to DON detoxification and sequestration, such as UDP-glycosyltransferase and ABC transporters and also transcripts of proteins related to oxidative stress and host cell death. Contrarily, many host defense-related transcripts were down-regulated (Foroud et al., 2011, Gardiner et al., 2010, Walter et al., 2008). Similarly, the polyamines putrescine and its precursor ornithine were detected in the wheat cultivars Sumai-3 and Roblin following DON inoculation (Gardiner et al., 2010, Paranidharan et al., 2008). However, a higher concentration of DON might mask many of the true host defense responses to infection induced by *F. graminearum*, due to the protein synthesis inhibition activity of DON.

Alternatively, the use of DON producing (*FgTri5*$^{+}$) and DON non-producing mutant strains of *F. graminearum* (*FgTri5*$^{-}$) have revealed the masked host defense mechanisms. Similar to DON treatment, transcripts related to DON detoxification, DON sequestration, and cell death were up-regulated when inoculated with *FgTri5*$^{+}$ but were not up-regulated by the *FgTri5*$^{-}$ mutant strain in barley (Boddu et al., 2007). In addition, *FgTri5*$^{+}$ suppressed the expression of 18 host defense related transcripts, in contrast to a single transcript by the *FgTri5*$^{-}$ mutant. In wheat, more DON resistance-related transcripts were up-regulated in the FHB resistant wheat near isogenic lines (NILs) GS1-EM0040 and GS1- GS-1-EM0168 compared to the susceptible cultivar Superb following *FgTri5*$^{+}$ inoculation, at all-time points tested, but not with *FgTri5*$^{-}$ inoculated samples. In contrast, more transcripts of ribosomal proteins were down-regulated in Superb compared to the resistant NILs (Foroud et al., 2011). However, studying the influence of DON at the protein and metabolite level could give more insight into the host defense mechanisms, as DON inhibits protein synthesis. More RR metabolites were detected in barley genotypes inoculated with *FgTri5*$^{-}$ compared to those inoculated with *FgTri5*$^{+}$. The necrotrophic plant signalling molecule jasmonic acid was induced at higher levels in response to *FgTri5*$^{+}$ than to the *FgTri5*$^{-}$ strain. Plant defense compounds in the phenylpropanoid

pathway were either highly induced or induced only in response to *FgTri5*$^{-}$ inoculation, indicating defense suppression action of DON (Kumaraswamy et al., 2011). Studies have not been reported on masked host defense mechanisms using DON non-producing strains of *F. graminearum* at the protein or metabolite level in wheat.

The wheat cultivar Sumai-3 and its derivative cultivars are potential sources of FHB resistance in wheat breeding worldwide (Bai and Shaner, 2004). Sumai-3 has been consistently used as a donor parent for the major QTLs *Fhb1* and *Fhb2* on chromosomes 3B and 6B, respectively, for resistance to disease spread (type II), *Fhb5* on chromosome 5A for resistance to intimal infection (type I), and a minor QTL on 3BSc for type II resistance near the centromere region of 3BS (Buerstmayr et al., 2009). In parallel, Sumai-3 contributed negative alleles for FHB resistance at QTL regions on chromosomes 2AL and 4B (Anderson et al., 2001, Waldron et al., 1999). Sumai-3 also possesses a susceptible allele at the QTL on chromosome 2D coding for a multidrug resistance-associated protein, which is reported to be involved in DON sequestration (Handa et al., 2008). Elucidating the genetic, molecular and biochemical host defense mechanisms in Sumai-3 could aid in selecting suitable genes when Sumai-3 is used as resistance source in breeding.

Functional genomic approaches including transcriptomics, proteomics and metabolomics on Sumai-3 and its derivative cultivars have revealed diverse host defense mechanisms. Transcripts related to DON detoxification, oxidative stress, cell death and PR-proteins were induced following *F. graminearum* or DON inoculation in the Sumai-3 derived cultivars Ning8331 (Golkari et al., 2007), Ning-7840 (Bernardo et al., 2007, Kong et al., 2007) and CM82036 (Steiner et al., 2009, Walter et al., 2008). The role of jasmonic acid (JA) and ethylene (ET) signalling in FHB resistance and DON detoxification in Sumai-3 was demonstrated based on up-regulated transcripts of JA and ET pathways and JA/ET induced defense pathway (Gottwald et al., 2012, Li and Yen, 2008). In consistence with transcripts, PR-proteins and proteins related to oxidative burst, such as superoxide dismutase, dehydroascorbate reductase, and glutathione S-transferases (GSTs) were up regulated in Ning-7840 following *F. graminearum* inoculation (Zhou et al., 2005). In parallel, metabolomics of Sumai-3 derived *Fhb1*-containing NILs revealed diverse

resistance mechanisms related to cell membrane disintegration and cell death (Gunnaiah and Kushalappa 2013; Chapter IV). The transcript and protein studies could reveal only induced resistance mechanisms, such as defense signalling and resistance to oxidative burst in the spikelets. Organ-specific transcript regulation in glume, lemma, palea, anther, ovary and rachis (Golkari et al., 2007) and metabolite accumulation in spikelets and rachis (Gunnaiah et al., 2012), suggest that the host deploys different resistance mechanisms in different organs. In parallel, accumulation of lignin and β-glucans at the rachis in FHB resistant genotypes indicate that constitutive resistance plays a significant role in FHB resistance to spread (Kang et al., 2008). Sumai-3 is reported to possess inherent type II resistance in resisting the spread of pathogen through the rachis and DON a pathogen aggressiveness factor is considered to reduce disease spread. Consequently, the present study was designed to elucidate the host biochemical resistance to FHB spread in the rachis of Sumai-3 in response to trichothecene producing and non-producing isolates of *F. graminearum*. The study revealed substantial association of the phenylpropanoid pathway with FHB resistance.

5.3 MATERIALS AND METHODS

5.3.1 Plant Material

Seeds of the wheat cultivars Sumai-3 and Roblin were obtained from Agriculture and Agri-Food Canada, Winnipeg, Canada. Sumai-3 is a Chinese cultivar, highly resistant to FHB with both type I and type II resistance. Roblin is a high-protein; marquis type quality, early-maturing cultivar for the eastern prairies of Canada, highly susceptible to FHB. Plants were grown in the greenhouse, maintained at 25 ± 2^0 C, 70±10 % relative humidity and alternating 16 hrs of light and 8 hrs of darkness. Seeds were sown in 6 inch diameter pots filled with Growing Mix-PV20 (Fafard, QC, Canada) and three plants were retained from each pot after germination. Plants were watered when required and fertilized with 200 mL of 0.3 % NPK and 0.035 % micronutrients fortnightly.

5.3.2 Pathogen, spore production and inoculation

F. graminearum Schwabe trichothecene producing isolates, GZ3639 (*FgTri5*+) and trichothecene non-producing strain (*FgTri5*-) (obtained from Dr. Proctor, USDA, USA)

(Proctor et al., 1995) were maintained on potato dextrose agar. For spore production, cultures were grown on rye B agar with half the concentration of sucrose under 16 hr light and 8 hr dark, alternatively, for three days at 23 $\pm 2^0$C. Later, the culture plates were shifted to UV light chamber and grown under 16 hr UV light and 8 hr dark, for the next four days at 23 $\pm 2^0$C. From the seven day old cultures, mycelium was scraped and suspended in sterile water. Macroconidia were harvested by filtering off the mycelia using double layer cheese cloth. A spore suspension was prepared by adjusting the spore concentration to 10^5 spores mL^{-1}. For metabolic profiling, wheat plants at the growth stage 65 (50 % anthesis) were selected for inoculation and three alternate pairs of spikelets at the middle of the spike were point inoculated. Each spikelet was inoculated with 10 µl *FgTri5+* or *FgTri5-* or sterile water, according to the treatments, using a syringe with an auto dispenser (GASTIGHT 1750DAD W/S, Hamilton, Reno, NV, USA). For disease severity analysis, a single pair of spikelets at the middle of the spike was inoculated.

5.3.3 Disease severity assessment

The number of spikelets diseased was recorded at 3 day intervals until 12 days post inoculation (dpi). From these data, the proportion of spikelets diseased (PSD = number of spikelets diseased/total number of spikelets in a spike) and area under the disease progress curve (AUDPC) were calculated. A student's *t*-test was applied using SAS 9.3 to compare the AUDPC variation between two cultivars.

5.3.4 Sample collection, metabolite extraction and LC/MS analysis

For metabolite extraction, *F. graminearum* or mock inoculated spikes were harvested at 3 dpi. Rachis in between the top and bottom inoculated spikelets were collected, frozen immediately in liquid nitrogen and stored at -80^0C freezer until further use. Rachises were ground in liquid nitrogen using pre cooled mortar and pestle and metabolites were extracted with pre cooled 60% aqueous methanol as described previously (Bollina et al., 2010). The metabolites were analyzed using liquid chromatography coupled with high resolution hybrid mass spectrometers (LC-ESI-LTQ-Orbitrap, Thermo Fisher, Waltham, MA) as described previously (Bollina et al., 2010, Gunnaiah et al., 2012)

5.3.5 LC-MS data processing

Thermo Scientific, Xcalibur RAW files were converted to mzXML files using ReAdW version 4.3.1. Data were processed using user interactive LC/MS data processing software, *mzMine2* with high sensitive peak detection algorithm, XCMS *centwave* (Pluskal et al., 2010). Metabolites were identified by searching matching *m/z* values in PlantCyc, KEGG, LIPIDMAPS, METLIN and in house McGill-MD databases with <5 ppm accurate mass error and were confirmed with MS/MS fragmentation pattern in in house spiked MS/MS library MASSBANK, METLIN, MS2T and *in silico* fragmentation as described previously (Gunnaiah et al., 2012). List of peaks (deprotanated *m/z* values) along with their corresponding retention time, putative annotation and peak intensity in a matrix is exported to MS-Excel for further data processing.

5.3.6 Identification of resistance related (RR) metabolites

Peaks containing adduct and complex ions were removed from the data matrix and subjected to pair wise student *t*-test in RM versus SM, R*FgTri5*$^{+}$ versus RM, R*FgTri5*$^{-}$ versus RM, S*FgTri5*$^{+}$ versus SM and S*FgTri5*$^{-}$ versus SM using SAS9.3, where RM= mock inoculated Sumai-3, SM= mock inoculated Roblin, R*FgTri5*$^{+}$ = *FgTri5*$^{+}$ inoculated Sumai-3, R*FgTri5*$^{-}$ = *FgTri5*$^{-}$ inoculated Sumai-3, *SFgTri5*$^{+}$ = *FgTri5*$^{+}$ inoculated Roblin and SFgTri5^{-} = *FgTri5*$^{-}$ inoculated Roblin. R and S were used to represent resistant and susceptible genotypes, respectively, for Sumai-3 and Roblin. Peaks with student *t*-test *P* values <0.05 is considered significant. Further resistance related constitutive (RRC) and resistance related induced (RRI) metabolites with greater peak intensity in Sumai-3 in comparison to Roblin (Fold change >1.5) were calculated as follows: RRC = RM > SM, RRI-*FgTri5*$^{+}$= PRr *FgTri5*$^{+}$> PRs*FgTri5*$^{+}$ and RRI-*FgTri5*$^{-}$= PRr *FgTri5*$^{-}$> PRs*FgTri5*$^{-}$, where, PRr-*FgTri5*$^{+}$=R*FgTri5*$^{+}$> RM, PRs-*FgTri5*$^{+}$=S*FgTri5*$^{+}$> SM, and PRr-*FgTri5*$^{-}$=R*FgTri5*$^{-}$ > RM and PRs-*FgTri5*$^{-}$ =S*FgTri5*$^{-}$ > SM. Further, to know the effect of trichothecene producing and non- producing *F. graminearum* on resistance, the metabolites were statistically compared in the combinations of PRr-*FgTri5*$^{+}$ > PRr-*FgTri5*$^{-}$ and PRs-*FgTri5*$^{+}$ > PRs-*FgTri5*$^{-}$, respectively, for Sumai-3 and Roblin. Metabolites with fold change >1were considered as *FgTri5*$^{+}$ DON induced metabolites and <1 were considered as *FgTri5*$^{+}$ DON repressed

metabolites, individually in Sumai-3 and Roblin. The RR metabolites were mapped on their respective metabolic pathways using Cytoscape 2.8 (Smoot et al., 2011).

5.4 RESULTS

5.4.1 FHB severity

FHB resistance in the wheat cultivars Sumai-3 and Roblin was assessed by quantifying the spread of disease symptoms from the point inoculated spikelet to the adjacent un-inoculated spikelets in a spike. Initial symptoms were observed as dark brown colored necrotic patches on the inoculated spikelets at 2 dpi in both Sumai-3 and Roblin following *FgTri5*$^{+}$ and *FgTri5*$^{-}$ inoculation. Necrotic patches were restricted to the inoculated spikelets in both Sumai-3 and Roblin in *FgTri5*$^{-}$ inoculated spikes, and only in Sumai-3 in *FgTri5*$^{+}$ inoculated spikes during the period of study. In contrast, necrotic symptoms were spread to spikelets above and below the *FgTri5*$^{+}$ inoculated spikelet in Roblin. In addition to necrotic symptoms, bleaching of spikelets was observed at 6 dpi in Roblin. On average, 2 bleached spikelets were observed at 6 dpi that increased to 5 bleached spikelets at 9 dpi and the entire spikelet was dried up by 12 dpi in Roblin. Bleached spikelets were not observed in Sumai-3 until 12 dpi. Both necrotic spikelets and bleached spikelets were considered as diseased spikelets in assessing disease severity. The disease progress, quantified based on proportion of spikelets PSD, varied drastically between cultivars (Fig. 5.1). The highest AUDPC was noted in Roblin (5.98), significantly (P<0.001) differing from Sumai-3 (1.35); in the latter, there was no spread of disease symptoms during the period of study.

5.4.2 Accumulation of DON, 3ADON and D3G

The *F. graminearum* produced trichothecene mycotoxins, DON and 3ADON, and the host detoxified product of DON, D3G, were quantified using standard curves developed by spiking different concentrations of DON, 3ADON and D3G, in high resolution LC/MS (Fig. 5.2). The amounts of DON (1.16 mg kg^{-1}) and 3ADON (0.56 mg kg^{-1}) were significantly (P<0.05) higher in the susceptible cultivar Roblin as compared to DON (0.59 mg kg^{-1}) and 3ADON (0.33 mg kg^{-1}) accumulated in Sumai-3. Accordingly, the amount of D3G (1.44 mg kg^{-1}) and TDP (2.59 mg kg^{-1}) accumulated was also

significantly higher in Roblin compared to D3G (0.86 mg kg^{-1}) and TDP (1.45 mg kg^{-1}) in Sumai-3. Surprisingly, the DON detoxification, measured as proportion of DON conversion (PDC), was quite high in both Sumai-3 (PDC=0.58) and Roblin (PDC=0.56), with no significant difference.

5.4.3 Differential accumulation of metabolites in Sumai-3 and Roblin

The metabolites in rachis at 3 dpi were profiled in Sumai-3 and Roblin following *F. graminearum* (*FgTri5*$^+$ and *FgTri5*$^-$) and water inoculation, based on high resolution LC-MS. 2618 consistent peaks were detected in all the treatment combinations. Following pairwise *t*-tests, 331 RRC metabolites were identified. To evaluate the role of DON on host resistance, RRI metabolites were separately identified for the *FgTri5*$^+$ and *FgTri5*$^-$ strains of *F. graminearum*, which are represented as RRI- *FgTri5*$^+$ and RRI-*FgTri5*$^-$. Comparatively, more metabolites were induced by *FgTri5*$^-$ (RRI-*FgTri5*$^-$ =139) compared to the wild type, *FgTri5*$^+$ (RRI-*FgTri5*$^+$ =98). Among them, 44 were common to both RRI-*FgTri5*+ and RRI-*FgTri5*- (Fig. 5.3) and for most of the metabolites, the fold change in abundance was higher in RRI-*FgTri5*$^-$ than in RRI-*FgTri5*$^+$. Eleven metabolites were common to RRC and RRI-*FgTri5*$^-$, but none of the RRC metabolites was identified as RRI-*FgTri5*$^+$. Putatively identified metabolites and their MS/MS fragmentation match are presented in Appendix 5.1. The majority of the RR metabolites (49 %) are in the phenylpropanoid pathway and can further be classified into downstream pathways of flavonoids, hydroxycinnamic acid amides, lignans, monolignols and their glucosides (Fig. 5.4). The second major class of metabolites belonged to terpenoids (14 %), including mono, di, tri and sesquiterpenoids and their glucose conjugates. Other RR metabolites detected were nine amino acids and their derivatives, six cell-wall bound carbohydrates and their conjugates, five each of antioxidant phenolic compounds and carboxylic acids and three each of fatty acids and alkaloids (Appendix 5.1).

5.4.4 Resistance related constitutive (RRC) metabolites

Of 331 RRC metabolites, 80 were putatively identified (Table 5.1). The majority were glucose conjugates of monolignols, flavonoids and terpenoids. Sumai-3 rachis was rich in syringyl lignin precursors: sinapoyl alcohol and sinapladehyde with > 2 fold change and

glucose conjugate of sinapoyl alcohol, syrinign (FC>1.54). In addition, guacoyl lignin monomer glucosides such as coniferin and dihydroconiferyl alcohol glucoside were also significantly higher in Sumai3 rachis. Diferulic acid, the most abundant hydroxycinnamic acid in wheat, was detected with high fold change (FC= 3.42). 22 metabolites belonging to flavonoid biosynthesis pathway were identified as RRC metabolites. These were mainly sugar conjugated isomers of kaempferol, naringenin, catechin, cyanidin, isooreintin and other flavonoids (Table 5.1). Flavonoids with high fold change (FC>4) were: pisatin (a phytoalexin), 5'-prenylhomoeriodictyol, pneumatopterin A, naringenin 7-O-(2",6"-di-O-alpha-rhamnopyranosyl)-beta-glucopyranoside, naringenin 7-O-(2",6"-di-O-alpha-rhamnopyranosyl)-beta-glucopyranoside, isovitexin 2"-O-(6"'-feruloyl)glucoside, and isoorientin 4'-O-glucoside-2"-O-(E)-caffeate. Interestingly, the abundance of flavonoid glucosides was decreased following *F. graminearum* inoculation and their reduction was higher when inoculated with *FgTri5*$^{+}$. Three lignans: pinoresinol, (+)-medioresinol di-O-beta-glucopyranoside, and carolignan-E also accumulated in rachis of Sumai-3 with high abundance (FC>4).

Of 18 the identified terpenoids, 14 were constitutively present with significantly higher abundance in Sumai-3. Among them, two antimicrobial monoterpene iridoids, lamioside (FC=10.78), harpagoside (FC=8.07), eleganin (a sesquiperpene lactone, FC=5.11) and two triterpenoids: bruceine B (FC=8.07) and isobruceine A (FC=8.11) were detected. Three amino acids: serine, histidine and L-tryptophan, and an amino acid derivative, N-succinyl-L-amino-6 oxopimelate were constitutively higher in Sumai-3 than in Roblin. Interestingly, the polyamine precursor amino acid, L-trytophan was found with very high abundance (FC=6.91) in Sumai-3. Apart from this large group of metabolites, many other precursor metabolites, carboxylic acids, fatty acids, carbohydrates and their conjugates, cell wall bound sugars and alkaloids with antimicrobial activity were also identified as RRC metabolites (Table 5.1, Appendix 5.1).

5.4.5 Resistance related induced (RRI) metabolites, following wild and mutant pathogen inoculation

Of 193 RRI metabolites, 53 were putatively identified (Table 5.1, Appendix 5.1). The RRI metabolites were classified as RRI-*FgTri5*$^{+}$ and RRI-*FgTri5*$^{-}$. Among 53 RRI

metabolites, 15 were common to both RRI-*FgTri5*$^{+}$ with greater fold change in RRI (*FgTri5*$^{-}$). 25 metabolites were exclusively identified as RRI-*FgTri5*$^{-}$ with decreased accumulation in RRI-*FgTri5*$^{+}$, and 13 were exclusively identified as RRI-*FgTri5*$^{+}$ with decreased accumulation in RRI-*FgTri5*$^{-}$.

Similar to RRC metabolites, the majority (22) of the RRI metabolites were phenylpropanoids. Coniferaldehyde was identified as an RRI metabolite in both pathogen treatments; however the fold change decreased with *FgTri5*$^{+}$ inoculation. Interestingly, four hydroxycinnamic acid amides (HCAAs) were detected as RRI-*FgTri5*$^{-}$ only with reduced abundance of 5-O-feruloylquinic acid and N-caffeoylputrescine, and in contrast there was no significant fold change in 4-coumaroyl-3-hydroxyagmatine and feruloylserotonin following *FgTri5*$^{+}$ inoculation in Sumai-3. Among flavonoids, 4 were identified as RRI-*FgTri5*$^{+}$ only, six were RRI-*FgTri5*$^{-}$ only and three flavonoids, lupinisoflavone G, chalconaringenin 2'-rhamnosyl-(1->4)-xyloside and (+)-syringaresinol O- β-D-glucoside, were common to both isolates. Seven lignans were identified as RRI-*FgTri5*$^{-}$ metabolites in contrast to just two in RRI-*FgTri5*$^{+}$. (+)-pinoresinol 4-o-(6-ogalloyl)-β-D-glucopyranoside was detected as an RRI metabolite in both isolates-inoculations, with very high fold change.

Surprisingly, the plant defense signalling compound jasmonic acid (JA) was not identified as an RR metabolite in either *FgTri5*$^{+}$ or *FgTri5*$^{-}$ inoculations. It was highly induced in Roblin compared to Sumai-3 following both *FgTri5*$^{+}$ and *FgTri5*$^{-}$ inoculations. The fold change in JA was higher in *FgTri5*$^{+}$ (PRr*FgTri5*$^{+}$=2.07, PRs*Tri5*$^{+}$ = 4.33) inoculations compared to *FgTri5*$^{-}$ inoculations (PRr*FgTri5*$^{-}$ =1.04, PRs*Tri5*$^{-}$ = 1.50) in both cultivars.

Among other RRI metabolites, five monoterpenoids were identified as RRI-*FgTri5*$^{-}$ against two in RRI-*FgTri5*$^{-}$. 7-deoxyloganin was accumulated with very high fold change, 14.58 and 8.08 as RRI-*FgTri5*$^{-}$ and RRI-*FgTri5*$^{+}$, respectively. Five phenolic compounds with antioxidant properties were identified as RRI-*FgTri5*$^{-}$ against three in RRI-*FgTri5*+. One alkaloid: vellosimine, two amino acids: L-asparagine and N-methyl β-alanine, dopaquinone and indole-3-butyryl-glucose were identified as RRI-*FgTri5*-metabolites. Oxaloacetic acid, a precursor metabolite for many primary and secondary

metabolites, was identified as RRI for both inoculations (*FgTri5*$^{-}$ and *FgTri5*$^{+}$), with higher fold change in RRI-*FgTri5*$^{-}$.

5.4.6 Relative accumulation of metabolites following inoculation with *FgTri5*$^{+}$ and *FgTri5*$^{-}$ isolates of *F. graminearum.*

To explore the host resistance mechanisms masked due to the protein synthesis inhibitory properties of DON, the differential accumulation of metabolites in rachis between *FgTri5*$^{+}$ and *FgTri5*$^{-}$ inoculated Sumai-3 and Roblin were compared. Surprisingly, *FgTri5*$^{+}$ (DON) induced metabolites were greater in the susceptible cultivar Roblin (249) than in the resistant cultivar in Sumai-3 (105). In contrary, more metabolites were repressed in Sumai-3 (74) than in Roblin (27). Most of the DON-induced metabolites in Sumai-3 were also identified as RRI-*FgTri5*$^{+}$ metabolites. The *FgTri5*$^{+}$ induced metabolites in Roblin mainly were in the polyamine biosynthesis pathway. Many of the *FgTri5*$^{+}$DON repressed metabolites in Sumai-3 were also identified as RRI-*FgTri5*$^{-}$ metabolites. Those repressed in Roblin mainly were in the phenylpropanoid, terpenoid and alkaloid pathway.

5.5 DISCUSSION

5.5.1 Resistance to Fusarium spread in Sumai-3 is associated with reduced spread of necrosis, bleaching and DON

A non-targeted metabolic profiling of rachis tissue was carried out to reveal the host resistance mechanisms in a FHB resistant wheat cultivar, Sumai-3, in comparison with a susceptible cultivar, Roblin, following inoculation with a DON producing isolate of *F. graminearum* (*FgTri5*$^{+}$), a DON non-producing isolate (*FgTri5*$^{-}$) and water as mock inoculation. FHB severity in terms of disease spread within a spike (type II resistance), assessed following point inoculation with (*FgTri5*$^{+}$) in the greenhouse, revealed significant difference in resistance between two cultivars. Confirming earlier findings, Sumai-3 exhibited absolute resistance to disease spread, with no symptoms spreading to the adjacent spikelets (Hamzehzarghani et al., 2005). In contrast, the susceptible cultivar Roblin was highly susceptible to *F. graminearum* infection. In addition to spread of necrotic symptoms due to colonization of the pathogen, spikelets were bleached ahead of

necrotic spikelets due to DON accumulation. Disease symptoms failed to spread to the adjacent spikelets in the *FgTri5*$^{-}$ inoculated spikes in both Sumai-3 and Roblin. DON is a pathogen aggressiveness factor for disease spread (Bai et al., 2002) and induces premature bleaching (Lemmens et al., 2005), leading to drying of entire spikes. Biochemical mechanisms of host resistance to *FgTri5*$^{+}$ and *FgTri5*$^{-}$ in Sumai-3 can be explained based on the metabolites that accumulated in high abundance in rachis.

***DON and conjugated products*:** Very low amounts of DON, D3G and TDP were accumulated in rachis of Sumai-3 at 3 dpi compared to Roblin. Even though PDC was moderately high in both Sumai-3 and Roblin, there was no significant difference between them (Fig. 5.2). DON is detoxified by host UDP-glycosyltransferases, which conjugate DON with glucose to produce the less toxic D3G (Poppenberger et al., 2003). Sumai-3 and its derivative genotypes which possess a resistant *Fhb1* allele was believed to localize or regulate the expression of a UDP-glycosyltransferase that detoxifies DON, and thus, resists the spread of *F. graminearum* (Lemmens et al., 2005). However, no significant difference in the proportion of DON conversion (PDC) was observed between the resistant cultivar Sumai-3 and the highly susceptible cultivar Roblin despite high disease spread in the latter. Homologous sequences to barley DON detoxifying UDP-glycosyltransferases (*HvUGT1324*) were located on wheat chromosomes other than *Fhb1* containing chromosome 3B: 2AS, 2BL, 2BS, 2DS, 5AL, 5BL, 5BS, 5DL and 5DS ((Schweiger et al., 2010); Chapter IV). Also, the expression of a wheat homologue of *HvUGT1324* correlated with the TDP, irrespective of the *Fhb1* allele. It was hypothesized that *Fhb1* neither localizes nor regulates UDP-glycosyltransferase. Instead, *Fhb1* localizes a non-functional *TaCaMBP_Fhb1* gene that rescues host cells from PCD and stops pathogen proliferation by depriving of nutrients to the necrotrophic *F. graminearum* (Chapter IV). Similar to Roblin in this study, a moderately high PDC was also observed in the NILs with susceptible genome background of a Canadian spring wheat 98B69*L47 (Gunnaiah et al., 2012). With evidences from these three different genotypes, we hypothesize that the susceptible wheat cultivars Roblin and 98B69*L47 also code for UDP-glycosyltransferases capable of detoxifying DON at a moderately high levels, similar to Sumai-3. Interestingly, at 3 dpi, DON and its glucose conjugate was not

detected in the rachis of either NIL with resistant and susceptible *Fhb1* alleles, which were developed by repeated backcrossing to Sumai-3 (Chapter IV). It is possible that during backcrossing, the NILs lost the Sumai-3 FHB susceptible allele at 2D, which is hypothesized to localize a gene coding for a DON sequestering, multidrug resistance-associated protein (MRP) (Handa et al., 2008). The Initial low amount of DON in the NILs might be sequestered by MRP compared to their resistant parent, Sumai-3. However, more studies are needed to confirm the variation in UDP-glycosyltransferase activity in detoxifying DON in Sumai-3 and its derivatives in comparison to other susceptible genotypes. Nevertheless, based on the evidence in the present investigation, we hypothesize that resistance to spread in Sumai-3 is due to biochemical mechanisms other than DON detoxification by UDP-glycosyltransferases.

5.5.2 Role of DON/trichothecenes in resistance and susceptibility

More RR metabolites accumulated in rachis of Sumai-3 following *FgTri5*$^{-}$ inoculation (RRI-*FgTri5*$^{-}$ = 139) compared to *FgTri5*$^{+}$inoculation (RRI-*FgTri5*$^{+}$ = 98), and also the RRI fold change was lower in the *FgTri5*$^{+}$ induced compared to *FgTri5*$^{-}$ induced, for most of the common RR metabolites. Reduced number of RR metabolites or reduced fold change following infection with a trichothecene producing strain of *F. graminearum* is caused by DON, which inhibits eukaryotic protein translation including enzymes catalyzing synthesis of several of the RR metabolites (Pestka, 2010). Similarly, fewer RR metabolites were induced in barley following trichothecene producing *F. graminearum* inoculation compared to its trichothecene non-producing counterpart (Kumaraswamy et al., 2011a). DON inhibitory action on host resistance was also evidenced at the transcript level with down regulated transcripts, following inoculation with DON or trichothecene producing *F. graminearum* in wheat (Foroud et al., 2011) and barley (Boddu et al., 2007).

5.5.3 Resistance to spread in Sumai-3 due to constitutive metabolites

***Phenylpropanoids*:** Sumai-3 had higher levels of several RRC metabolites, most strikingly the precursors of lignin, lignans, a cinnamic acid, diferulic acid and flavonoids. Sinapaldehyde and sinapyl alcohol are precursors of syringyl lignin biosynthesis. Coniferin and syringin are stored glucosides of monolignols, coniferyl alcohol and

sinapyl alcohol respectively, which are incorporated into lignin (Rolando et al., 2004, Vanholme et al., 2010). Higher amounts of preformed monolignol glucosides and syringyl lignin precursors in the rachis of Sumai-3 and further reduction in their abundance following pathogen inoculation implicates, that these monolignols are polymerized into lignin with syringyl rich units and enhance cell wall thickening to restrict the spread of pathogen. Similarly, a higher density of lignin was deposited at the cell walls of infected tissue in Sumai-3 compared to the susceptible cultivar (Kang et al., 2008). Concurrently, syringyl lignin units were increased in the cell walls of resistant wheat cultivars following rust elicitor treatment, increasing the syringyl/guacoyl (S/G) lignin ratio, which confers high resistance to pathogen attack (Menden et al., 2007). Concurrently, three lignans: (+)-pinoresinol, (+)-medioresinol di-O-beta-glucopyranoside and threo-carolignan E were also detected in the rachis of Sumai-3 in high abundance. The precursor of guacoyl lignin, coniferyl alcohol is diverted to form lignans, thus reducing guacoyl lignin and consequently increasing the S/G ratio, which also boosts resistance with their antimicrobial properties. Further, a cinnamic acid (diferulic acid, RRC FC=3.42) can play dual roles. Cinnamic acids, including ferulic acid, reduce the growth of *F. graminearum* and also the biosynthesis of trichothecenes (Bollina and Kushalappa, 2011, Boutigny et al., 2009). In addition, ferulic acid plays a pivotal role in cross linking lignin and flavonoids with other RRC metabolites, such as cell wall bound sugars 1,4-β-xylobiose, feruloyl-3-(arabinosylxylose), cis-*p*-coumaric acid 4-[apiosyl-(1->2)-glucoside], β-D-fructosyl-a-D-(6-O-(E))-feruloylglucoside (Ralph et al., 1998).

Flavonoids: 22 metabolites belonging to shunt phenylpropanoid/flavonoid biosynthesis pathway accumulated in the rachis of Sumai-3 as RRC metabolites. The RRC catechins catechin 5,7,3'-trimethyl ether, epicatechin 3-O-(3-O-methylgallate) and 4-methyl-(-)-epigallocatechin 7-glucuronide are precursors of proanthocyanidins. The preformed flavonoids pisatin (FC=9.8) and naringenin 7-O-(2",6"-di-O-α-rhamnopyranosyl)-β-glucopyranoside and other *flavones:* isoorientin 4'-O-glucoside-2"-O-(E)-caffeate (a luteolin), isovitexin 2"-O-(6"'-feruloyl) glucoside (an apigenin) and other kaempferol glucosides (Table 5.1) are strong antioxidants. Flavan-3-ols (+)-catechin and (–)-epicatechin are the building blocks of proanthocyanidins (Dixon et al., 2005). The

catechin polymers, proanthocyanidins, are deposited at the cell walls, making them more rigid along with the syringyl rich lignin, reducing pathogen spread. Similarly, preformed proanthocyanidins in the testa layer prevented the penetration of hyphae of *Fusarium* spp. in barley (Skadhauge et al., 1997) and flavonoids were accumulated at the cell wall of wheat rachis following *F. graminearum* inoculation (Gunnaiah et al., 2012). Dihydroxy B ring flavonoids, quercitins and luteolin and monohydroxy B ring flavonoids, apigenin and kampferol are oxygen radical scavengers during biotic and abiotic stresses, the former dihydroxy B ring flavonoids being stronger (Agati et al., 2012, Hernández et al., 2009). These flavones are transported to the site of ROS generation as glucosides and glutathione conjugates. Scavenging of ROS by these flavones is catalyzed by the flavonoid oxidizing P450 monooxygenases, peroxidases and polyphenol oxidases (Hernández et al., 2009). Other flavonoids such as pisatin, naringenin and their glucosides have been reported to have antifungal activities (Huang et al., 2010). Naringenin, kaempferol and their glucosides were often identified as RRC metabolites in barley, and naringenin inhibited the growth *F. graminearum in vitro* (Bollina et al., 2010, Bollina et al., 2011, Kumaraswamy et al., 2011, Kumaraswamy et al., 2011).

5.5.4 Resistance to spread in Sumai-3 due to induced metabolites

Increased cell wall thickening

Importance of the phenylpropanoid pathway in Sumai-3 against FHB was also evidenced with many of the RRI metabolites belonging to the class of hydroxycinnamic acid amides (HCAA), flavonoids and lignans. HCAAs that play dual roles in pathogen resistance as phytoalexins and cell wall strengthening agents were induced by *F. graminearum* infection. However, only three HCAAs, N-caffeoylputrescine, 4-coumaroyl-3-hydroxyagmatine and feruloylserotonin, were identified as RRI metabolites in Sumai-3 and the rest were highly induced in both Sumai-3 and Roblin, with significant differences between them. Roblin is highly resistant to rust and HCAAs were induced in response to any stress (Bassard et al., 2010, Campbell and Czarnecki, 1987). Similarly, HCAAs were induced in the NIL with the resistant *Fhb1* allele derived from Nyuabi, and in both the NILs carrying resistant and susceptible alleles derived from the Sumai-3, following *F. graminearum* inoculation, which were shown to deposited at the cell walls enhancing

resistance to spread (Gunnaiah et al., 2012); chapter IV). It should be noted that the former NIL had a susceptible genetic background while the latter had resistant. Deposition of induced HCAAs further increased the cell wall thickening, thus reducing pathogen spread among spikelets within spike.

5.5.4 Inhibition of pathogen growth and trichothecene biosynthesis by antimicrobial and anti-oxidant metabolites: Flavonoids, especially flavones, flavonones and isoflavonoids, lignans and other phenolic compounds were induced in Sumai-3 following *F. graminearum* inoculation (Table 5.1). Flavonoids such as furano[2',3':6,7] aurone, epigallocatechin, lupinisoflavone G, apigenin 7-o-rutinoside and 3,4\',6\'-trihydroxy-4,2\'-dimethoxychalcone 4\'-O-rutinoside, which are induced by both *FgTri5*$^{+}$ and *FgTri5*$^{-}$ or only by *FgTri5*$^{-}$ inhibit the growth of *F. graminearum*. Rhamnetin, 4',5,6,7-tetramethoxyflavone, kaempferol-3-rhamnoside and chalconaringenin 2'-rhamnosyl-(1->4)-xyloside induced by *FgTri5*$^{+}$ either inhibit the growth of the pathogen or neutralize ROS produced by DON. Most of the flavonoids are either antioxidants in neutralizing ROS produced under various stress or antimicrobial (Agati et al., 2012, Huang et al., 2010). Both preformed flavonoids and induced flavonoids inhibit the growth of *F. graminearum* and (or) biosynthesis of trichothecenes, similar to antioixidants (Boutigny et al., 2008). Many flavonoids were also induced following *F. graminearum* inoculation in barley cultivars (Bollina et al., 2010, Kumaraswamy et al., 2011) and in wheat (Gunnaiah et al., 2012); Chapter IV). Eight metabolites belonging to lignans were also identified as RRI metabolites. Lignans are dimerized isomers of phenylpropanes, especially coniferyl alcohol (Naoumkina et al., 2010). Lignans such as (+) – pinoresinol, which also is the precursor of many other oligomeric lignans, have shown antifungal and cytotoxic activities (Hwang et al., 2010). In addition, ligans might also neutralize the DON induced ROS, in the presence of oxidases during radical coupling of monomers into lignans, catalyzed by the host proteins (Davin and Lewis, 2000).

Phenylpropanoids are plant secondary metabolites implicated in host defense function as signalling molecules, preformed phytoanticipins and inducible phytoalexins (Naoumkina et al., 2010). The importance of the phenylpronapoid pathway in FHB resistance is also evidenced at the transcript level, with up-regulation of transcripts of phenylalanine

ammonia lyase, the driver of the phenylpropanoid pathway in resistant genotypes following *F. graminearum* inoculation (Foroud et al., 2011, Golkari et al., 2009, Steiner et al., 2009). Increased cell wall thickening in Sumai-3 due to deposition of syringyl lignin, flavonoids and HCAAs reduce the spread of pathogen leading to low pathogen biomass in host tissues that produce less DON. Consequently, low DON is converted to D3G by host UDP-glycosyltransferases and ROS such as H_2O_2 induced by DON is neutralized by the antioxidant phenolic acids, flavonoids and lignans.

Signaling molecules: Surprisingly, jasmonic acid (JA), which is often associated with FHB resistance, was not identified as an RRI metabolite. It was induced in both Sumai-3 and Roblin with higher abundance following infection with trichothecene producing *F. graminrearum.* DON kills host tissue by inhibiting protein synthesis and inducing ROS such as H_2O_2 that promotes necrosis for the pathogen to feed on dead tissues. The host senses the necrotrophy and induces JA signalling, which further induces downstream host defenses. JA signalling is induced in both Sumai-3 and Roblin. However, Roblin failed to induce downstream defense response as in Sumai-3. Similarly, transcripts of the JA signalling pathway were induced in Sumai-3 following *F. graminearum* inoculation (Gottwald et al., 2012, Li and Yen, 2008) and in another type II FHB resistant wheat landrace, Wangshuibai and its FHB susceptible mutant with deleted *Fhb1* region, but the transcripts of downstream defense responses were induced only in Wangshuibai (Xiao et al., 2013). JA signalling is induced as a defense response to necrotrophs but its downstream defense responses regulate the host resistance.

Resistance to FHB spread in Sumai-3 was mainly associated with phenylpropanoids and its shunt pathways through cell wall thickening by deposition of lignins, preformed flavonoids and induced HCAAs. The resistance is further enhanced by the antifunagl cinnamic acids such as ferulic acid and elimination of DON induced ROS by the isoflavones and lignans. However, the genes regulating the biosynthesis of phenylpropanoids were not found on the major QTL, *Fhb1,* except a putatively identified gene, near to *Fhb1* locus, coding for hydroxyl cinnamoyltransferase that catalyzes the biosynthesis of HCAAs (Choulet et al., 2010, Gunnaiah et al., 2012). Other major QTLs, *Fhb5* and *Fhb2* on the chromosomes 5A and 6B, respectively, have to be explored to

better explain the mechanisms. DON detoxification by UDP-glycosyltransferases in Sumai-3 was similar to the susceptible cultivar Roblin, and the trichothecene producing *F. graminearum* repressed many inherent host resistance mechanisms. The inherent host resistance, otherwise repressed by DON, can be further exploited in wheat breeding with stacking genes that detoxifies or sequesters DON, such as UDP-glycosyltransferases (Schweiger et al., 2010) and multi-drug resistance proteins (Handa et al., 2008).

Table 5.1: Resistance related metabolites induced in rachis of wheat cultivar Sumai-3, inoculated with water or *F. graminearum*, relative to a susceptible cultivar Roblin

Observed mass (Da)[a]	**Metabolite Name**	**RRC**	**RRI-** ***FgTri5+***	**RRI-** ***FgTri5-***
Phenylpropanoids (Aldehydes, monolignols and monolignol glucosides)				
178.0627	Coniferaldehyde	0.81^{NS}	**1.33****	**2.15****
208.0578	Sinapaldehyde	**2.42***	0.16	0.76
210.0888	Sinapyl-alcohol	**2.19*****	0.91	1.11
312.12	4-Hydroxycinnamyl alcohol 4-D-glucoside	0.92 ^{NS}	**1.64***	1.9
342.1305	Coniferin	**1.77****	0.44	0.95
344.1462	Dihydroconiferyl alcohol glucoside	**2.81****	1.58	1.45
372.1407	Syringin	**1.54***	1.02	0.79
386.0978	Diferulic acid	**3.42****	0.92	0.89
Phenylpropanoids (Hydroxycinnamic acid amides)				
250.1282	N-Caffeoylputrescine	ND	0.56	**1.25***
292.1529	4-coumaroyl-3-hydroxyagmatine	ND	1.06	**1.39***
352.1416	Feruloylserotonin	ND	1.06	**2.77***
368.1097	5-O-Feruloylquinic acid	ND	0.26	**2.15*****
474.1725	6-Feruloylglucose 2,3,4-trihydroxy-3-methylbutylglycoside	0.3NS	**1.5****	**1.62****
Phenylpropanoids (Flavonoids)				
262.0655	Furano[2",3":6,7] aurone	1.47 ^{NS}	1.21	**1.62***
306.0753	Epigallocatechin	1.04 ^{NS}	0.34	**1.34***
316.0786	Rhamnetin	0.38NS	**1.89***	1.71
316.094	(+)-Pisatin	**9.28*****	0.96	1.47
326.0992	Jacareubin	**2.62*****	1.26	1.09
326.1147	Methylophiopogonone B	**2.4*****	0.99	1.33
332.1253	Catechin 5,7,3'-trimethyl ether	**3.84****	1.02	1.39
340.1303	Sophoraflavanone B	**2.73****	1.19	1.61

342.1089	4',5,6,7-Tetramethoxyflavone	0.46NS	**1.63***	1.45
344.0889	Quercetin 7,3',4'-trimethyl ether	**2.03***	0.63	0.71
370.1408	5'-Prenylhomoeriodictyol	**4.51****	1.48	1.84
388.1148	5-Hydroxy-7,2',3',4',5'-pentamethoxyflavone	**1.87***	1.17	1.36
402.1485	Ulexone B	**2.41***	0.64	0.73
422.1712	Lupinisoflavone G	0.18NS	**2.62*****	**5.35****
432.1047	kaempferol-3-rhamnoside	0.26NS	**7.83****	4.2
456.1077	Epicatechin 3-O-(3-O-methylgallate)	**2.59*****	0.41	0.69
462.1184	Isoscoparine	**2.62***	0.83	0.86
490.1831	5-Hydroxy-7,4'-dimethoxy-6,8-di-C-prenylflavanone 5-O-galactoside	**2.08****	0.38	**1.2***
492.1258	Malvidin 3-O-glucoside	**2.25***	0.56	0.74
496.1204	4-Methyl-(-)-epigallocatechin 7-glucuronide	0.6NS	0.89	**1.27****
550.1672	Chalconaringenin 2'-rhamnosyl-(1->4)-xyloside	1NS	**2.51*****	**2.45****
578.168	Apigenin 7-o-rutinoside	**2.56*****	1.12	**1.56***
624.2022	3,4\',6\'-Trihydroxy-4,2\'-dimethoxychalcone 4\'-O-rutinoside	0.39NS	1.18	**1.27***
626.2182	Pneumatopterin A	**10.74*****	0.57	1.21
638.2183	4'-Hydroxy-5,7,2'-trimethoxyflavanone 4'-rhamnosyl-(1->6)-glucoside	**1.65*****	0.83	0.94
726.2339	Naringenin 7-O-(2",6"-di-O-alpha-rhamnopyranosyl)-beta-glucopyranoside	**6.56****	0.56	1
770.2024	Isovitexin 2"-O-(6"'-feruloyl)glucoside	**4.62****	0.77	0.75
772.1819	Isoorientin 4'-O-glucoside-2"-O-(E)-caffeate	**4.91****	1.54	1.58
862.2136	Cyanidin 3-[6-(6-p-hydroxybenzoylglucosyl)-2-	**1.79****	0.85	0.83

	xylosylgalactoside]			
884.2323	Salviamalvin	**1.97***	0.25	0.85
934.2336	Isoorientin 4'-O-glucoside-2"-(4-glucosylcaffeate)	**1.7***	0.85	0.83
Phenylpropanoids (Lignans)				
358.141	(+)-pinoresinol	**7.27****	0.45	0.69
360.1564	(+)-lariciresinol	1.57NS	0.79	**1.3***
374.1357	Hydroxypinoresinol	0.92NS	1.09	**1.54***
414.1278	(-)-Podophyllotoxin	0.27NS	1.11	**2.59****
540.1652	Cleistanthin A	0.76NS	0.73	**1.78****
580.2146	(+)-Syringaresinol O-beta-D-glucoside	0.32NS	**1.55*****	**3.98*****
596.2234	Kadsulignan	1.37NS	**1.24****	**1.35***
672.2069	(+)-pinoresinol 4-o-(6-ogalloyl)-bets-D-glucopyranoside	0.13NS	**5.2*****	**7.14***
702.2173	Ramontoside	0.87NS	0.31	**2.2***
712.2563	(+)-Medioresinol di-O-beta-glucopyranoside	**4.22*****	1.03	0.37
730.2608	threo-carolignan E	**4.15*****	0.59	1.32
Terpenoids				
328.115	Anisatin	**2.26***	1.22	1.28
330.1459	Podolide /Gibberlin A7	**2.02****	0.88	1.33
346.1254	Aucubin	**1.79****	1.12	**1.52***
358.1255	Tarennoside	0.25NS	**1.24*****	**3.3****
374.1202	Secologanate	1.0NS	0.24	**1.24*****
374.1559	7-deoxyloganin	0.05NS	**8.08*****	**14.5****
376.1513	Ailanthone	**2.21****	0.79	0.45
376.1515	Ailanthone	**2.78****	0.94	0.76
390.1514	loganin	**1.72****	1.05	0.98
420.1615	Lamioside	**10.78*****	0.67	1.26

426.1928	(+)-Abscisyl beta-D-glucopyranoside	1.53NS	1.8	**1.75***
434.1567	Eleganin	**5.11****	0.7	0.9
440.1131	Hallactone B	**2.02***	0.6	0.97
480.162	Bruceine B	**8.07****	0.25	0.63
488.2618	alpha-Ionol O-[arabinosyl-(1->6)-glucoside]	**1.7***	1.06	0.94
494.1775	Harpagoside	**7.33*****	1.14	1.21
520.2496	3b,6a-Dihydroxy-alpha-ionol 9-[apiosyl-(1->6)-glucoside]	**2.09****	1.13	0.64
522.2086	Isobrucein A	**8.11*****	0.9	1.17
Carbohydrates and conjugates				
180.0632	β-D-glucose	0.88NS	1.43*	1.81
185.9927	2-phospho-D-glycerate	1.0NS	1.79***	1.0
282.0945	(1,4)-β-xylobiose	2.74***	0.79	1.24
458.1404	Feruloyl-3-(arabinosylxylose), cis-p-Coumaric acid 4-[apiosyl-(1->2)-glucoside]	1.84**	0.74	0.82
472.157	β-D-fructosyl-a-D-(6-O-(E))-feruloylglucoside	4.12**	0.78	0.93
474.1725	6-Feruloylglucose 2,3,4-trihydroxy-3-methylbutylglycoside	0.3NS	1.5**	1.62**
Amino acids and their derivatives				
103.0635	N-methyl-β-alanine	0.87NS	1.04	**1.48****
105.0427	D-serine	**1.74***	0.46	0.65
119.0583	D-threonine	0.48NS	**1.62*****	1.04
132.0535	L-asparagine	1.05NS	1.03	1.29*
146.0691	L-glutamine	0.45NS	**1.78***	1.28
155.0694	Histidine	**3.78*****	0.67	1.03
204.0818	L-tryptophan,	**6.91****	0.81	1.13
261.0426	O-phospho-L-tyrosine	0.35NS	**1.51***	1.5

289.0844	N-Succinyl-L-amino-6-oxopimelate	**10.38*** **	0.93	0.89
Carboxylates				
74.0006	Glyoxylate/Oxaloacetiec acid	0.86NS	**1.4** **	**2.05** **
116.011	maleate	**2.26***	0.51	0.72
134.0215	(S)-Malate	**1.61** **	0.77	0.87
192.0632	L-quinate	0.57NS	**1.54** **	1.98
270.1097	Benzoyl -β -D -glucopyranoside	**2.69** **	1.02	1.02
Fatty acids and conjugates				
254.188	3-hydroxy-15-dihydrolubimin	1.9**	1.2	1.38
322.1628	Butyl 3-O-β -D-glucopyranosyl-butanoate	9.52***	0.83	0.67
332.1827	(2S,3S)-2-hydroxytridecane-1,2,3-tricarboxylate	0.83NS	1.32**	1.96**

[@] Fold change calculation: were based on relative intensity of metabolites, RRC= RM/SM, RRI= (RP/RM)/(SP/SM)

RRC: resistant related constitutive, RRI-*FgTri5*$^{+}$: resistant related metabolites induced by trichothecene producing *F. graminearum*, RRI-*FgTri5*$^{-}$: resistant related metabolites induced by trichothecene non-producing *F. graminearum*, Da: Daltons,

Student t-test *P* value: *** <0.001, ** <0.01, * <0.05, NS-Non significant

Fig.5.1: Fusarium head blight progress in wheat cultivars, Sumai-3 and Roblin, inoculated with *Fusarium graminearum*. PSD: Proportion of spikelets diseased=no. of diseased spikelets/total no. of spikelets in a spike, dpi: days post inoculation

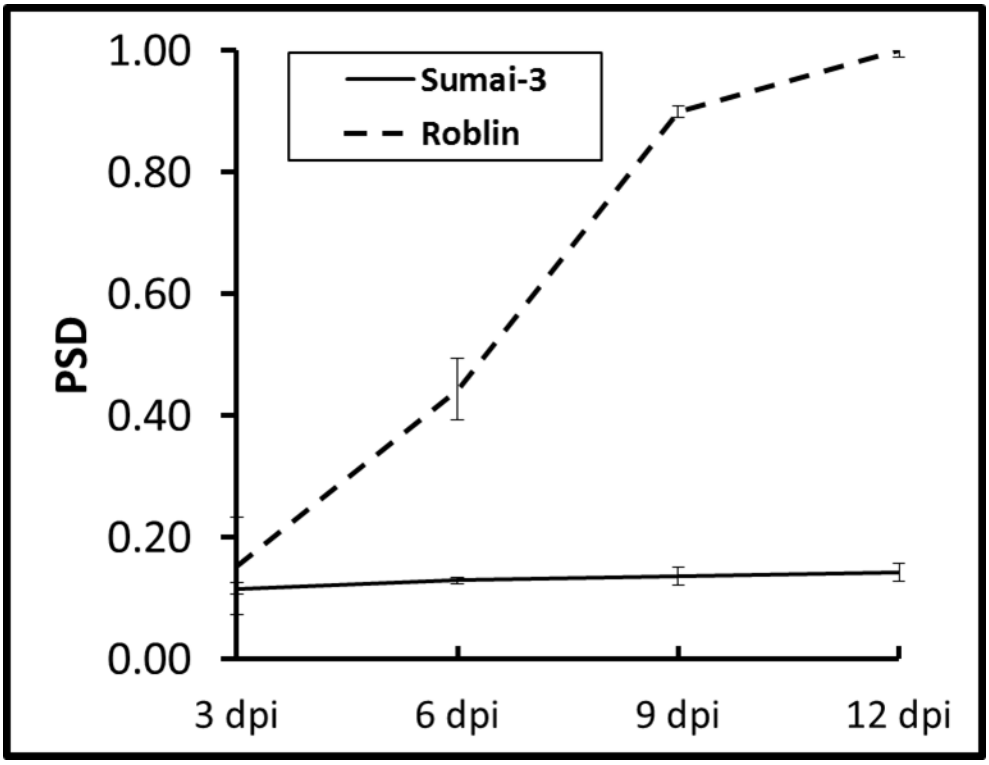

Fig. 5.2: Accumulation of deoxynivalenol (DON), 3-acetyl DON (3-ADON) and DON-3-O-glucoside (D3G), in the rachis of wheat cultivars, Sumai-3 and Roblin inoculated with *Fusarium graminearum*. TDP= total DON produced, PDC=proportion of TDP converted to D3G. Error bars indicate standard error of mean

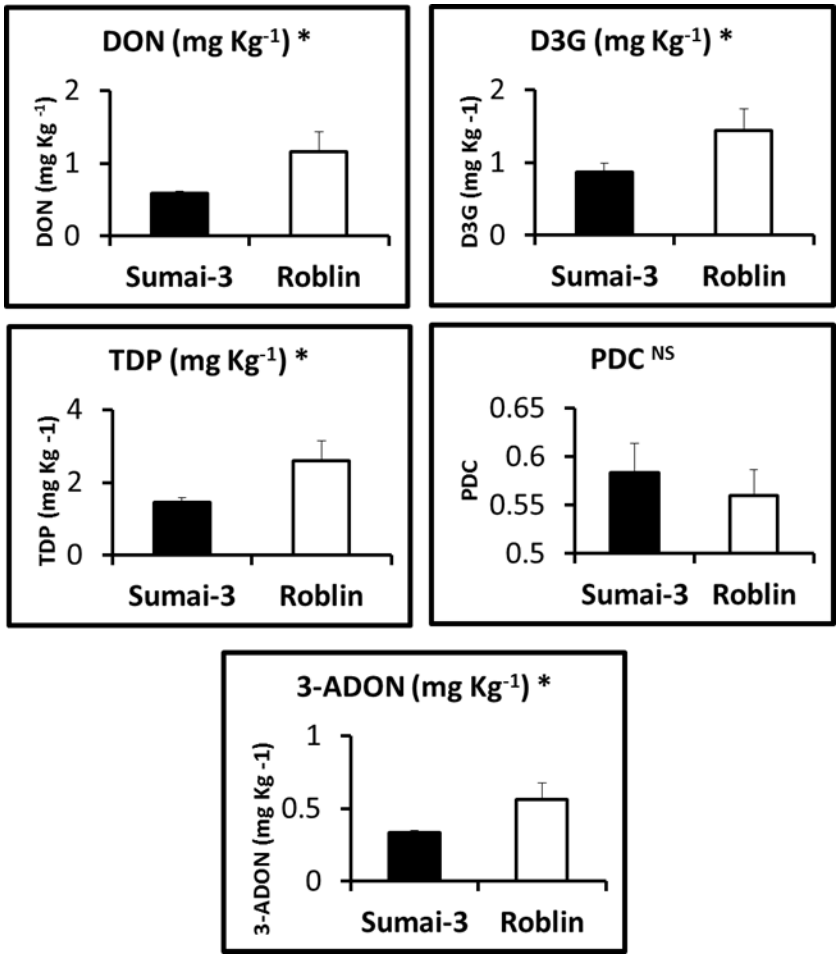

Fig. 5.3: Number of resistance related metabolites identified in the rachis of wheat cultivar, Sumai-3, inoculated with water or *F. graminearum.* RRC=resistance related constitutive, RRI (*FgTri5+*) =resistance related induced metabolites, induced by trichothecene producing *F. graminearum*, RRI (*FgTri5-*) =resistance related induced metabolites, induced by trichothecene non-producing *F. graminearum*

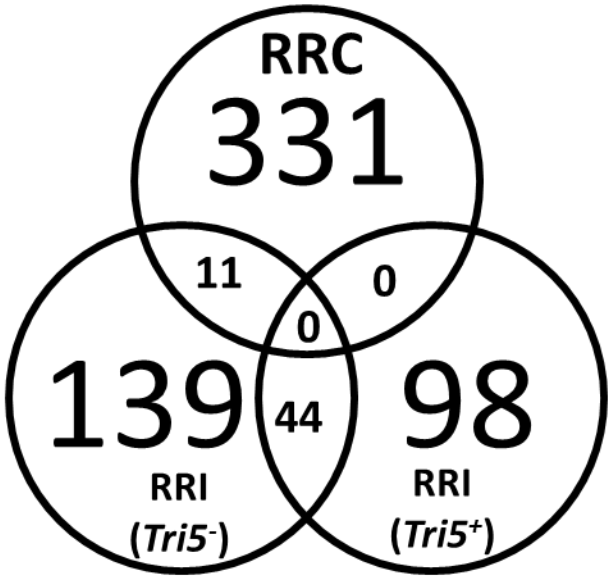

Fig. 5.4: Diverse groups of resistance related metabolites induced in the rachis of wheat cultivar, Sumai-3, inoculated with water or *F. graminearum.*

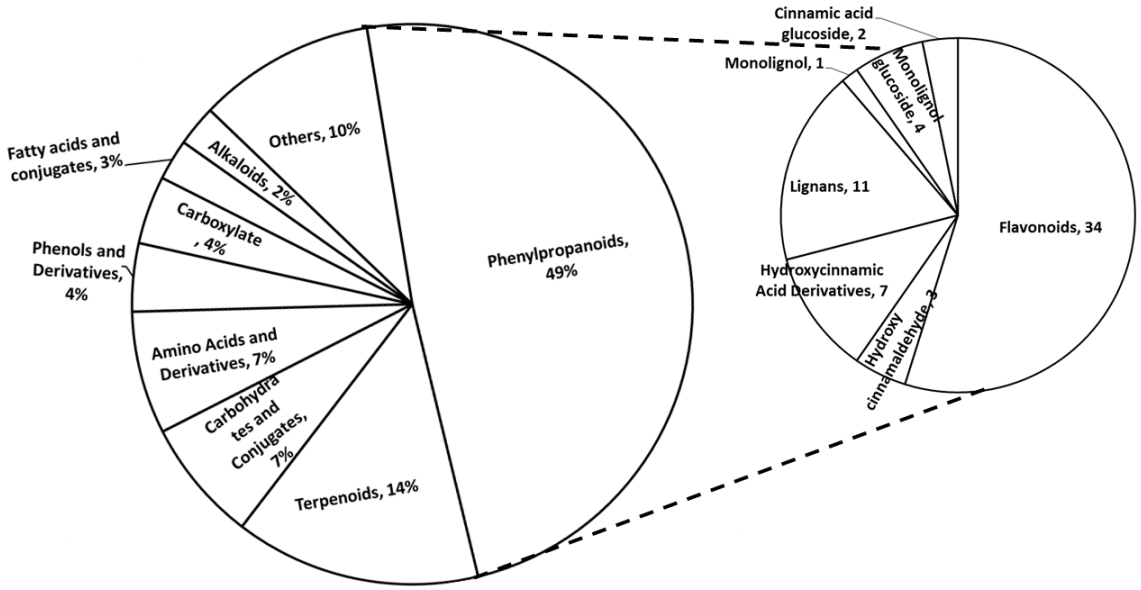

CHAPTER VI

GENERAL DISCUSSION, SUMMARY AND SUGGESTIONS FOR FUTURE RESEARCH

6.1 GENERAL DISCUSSION AND SUMMARY

Fusarium head blight (FHB) of wheat (*Triticum aestivum* L) caused by *Fusarium graminearum* Schwabe [teleomorph *Gibberella zeae* (Schweinitz) Petch] has re-emerged as a disease of global significance. The fungus survives saprophytically in crop residues, spores are disseminated through wind, rain and insects, and infects the plants during anthesis and grain development under favourable warm and humid conditions (Bushnell et al., 2003). During infection, *F. graminearum* produces a group of sesquiterpenoid trichothecene mycotoxins. Type B trichothecenes such as deoxynivalenol (DON), and its acetylated derivatives 3-acetyl DON (3ADON) and 15-acetyl DON (15ADON), and nivalenol (NIV) are most commonly produced by *F. graminearum* (Xu and Nicholson, 2009). DON is a pathogen aggressiveness factor for FHB spread from spikelet to spikelet through the rachis, which kills host tissue in advance for fungal saprophytic feeding (Bai et al., 2002, Jansen et al., 2005, Kang and Buchenauer, 1999). Seeds if developed in the FHB infected spikes will be shrivelled due to wilting and drastically reduces the grain yield (Steffenson et al., 2003). Seeds from FHB infected spikes are contaminated with trichothecene mycotoxins, which cause serious health risks in animals and human beings, and reduce the crop value in the market (Pestka, 2010). Development of resistant genotypes is considered as the most efficient, viable and environmentally friendly approach for management of FHB (Bai and Shaner, 2004).

Host resistance to FHB is quantitatively inherited and development of resistant genotypes through conventional breeding is challenging (Bai and Shaner, 1994). For convenience, FHB resistance in wheat has been classified into five components, however only three types: type I resistance (resistance to initial infection), type II resistance (resistance to spread) and type III resistance (resistance to DON accumulation) are commonly followed in wheat breeding (Bai and Shaner, 2004, Schroeder and Christensen, 1963, Wang and Miller, 1988). More than 100 FHB resistant quantitative trait loci (QTLs) have been

identified in wheat and few major QTLs *Fhb1*, *Fhb2*, *Fhb4* and *Fhb5* and a QTL on 2D have been identified, in different mapping populations and validated (Buerstmayr et al., 2009). However, the resistance mechanisms governed by these QTLs are poorly understood.

Fhb1 is the most consistent and largest effect QTL for resistance to FHB spread identified from different resistant genotypes: Sumai-3 and its derivatives (Anderson et al., 2001, Waldron et al., 1999), Wangshuibai (Lin et al., 2004) and Nyubai (Somers et al., 2003). *Fhb1* was fine mapped as a Mendelian gene within 1.2 cM between STS142 and STS180 (Cuthbert et al., 2006) and was further narrowed down to a 261 Kb region that localizes seven genes (Liu et al., 2008). However, none of the genes showed resistance on transfer to a susceptible cultivar. *Fhb1* was hypothesized to co-localize with a gene for UDP glycosyltransferase, which detoxifies DON into the less toxic DON-O-glucoside (D3G), or regulates its expression (Lemmens et al, 2005). Conversely, *Fhb1* doesn't localize any genes coding for UDP-glycosyltransferase (Choulet et al., 2010) and regulation of UDP-glycosyltransferase by *Fhb1* remains to be investigated. A few comparative transcript analysis studies have hinted association of *Fhb1* with susceptibility (Jia et al., 2009, Xiao et al., 2013, Zhuang et al., 2013). Nonetheless, *Fhb1* candidate genes are still unknown.

"Omics" have been well utilized in elucidating host resistance mechanisms against FHB (Kushalappa and Gunnaiah, 2013). Host defense responses in wheat and barley through defense signalling, production of PR proteins and anti-oxidative proteins, DON detoxification, and production of antifungal metabolites have been revealed based on non-targeted transcript profiling (Foroud et al., 2011, Gardiner et al., 2010, Jia et al., 2009), protein profiling (Geddes et al., 2008, Zhou et al., 2005) and metabolic profiling (Bollina et al., 2010, Bollina et al., 2011, Hamzehzarghani et al., 2005, Kumaraswamy et al., 2011, Kumaraswamy et al., 2011). The integration of transcriptomics, proteomics and metabolomics using bioinformatics tools can be used to identify the function of un-annotated genes (Tohge and Fernie, 2010). This study was planned to identify FHB resistance related genes localized at the major FHB resistant QTL in wheat, *Fhb1*, by non-targeted profiling of metabolites and proteins that are associated with the phenotype.

It was hypothesised that wheat near isogenic lines (NILs) with resistant and susceptible *Fhb1* alleles differentially accumulate constitutive and *F. graminearum* induced resistance related metabolites and proteins, and the differential accumulation is governed by genes localized at the *Fhb1* locus. To test this hypothesis, three objectives were formulated: 1) To determine host's biochemical resistance mechanisms governed by wheat FHB QTL *Fhb1,* derived from the cultivar Nyubai, against spread of *F. graminearum* based on non-targeted metabolomics and proteomics profiling of NILs with resistant and susceptible *Fhb1* alleles; 2) To confirm the function of *Fhb1* candidate genes derived from wheat cultivar Nyubai, with those derived from wheat cultivar Sumai-3, based on differentially accumulating metabolites and/or proteins and validating the candidate genes by transcript expression analysis and 3) To confirm host resistance mechanisms in a FHB resistant cultivar Sumai-3 in comparison to a susceptible cultivar Roblin. Accordingly, the investigation was divided into three studies to test and confirm the hypothesis presented, as three chapters III, IV and V.

In chapter III, non-targeted metabolic profiling of wheat NILs carrying resistant (NIL-R) or susceptible (NIL-S) *Fhb1* alleles derived from the moderately resistant cultivar Nyubai, with a susceptible genome background were carried out. Wheat plants were grown under greenhouse conditions until anthesis (Growth stage (GS)-65). Three pairs of alternative spikelets on a spike were inoculated with either spore suspension of *F. graminearum* (10 µl of 10^5 spores mL^{-1} per spikelet) or sterile water, for metabolic and proteomic profiling. For FHB severity assessment, a single pair of spikelets at the middle of the spike was inoculated and incubated. Inoculated spikelets and rachis between two extreme inoculated spikelets were harvested at 72 hpi, immediately frozen in liquid nitrogen and stored at -70 ± 5^0 C. FHB severity was assessed by counting number of diseased spikelets at every three day interval. Metabolites and proteins were extracted from the collected tissue and analysed in a high resolution LC-MS. Resistance related (RR) metabolites and proteins, that were present with high abundance the resistant genotype were identified. Host biochemical resistance mechanisms were explained based on the RR metabolites and proteins.

FHB severity (necrosis) was significantly high in NIL-S compared to NIL-R until 9 dpi, and later, the spikelets wilted and dried in both the genotypes due to DON bleaching (Fig. 3.1). Nevertheless, AUDPC was significantly high in NIL-S (AUDPC = 10.45) compared to NIL-R (AUDPC = 6.08) suggesting NIL-R defends the pathogen through biochemical mechanisms other than DON detoxification. Total DON (DON +D3G) accumulation was high in both the NILs, with no significant difference between NILs (Fig. 3.4a, Table 3.3). However, the total DON accumulation was higher in spikelets than in rachis, and conversely, the PDC was higher in rachis, suggesting a higher DON detoxification at lower DON concentrations, as DON is a host protein inhibitor inclusive of UDP-glycosyltransferase (Fig. 3.4b). In addition, other host resistance mechanisms were also explored. A total of 235 RRC and 473 RRI metabolites in rachis and 71 RRC and 340 RRI metabolites in spikelets were identified (Fig. 3.2). The putatively identified RR metabolites mainly belonged to phenylpropanoid, flavonoid, fatty acid, terpenoid and alkaloid pathways (Table 3.1 and 3.2). Among them, hydroxycinnamic acids, flavonoids and phenolic glucosides were accumulated with very high fold changes (>10), especially in rachis (Table 3.1). A parallel proteomic profiling of rachis also confirmed the up-regulation of phenylpropanoid pathway, with the up-regulated enzymes of cysteine and methionine metabolism, and phenylpropanoid biosynthesis in NIL-R (Table 3.4). Histochemical localization HCAAs and flavonoids in the rachis revealed that, HCAAs and flavonoids were mainly deposited at the cell walls (Fig. 3.5). Coincidentally, a protein coding gene (GenBank: *CBH32656.1*) near the *Fhb1* locus contained a 'hydroxycinnamoyl transferase domain" and it was putatively annotated as hydroxycinnamoyl transferase (*HCT*), that catalyze the biosynthesis of HCAAs. Higher expression of *HCT* was confirmed by qRT-PCR expression of wheat agmatine coumaroyltransferase (Fig, 3.7). With evidences from transcript, protein and metabolite expression and histo-chemical localization, it was postulated that, *Fhb1* derived from the wheat genotype Nyubai is mainly associated with cell wall thickening due to the deposition of hydroxycinnamic acid amides, phenolic glucosides and flavonoids, but not with the conversion of deoxynivalenol to less toxic deoxynivalenol 3-*O*-glucoside. HCAAs and flavonoids deposited at the cell walls are synthesized in a shunt

phenylpropanoid pathway (Fig. 3.8) by the condensation of hydroxycinnamoyl-CoA thioesters of the phenylpropanoid pathway, with aromatic amines such as serotonin, agmatine, putrescine, spermine, spermidine and tyramine, by amine specific hydroxyl cinnamoyltransferases (Fig 3.9) (Bassard et al., 2010, Edreva et al., 2007, Facchini et al., 2002). Hydroxycinnamoyl moieties of HCAAs also cross link with polysaccharides, lignin and suberin of the cell wall by etheric linkage and are deposited as cell wall appositions at the inner side of plant cell walls (Buanafina de O, 2009). Deposition of flavonoids further strengthen the cell wall (Gang et al., 1999) and phenolic glucosides might serve as substrates for monolignols involved in the synthesis of syringyl rich lignin (Menden et al., 2007, Suzuki et al., 2010). Deposition of lignin, HCAAs and flavonoids increase cell wall thickening at the rachis and block the intruding pathogen from spreading to other un-inoculated spikelets through the rachis (Kang and Buchenauer, 2000). However, *HCT* as *Fhb1* candidate gene was ambiguous as more than one *HCT* are involved in HCAA biosynthesis and also it was outside the fine mapped FHB region. Nevertheless the cell wall strengthening at the rachis, spikelets were bleached at advanced stages of infection due to high DON accumulation even in resistant NILs, and hence the resistance to DON accumulation, key determinant of pathogenicity, could not be explained. The study hinted that, DON detoxifying UDP-glycosyltransferase is not regulated by *Fhb1* region and is located outside the *Fhb1* region as both the NILs accumulated high DON due to susceptible genotype background.

Chapter IV was conducted to confirm the function of ambiguous *Fhb1* candidate gene hydroxyl cinnamoyltransferases in FHB resistance, due to increased cell wall thickening, using another *Fhb1* QTL, derived from cultivar Sumai-3. In this study NILs derived from a highly FHB resistant cultivar Sumai-3, with resistance genome background (developed by backcrossing to Sumai-3), were chosen to identify the mechanisms responsible for low DON accumulation. Inoculation, sample collection and metabolic profiling were carried out as explained in chapter III. Samples were collected at 7 dpi, in addition to 3 dpi, to assess the resistance mechanisms at advanced stages of infection. Unlike NILs derived from a moderately resistant cultivar Nyubai, the FHB severity was significantly higher in NIL-S than in NIL-R throughout the study period. Disease symptoms, neither necrosis

nor bleaching were spread to the un-inoculated spikelets in the NIL-R (AUDPC=1.5), indicating low DON accumulation. While in NIL-S, the necrotic symptoms were spread to adjacent top and bottom spikelets, at 6 dpi, and the entire spikes were dried up due to DON bleaching by 12 and 15 dpi (AUDPC=5.58). Surprisingly, none of the trichothecenes and their glucose conjugates was detected, in either of the NILs at 3 dpi. Similarly, many differentially accumulating metabolites were also not detected. Profiling of metabolites from spikelets revealed that, several antimicrobial and anti-oxidative metabolites belonging to phenylpropanoid, flavonoid and terpenoid pathway were accumulated in both the NILs, with a little higher fold change in the NIL-R (Table 4.3). Accumulation of DON was higher in NIL-S (2.32 mg kg^{-1}) than in NIL-R (1.2 mg kg^{-1}) (Fig. 4.1 A, Table 4.2). A low amount of D3G was accumulated only in NIL-R (0.93 mg kg^{-1}). Expression of UDP-glycosyltransferase was also low in both the NILs with no significant difference, at 3 dpi in spikelets (Fig. 4.2). HCAAs, which were accumulated at high abundance in NIL-R derived from Nyubai, were also highly abundant in both the NILs derived from Suami-3, at 3dpi (Table 4.5). Similarly, the expression of agmatine coumaroyltransferase was also high, in both the NILs, with no significant difference between NILs derived from Sumai-3. In continuation of our objective to decipher the host resistance mechanisms to FHB spread at rachis, metabolites accumulated at 7 dpi were profiled. Very low amount of DON was detected in NIL-R (0.5 mg kg^{-1}) compared to NIL-S (1.36 mg kg^{-1}) (Table 4.2, Fig. 4.1). Surprisingly, DON detoxification (PDC) was moderately high in both the NILs with no significant difference between the NILs (Fig. 4.1). The expression of UDP-glycosyltransferase was higher in NIL-S (Fig. 4.2), and its expression correlated with TDP (DON + D3G), irrespective of NILs (Fig. 4.5). Interestingly, many glycerophospholipids that were constitutively present in both the NILs were absent in pathogen inoculated NIL-S (Table 4.4). The glycerophospholipids are the structural components of cellular membranes that play a key role in maintaining the cell membrane integrity, cell fluidity and ion permeability (Farooqui, 2009). The rupture of plasma membrane and sequestration of membrane bound glycerophospholipids is a characteristic feature of the programmed cell death (PCD) in plants (Van Doorn, et al., 2011), suggesting PCD in the NIL-S. In confirmation, genomic DNA (gDNA)

laddering, a characteristic of programmed cell death was observed only in the NIL-S, while the gDNA was intact in the NIL-R (Fig. 4.6). Coincidentally, the transcript expression of a gene localized on *Fhb1* locus, which encodes calmodulin binding protein (*TaCaMBP_Fhb1*), was significantly up-regulated in NIL-S, following pathogen inoculation (Fig. 4.3). The resistant allele of *TaCaMBP_Fhb1* is non-functional due to deletion of a promoter region (Fig. 4.7) and rescues the host plants from programmed cell death induced by Ca^{2+} signalling activated by *TaCaMBP_Fhb1* by binding to Ca^{2+}activated CaM. In addition, the abundances of HCAAs were quite high in both the NILs, and accordingly, the *HCT* as an *Fhb1* candidate gene was ruled out, and also this gene is present outside the fine mapped *Fhb1* region. It was concluded that the *Fhb1* candidate gene, *TaCaMBP_Fhb1*, was responsible for high DON accumulation in susceptible NIL, because *TaCaMBP_Fhb1* promotes cell death, facilitating pathogen growth and DON accumulation in NIL-S. Conversely, the low expression of *TaCaMBP_Fhb1* in NIL-R accumulated low DON because of lack of host cell death, leading to reduced pathogen growth. Allelic variation between the resistant and susceptible genotypes has to be investigated.

Chapter V was planned to confirm the findings of Chapter III (HCAA) and Chapter IV (low DON accumulation) by metabolic profiling of a highly FHB resistant cultivar Sumai-3 and a susceptible cultivar Roblin. Also to determine the effect of DON on host resistance mechanisms, the differentially accumulated metabolites were compared in response to trichothecene producing (*FgTri5*$^{+}$) and non-producing (*FgTri5*$^{+}$) isolates of *F. graminearum*. Experimental procedures remained the same, as explained in Chapter III. Sumai-3 exhibited absolute resistance to disease spread, with no symptoms spreading to the adjacent spikelets (Fig. 5.1) (Hamzehzarghani, et al., 2005). In contrast, the susceptible cultivar, Roblin, exhibited high susceptibility to *F. graminearum* infection, and spikelets were bleached ahead of necrotic spikelets, due to DON accumulation. Very low amounts of DON, D3G and TDP were accumulated in rachis of Sumai-3, at 3 dpi, as compared to Roblin. Even though the PDC was moderately high in both Sumai-3 and Roblin, there was no significant difference between them (Fig. 5.2). Similarly, the DON detoxification was moderately high in Nyubai NILs, even though the amount of total

DON produced were high in both the NILs, that had a Canadian FHB susceptible cultivar 98B69*L47 genome background. With the evidences from three different pairs of genotypes studied, we hypothesize that, the susceptible wheat cultivars Roblin and 98B69*L47 also code for UDP-glycosyltransferases, capable of detoxifying DON at a moderately high levels, similar to Sumai-3. More RR metabolites accumulated in rachis of Sumai-3, following *FgTri5*$^{-}$ inoculation (RRI-*FgTri5*$^{-}$ = 139), compared to *FgTri5*$^{+}$ inoculation (RRI-*FgTri5*$^{+}$ = 98) (Fig. 5.3), and also the RRI metabolites fold change was lower in the *FgTri5*$^{+}$ induced as compared to *FgTri5*$^{-}$ induced, for most of the common RR metabolites. Reduced number and fold change of RR metabolites, following inoculation of trichothecene producing strain of *F. graminearum* was because of DON, which inhibited eukaryotic protein translation, including enzymes catalyzing several of the RR metabolites (Pestka, 2010). Similarly, less number of RR metabolites was induced in barley following trichothecene producing *F. graminearum* inoculation as compared to its trichothecene non-producing counterpart (Kumaraswamy et al., 2011a). Sumai-3 had higher levels of several RRC metabolites, most strikingly, the precursors of lignin, lignans, a cinnamic acid, diferulic acid and flavonoids, and also several RRI metabolites belonging to hydroxycinnamic acid amides (HCAA), flavonoids and lignans (Table 5.1; Fig. 5.4). The resistance in Sumai-3 to FHB was mainly associated with phenylpropanoid pathway: i) preformed syringyl rich monolignols and their glucosides formed lignin (Kang and Buchenauer, 2000, Menden et al., 2007); ii) preformed flavonoids were antimicrobial (Agati et al., 2012, Hernández et al., 2009); iii) induced hydroxycinnamic acid amides enhanced cell wall thickening (Gunnaiah et al., 2012); iv) cinnamic acids and iso-flavonoids were antimicrobial (Bollina and Kushalappa, 2011, Boutigny et al., 2009); v) lignans reduced reactive oxygen species that were induced by deoxynivalenol (Davin and Lewis, 2000). In confirmation with our previous two studies (Chapter III and IV), this study also proved that, the phenylpropanoid pathway play a major role in host resistance to FHB spread, by strengthening cell walls mainly at the rachis, due to lignification and deposition of HCCAs and flavonoids, that blocks the fungal colonization, thus reducing fungal biomass accumulation. As antioxidants, the cinnamic acids, iso-flavonoids and lignans inhibit the growth of *F. graminearum*, reduce

trichothecene production and neutralize the ROS induced by DON. Activity of UDP-glycosyltransferase in DON detoxification might be similar in all the wheat cultivars. Susceptibility due to *TaCaMBP_Fhb1* in Roblin has to be explored at advanced stages of infection.

6.2. SUGGESTIONS FOR FUTURE RESEARCH

- Sequencing and cloning of *TaCaMBP_Fhb1* across several resistant and genotypes to identify potential SNP markers and their validation
- Function of *TaCaMBP_Fhb1* in FHB resistance/susceptibility has to be validated by either gain of function or loss of function studies.
- Function of *TaCaMBP_Fhb1* in other physiological functions of cell has to be identified to consider it as a potential candidate gene for knocking out or editing, to enhance the resistance.
- *Fhb1* is not associated with DON detoxification gene. It should be further explored to enhance the FHB resistance.
- Absolute type II resistance in barley is possibly due to high syringyl/guacoyl (S/G) lignin ratio, as we found more syringyl lignin in Sumai-3. Comparison of wheat and barley for S/G lignin could reveal the mechanisms and S/G ratio can be used as potential biomarker for type II FHB resistance.

REFERENCES

Agati, G., E. Azzarello, S. Pollastri and M. Tattini. 2012. Flavonoids as antioxidants in plants: Location and functional significance. Plant Science 196: 67-76.

Aldini, G., L. Regazzoni, A. Pedretti, M. Carini, S.M. Cho, K.M. Park, et al. 2011. An integrated high resolution mass spectrometric and informatics approach for the rapid identification of phenolics in plant extract. Journal of Chromatography A 1218: 2856-2864.

Alemanno, L., T. Ramos, A. Gargadenec, C. Andary and N. Ferriere. 2003. Localization and identification of phenolic compounds in *Theobroma cacao* L. somatic embryogenesis. Annals of Botany 92: 613-623.

Allwood, J. and R. Goodacre. 2010. An introduction to liquid chromatography-mass spectrometry instrumentation applied in plant metabolomic analyses. Phytochemical Analysis 21: 33-47.

Allwood, W.J., A. Clarke, R. Goodacre and L.A. Mur. 2010. Dual metabolomics: a novel approach to understanding plant–pathogen interactions. Phytochemistry 71: 590-597.

Anderson, J.A., R. Stack, S. Liu, B. Waldron, A. Fjeld, C. Coyne, et al. 2001. DNA markers for Fusarium head blight resistance QTLs in two wheat populations. Theoretical and Applied Genetics 102: 1164-1168.

Anil Kumar, K., S. Kumar Singh, B. Siva Kumar and M. Doble. 2007. Synthesis, anti-fungal activity evaluation and QSAR studies on podophyllotoxin derivatives. Central European Journal of Chemistry 5: 880-897.

Arbona, V., M. Manzi, C.d. Ollas and A. Gómez-Cadenas. 2013. Metabolomics as a Tool to Investigate Abiotic Stress Tolerance in Plants. International journal of molecular sciences 14: 4885-4911.

Arrizabalaga, G., F. Ruiz, S. Moreno and J.C. Boothroyd. 2004. Ionophore-resistant mutant of Toxoplasma gondii reveals involvement of a sodium/hydrogen exchanger in calcium regulation. The Journal of cell biology 165: 653-662.

Bai, G., F.L. Kolb, G. Shaner and L.L. Domier. 1999. Amplified fragment length polymorphism markers linked to a major quantitative trait locus controlling scab resistance in wheat. Phytopathology 89: 343-348.

Bai, G. and G. Shaner. 2004. Management and resistance in wheat and barley to Fusarium head blight 1. Annual Review of Phytopathology 42: 135-161.

Bai, G.H., A. Desjardins and R. Plattner. 2002. Deoxynivalenol-nonproducing *Fusarium graminearum* causes initial infection, but does not cause disease spread in wheat spikes. Mycopathologia 153: 91-98.

Bai, G.H., R. Plattner, A. Desjardins, F. Kolb and R. McIntosh. 2001. Resistance to Fusarium head blight and deoxynivalenol accumulation in wheat. Plant Breeding 120: 1-6.

Bai, S. and G. Shaner. 1994. Scab of wheat: prospects for control. Plant Disease 78: 760-766.

Ballini, E., J.B. Morel, G. Droc, A. Price, B. Courtois, J.L. Notteghem, et al. 2008. A genome-wide meta-analysis of rice blast resistance genes and quantitative trait loci provides new insights into partial and complete resistance. Molecular Plant-Microbe Interactions 21: 859-868.

Bassard, J.E., P. Ullmann, F. Bernier and D. Werck-Reichhart. 2010. Phenolamides: Bridging polyamines to the phenolic metabolism. Phytochemistry 71: 1808-1824.

Bernardo, A., G. Bai, P. Guo, K. Xiao, A.C. Guenzi and P. Ayoubi. 2007. *Fusarium graminearum*-induced changes in gene expression between Fusarium head blight-resistant and susceptible wheat cultivars. Functional & Integrative Genomics 7: 69-77.

Bernardo, A.N., H. Ma, D. Zhang and G. Bai. 2012. Single nucleotide polymorphism in wheat chromosome region harboring *Fhb1* for Fusarium head blight resistance. Molecular Breeding 29: 477-488.

Bhadauria, V., S. Banniza, L. Wang, Y. Wei and Y. Peng. 2010. Proteomic studies of phytopathogenic fungi, oomycetes and their interactions with hosts. European Journal of Plant Pathology 126: 81-95.

Bhat, R., Y. Ramakrishna, S. Beedu and K. Munshi. 1989. Outbreak of trichothecene mycotoxicosis associated with consumption of mould-damaged wheat products in Kashmir Valley, India. The Lancet 333: 35-37.

Bhuiyan, N.H., W. Liu, G. Liu, G. Selvaraj, Y. Wei and J. King. 2007. Transcriptional regulation of genes involved in the pathways of biosynthesis and supply of methyl units in response to powdery mildew attack and abiotic stresses in wheat. Plant Molecular Biology 64: 305-318.

Boddu, J., S. Cho and G.J. Muehlbauer. 2007. Transcriptome analysis of trichothecene-induced gene expression in barley. Molecular Plant-Microbe Interactions 20: 1364-1375.

Boerjan, W., J. Ralph and M. Baucher. 2003. Lignin biosynthesis. Annual Review of Plant Biology 54: 519-546.

Bollina, V., G. Kumaraswamy, A.C. Kushalappa, T. Choo, Y. Dion, S. Rioux, et al. 2010. Mass spectrometry-based metabolomics application to identify quantitative resistance-related metabolites in barley against Fusarium head blight. Molecular Plant Pathology 11: 769-782.

Bollina, V. and A.C. Kushalappa. 2011. In vitro inhibition of trichothecene biosynthesis in *Fusarium graminearum* by resistance-related endogenous metabolites identified in barley. Mycology 2: 291-296.

Bollina, V., A.C. Kushalappa, T.M. Choo, Y. Dion and S. Rioux. 2011. Identification of metabolites related to mechanisms of resistance in barley against *Fusarium graminearum*, based on mass spectrometry. Plant Molecular Biology 77: 355-370.

Boutigny, A.-L., V. Atanasova-Pénichon, M. Benet, C. Barreau and F. Richard-Forget. 2010. Natural phenolic acids from wheat bran inhibit *Fusarium culmorum* trichothecene biosynthesis in vitro by repressing *Tri* gene expression. European Journal of Plant Pathology 127: 275-286.

Boutigny, A.L., C. Barreau, V. Atanasova-Penichon, M.N. Verdal-Bonnin, L. Pinson-Gadais and F. Richard-Forget. 2009. Ferulic acid, an efficient inhibitor of type B trichothecene biosynthesis and *Tri* gene expression in Fusarium liquid cultures. Mycological research 113: 746-753.

Boutigny, A.L., F. Richard-Forget and C. Barreau. 2008. Natural mechanisms for cereal resistance to the accumulation of Fusarium trichothecenes. European Journal of Plant Pathology 121: 411-423.

Braun, H.J., Atlin G. and P. T. 2010. Multi-location testing as a tool to identify plant response to global climate change. In: M. P. Reynolds, editor Climate change and crop production. Cabi, U.K. p. 115–138.

Brown, N.A., M. Urban, A.M.L. Van de Meene and K.E. Hammond-Kosack. 2010. The infection biology of *Fusarium graminearum*: Defining the pathways of spikelet to spikelet colonisation in wheat ears. Fungal Biology 114: 555-571.

Buanafina de O, M.M. 2009. Feruloylation in grasses: current and future perspectives. Molecular Plant 2: 861-872.

Buerstmayr, H., G. Adam and M. Lemmens. 2012. 12 Resistance to head blight caused by *Fusarium* spp. in wheat. Disease Resistance in Wheat: 236.

Buerstmayr, H., T. Ban and J.A. Anderson. 2009. QTL mapping and marker-assisted selection for Fusarium head blight resistance in wheat: a review. Plant Breeding 128: 1-26.

Buerstmayr, H., M. Lemmens, L. Hartl, L. Doldi, B. Steiner, M. Stierschneider, et al. 2002. Molecular mapping of QTLs for Fusarium head blight resistance in spring wheat. I. Resistance to fungal spread (Type II resistance). Theoretical and Applied Genetics 104: 84-91.

Buerstmayr, H., B. Steiner, L. Hartl, M. Griesser, N. Angerer, D. Lengauer, et al. 2003. Molecular mapping of QTLs for Fusarium head blight resistance in spring wheat. II. Resistance to fungal penetration and spread. Theoretical and Applied Genetics 107: 503-508.

Bushnell, W., B. Hazen, C. Pritsch and K. Leonard. 2003. Histology and physiology of Fusarium head blight. Fusarium head blight of wheat and barley. p. 44-83.

Bushnell, W., P. Perkins-Veazie, V. Russo, J. Collins and T. Seeland. 2010. Effects of deoxynivalenol on content of chloroplast pigments in barley leaf tissues. Phytopathology 100: 33-41.

Campbell, A. and E. Czarnecki. 1987. Roblin hard red spring wheat. Canadian Journal of Plant Science 67: 803-804.

Carpinella, M.C., L.M. Giorda, C.G. Ferrayoli and S.M. Palacios. 2003. Antifungal effects of different organic extracts from *Melia azedarach* L. on phytopathogenic fungi and their isolated active components. Journal of Agricultural and Food Chemistry 51: 2506-2511.

Cerretani, L., A. Giuliani, R.M. Maggio, A. Bendini, T. Gallina Toschi and A. Cichelli. 2010. Rapid FTIR determination of water, phenolics and antioxidant activity of olive oil. European Journal of Lipid Science and Technology 112: 1150-1157.

Chakraborty, S. and A.C. Newton. 2011. Climate change, plant diseases and food security: An overview. Plant Pathology 60: 2-14.

Chen, L., Y. Song, Y. Xu, L. Nie and L. Xu. 1997. Comparison of activities of superoxide dismutase and catalase between scab-resistant and susceptible wheat varieties. Acta Phytopathologica Sinica 27: 209-213.

Choulet, F., T. Wicker, C. Rustenholz, E. Paux, J. Salse, P. Leroy, et al. 2010. Megabase level sequencing reveals contrasted organization and evolution patterns of the wheat gene and transposable element spaces. The Plant Cell 22: 1686-1701.

Cloutier, P., R. Al-Khoury, M. Lavallée-Adam, D. Faubert, H. Jiang, C. Poitras, et al. 2009. High-resolution mapping of the protein interaction network for the human transcription machinery and affinity purification of RNA polymerase II-associated complexes. Methods 48: 381-386.

Cossette, F. and J.D. Miller. 1995. Phytotoxic effect of deoxynivalenol and gibberella ear rot resistance of com. Natural Toxins 3: 383-388.

Cuthbert, P.A., D.J. Somers and A. Brulé-Babel. 2007. Mapping of *Fhb2* on chromosome 6BS: a gene controlling Fusarium head blight field resistance in bread wheat (*Triticum aestivum* L.). Theoretical and Applied Genetics 114: 429-437.

Cuthbert, P.A., D.J. Somers, J. Thomas, S. Cloutier and A. Brulé-Babel. 2006. Fine mapping *Fhb1*, a major gene controlling fusarium head blight resistance in bread wheat (*Triticum aestivum* L.). Theoretical and Applied Genetics 112: 1465-1472.

Danan, S., J.B. Veyrieras and V. Lefebvre. 2011. Construction of a potato consensus map and QTL meta-analysis offer new insights into the genetic architecture of late blight resistance and plant maturity traits. BMC Plant Biology 11: 16.

Dash, S., J. Van Hemert, L. Hong, R.P. Wise and J.A. Dickerson. 2012. PLEXdb: gene expression resources for plants and plant pathogens. Nucleic acids research 40: D1194-D1201.

Davin, L.B. and N.G. Lewis. 2000. Dirigent proteins and dirigent sites explain the mystery of specificity of radical precursor coupling in lignan and lignin biosynthesis. Plant Physiology 123: 453-462.

Degenhardt, J., T.G. Köllner and J. Gershenzon. 2009. Monoterpene and sesquiterpene synthases and the origin of terpene skeletal diversity in plants. Phytochemistry 70: 1621-1637.

Desmond, O.J., J.M. Manners, P.M. Schenk, D.J. Maclean and K. Kazan. 2008. Gene expression analysis of the wheat response to infection by *Fusarium pseudograminearum*. Physiological and Molecular Plant Pathology 73: 40-47.

Desmond, O.J., J.M. Manners, A.E. Stephens, D.J. MacLean, P.M. Schenk, D.M. Gardiner, et al. 2008. The Fusarium mycotoxin deoxynivalenol elicits hydrogen peroxide production, programmed cell death and defence responses in wheat. Molecular Plant Pathology 9: 435-445.

Dharmawardhana, D.P., B.E. Ellis and J.E. Carlson. 1995. A [beta]-Glucosidase from lodgepole pine xylem specific for the lignin precursor coniferin. Plant Physiology 107: 331-339.

Ding, L., H. Xu, H. Yi, L. Yang, Z. Kong, L. Zhang, et al. 2011. Resistance to hemi-biotrophic *F. graminearum* infection is associated with coordinated and ordered expression of diverse defense signaling pathways. PloS one 6: p.e19008. doi:doi: 10.1371/journal.pone.0019008.

Dixon, R.A. 2001. Natural products and plant disease resistance. Nature 411: 843-847.

Dixon, R.A., D.Y. Xie and S.B. Sharma. 2005. Proanthocyanidins–a final frontier in flavonoid research? New Phytologist 165: 9-28.

Du, L., T. Yang, S.V. Puthanveettil and B. Poovaiah. 2011. Decoding of calcium signal through calmodulin: calmodulin-binding proteins in plants. Coding and Decoding of Calcium Signals in Plants. Springer. p. 177-233.

Dubin, H.J. 1997. Fusarium Head Scab: Global Status and Future Prospects: Proceedings of a Workshop Held at CIMMYT, El Batan, Mexico, 13-17 October, 1996Cimmyt.

Edreva, A., V. Velikova and T. Tsonev. 2007. Phenylamides in plants. Russian Journal of Plant Physiology 54: 287-301.

Eeuwijk, F., A. Mesterhazy, C.I. Kling, P. Ruckenbauer, L. Saur, H. Buerstmayr, et al. 1995. Assessing non-specificity of resistance in wheat to head blight caused by inoculation with European strains of *Fusarium culmorum*, *F. graminearum* and *F. nivale* using a multiplicative model for interaction. Theoretical and Applied Genetics 90: 221-228.

Evans, A.M., C.D. DeHaven, T. Barrett, M. Mitchell and E. Milgram. 2009. Integrated, nontargeted ultrahigh performance liquid chromatography/electrospray ionization tandem mass spectrometry platform for the identification and relative quantification of the small-molecule complement of biological systems. Analytical chemistry 81: 6656-6667.

Facchini, P.J., J. Hagel and K.G. Zulak. 2002. Hydroxycinnamic acid amide metabolism: physiology and biochemistry. Canadian Journal of Botany 80: 577-589.

Farooqui, A.A. 2009. Glycerophospholipids. eLS.

Fernie, A. and N. Schauer. 2009. Metabolomics-assisted breeding: a viable option for crop improvement? Trends in Genetics 25: 39-48.

Foroud, N., T. Ouellet, A. Laroche, B. Oosterveen, M. Jordan, B. Ellis, et al. 2011. Differential transcriptome analyses of three wheat genotypes reveal different host response pathways associated with Fusarium head blight and trichothecene resistance. Plant Pathology 61: 296-314.

Gang, D.R., H. Kasahara, Z.Q. Xia, K. Vander Mijnsbrugge, G. Bauw, W. Boerjan, et al. 1999. Evolution of plant defense mechanisms. Journal of Biological Chemistry 274: 7516-7527.

Garcia-Canas, V., C. Simo, C. Leon, E. Ibanez and A. Cifuentes. 2011. MS-based analytical methodologies to characterize genetically modified crops. Mass spectrometry reviews 30: 396-416.

Gardiner, D.M., K. Kazan, S. Praud, F.J. Torney, A. Rusu and J.M. Manners. 2010. Early activation of wheat polyamine biosynthesis during Fusarium head blight implicates putrescine as an inducer of trichothecene mycotoxin production. BMC Plant Biology 10: 289.

Gardiner, S.A., J. Boddu, F. Berthiller, C. Hametner, R.M. Stupar, G. Adam, et al. 2010. Transcriptome analysis of the barley-deoxynivalenol interaction: evidence for a role of glutathione in deoxynivalenol detoxification. Molecular Plant-Microbe Interactions 23: 962-976.

Geddes, J., F. Eudes, A. Laroche and L.B. Selinger. 2008. Differential expression of proteins in response to the interaction between the pathogen *Fusarium graminearum* and its host, *Hordeum vulgare*. Proteomics 8: 545–554.

Golkari, S., J. Gilbert, S. Prashar and J.D. Procunier. 2007. Microarray analysis of *Fusarium graminearum* induced wheat genes: identification of organ specific and differentially expressed genes. Plant biotechnology journal 5: 38-49.

Golkari, S.G.S., J.G.J. Gilbert, T.B.T. Ban and J.D.P.J. Procunier. 2009. QTL-specific microarray gene expression analysis of wheat resistance to Fusarium head blight in Sumai-3 and two susceptible NILs. Genome 52: 409-418.

Gottwald, S., B. Samans, S. Lück and W. Friedt. 2012. Jasmonate and ethylene dependent defence gene expression and suppression of fungal virulence factors: Two essential mechanisms of Fusarium head blight resistance in wheat? BMC Genomics 13: 369.

Govrin, E.M. and A. Levine. 2000. The hypersensitive response facilitates plant infection by the necrotrophic pathogen< i> Botrytis cinerea</i>. Current Biology 10: 751-757.

Grabber, J.H., J. Ralph and R.D. Hatfield. 1998. Ferulate cross-links limit the enzymatic degradation of synthetically lignified primary walls of maize. Journal of Agricultural and Food Chemistry 46: 2609-2614.

Gunnaiah, R., A.C. Kushalappa, R. Duggavathi, S. Fox and D.J. Somers. 2012. Integrated metabolo-proteomic approach to decipher the mechanisms by which wheat qtl (*Fhb1*) contributes to resistance against *Fusarium graminearum*. PloS one 7.

Hamzehzarghani, H., A.C. Kushalappa, Y. Dion, S. Rioux, A. Comeau, V. Yaylayan, et al. 2005. Metabolic profiling and factor analysis to discriminate quantitative resistance in wheat cultivars against fusarium head blight. Physiological and Molecular Plant Pathology 66: 119-133.

Hamzehzarghani, H., V. Paranidharan, Y. Abu-Nada, A. Kushalappa, Y. Dion, S. Rioux, et al. 2008. Metabolite profiling coupled with statistical analyses for potential high-throughput screening of quantitative resistance to Fusarium head blight in wheat. Canadian Journal of Plant Pathology 30: 24-36.

Hamzehzarghani, H., V. Paranidharan, Y. Abu-Nada, A. Kushalappa, O. Mamer and D. Somers. 2008. Metabolic profiling to discriminate wheat near isogenic lines, with quantitative trait loci at chromosome 2DL, varying in resistance to fusarium head blight. Canadian Journal of Plant Science 88: 789-797.

Handa, H., N. Namiki, D. Xu and T. Ban. 2008. Dissecting of the FHB resistance QTL on the short arm of wheat chromosome 2D using a comparative genomic approach: From QTL to candidate gene. Molecular Breeding 22: 71-84.

Hao, C., M. Perretant, F. Choulet, L. Wang, E. Paux, P. Sourdille, et al. 2010. Genetic diversity and linkage disequilibrium studies on a 3.1-Mb genomic region of chromosome 3B in European and Asian bread wheat (*Triticum aestivum* L.) populations. TAG Theoretical and Applied Genetics 121: 1209-1225.

Hayashi, M., H. Takahashi, K. Tamura, J. Huang, L.-H. Yu, M. Kawai-Yamada, et al. 2005. Enhanced dihydroflavonol-4-reductase activity and NAD homeostasis leading to cell death tolerance in transgenic rice. Proceedings of the National Academy of Sciences of the United States of America 102: 7020-7025.

Hegeman, A. 2010. Plant metabolomics--meeting the analytical challenges of comprehensive metabolite analysis. Briefings in Functional Genomics and Proteomics 9: 139.

Hegeman, A.D., C.F. Schulte, Q. Cui, I.A. Lewis, E.L. Huttlin, H. Eghbalnia, et al. 2007. Stable isotope assisted assignment of elemental compositions for metabolomics. Analytical chemistry 79: 6912-6921.

Hernández, I., L. Alegre, F. Van Breusegem and S. Munné-Bosch. 2009. How relevant are flavonoids as antioxidants in plants? Trends in plant science 14: 125-132.

Huang, X. and F. Regnier. 2008. Differential metabolomics using stable isotope labeling and two-dimensional gas chromatography with time-of-flight mass spectrometry. Anal. Chem 80: 107-114.

Huang, Z., K. Hashida, R. Makino, S. Ohara, S. Amartey and P. Gillah. 2010. Flavonoids with antifungal activity from heartwood of Tanzanian wood species: Commiphora mollis (Burseraceae). International Wood Products Journal 1: 93-95.

Hwang, B., J. Lee, Q.-H. Liu, E.-R. Woo and D.G. Lee. 2010. Antifungal effect of (+)-pinoresinol isolated from *Sambucus williamsii*. Molecules 15: 3507-3516.

Hwang, I., J.F. Harper, F. Liang and H. Sze. 2000. Calmodulin activation of an endoplasmic reticulum-located calcium pump involves an interaction with the N-terminal autoinhibitory domain. Plant Physiology 122: 157-168.

Iijima, Y., Y. Nakamura, Y. Ogata, K. Tanaka, N. Sakurai, K. Suda, et al. 2008. Metabolite annotations based on the integration of mass spectral information. The Plant Journal 54: 949-962.

Ilgen, P., B. Hadeler, F.J. Maier and W. Schäfer. 2009. Developing kernel and rachis node induce the trichothecene pathway of *Fusarium graminearum* during wheat head infection. Molecular Plant-Microbe Interactions 22: 899-908.

Imaishi, H. and M. Petkova-Andonova. 2007. Molecular Cloning of CYP76B9, a Cytochrome P450 from Petunia hybrida, Catalyzing the. OMEGA.-Hydroxylation of Capric Acid and Lauric Acid. Bioscience, Biotechnology and Biochemistry 71: 104-113.

Ishihara, A., Y. Hashimoto, C. Tanaka, J.G. Dubouzet, T. Nakao, F. Matsuda, et al. 2008. The tryptophan pathway is involved in the defense responses of rice against pathogenic infection via serotonin production. The Plant Journal 54: 481-495.

Jansen, C., D. Von Wettstein, W. Schäfer, K.H. Kogel, A. Felk and F.J. Maier. 2005. Infection patterns in barley and wheat spikes inoculated with wild-type and trichodiene synthase gene disrupted *Fusarium graminearum*. Proceedings of the National Academy of Sciences of the United States of America 102: 16892-16897.

Jia, G., P. Chen, G. Qin, G. Bai, X. Wang, S. Wang, et al. 2005. QTLs for Fusarium head blight response in a wheat DH population of Wangshuibai/Alondra‘s’. Euphytica 146: 183-191.

Jia, H., S. Cho and G.J. Muehlbauer. 2009. Transcriptome analysis of a wheat near-isogenic line pair carrying Fusarium head blight-resistant and-susceptible alleles. Molecular Plant-Microbe Interactions 22: 1366-1378.

Kang, Z. and H. Buchenauer. 1999. Immunocytochemical localization of fusarium toxins in infected wheat spikes by *Fusarium culmorum*. Physiological and Molecular Plant Pathology 55: 275-288.

Kang, Z. and H. Buchenauer. 2000. Ultrastructural and immunocytochemical investigation of pathogen development and host responses in resistant and susceptible wheat spikes infected by *Fusarium culmorum*. Physiological and Molecular Plant Pathology 57: 255-268.

Kang, Z.S., H. Buchenauer, L.L. Huang, Q.M. Han and H.C. Zhang. 2008. Cytological and immunocytochemical studies on responses of wheat spikes of the resistant Chinese cv. Sumai 3 and the susceptible cv. Xiaoyan 22 to infection by *Fusarium graminearum*. European Journal of Plant Pathology 120: 383-396. doi:DOI 10.1007/s10658-007-9230-9.

Keurentjes, J.J.B., J. Fu, A. Lommen, R.D. Hall, R.J. Bino, R.C. Jansen, et al. 2006. The genetics of plant metabolism. Nature Genetics, 38: 842-849.

Kiefer, P., J. Portais and J. Vorholt. 2008. Quantitative metabolome analysis using liquid chromatography-high-resolution mass spectrometry. Analytical Biochemistry 382: 94-100.

Kind, T. and O. Fiehn. 2007. Seven golden rules for heuristic filtering of molecular formulas obtained by accurate mass spectrometry. BMC Bioinformatics 8: 105.

Kleczkowski, L.A., S. Kunz and M. Wilczynska. 2010. Mechanisms of UDP-glucose synthesis in plants. Critical reviews in plant sciences 29: 191-203.

Kong, L., H.W. Ohm and J.M. Anderson. 2007. Expression analysis of defense-related genes in wheat in response to infection by *Fusarium graminearum*. Genome 50: 1038-1048.

Kuhl, C., R. Tautenhahn and S. Neumann. 2009. LC-MS Peak Annotation and Identification with CAMERA. Online: http://watson.nci.nih.gov/bioc_mirror/packages/2.7/bioc/vignettes/CAMERA/inst/doc/CAMERA.pdf Accessed 24th october 2011.

Kumaraswamy, G.K., Kushalappa A. C., Choo T., Dion Y. and S. Rioux. 2011. Differential metabolic response of barley genotypes, varying in resistance, to trichothecene-producing and-nonproducing (*tri5*−) isolates of *Fusarium graminearum*. Plant Pathology 61: 509-521.

Kumaraswamy, G.K., V. Bollina, A.C. Kushalappa, T.M. Choo, Y. Dion, S. Rioux, et al. 2011. Metabolomics technology to phenotype resistance in barley against *Gibberella zeae*. European Journal of Plant Pathology 130: 29-43.

Kumaraswamy, G. K., A.C. Kushalappa, T.M. Choo, Y. Dion and S. Rioux. 2011. Mass Spectrometry Based Metabolomics to Identify Potential Biomarkers for Resistance in Barley against Fusarium Head Blight (*Fusarium graminearum*). Journal of Chemical Ecology 37: 846-856.

Kusano, M., T. Tohge, A. Fukushima, M. Kobayashi, N. Hayashi, H. Otsuki, et al. 2011. Metabolomics reveals comprehensive reprogramming involving two independent metabolic responses of Arabidopsis to UV B light. The Plant Journal 67: 354-369.

Kushalappa, A.C. 2011. http://metabolomics.mcgill.ca.

Kushalappa, A.C. and R. Gunnaiah. 2013. Metabolo-proteomics to discover plant biotic stress resistance genes. Trends in Plant Science. doi:http://dx.doi.org/10.1016/j.tplants.2013.05.002.

Lemmens, M., U. Scholz, F. Berthiller, C. Dall'Asta, A. Koutnik, R. Schuhmacher, et al. 2005. The ability to detoxify the mycotoxin deoxynivalenol colocalizes with a major quantitative trait locus for Fusarium head blight resistance in wheat. Molecular Plant-Microbe Interactions 18: 1318-1324.

Li, G. and Y. Yen. 2008. Jasmonate and ethylene signaling pathway may mediate Fusarium head blight resistance in wheat. Crop Science 48: 1888-1896.

Li, L., C. Li, G.I. Lee and G.A. Howe. 2002. Distinct roles for jasmonate synthesis and action in the systemic wound response of tomato. Proceedings of the National Academy of Sciences 99: 6416-6421.

Lim, E.K., R.G. Jackson and D.J. Bowles. 2005. Identification and characterisation of Arabidopsis glycosyltransferases capable of glucosylating coniferyl aldehyde and sinapyl aldehyde. FEBS letters 579: 2802-2806.

Lin, F., Z. Kong, H. Zhu, S. Xue, J. Wu, D. Tian, et al. 2004. Mapping QTL associated with resistance to Fusarium head blight in the Nanda2419× Wangshuibai population. I. Type II resistance. Theoretical and Applied Genetics 109: 1504-1511.

Lin, F., S. Xue, Z. Zhang, C. Zhang, Z. Kong, G. Yao, et al. 2006. Mapping QTL associated with resistance to Fusarium head blight in the Nanda2419× Wangshuibai population. II: Type I resistance. Theoretical and Applied Genetics 112: 528-535.

Lisec, J., M. Steinfath, R.C. Meyer, J. Selbig, A.E. Melchinger, L. Willmitzer, et al. 2009. Identification of heterotic metabolite QTL in *Arabidopsis thaliana* RIL and IL populations. The Plant Journal 59: 777-788.

Liu, S., Z. Abate, H. Lu, T. Musket, G.L. Davis and A. McKendry. 2007. QTL associated with Fusarium head blight resistance in the soft red winter wheat Ernie. Theoretical and Applied Genetics 115: 417-427.

Liu, S., M.D. Hall, C.A. Griffey and A.L. McKendry. 2009. Meta-analysis of QTL associated with Fusarium head blight resistance in wheat. Crop Science 49: 1955-1968.

Liu, S., M.O. Pumphrey, B.S. Gill, H.N. Trick, J.X. Zhang, J. Dolezel, et al. 2008. Toward positional cloning of *Fhb1*, a major qtl for fusarium head blight resistance in wheat. Cereal Research Communications 36: 195-201.

Liu, S., X. Zhang, M.O. Pumphrey, R.W. Stack, B.S. Gill and J.A. Anderson. 2006. Complex microcolinearity among wheat, rice, and barley revealed by fine mapping of the genomic region harboring a major QTL for resistance to Fusarium head blight in wheat. Functional and Integrative Genomics 6: 83-89.

Lloyd, A.J., J. William Allwood, C.L. Winder, W.B. Dunn, J.K. Heald, S.M. Cristescu, et al. 2011. Metabolomic approaches reveal that cell wall modifications play a major role in ethylene-mediated resistance against *Botrytis cinerea*. The Plant Journal 67: 852-868.

Löffler, M., C.-C. Schön and T. Miedaner. 2009. Revealing the genetic architecture of FHB resistance in hexaploid wheat (*Triticum aestivum* L.) by QTL meta-analysis. Molecular Breeding 23: 473-488.

Luz, W.d., C. Stockwell, G. Bergstrom, K. Leonard and W. Bushnell. 2003. Biological control of *Fusarium graminearum*. Fusarium head blight of wheat and barley: 381-394.

Matern, U., B. Grimmig and R.E. Kneusel. 1995. Plant cell wall reinforcement in the disease-resistance response: molecular composition and regulation. Canadian Journal of Botany 73: 511-517.

Matros, A., S. Kaspar, K. Witzel and H.P. Mock. 2011. Recent progress in liquid chromatography-based separation and label-free quantitative plant proteomics. Phytochemistry 72: 963-974.

Matsuda, F., Y. Okazaki, A. Oikawa, M. Kusano, R. Nakabayashi, J. Kikuchi, et al. 2012. Dissection of genotype–phenotype associations in rice grains using metabolome quantitative trait loci analysis. The Plant Journal 70: 624-636.

Matsuda, F., K. Yonekura Sakakibara, R. Niida, T. Kuromori, K. Shinozaki and K. Saito. 2009. MS/MS spectral tag based annotation of non targeted profile of plant secondary metabolites. The Plant Journal 57: 555-577.

McCartney, C., D. Somers, G. Fedak, R. DePauw, J. Thomas, S. Fox, et al. 2007. The evaluation of FHB resistance QTLs introgressed into elite Canadian spring wheat germplasm. Molecular Breeding 20: 209-221.

McLusky, S.R., M.H. Bennett, M.H. Beale, M.J. Lewis, P. Gaskin and J.W. Mansfield. 1999. Cell wall alterations and localized accumulation of feruloyl 3 methoxytyramine in onion epidermis at sites of attempted penetration by *Botrytis allii* are associated with actin polarisation, peroxidase activity and suppression of flavonoid biosynthesis. The Plant Journal 17: 523-534.

Menden, B., M. Kohlhoff and B.M. Moerschbacher. 2007. Wheat cells accumulate a syringyl-rich lignin during the hypersensitive resistance response. Phytochemistry 68: 513-520.

Mesterhazy, A. 1995. Types and components of resistance to Fusarium head blight of wheat. Plant Breeding 114: 377-386.

Mesterházy, Á. 2002. Role of deoxynivalenol in aggressiveness of *Fusarium graminearum* and *F. culmorum* and in resistance to Fusarium head blight. European Journal of Plant Pathology 108: 675-684.

Miller, D.J. and P.G. Arnison. 1986. Degradation of deoxynivalenol by suspension cultures of the Fusarium head blight resistant wheat cultivar Frontana. Canadian Journal of Plant Pathology 8: 147-150.

Miller, J., J. Young and D. Sampson. 1985. Deoxynivalenol and Fusarium head blight resistance in spring cereals. Journal of Phytopathology 113: 359-367.

Miller, J.D. and M.A. Ewen. 1997. Toxic effects of deoxynivalenol on ribosomes and tissues of the spring wheat cultivars Frontana and Casavant. Natural Toxins 5: 234-237.

Mirocha, C., W. Xie, K. Leonard and W. Bushnell. 2003. Chemistry and detection of Fusarium mycotoxins. Fusarium head blight of wheat and barley: 144-164.

Naoumkina, M.A., Q. Zhao, L. Gallego-giraldo, X. Dai, P.X. Zhao and R.A. Dixon. 2010. Genome-wide analysis of phenylpropanoid defence pathways. Molecular Plant Pathology 11: 829-846.

O'Donnell, K., H.C. Kistler, B.K. Tacke and H.H. Casper. 2000. Gene genealogies reveal global phylogeographic structure and reproductive isolation among lineages of *Fusarium graminearum,* the fungus causing wheat scab. Proceedings of the National Academy of Sciences 97: 7905-7910.

Paoletti, A.C., T.J. Parmely, C. Tomomori-Sato, S. Sato, D. Zhu, R.C. Conaway, et al. 2006. Quantitative proteomic analysis of distinct mammalian Mediator complexes using normalized spectral abundance factors. Proceedings of the National Academy of Sciences 103: 18928-18933.

Paranidharan, V.P.V., Y.A.-N.Y. Abu-Nada, H.H.H. Hamzehzarghani, A.K.A. Kushalappa, O.M.O. Mamer, Y.D.Y. Dion, et al. 2008. Resistance-related metabolites in wheat against *Fusarium graminearum* and the virulence factor deoxynivalenol (DON). Botany 86: 1168-1179.

Parry, D., P. Jenkinson and L. McLeod. 1995. Fusarium ear blight (scab) in small grain cereals—a review. Plant Pathology 44: 207-238.

Penninckx, I.A.M.A., K. Eggermont, F.R.G. Terras, B.P.H.J. Thomma, G.W.D. Samblanx, A. Buchala, et al. 1996. Pathogen-induced systemic activation of a plant defensin gene in Arabidopsis follows a salicylic acid-independent pathway. The Plant Cell 8: 2309-2323.

Pestka, J.J. 2007. Deoxynivalenol: toxicity, mechanisms and animal health risks. Animal Feed Science and Technology 137: 283-298.

Pestka, J.J. 2010. Deoxynivalenol: mechanisms of action, human exposure, and toxicological relevance. Archives of Toxicology 84: 663-679.

Pestka, J.J. and A.T. Smolinski. 2005. Deoxynivalenol: toxicology and potential effects on humans. Journal of Toxicology and Environmental Health. Part B, Critical reviews 8: 39.

Pluskal, T., S. Castillo, A. Villar-Briones and M. Orešič. 2010. MZmine 2: modular framework for processing, visualizing, and analyzing mass spectrometry-based molecular profile data. BMC Bioinformatics 11: 395.

PMN. 2011. http://www.plantcyc.org/tools/tools_overview.faces on www.plantcyc.org Accessed 7th Septemeber 2011.

Ponts, N., L. Pinson-Gadais, A.-L. Boutigny, C. Barreau and F. Richard-Forget. 2011. Cinnamic-derived acids significantly affect *Fusarium graminearum* growth and in vitro synthesis of type B trichothecenes. Phytopathology 101: 929-934.

Poppenberger, B., F. Berthiller, D. Lucyshyn, T. Sieberer, R. Schuhmacher, R. Krska, et al. 2003. Detoxification of the Fusarium mycotoxin deoxynivalenol by a UDP-glucosyltransferase from *Arabidopsis thaliana*. Journal of Biological Chemistry 278: 47905-47914.

Pritsch, C., G.J. Muehlbauer, W.R. Bushnell, D.A. Somers and C.P. Vance. 2000. Fungal development and induction of defense response genes during early infection of wheat spikes by *Fusarium graminearum*. Molecular Plant-Microbe Interactions 13: 159-169.

Proctor, R.H., T.M. Hohn and S.P. McCormick. 1995. Reduced virulence of *Gibberella zeae* caused by disruption of a trichthecine toxin biosynthetic gene. Molecular Plant Microbe Interactions 8: 1995-1908.

Pumphrey, M.O., R. Bernardo and J.A. Anderson. 2007. Validating the *Fhb1* QTL for fusarium head blight resistance in near-isogenic wheat lines developed from breeding populations. Crop Science 47: 200-206.

Qi, X., R.E. Niks, P. Stam and P. Lindhout. 1998. Identification of QTLs for partial resistance to leaf rust (*Puccinia hordei*) in barley. Theoretical and Applied Genetics 96: 1205-1215.

Quirino, B., E. Candido, P. Campos, O. Franco and R. Krueger. 2009. Proteomic approaches to study plant-pathogen interactions. Phytochemistry.

1998. Cell wall cross-linking in grasses by ferulates and diferulates. ACS Symposium Series, ACS Publications.

Reboul, R., C. Geserick, M. Pabst, B. Frey, D. Wittmann, U. Lütz-Meindl, et al. 2011. Down-regulation of UDP-glucuronic acid biosynthesis leads to swollen plant cell walls and severe developmental defects associated with changes in pectic polysaccharides. Journal of Biological Chemistry 286: 39982-39992.

Reddy, V.S., G.S. Ali and A. Reddy. 2003. Characterization of a pathogen-induced calmodulin-binding protein: mapping of four Ca2+-dependent calmodulin-binding domains. Plant Molecular Biology 52: 143-159.

Rolando, C., N. Daubresse, B. Pollet, L. Jouanin and C. Lapierre. 2004. Lignification in poplar plantlets fed with deuterium-labelled lignin precursors. Comptes Rendus Biologies 327: 799-807.

SAS v 9.2. 2004. SAS Institute Inc Cary, North Carolina, USA.

Schroeder, H.W. and J.J. Christensen. 1963. Factors affecting resistance of wheat to scab by *Gibberella zeae*. Phytopathology 53: 831–838.

Schweiger, W., J. Boddu, S. Shin, B. Poppenberger, F. Berthiller, M. Lemmens, et al. 2010. Validation of a candidate deoxynivalenol-inactivating UDP-glucosyltransferase from barley by heterologous expression in yeast. Molecular Plant-Microbe Interactions 23: 977-986.

Schweiger, W., B. Steiner, C. Ametz, G. Siegwart, G. Wiesenberger, F. Berthiller, et al. 2013. Transcriptomic characterization of two major Fusarium resistance quantitative trait loci (QTLs), Fhb1 and Qfhs. ifa-5A, identifies novel candidate genes. Molecular Plant Pathology.

Shen, X., M. Zhou, W. Lu and H. Ohm. 2003. Detection of Fusarium head blight resistance QTL in a wheat population using bulked segregant analysis. Theoretical and Applied Genetics 106: 1041-1047.

Skadhauge, B., K.K. Thomsen and D. Wettstein. 1997. The role of the barley testa layer and its flavonoid content in resistance to Fusarium infections. Hereditas 126: 147-160.

Smith, C.A., J. Elizabeth, G. O'Maille, R. Abagyan and G. Siuzdak. 2006. XCMS: processing mass spectrometry data for metabolite profiling using nonlinear peak alignment, matching, and identification. Analytical chemistry 78: 779-787.

Smoot, M.E., K. Ono, J. Ruscheinski, P.-L. Wang and T. Ideker. 2011. Cytoscape 2.8: new features for data integration and network visualization. Bioinformatics 27: 431-432.

Snijders, C. and F. Eeuwijk. 1991. Genotype x strain interactions for resistance to Fusarium head blight caused by *Fusarium culmorum* in winter wheat. Theoretical and Applied Genetics 81: 239-244.

Somers, D.J., G. Fedak and M. Savard. 2003. Molecular mapping of novel genes controlling Fusarium head blight resistance and deoxynivalenol accumulation in spring wheat. Genome 46: 555-564.

Somers, D.J., J. Thomas, R. DePauw, S. Fox, G. Humphreys and G. Fedak. 2005. Assembling complex genotypes to resist Fusarium in wheat (*Triticum aestivum* L.). Theoretical and Applied Genetics 111: 1623-1631.

Staswick, P.E. and I. Tiryaki. 2004. The oxylipin signal jasmonic acid is activated by an enzyme that conjugates it to isoleucine in Arabidopsis. The Plant Cell Online 16: 2117-2127.

Steffenson, B., K. Leonard and W. Bushnell. 2003. Fusarium head blight of barley: impact, epidemics, management, and strategies for identifying and utilizing genetic resistance. Fusarium head blight of wheat and barley. p. 241-295.

Steiner, B., H. Kurz, M. Lemmens and H. Buerstmayr. 2009. Differential gene expression of related wheat lines with contrasting levels of head blight resistance after *Fusarium graminearum* inoculation. TAG Theoretical and Applied Genetics 118: 753-764.

Stępień, Ł. and J. Chełkowski. 2010. Fusarium head blight of wheat: pathogenic species and their mycotoxins. World Mycotoxin Journal 3: 107-119.

Strange, R., J. Majer and H. Smith. 1974. The isolation and identification of choline and betaine as the two major components in anthers and wheat germ that stimulate *Fusarium graminearum in vitro*. Physiological Plant Pathology 4: 277-290.

Sutton, J. 1982. Epidemiology of wheat head blight and maize ear rot caused by *Fusarium graminearum*. Canadian Journal of Plant Pathology 4: 195-209.

Suzuki, S., N. Sakakibara, L. Li, T. Umezawa and V.L. Chiang. 2010. Profiling of phenylpropanoid monomers in developing xylem tissue of transgenic aspen (*Populus tremuloides*). Journal of Wood Science 56: 71-76.

Taiakina, V., A.N. Boone, J. Fux, A. Senatore, D. Weber-Adrian, J.G. Guillemette, et al. 2013. The Calmodulin-Binding, Short Linear Motif, NSCaTE Is Conserved in L-Type Channel Ancestors of Vertebrate Cav1. 2 and Cav1. 3 Channels. PloS one 8: e61765.

Tautenhahn, R., C. Böttcher and S. Neumann. 2008. Highly sensitive feature detection for high resolution LC/MS. BMC bioinformatics 9: 504.

Tautenhahn, R., G.J. Patti, E. Kalisiak, T. Miyamoto, M. Schmidt, F.Y. Lo, et al. 2011. metaXCMS: Second-order analysis of untargeted metabolomics data. Analytical Chemistry 83: 696-700.

Tohge, T. and A.R. Fernie. 2010. Combining genetic diversity, informatics and metabolomics to facilitate annotation of plant gene function. Nature Protocols 5: 1210-1227.

Tohge, T., Y. Nishiyama, M.Y. Hirai, M. Yano, J.i. Nakajima, M. Awazuhara, et al. 2005. Functional genomics by integrated analysis of metabolome and transcriptome of Arabidopsis plants over-expressing an MYB transcription factor. The Plant Journal 42: 218-235.

Trucksess, M.W., F. Thomas, K. Young, M.E. Stack, W.J. Fulgueras and S.W. Page. 1995. Survey of deoxynivalenol in US 1993 wheat and barley crops by enzyme-linked immunosorbent assay. Journal of AOAC International 78: 631.

Umezawa, T. 2010. The cinnamate/monolignol pathway. Phytochemistry Reviews 9: 1-17.

Vanholme, R., B. Demedts, K. Morreel, J. Ralph and W. Boerjan. 2010. Lignin biosynthesis and structure. Plant Physiology 153: 895.

Vorst, O., C. Vos, A. Lommen, R. Staps, R. Visser, R. Bino, et al. 2005. A non-directed approach to the differential analysis of multiple LC–MS-derived metabolic profiles. Metabolomics 1: 169-180.

Waldron, B., B. Moreno-Sevilla, J. Anderson, R. Stack and R. Frohberg. 1999. RFLP mapping of QTL for Fusarium head blight resistance in wheat. Crop Science 39: 805-811.

Walter, S., J.M. Brennan, C. Arunachalam, K.I. Ansari, X. Hu, M.R. Khan, et al. 2008. Components of the gene network associated with genotype-dependent response of wheat to the Fusarium mycotoxin deoxynivalenol. Functional & Integrative Genomics 8: 421-427.

Walter, S., P. Nicholson and F.M. Doohan. 2010. Action and reaction of host and pathogen during Fusarium head blight disease. New Phytologist 185: 54-66.

Wang, J. and B. Hou. 2009. Glycosyltransferases: key players involved in the modification of plant secondary metabolites. Frontiers of Biology in China 4: 39-46.

Wang, Y. and J. Miller. 1988. Effects of *Fusarium graminearum* metabolites on wheat tissue in relation to Fusarium head blight resistance. Journal of Phytopathology 122: 118-125.

Wang, Y., L. Yang, H. Xu, Q. Li, Z. Ma and C. Chu. 2005. Differential proteomic analysis of proteins in wheat spikes induced by *Fusarium graminearum*. Proteomics 5: 4496-4503.

Watanabe, M., M. Kusano, A. Oikawa, A. Fukushima, M. Noji and K. Saito. 2008. Physiological roles of the β-substituted alanine synthase gene family in Arabidopsis. Plant Physiology 146: 310-320.

Wei, S. 2010. Methyl jasmonic acid induced expression pattern of terpenoid indole alkaloid pathway genes in *Catharanthus roseus* seedlings. Plant Growth Regulation 61: 243-251.

Wilkins, M., J. Sanchez, A. Gooley, R. Appel, I. Humphery-Smith, D. Hochstrasser, et al. 1995. Progress with proteome projects: why all proteins expressed by a genome should be identified and how to do it. Biotechnology & genetic engineering reviews 13: 19-50.

Wink, M. 1988. Plant breeding: importance of plant secondary metabolites for protection against pathogens and herbivores. TAG Theoretical and Applied Genetics 75: 225-233.

Xia, J. and D.S. Wishart. 2011. Web-based inference of biological patterns, functions and pathways from metabolomic data using MetaboAnalyst. Nature Protocols 6: 743-760.

Xiao, J., X. Jin, X. Jia, H. Wang, A. Cao, W. Zhao, et al. 2013. Transcriptome-based discovery of pathways and genes related to resistance against Fusarium head blight in wheat landrace Wangshuibai. BMC Genomics 14: 197.

Xu, D., H. Juan, M. Nohda and T. Ban. 2001. QTLs mapping of type I and type II resistance to FHB in wheat. National Fusarium Head Blight Forum Proceedings. p. 40.

Xu, X. and P. Nicholson. 2009. Community ecology of fungal pathogens causing wheat head blight. Annual Review of Phytopathology 47: 83-103.

Xue, S., G. Li, H. Jia, F. Xu, F. Lin, M. Tang, et al. 2010. Fine mapping *Fhb4*, a major QTL conditioning resistance to Fusarium infection in bread wheat (*Triticum aestivum* L.). Theoretical and Applied Genetics 121: 147-156.

Xue, S., F. Xu, M. Tang, Y. Zhou, G. Li, X. An, et al. 2011. Precise mapping Fhb5, a major QTL conditioning resistance to Fusarium infection in bread wheat (Triticum aestivum L.). Theoretical and Applied Genetics 123: 1055-1063.

Xue, Y.J., L. Tao and Z.M. Yang. 2008. Aluminum-induced cell wall peroxidase activity and lignin synthesis are differentially regulated by jasmonate and nitric oxide. Journal of Agricultural and Food Chemistry 56: 9676-9684.

Yang, F., J.D. Jensen, B. Svensson, H.J.L. Jørgensen, D.B. Collinge and C. Finnie. 2010. Analysis of early events in the interaction between *Fusarium graminearum* and the susceptible barley (*Hordeum vulgare*) cultivar Scarlett. Proteomics 10: 3748-3755.

Yang, J., G. Bai and G.E. Shaner. 2005. Novel quantitative trait loci (QTL) for Fusarium head blight resistance in wheat cultivar Chokwang. Theoretical and Applied Genetics 111: 1571-1579.

Yang, S., S.H. Lu and Y.J. Yuan. 2008. Lipidomic analysis reveals differential defense responses of *Taxus cuspidata* cells to two elicitors, methyl jasmonate and cerium (Ce4+). Biochimica et Biophysica Acta - Molecular and Cell Biology of Lipids 1781: 123-134.

Yang, Z., J. Gilbert, G. Fedak and D.J. Somers. 2005. Genetic characterization of QTL associated with resistance to Fusarium head blight in a doubled-haploid spring wheat population. Genome 48: 187-196.

Young, N. 1996. QTL mapping and quantitative disease resistance in plants. Annual Review of Phytopathology 34: 479-501.

Zhang, C., Y. Shen, J. Chen, P. Xiao and J. Bao. 2008. Nondestructive prediction of total phenolics, flavonoid contents, and antioxidant capacity of rice grain using near-infrared spectroscopy. Journal of Agricultural and Food Chemistry 56: 8268-8272.

Zhang, X., M. Zhou, L. Ren, G. Bai, H. Ma, O.E. Scholten, et al. 2004. Molecular characterization of Fusarium head blight resistance from wheat variety Wangshuibai. Euphytica 139: 59-64.

Zhou, W., F. Eudes and A. Laroche. 2006. Identification of differentially regulated proteins in response to a compatible interaction between the pathogen *Fusarium graminearum* and its host, *Triticum aestivum*. Proteomics 6: 4599-4609.

Zhou, W., F.L. Kolb and D.E. Riechers. 2005. Identification of proteins induced or upregulated by Fusarium head blight infection in the spikes of hexaploid wheat (Triticum aestivum). Genome 48: 770-780.

Zhou, W., F.L. Kolb, J. Yu, G. Bai, L.K. Boze and L.L. Domier. 2004. Molecular characterization of Fusarium head blight resistance in Wangshuibai with simple sequence repeat and amplified fragment length polymorphism markers. Genome 47: 1137-1143.

Zhou, W.C., F. Kolb, G.H. BAI, L. Domier and J.B. YAO. 2002. Effect of individual Sumai 3 chromosomes on resistance to scab spread within spikes and deoxynivalenol accumulation within kernels in wheat. Hereditas 137: 81-89.

Zhuang, Y., A. Gala and Y. Yen. 2013. Identification of Functional Genic Components of Major Fusarium Head Blight Resistance Quantitative Trait Loci in Wheat Cultivar Sumai 3. Molecular Plant-Microbe Interactions 26: 442-450.

Appendices

Appendix 3.1: Fusarium head blight resistance related metabolites in wheat QTL *Fhb1* identified in **rachis**, following *F. graminearum* or mock inoculation

Observed mass (Da)	**Exact mass (Da)**	**AME**	**RT (min)**	**Putative** inoculation **name**	**Observed fragmentation**	**Database fragmentation**	**Fold change[@]**	**Chemical group**	**Database ID[$]**
130.0270	130.0266	2.92	1.61	Itaconic acid	**129.10**, **111.07**, 101.25, 99.11, **85.20**	129.01, 111.04, 85.02, 41.04	1.30 (RRI), 1.7 (PRr),	Fatty acids and Conjugates	44764, C00490, **KOX00366**, LMFA01170063
132.0426	132.0423	2.00	1.60	2-methylenesuccinic acid	**113.18, 87.30**	131.03, 113.02, 87.04, 69.03	1.69*(RRI), 2.2*(PRr)	Fatty acids and Conjugates	3254, C00489, **KOX00277**, LMFA01170046
134.0370	134.0368	1.00	13.58	6Z-Octene-2,4-diynoic acid	115.28, 75.18, 59.10		4.9*(RRI), 5.8*(PRr)	Fatty Acids and Conjugates	35332
136.0527	136.0524	1.00	14.70	Hydroxyacetophenone	135.18, 107.23, 91.31, 75.25		3.8*(***RRI***)	Phenylpropanoid	64173, C06224
136.0527	136.0524	1.00	13.54	Methylbenzoate	135.27, 117.54, 107.25, **91.24, 75.30**	135.04, 91.05, 89.01, 75.00, 59.01,	3.9*(***RRI***)	Aldehydes	63506, C03765, **KOX00415**
138.0320	138.0317	2.52	14.16	Salicylic acid	**136.84,** 118.99, 108.93, **92.84**	137.02, 93.03, 65.03	3.2*(***RRI***)	Phenol	3263, C00156, **KOX00321**
148.0527	148.0524	2.09	1.66	*trans*-Cinnamic acid	129.13, 103.11, 87.17, 85.18	147.0, 103.05, 101.04, 77.04	1.27*(RRI), 1.9*(PRr)	Phenylpropanoid	63104, C00423, **PR050604**
162.0681	162.0680	1.00	1.60	Methylcinnamate	161.03, 143.14, 131.05, 117.24,		1.13*(RRI), 1.7*(PRr)	Phenylpropanoid	3793
166.0631	166.0630	0.70	18.01	Caffeyl alcohol	**149.13, 135.18,** 121.30, **109.26,** 97.12	149.13, 135.18, 109.26	1.35*(RRI), 10*(PRr)	Phenylpropanoid	64162, C12206, ***In silico***
175.0635	175.0633	1.00	9.75	3-Indoleacetic Acid	**174.01,** 146.04, **130.15,** 129.09, 115.09	174.05, 130.06, 128.04	123.9*(***RRI***)	Auxin	70, **KOX00380**
176.0941	176.0940	0.80	35.14	Serotonin	175.23, 147.13, 131.08		1.33*(RRI), 1.6*(PRr)	Amines	C00780, PMN
180.0636	180.0634	1.21	1.59	Myoinositol	179.12, **161.06, 143.11**, **125.08,** 99.12, 97.06	180.03, 161.0, 149.0, 143.1, 131.0, 125.1, 119.1, 113.1, 89.1	1.8*(***RRI***)	Carbohydrates and Carbohydrate conjugates	C00137**, MT000112**
192.0634	192.0634	0.19	1.51	Quinic acid	**191.26, 173.07, 171.0, 110.96**	191.3, 173.4, 170.8, 127.0, 111.4, 93.0, 96.1	1.13*(RRI), 2.5*(PRr)	Carboxylic acid	3329, C00296, **KO001747**
202.1206	202.1205	0.26	18.31	Sebacic acid	**201.09,** 157.13, 118.97, 58.89	201.0, 183.0, 139.0	1.25*(RRI), 1.5*(PRr)	Fatty Acids and Conjugates	4240, C08277, **PR051363,** LMFA01170006, C00001202

208.0722	208.0736	6.45	22.44	Sinapaldehyde	**206.90**, **192.06, 177.33,** 163.20, **146.8,** 133.18, 120.09, 103.05	207.0, 192.0, 177.0,149.0, 93.0	2.22*(RRI), 14.2*(PRr)	Phenylpropanoid	44806, C05610, **PR051195**, C00002775, **McGill MD**
210.1255	210.1256	0.35	17.07	Jasmonic acid	194.12, **191.01, 165.03,** 149.94, **143.01,** 127.18, 111.04	209.29, 191.00, 165.40, 143.05, 133.67	1.14**(RRI), 4**(PRr)	Jasmonate	**62988**, C08491, C00001314, **McGill MD**
224.0700	224.0685	7.00	19.94	Sinapic acid	**223.18, 208.0,** 179.02, 145.04, **141.04**	223.08, 208.03, 193.01, 164.04, 149.02, 141.01	2.6*(RRC)	Phenylpropanoid	45738, C00482, **KOX00565, McGill MD**
234.1367	234.1368	-0.34	14.23	*p*-Coumaroylputrescine	**233.11, 218.25,** 191.13,**119.01**	119.04, 190.08, 218.11, 233.12	24.6** (***RRI***)	Hydroxycinnamic acid amide	C18326, PMN, J817.813E, ***In silico,* (Muroi et al., 2009)**
248.1423	248.1412	4.34	15.36	Abscisic aldehyde	247.10, **219.38,** 186.17, **179.06**	219.38, 179.06	163.1* (***RRI***)	Terpenoid	C13455, J489.427H, PMN, ***In silico***
250.1568	250.1569	0.54	24.50	Xanthoxin	249.53, 205.23, 181.00, 125.23, 119.13		2.68*(RRI), 13.9*(PRr)	Terpenoid	64102, C13453
250.1568	250.1569	0.44	20.71	Abscisic alcohol	119.14		2.67*(RRI), 15.8*(PRr)	Terpenoid	64130, C13456,
264.1036	264.1030	2.42	13.58	2-(6'-methylthio)hexylmalate	248.01, 245.07, 235.23, 219.22, 176.22		1.01*(RRI), 20.6*(PRr)	Glucosinolate	PMN
264.1473	264.1474	0.32	15.11	Feruloylputrescine	**248.04,** 235.32, 219.33, **176.19,** 160.25	176.04, 248.12	407.8* (***RRI***)	Hydroxycinnamic acid amide	C10497, J11.793E , ***In silico,* (Muroi et al., 2009)**
267.1268	267.1259	3.21	13.55	Cinnamoyltyramine	135.32, **136.13,** 182.35	131.04, 136.07	262.8* (***RRI***)	Hydroxycinnamic acid amide	PMN, J466.382I, ***In silico***
272.2352	272.2351	0.00	31.64	4-Hydroxy palmitic acid	271.38, 253.43, 243.23, 227.27		1.6*(RRI), 1.6*(PRr)	Fatty Acids and Conjugates	35428, LMFA01050050
276.0244	276.0246	0.84	1.40	6-Phospho-D-gluconate	**257.16, 177.07, 159.16, 97.10**		1.18*(RRI), 1.3*(PRr)	Carbohydrates and Carbohydrate conjugates	367, C00345
276.1584	276.1586	0.96	16.16	*cis-p*-Coumaroylagmatine	**258.29, 233.30, 119.18**	119.04, 233.129, 258.14	44.3* (***RRI***)	Hydroxycinnamic acid amide	C00028060, ***In silico* , (Muroi et al., 2009)**
280.1085	280.1099	5.10	13.56	Magnaldehyde B	264.28, 239.27, 149.16, 134.12		1.33*(RRI), 189.8*(PRr)	Lignan	C00030707
280.1309	280.1311	0.79	22.44	8'-hydroxyabscisate	279.21, 261.29, 195.07		529.4* (***RRI***)	Terpenoid	PMN
280.2403	280.2402	0.08	31.90	Linoleic acid	**279.26, 261.24, 235.38, 191.09,**	279.23, 261.22, 235.16, 219.17, 191.12	1.5*(RRC)	Fatty Acids and Conjugates	191, C01595, **KOX00402,** LMFA01030120, **McGill MD**
282.0887	282.0892	1.00	12.69	5,6-Dimethoxyflavone	281.10, 263.14, 237.11, 219.28, 179.21		126.6* (***RRI***)	Flavonoids	48536, , , LMPK12110102
288.0622	288.0633	3.78	13.57	2-Hydroxyisoflavanone naringenin	277.24, 257.10, 249.31,		16.3* (***RRI***)	Flavonoids	PMN

292.1560	292.1575	5.07	16.05	16-epivellosimine	274.14, 249.26, 119.14		35.3* (***RRI***)	Alkaloid	PMN
296.2351	296.2351	0.18	29.98	9S-hydroxy-10E,12Z-octadecadienoic acid (9(S)-HODE)	**295.37, 277.36, 171.27**	295.22, 277.21, 171.10	1.6*(RRC)	Fatty Acids and Conjugates	**45662,** LMFA02000057
300.0841	300.0845	1.33	11.38	Salicylic acid O-β-D-glucoside	239.13, 209.20, **179.26, 137.15**	179.26, 137.15	1.03*(RRI), 3.1*(PRr)	Aryl glucoside	PMN, J355.695F, ***In silico*, (Torras-Claveria et al., 2011)**
306.1362	306.1368	1.96	14.71	Cinnamoylserotonin	**289.24, 219.23,** 175.16, 97.13	175.08, 289.13	1.06*(RRI), 33.7*(PRr)	Hydroxycinnamic acid amide	PMN, J958.892B, ***In silico***
306.1688	306.1692	1.25	16.85	Feruloylagmatine	**289.25, 263.15, 177.41, 149.12,** 134.18	289.14, 263.13, 177.05, 149.06	104.2 * (***RRI***)	Hydroxycinnamic acid amide	PMN, J817.816J, ***In silico* , (Muroi et al., 2009)**
309.1935	309.1940	1.52	14.71	Jasmonoyl valine			79.1* (***RRI***)	Jasmonate	PMN, J2.953.029G
310.2138	310.2144	1.95	26.99	13(S)-Hydroperoxylinolenic acid	**291.23, 209.12,** 171.13, **165.22,** 155.07	309.20, 291.19, 247.19, 209.11, 165.22	1.5*(RRC)	Fatty Acids and Conjugates	36025, C16321, **UT000087**
320.0888	320.0896	2.46	25.45	4-coumaroylshikimate	301.23, **172.20**	172.03	85.1* (***RRI***)	Phenylpropanoid	PMN, J2.380.119A, ***In silico***
322.1321	322.1317	1.03	15.94	*p*-coumaroylserotonin	97.19, 149.08, **175.16, 219.17, 289.17**	289.13, 175.08	99.1* (***RRI***)	Hydroxycinnamic acid amide	PMN, J2.159.664G, ***In silico***
323.2093	323.2096	0.79	23.57	(+)-7-iso-jasmonoyl-L-isoleucine	**304.34, 278.28,** 182.34, **130.16**	304.34, 278.28, 130.16	1.76*(RRI), 4.6*(PRr)	Jasmonate	PMN, J272.686F, ***In silico***
326.1523	326.1518	1.59	11.45	Dehydrodiisoeugenol	265.19, 324.19, 281.05, 227.02, 163.09, 296.85		1.7*(RRC)	Lignan	C10650, C00002611
328.1880	328.1889	2.72	17.80	1-pentyl-sn-glycero-3-phosphocholine	312.23, 309.25, 291.14, 267.21, 175.07		97* (***RRI***)	Glycerophospholipid	40394, LMGP01060020
338.0993	338.1001	2.35	13.52	4-coumaroylquinate	161.21, **191.19,** 235.26, **277.25, 293.21,** 318.70	293.10, 191.09, 277.01	43.1* (***RRI***)	Phenylpropanoid	PMN, , ***In silico*, Torras-Claveria et al. (2011)**
338.1258	338.1266	2.30	17.86	Caffeoylserotonin	**175.15,** 249.25, 269.03, 291.05	175.08	2.45*(RRI), 167.2*(PRr)	Hydroxycinnamic acid amide	PMN, ***In silico***
340.0592	340.0583	2.77	1.57	7-Methoxy-5,6:3\',4\'-bis(methylenedioxy)flavone	320.93, 278.13, 241.22, 159.17, 154.19		1.6*(RRC)	Flavonoids	49668, LMPK12111244
342.1002	342.0950	5.20	20.95	β-D-glucopyranosyl-caffeic acid	113.20, 143.16, 161.06, **179.05,** 297.16	163.06, 179.03	2.6 (RRI), 4.0 *(PRr)	Phenylpropanoid	J460.644B, *In silico*, **Torras-Claveria et al. (2011)**
342.1308	342.1315	2.00	12.73	Coniferin	294.96, 281.31, 265.25, **179.11, 163.24**	179.11, 163.24	4.0* (PRr)	Phenylpropanoid	64182, C00761
344.0891	344.0896	1.39	22.83	3',5-Dihydroxy-4',6,7-trimethoxyflavone	328.15, 275.27		1.4**(RRC)	Flavonoids	43851, LMPK12111239

344.0894	344.0896	0.47	21.65	5,6-Dihydroxy-7,8,4'-trimethoxyflavone	328.16, 275.20		1.7*(RRC)	Flavonoids	49872, LMPK12111449
344.1458	344.1471	4.00	17.06	Dihydroconiferyl alcohol glucoside	275.21		10** (***RRI***)	Terpenoid	41169, C11653, LMPR0102070024,
346.1260	346.1263	1.99	11.87	Aucubin	330.84, 299.22, 281.16		2.6* (***RRI***)	Terpenoid	41151, C09771, LMPR0102070006
346.1261	346.1263	0.00	13.98	Deutzioside	331.00, 299.11, 281.09, 227.22		1.56*(RRI), 6.4*(PRr)	Terpenoid	41181, C11671, LMPR0102070036
350.1636	350.1630	1.52	14.60	Vomilenine	333.26, 319.28, 305.41, 291.39, 255.77		1054.4** (***RRI***)	Alkaloid	PMN
352.1421	352.1423	0.65	20.67	Feruloylserotonin	**336.16,** 237.21, 201.31, **175.18, 177.01, 161.23, 135.20**	135.04, 175.08, 177.05, 336.11	1194.8* (***RRI***)	Hydroxycinnamic acid amide	PMN, J1.973.598B, ***In silico***
356.1101	356.1107	1.00	16.63	Ferulic acid 7-O-glucoside	217.06, 193.01, 175.01	163.06, 193.02	28.7 * (***RRI***)	Phenylpropanoid	J322.813D, ***In silico,*** **(Torras-Claveria et al., 2011)**
360.1416	360.1420	1.06	13.05	7-Deoxyloganate	340.17, 299.21, 239.18, 197.23		1.4* (RRC)	Terpenoid	64040, C11636
360.1566	360.1573	1.95	20.26	Lariciresinol	**344.15,** 327.12, 299.15, 239.00, 197.08	344, 313	1.95*(RRI), 13.5*(PRr)	Lignan	C10646, C00000602, (Eklund et al., 2008)
370.1265	370.1264	0.32	18.48	Sinapaldehyde glucoside			93.1* (***RRI***)	Phenylpropanoid	PMN,
370.1790	370.1780	2.59	22.29	Unanisoflavan	354.07, 323.27, 201.12, 185.02, 166.93		2.5*(RRC)	Flavonoids	48254, LMPK12080009, C00009734
372.1425	372.1420	1.16	13.03	Syringin	**353.27,** 310.6, **249.26, 209.23,** 149.13	353, 311, 209	1.92 (RRI), 60* (PRr)	Phenylpropanoid	64181, C01533,
373.1294	373.1287	1.96	1.49	7-Oxomatairesinol	356.10, 288.69, 249.04, 231.20, 175.24, 120.94		1.04*(RRI), 4.5*(PRr)	Lignan	
384.1209	384.1215	1.58	17.87	2-S-adenosyl-L-homocysteine	365.24, 355.13, 337.06, 307.11, 296.02, 247.28		132.6* (***RRI***)	non-standard alpha amino acid	PMN
386.1210	386.1212	0.8	16.98	β -D-glucopyranosyl-sinapic acid	**223.24,** 247.14, 342.74	223.06, 163.06	2.8 (RRI), 4.8*(PRr)	Phenylpropanoid	J1.426.998C, ***In silico***
390.1508	390.1526	4.00	16.02	Loganin	371.42, 341.22, 291.16		1.70*(RRI), 18.8*(PRr),	Terpenoid	41146, C01433, LMPR0102070001
398.1356	398.1366	2.41	20.79	Deoxypodophyllotoxin	379.22, 336.86, 329.26, 311.40		1.4*(RRC)	Lignan	2040, C10556,
399.1437	399.1450	3.18	24.29	S-adenosyl-L-methionine	329.38		Inf* (***RRI***)	non-standard alpha amino acid	PMN

402.1519	402.1526	1.62	13.79	Benzyl alcohol beta-D-xylopyranosyl (1->6)-beta-D-glucopyranoside	383.23, 357.37, 179.25		23.3* (***RRI***)	Carbohydrates and Carbohydrate conjugates	PMN
406.1467	406.1475	1.00	13.99	10-Hydroxyloganin	387.34, 344.93, 183.28, 161.02		1.01*(RRI), 7.3*(PRr)	Terpenoid	41173, C11659, LMPR0102070028
426.1881	426.1890	2.14	22.36	Abscisic acid glucose ester	305.18, 275.25, 261.24		189.1* (***RRI***)	Terpenoid	PMN
428.1462	428.1471	0.00	20.88	5,4\'-Dihydroxy-3,6,3\'-trimethoxy-7-prenyloxyflavone	409.19, 395.10, 351.17, 281.16, 263.13, 249.06		1.20*(RRI), 7*(PRr)	Flavonoids	51635, LMPK12113223
434.1219	434.1213	1.32	20.69	Naringenin 7-O-β-D-glucoside	403.38, 373.29, 364.86, 351.25, 312.14, 206.86		23.7* (***RRI***)	Flavonoids	52730, PMN
446.1567	446.1577	2.00	20.90	5-Hydroxy-7,8-dimethoxyflavanone 5-rhamnoside	429.60, 417.11, 353.29, 327.23		74.4* (***RRI***)	Flavonoids	53130, PMN
550.1678	550.1686	1.00	16.32	Chalconaringenin 2\'-rhamnosyl-(1->4)-xyloside	530.64, 387.22, 369.17, 265.11		6.7***(RRC)	Flavonoids	52056, LMPK12120252
550.2036	550.2050	2.62	20.37	Medioresinol 4'-O-beta-D-glucopyranoside	531.26, 504.42, 327.09		1.6* ***(RRI)***	Lignan	PMN
552.1468	552.1479	0.00	23.18	5,2',5'-Trihydroxy-3,6,7,4'-tetramethoxyflavone 5'-glucoside	367.16, 343.33		1.7*(RRC)	Flavonoids	51455, LMPK12113043
566.1624	566.1636	1.00	23.18	5,7,4\'-Trihydroxyflavonone 4\'-O-xylosylglucoside	367.16, 343.33		2.9***(RRC)	Flavonoids	52740, LMPK12140252
566.1626	566.1636	1.00	19.62	5,7,4\'-Trihydroxyflavanone 7-O-arabinosylglucoside	546.06, 504.14, 474.09, 444.14, 384.16, 354.21		1.7*(RRC)	Flavonoids	52737, LMPK12140249
578.1616	578.1636	3.42	19.05	Kaempferitrin	559.3, 503.19, 473.30, 457.27, 383.32, 354.81, 337.21, 325.17	431.09, 430.08, 286.04, 285.03, 283.02	4.8*(RRC)	Flavonoids	50281, LMPK12111865
578.1629	578.1636	1.10	14.34	Kaempferol 3-rhamnoside-(1->2)-rhamnoside	497.32		2.4*(RRC)	Flavonoids	50323, LMPK12111907
592.1417	592.1428	1.00	21.64	Kaempferol 3-[6\'\'-(3-hydroxy-3-methylglutaryl)glucoside]	573.25, 561.32, 353.21		1.6*(RRC)	Flavonoids	50201, LMPK12111785
674.1447	674.1424	0.00	21.66	Phyllanthusmin B	655.10, 477.26, 459.27		1.5*(RRC)	Lignan	C00031017
686.2743	686.2786	6.23	21.35	Secoisolariciresinol di-O-glucoside	670.58, 643.09, 625.27, 601.08, 583.10		1.46*(RRI), 4.1*(PRr)	Lignan	C00000652

710.2085	710.2058	3.73	25.01	Kaempferol 3-rhamnoside-7-xylosyl-(1->2)-rhamnoside	649.29, 634.93, 517.27, 443.32, 441.22, 367.04		34.9* (***RRI***)	Flavonoids	50340
861.2420	861.2453	3.00	25.01	Pelargonidin 3-rutinoside-7-(6-(p-hydroxybenzoyl)glucoside)	819.24, 801.15, 777.15, 759.25, 685.11, 643.14		1.14*(RRI), 3.9**(PRr)	Flavonoids	46849, LMPK12010082

AME: Accurate Mass Error= ((Observed mass - expected mass) / expected mass) X $10^{6,}$ **RT:** Retention time, **RRC:** Resistance related constitutive, **PRr:** Pathogen related in resistant NIL, **RRI:** Resistance related induced, ***RRI***: Detected only in resistant NIL

[@] **Fold change calculation**: were based on relative intensity of metabolites, RRC= RM/SM, PRr= RP/RM, RRI= (RP/RM)/(SP/SM); ***RRI***= RP/RM, PRr fold change is reported for the metabolites detected only in NIL-R. RP: resistant NIL with pathogen inoculation, RM: resistant NIL with mock inoculation, SP: susceptible NIL with pathogen inoculation, SM: susceptible NIL with mock inoculation.

***** *t* test significance at $P<0.05$, ****** *t* test significance at $P<.01$, *** *t* test significance at $P<.001$

Database ID examples: Number-METLIN, **LMP**-LIPIDMAPS, **KEGG**-C05610, **KNAPSACK**- C00002775, **MASSBANK**-PR051195, KOX00020, **NIKKAJI:** J355.695F, and **PMN**-Plant Metabolic Network, ***In silico:*** In silico fragmentation

[$]Database ID in bold is the fragmentation match

References:

Eklund P.C., Backman M.J., Kronberg L.Å., Smeds A.I., Sjöholm R.E. (2008) Identification of lignans by liquid chromatography-electrospray ionization ion-trap mass spectrometry. Journal of Mass Spectrometry 43:97-107.

Muroi A., Ishihara A., Tanaka C., Ishizuka A., Takabayashi J., Miyoshi H., Nishioka T. (2009) Accumulation of hydroxycinnamic acid amides induced by pathogen infection and identification of agmatine coumaroyltransferase in Arabidopsis thaliana. Planta 230:517-527.

Torras-Claveria L., Jáuregui O., Codina C., Tiburcio A.F., Bastida J., Viladomat F. (2011) Analysis of phenolics compounds by high-performance liquid chromatography coupled to electrospray ionization tandem mass spectrometry in senescent and water-stressed tobacco. Plant Science 182:71-78.

Appendix 3.2: Fusarium head blight resistance related metabolites in identified in ***spikelets*** of wheat NILs harboring *Fhb1* resistant allele, following F. graminearum or mock inoculation

Observed mass (Da)	**Exact mass (Da)**	**AME**	**RT (min)**	**Putative name**	**Observed fragmentation**	**Database fragmentation**	**Fold change[@]**	**Chemical group**	**Database ID[$]**
124.0519	124.0524	4.00	39.18	4-Methylcatechol	108.33, 105.41, 80.97	108.02, 105.03, 80.02	1.2* (RRC)	Phenol	**64945,** C06730
131.0582	131.0582	4.00	16.15	*trans*-Hydroxy-D-proline	**130.28, 112.03, 86.38, 62.17**	130.05, 112.04, 86.02, 84.04, 68.04, 66.03, 57.03	1.50 (RRI), 59* (PRr)	Aldehyde	**257,** C01157
133.0371	133.0375	3.00	1.67	L-aspartate	**132.23, 115.15, 114.19, 88.21**	132.0, 115.0, 103.0, 88.0, 71.0	3.45 (RRI), 3.8* (PRr)	Amino acid	C00049, **PR051379**, C00001342
148.0532	148.0524	5.15	14.19	*trans*-Cinnamic acid	**147.12,** 119.19, **103.05, 77.02**	147, 103.05, 101.04, 77.04	2.0 (RRI), 1.7* (PRr)	Phenylpropanoid	**63104,** C00423, **PR050604, McGill MD**
165.0797	165.0790	4.53	7.72	L-phenylalanine	**164.01, 147.13, 103.16,** 91.15, **72.14**	164.0, 147.0, 103.0, 72.0	1.56 (RRI), 2.5** (PRr)	Phenylpropanoid	**28,** C00079, **PR050152**, **McGill MD** C00001386
174.0172	174.0164	4.58	1.60	*cis*-aconitate	**173.11,** 155.06, **129.0, 110.99,** 70.97, **59.0**	173.00, 129.01, 112.98, 111.00, 85.02, 59.01	2.32 (RRI), 11.6*** (PRr)	Carboxylic acid	C00417, **KOX00020**
175.0639	175.0633	3.31	23.07	Indole-3-acetate	**174.01,** 146.04, **130.15,** 129.09, 115.09	174.05, 130.06, 128.04	1.11 (RRI), 69.5* (PRr)	Auxin	70, C00954, **KOX00380**
178.0626	178.0630	1.00	22.49	Coniferyl aldehyde	**177.03, 162.00,** 145.04, 117.99	177.0, 162.0, 134.0	1.08 (RRI), 72.2* (PRr)	Phenylpropanoid	C02666, **PR051058**, **McGill MD** C00002728
182.0786	182.079	2.43	1.93	D Mannitol	**163.14,** 131.17, **119.07**, **101.11, 89.18**	181.07, 163.06, 119.03, 101.02, 89.02, 71.01, 59.04	15.31 (RRI), 19.9* (PRr)	Sugar	**142, C00392, PR051123**
191.0588	191.0582	3.07	9.03	5-Hydroxyindoleacetic acid	175.15, **146.16**	146.06, 144.04, 131.03	1.31 (RRI), 2.5* (PRr)	Auxin	**44806,** C05635, **KO001068**
208.0788	208.0736	4.00	23.62	Sinapaldehyde	**207.08, 192.04,** 178.96, 164.92, 147.27, 121.33, 101.08	207.0, 192.0, 177.0,149.0, 93.0	3.36 (RRI), 20.2* (PRr)	Phenylpropanoid	**44806**, C05610, **McGill MD**
210.1263	210.1256	3.25	16.65	Jasmonic acid	194.12, **191.01, 165.03,** 149.94, **143.01,** 127.18, 111.04	209.29, 191.00, 165.40, 143.05, 133.67	1.52 (RRI), 2.9* (PRr)	Fatty acid and conjugates	**62988,** C08491, **McGill MD**
234.1375	234.1386	5.00	15.93	*p*-Coumaroylputrescine	**233.11, 218.25,** 191.13,**119.01**	119.04, 190.08, 218.11, 233.12	1.93 (RRI), 6.2* (PRr)	Hydroxycinnamaic acid	PMN, ***In silico,*** **(Muroi et al., 2009)**

248.1419	248.1412	2.76	15.86	Abscisic aldehyde	247.29, 205.17, 119.00	219.38, 179.06	1.22 (RRI), 32.6* (PRr)	Terpenoid	C13455, PMN, ***In silico***
250.1478	250.1569	5.00	16.17	4-Coumaroylcholine	119.12		1.72 (RRI), 23.6* (PRr)	Phenylpropanoid	PMN
254.0201	254.0192	3.72	1.40	Shikimic acid 3-phosphate	253.11, 237.82, 209.12, 193.04		1.3* (RRC)		3384, C03175
272.0683	272.0685	1.00	22.97	Naringenin	**271.10,** 270.05, 226.13, 203.16, 181.09, **118.86**	271.0, 151.0, 119.0	1.2* (RRC)	Flavonoid	3401, C00509, **PR051071,** C00000982, **McGill MD**
276.1591	276.1586	1.8		*cis-p*-Coumaroylagmatine	**258.29, 233.30, 119.18**	119.04, 233.129, 258.14	41** (***RRI***)	Hydroxycinnamaic acid	PMN, ***In silico*** , **(Muroi et al., 2009)**
278.2257	278.2246	4.08	30.66	α-Linolenate	**277.22, 259.41,** 233.34, 80.16	277.21, 259.20, 59.01	2.79 (RRI), 3.2** (PRr)	Fatty acid and conjugates	**192**, C06426, C00001226, **McGill MD**
280.2409	280.2402	2.39	31.39	Linoleate	**279.40, 261.36, 259.27, 243.05,**	279.4, 261.1, 259.3, 243.5, 219.5, 59.1	2.61 (RRI), 2.7* (PRr)	Fatty acid and conjugates	**191,** C01595, **KO001297, McGill MD**
298.1207	298.1205	0.79	21.66	Enterolactone			1.47 (RRI), 52.5*** (PRr)	Lignan	64734, C18165
316.1163	316.1158	1.50	14.89	Vanilloloside	297.31, 233.34, 201.32, 130.22		1.13 (RRI), 2.5* (PRr)	Phenylpropanoid	C00032471
318.1106	318.1103	0.94	26.03	Catechin 7,4'-dimethyl ether	328.12, 302.15, 286.38, 249.33		1.41 (RRI), 25.3** (PRr)	Flavonoid	47359, LMPK12020143
322.1043	322.1053	3.00	13.35	4-O-Cinnamoylquinic acid	277.14, 253.14, 249.31, 235.17, 176.15, 119.16		1.7* (RRC)	Phenylpropanoid	C00029541, ***In silico***
336.0836	336.0845	3.00	9.48	5-O-Caffeoylshikimic acid			2.3** (RRC)	Phenylpropanoid	C00002720,
338.0989	338.1002	4.00	1.98	1-Caffeoyl-4-deoxyquinic acid	318.21, 294.38, 277.16, 153.33		2.7* (RRC)	Monolignol	C00002717
338.1282	338.1266	4.87	18.02	Caffeoylserotonin	322.27, 314.86, 307.27, 294.05, 217,13, 173.35		16.1 * (***RRI***)		***In silico,*** PMN
340.1315	340.1311	1.27	18.33	6-Prenylnaringenin	324.16, 321.30, 271.41, 249.04, 163.22, 130.29		1.30 (RRI), 1.7* (PRr)	Flavonoid	52761, LMPK12140277
342.1319	342.1315	1.25	14.13	Coniferin	341.33, 280.67, **179.03, 160.98,** 143.02, 113.12	179.03, 161	1.41 (RRI), 16.5* (PRr)	Phenylpropanoid	64182, C00761

342.1683	342.1681	0.51	12.76	2-valeryl-sn-glycero-3-phosphocholine	295.10, 281.10, 265.16		1.90 (RRI), 400.5* (PRr)	Glycerophospholipids	40358, LMGP01050092
344.0851	344.0896	5.00	21.25	6-Hydroxykaempferol 3,7,4\'-trimethyl ether	325.19, 257.33, 247.20, 195.20		2.22 (RRI), 9.8** (PRr)	Flavonoid	51285, LMPK12112873
344.0898	344.0896	0.72	18.48	Quercetin 3,5,3'-trimethyl ether	325.25, 307.32, 289.35, 237.24, 229.18, 209.25, 201.15, 171.21		1.72 (RRI), 12.8** (PRr)	Flavonoid	51167, LMPK12112753
344.1471	344.1471	0.12	15.75	Iridotrial glucoside			12.3* (***RRI***)	Terpenoid	C11653
344.1475	344.1471	1.33	17.33	Dihydroconiferyl alcohol glucoside	325.32, 275.28		1.16 (RRI), 2.9** (PRr)	Phenylpropanoid	C11652
344.1761	344.1776	4.00	25.69	alpha,alpha\'-diethyl-4,4\'-bis(2-propynyloxy)stilbene	328.18, 310.29, 292.39, 225.15, 171.24		1.4* (RRC)	Stilbene	53252, C15066, LMPK13090025
350.1639	350.1630	2.45	16.40	Vomilenine	330.72, 304.09, 255.24, 233.22, 187.18		8.21 (RRI), 11.5** (PRr)	Alkaloids	64326, C11680,
352.1417	352.1423	-1.78	22.75	Feruloylserotonin	336.32, 33.28, 201.16, 161.16, 135.22		30.7* (***RRI***)		PMN, J1.973.598B, ***In silico***
360.1410	360.1420	3.00	16.29	7-Deoxyloganate	341.26, 291.19, 201.27, 171.25		1.30 (RRI), 31.6** (PRr)	Flavonoid	64040
360.1576	360.1573	1.05	20.41	Lariciresinol	341.33, 315.28, **299.23,** 291.21	299, 284, 192, 178, 160	1.23 (RRI), 8.9* (PRr)	Lignan	C10646, **(Eklund et al., 2008)**
370.1268	370.1264	1.05	14.07	Sinapaldehyde glucoside	360.21, 351.22, 249.29, 147.12		1.14 (RRI), 57.7* (PRr)	Phenylpropanoid	PMN
372.1425	372.1420	1.16	13.03	Syringin	**353.27,** 310.6, **249.26, 209.23,** 149.13	353, 311, 209	2.09 (RRI), 19.9* (PRr)	Phenylpropanoid	64181, C01533
388.1161	388.1158	0.85	18.52	Quercetagetin 5,6,7,3',4'-pentamethyl ether	369.23, 265.16		6.4*** (RRC)	Flavonoid	51431
388.1524	388.1522	0.59	20.65	Trachelogenin/Medioresinol	369.12, 351.09, 343.23, 327.16, 265.25,		1.13 (RRI), 7* (PRr)	Lignan	52090, LMPK12120287
432.1420	432.1420	0.05	21.19	Heptamethoxyflavone	413.35, 341.13, 311.13, 269.18		1.11 (RRI), 1.9** (PRr)	Flavonoid	49055, LMPK12110625
434.1212	434.1213	0.11	24.59	Naringenin-7-O-Glucoside	401.03, 328.11		1.83 (RRI), 2.2* (PRr)	Flavonoid	52730, LMPK12140242

448.2452	448.2468	3.00	31.41	Glutathionylaminopropylcadaverine	279.37		1.2 (RRI), 4.2** (PRr)	Glutathione metabolism	63644, C16566
476.1317	476.1319	0.35	25.22	Naringenin 7-O-beta-D-glucoside 6\'\'-acetate	328.04, 307.35, 289.25, 245.34, 209.25, 191.37		1.47 (RRI), 65.4* (PRr)	Flavonoid	52745, LMPK12140257
478.1474	478.1475	0.17	14.35	2',4',4-Trihydroxy-3',3-dimethoxychalcone 4'-O-glucoside	395.86, 297.54, 233.07		2.2* (RRC)	Flavonoid	51984, LMPK12120180
478.1475	478.1475	0.09	26.14	Persiconin	459.11, 329.23, 309.20, 291.29, 209.24		2.04 (RRI), 44.2* (PRr)	Flavonoid	53063, LMPK12140586
510.2962	510.2957	1.02	31.84	1-(9E-octadecenoyl)-sn-glycero-3-phospho-(1'-sn-glycerol)	493.27, 423.29, 281.37		1.22 (RRI), 6** (PRr)	Glycerophospholipids	40878, LMGP04050006
530.1396	530.1424	5.00	20.28	Luteolin 7-glucoside-4\'-(Z-2-methyl-2-butenoate)	510.67, 461.25		1.11 (RRI), 2.9* (PRr)	Flavonoid	49214, LMPK12110784
550.1491	550.1475	2.96	16.50	Formononetin 7-O-(2\'\'-p-hydroxybenzoylglucoside)	531.37, 387.24, 369.25, 265.25		4.9*** (RRC)	Flavonoid	47549, LMPK12050026
566.0553	566.0550	0.56	1.57	UDP-glucose	466.68, **384.94, 323.16, 240.98 211.20**	565.04, 384.98, 323.02, 241.01, 78.95	1.61 (RRI), 2.1* (PRr)	carbohydrates and conjugates	**3598,** C00029
572.2962	572.2962	0.03	31.59	1-Hexadecanoyl-sn-glycero-3-phospho-(1'-myo-inositol)	554.47, 485.18, 391.36, 315.19, 255.35, 241.10		1.67 (RRI), 10.5** (PRr)	Glycerophospholipids	46744, LMGP06050002
598.3120	598.3118	0.38	31.69	1-(9Z-octadecenoyl)-sn-glycero-3-phospho-(1'-myo-inositol)	417.27, 315.16, 281.46, 241.14, 223.05		1.10 (RRI), 10.9** (PRr)	Glycerophospholipids	46747, LMGP06050005

AME: Accurate Mass Error= ((Observed mass - expected mass) / expected mass) X $10^{6,}$ **RT:** Retention time, **RRC:** Resistance related constitutive, **PRr:** Pathogen related in resistant NIL, **RRI:** Resistance related induced, ***RRI***: Detected only in resistant NIL, [@] **Fold change calculation**: were based on relative intensity of metabolites, RRC= RM/SM, PRr= RP/RM, RRI= (RP/RM)/(SP/SM); ***RRI***= RP/RM, PRr fold change is reported for the metabolites detected only in NIL-R. RP: resistant NIL with pathogen inoculation, RM: resistant NIL with mock inoculation, SP: susceptible NIL with pathogen inoculation, SM: susceptible NIL with mock inoculation.
***** *t* test significance at $P<0.05$, ****** *t* test significance at $P<.01$, *** *t* test significance at $P<.001$
Database ID examples: Number-METLIN, **LMP**-LIPIDMAPS, **KEGG**-C05610, **KNAPSACK**- C00002775, **MASSBANK**-PR051195, KOX00020, **NIKKAJI:** J355.695F, and **PMN**-Plant Metabolic Network, ***In silico:*** In silico fragmentation [$]Database ID in bold is the fragmentation match

References:

Eklund, P.C., M.J. Backman, L.Å. Kronberg, A.I. Smeds and R.E. Sjöholm. 2008. Identification of lignans by liquid chromatography-electrospray ionization ion-trap mass spectrometry. Journal of Mass Spectrometry 43: 97-107.
Muroi, A., A. Ishihara, C. Tanaka, A. Ishizuka, J. Takabayashi, H. Miyoshi, et al. 2009. Accumulation of hydroxycinnamic acid amides induced by pathogen infection and identification of agmatine coumaroyltransferase in Arabidopsis thaliana. Planta 230: 517-527.
Torras-Claveria, L., O. Jáuregui, C. Codina, A.F. Tiburcio, J. Bastida and F. Viladomat. 2011. Analysis of phenolics compounds by high-performance liquid chromatography coupled to electrospray ionization tandem mass spectrometry in senescent and water-stressed tobacco. Plant Science 182: 71-78.

Appendix 4.1

Fusarium head blight resistance related metabolites in the rachis (3dpi) wheat NILS with resistant and susceptible *Fhb1* alleles derived from Sumai-3 following *F. graminearum* or mock inoculation

Observed mass (Da)	row retention time	ID	Molecular formula	Name	observe fragments	URL	Fold change	
							RRC	RRI
76.0167	2.14	GLYCOLLATE	H3O3C2	Glycolate	no ms	http://pmn.plantcyc.org/PLANT/NEW-IMAGE?type=COMPOUND&object=GLYCOLLATE	0.88	1.59
120.043	16.57	PURINE	C4H8O4	Dihydroxybutanoic acid	75.0,73.1,71.9,118.9		0.88	1.25
120.0431	1.51	PURINE	H4N4C5	purine	59.7,75.1,58.9,72.1	http://pmn.plantcyc.org/PLANT/NEW-IMAGE?type=COMPOUND&object=PURINE	0.99	1.37
120.0431	20.06	PURINE	H4N4C5	Purine	58.7(confu)	http://pmn.plantcyc.org/PLANT/NEW-IMAGE?type=COMPOUND&object=PURINE	0.84	1.41
159.9972	2.65			[2M-H]- 2.0000 m/z adduct of 156.9918 m/z	59.12,115.05,129.1,141.2		1.13	0.9
160.0381	1.57			2-Oxo-adipate	no MS		1.06	1.22
174.0537	24.49	SHIKIMATE	H9C7O5	Shikimate	129.08,111.2,145.17,155.03,173.4	http://pmn.plantcyc.org/PLANT/NEW-IMAGE?type=COMPOUND&object=SHIKIMATE	1.22	0.8
180.0644	30.54	1-7-DIMETHYLXANTHINE	H8O2N4C7	Paraxanthine	no ms	http://pmn.plantcyc.org/PLANT/NEW-IMAGE?type=COMPOUND&object=1-7-DIMETHYLXANTHINE	0.94	1.27
186.163	26.6	C17715	C11H22O2	Undecanoic acid	141.19,185.2,167.2,123.1,119.2,103.3, 115.1	http://www.kegg.jp/entry/C17715	1.19	0.93
204.0644	1.6			3-o- Ethyl ascorbic acid			0.98	1.3
206.0437	1.61			2-Methylcitrate	no MS		0.59	1.96
222.0702	1.5			Cystathionine			0.7	1.72
222.0751	1.44	C02655	C8H14O7	6-Acetyl-D-glucose	145.2,161.2,177.1,124.2	http://www.kegg.jp/entry/C02655	0.96	1.38
240.0856	25.54		C14H12N2O2	β-Carboline-1-propionic acid	223.08,171,178,221,209,	240.0898776	0.81	1.29
282.0965	1.35		C10H18O9	Xylobiose	438.9,481.1,400.1,437.2,325.2		1.09	1.29
492.1291	23.42	C10303	C23H24O12	Aurantio-obtusin beta-D-glucoside	329.03,476.0,371.0,343.1	http://www.kegg.jp/entry/C10303	1.22	0.74
502.1149	2.01		C24H22O12	Apigenin 7-(2"-acetyl-6"-	no ms	502.1111262	2.23	0.68

				methylglucuronide)				
502.2437	16.6	C17888	C24H38O11	Eriojaposide A	441.08,382.1,456.6,492.4,474.3,194.1	http://www.kegg.jp/entry/C17888	2.06	0.87
520.2542	15.6	LMST03020612	C29H45BrO3	25-Hydroxyvitamin D3-bromoacetate	confu	http://www.lipidmaps.org/data/LMSDRecord.php?LMID=LMST03020612	1.96	0.95
566.2024	17.76		C27H34O13	Fraxiresinol 4'-O-beta-D-glucopyranoside	474.2,444.2,504.1,354.2,384.1,546.0	566.1999412	0.66	1.22
598.2077	20.95	C18684	C31H34O12	Landomycin D	401.0,549.1,357.2	http://www.kegg.jp/entry/C18684	1.8	0.64
836.2771	18.72	UROPORPHYRINOGEN-III	H36O16N4C40	Eroporphyrinogen-III	no ms	http://pmn.plantcyc.org/PLANT/NEW-IMAGE?type=COMPOUND&object=UROPORPHYRINOGEN-III	1.59	0.89

Appendix 4.1 continued

Fusarium head blight resistance related metabolites in the spikelets (3dpi) wheat NILS with resistant and susceptible *Fhb1* alleles derived from Sumai-3 following *F. graminearum* or mock inoculation

Observed mass (Da)	retention time	ID	Molecular formula	Name	Observed fragments	Database fragmentation	URL	Chemical group	Fold change	
									RRC	RRI
116.0112	1.24	MALEATE	H2C4O4	maleate	115.23, 97.22, 87.28, 71.21, 69.31, 59.34		http://pmn.plantcyc.org/PLANT/NEW-IMAGE?type=COMPOUND&object=MALEATE	Carboxylate	0.9332	1.14*
118.0239	1.32	SUC	H4C4O4	succinate			http://pmn.plantcyc.org/PLANT/NEW-IMAGE?type=COMPOUND&object=SUC	Carboxylate	6.2719	6.27**
134.0581	1.48	3-DEAZAADENINE	H7N4C6	3-deazaadenine	133.24, 115.15, 107.95, 87.26, 71.28		http://pmn.plantcyc.org/PLANT/NEW-IMAGE?type=COMPOUND&object=3-DEAZAADENINE	Others	0.6755	1.42*
136.0259	1.24	JP010516	C6H4N2O2	BENZOFUROXAN; EI-B; MS	No MS		http://www.massbank.jp/jsp/FwdRecord.jsp?id=JP010516	Others	0.9427	1.17*
136.0374	1.41	C01620 ,	C4H8O5	Threonate	No MS	135.02, 89.02, 76.01, 59.01, 56.99	http://www.genome.jp/dbget-bin/www_bget?cpd:C01620	Fatty acid	0.6832	1.24*
137.024	14.27	Arabidopsis thaliana	C7H7NO2	Anthranilic acid	137.0476785	0.023678475	http://pmn.plantcyc.org/PLANT/new-image?type=COMPOUND&object=ANTHRANILATE	Organic acid	0.5084	2.16*

140.0462	27.27	CPD-9494	H8O3C7	3,5-dihydroxyanisole	No MS		http://pmn.plantcyc.org/PLANT/NEW-IMAGE?type=COMPOUND&object=CPD-9494	Phenolic compound	1.0203	1.89**
148.0525	4.29	DIHYDROCOUMARIN	H8O2C9	*trans*-cinnamic acid	No MS	103.05, 101.04, 78.04	http://pmn.plantcyc.org/PLANT/NEW-IMAGE?type=COMPOUND&object=DIHYDROCOUMARIN	phenylpropanoid	0.6297	1.24*
152.0474	14.26	VANILLIN	H8C8O3	Vanillin	No MS	136.01, 108.02, 92.02	http://pmn.plantcyc.org/PLANT/NEW-IMAGE?type=COMPOUND&object=VANILLIN	Phenolic compound	0.4597	2.34*
154.1359	23.8	CPD-8997	H18O1C10	(3S)-linalool	No MS	(+ mode) 107.08, 95.08, 81.07, 79.05, 67.05, 58.98	http://pmn.plantcyc.org/PLANT/NEW-IMAGE?type=COMPOUND&object=CPD-8997	Terpenoid	1.0436	1.29*
164.0473	4.99	KOX00142	H7O3C9	4-Coumaric acid	148.25, 135.11, 131.14, 119.16, 91.45	163.03, 147.04, 135.05, 119.05, 91.05	http://pmn.plantcyc.org/PLANT/NEW-IMAGE?type=COMPOUND&object=PHENYL-PYRUVATE	Phenylpropanoid	0.4714	1.45***
164.0474	7.59	C00166, 328	C9H8O3	Phenylpyruvic acid	135.44, 133.16, 131.17, 119.14, 117.33, 101.09, 91.31	117.03, 101.03, 91.05,	http://metlin.scripps.edu/metabo_info.php?molid=328	Organic acid	0.7452	1.55*
164.0571	1.58	C07326, MT000011	C6H12O5	1,5-Anhydro-D-glucitol	145.11, 131.16, 121.33, 119.15, 118.48, 97.15	145.1, 143.1, 131.0, 119.1, 118.1, 113.1, 101.1, 97.2	http://www.genome.jp/dbget-bin/www_bget?cpd:C07326	Sugar	0.9693	1.23*
172.1464	25.78	CPD-3617, 336	H19O2C10	Caprate	171.20, 153.05, 127.23, 113.51, 99.41, 59.21	171.139, 153.11, 76.95, 68.99, 59.01	http://pmn.plantcyc.org/PLANT/NEW-IMAGE?type=COMPOUND&object=CPD-3617	Fatty acids	0.7172	1.78*
180.0599	1.53	CE000286	C6H12O6	Mannose	179.31, 161.16, 159.20, 143.14, 135.26, 117.21, 99.22	(+ mode) 181.04, 163.03, 145.049, 137.05, 127.03	http://pmn.plantcyc.org/PLANT/new-image?type=COMPOUND&object=MANNOSE	Sugar	1.1035	1.13*
180.0634	14.51	BETA-D-FRUCTOSE	H12C6O6	β-D-fructofuranose	164.28, 161.25, 159.27, 151.26, 146.37, 141.33, 117.28		http://pmn.plantcyc.org/PLANT/NEW-IMAGE?type=COMPOUND&object=BETA-D-FRUCTOSE	Sugar	1.0094	1.09***
185.9682	3.32	Oryza sativa	C3H7O7P	2-phosphoglycerate	185.9929391	0.024739069		Organic acid	Inf	Inf
198.1256	23.8	C05575	C9H16N3O2	Hercynine	179.25, 153.33, 139.23, 135.41, 122.29, 107.36, 97.34		http://www.kegg.jp/entry/C05575		1.0265	1.28*

200.1813	27.94	357, LMFA01010012	C12H24O2	Lauric acid	199.64, 184.16, 181.43, 167.26, 155.40, 139.07, 131.29, 127.29, 117.26, 113.51, 99.33, 80.37, 87.05	199.169, 181.15, 176.62, 79.95,	http://metlin.scripps.edu/metabo_info.php?molid=357	Organic acid	0.6944	1.84*
204.0899	8.74	33	H12O2N2C11	L-tryptophan	203.49, 186.19, 173.31, 159.25, 142.23, 116.19, 74.31	203.08, 186.05, 159.09, 142.06, 116.05, 74.02	http://pmn.plantcyc.org/PLANT/NEW-IMAGE?type=COMPOUND&object=TRP	Amino acid	0.5527	1.14*
206.0579	18.97	CPD-12208	H9O4C11	*p*-coumaroyldiketide	No MS		http://pmn.plantcyc.org/PLANT/NEW-IMAGE?type=COMPOUND&object=CPD-12208	phenylpropanoid	0.5585	2.09*
210.0891	16.29	44805	H14C11O4	Sinapyl-alcohol	No MS	194.05, 179.03, 161.02, 151.03, 133.02, 105.03	http://pmn.plantcyc.org/PLANT/NEW-IMAGE?type=COMPOUND&object=SINAPYL-ALCOHOL	Phenylpropanoid	0.3706	4.4*
238.084	18.95	6705	C12H14O5	Sinapic acid methyl ester	No MS	237.07, 133.06,103.05		phenylpropanoid	0.4623	2.99*
240.0898	1.59		C14H12N2O2	β-Carboline-1-propionic acid	221.24, 195.15, 179.13, 174.37, 145.32		240.0898776	Alkaloid	0.7955	1.3*
250.1346	14.27	C03002	C13H18N2O3	N-caffeoylputrescine	249.35, 233.82, 219.04, 205.08, 189.00, 174.09, 164.16, 119.20, 108.23		http://www.kegg.jp/entry/C03002	phenylpropanoid	0.8273	1.11*
290.0399	1.25	D-SEDOHEPTULOSE-7-P	H13P1O10C7	D-sedoheptulose-7-phosphate	No MS		http://pmn.plantcyc.org/PLANT/NEW-IMAGE?type=COMPOUND&object=D-SEDOHEPTULOSE-7-P	Sugar	0.8838	1.14*
297.0893	15.29	C00170, 3425	C11H15N5O3S	5'-Methylthioadenosine	No MS	(+ mode) 298.098, 163.04, 145.03, 136.06	http://www.kegg.jp/entry/C00170	others	0.424	1.9*
298.1047	11.39	C01961	C14H18O7	Picein (4-Hydroxyacetophenone 4-glucoside)	No MS		http://www.kegg.jp/dbget-bin/www_bget?cpd:C10720		0.7293	1.39*
307.0835	1.34	GLUTATHIONE	H16S1O6C10N3	Glutathione	No MS		http://pmn.plantcyc.org/PLANT/NEW-IMAGE?type=COMPOUND&object=GLUTATHIONE	Organo sulphur compound	0.9423	1.47**
328.1306	19.82	LMPK12120341, 52144	C19H20O5	2,3,4,6-tetramethoxychalocone	312.30, 309.38, 291.28, 239.25, 229.28, 221.22, 211.28, 209.30, 171.31		http://www.lipidmaps.org/data/LMSDRecord.php?LMID=LMPK12120341	Flavonoid	0.6954	1.54*
340.1306	19.8	CPD-9440, 52761	C20H19O5	6-Prenylnaringenin	No MS		http://pmn.plantcyc.org/PLANT/NEW-IMAGE?type=COMPOUND&object=CPD-9440	Flavonoid	0.823	1.3**

342.097	1.46	C10431, 68323	C15H18O9	Caffeic acid 3-glucoside	323.17, 295.18, 281.01, 220.85,179.22, 161.30, 143.26, 119.14, 113.25		http://www.kegg.jp/entry/C10431	Phenylpropanoid	1.003	1.64*
353.1104	10.23	CPD-9592	H19N1O8C16	2-oxindole-3-acetyl-beta-D-glucose	No MS		http://pmn.plantcyc.org/PLANT/NEW-IMAGE?type=COMPOUND&object=CPD-9592	Auxin	0.6236	1.64*
356.1104	14.48	64481, C17759	C16H20O9	1-O-feruloyl-β-D-glucose	337.08, 295.18, 235.29,217.25, 193.16, 175.17, 160.19, 134.16		http://www.genome.jp/dbget-bin/www_bget?cpd:C17759	Phenylpropanoid	0.8376	1.49*
358.1411	19.8	CPD-8905	H22O6C20	(+)-pinoresinol	342.15, 339.17, 327.21, 275.27, 221.24, 203.19, 191.23		http://pmn.plantcyc.org/PLANT/NEW-IMAGE?type=COMPOUND&object=CPD-8905	Phenylpropanoid	0.8224	1.24**
365.1469	14.61	CPD-12621	H23O7N1C18	Indole-3-butyryl-glucose	No MS		http://pmn.plantcyc.org/PLANT/NEW-IMAGE?type=COMPOUND&object=CPD-12621	Auxin	0.6395	1.44**
372.1203	20.12	CPD-8927	H20O7C20	(+)-sesamolinol	No MS		http://pmn.plantcyc.org/PLANT/NEW-IMAGE?type=COMPOUND&object=CPD-8927	Phenylpropanoid	0.4474	1.81***
376.1361	9.4	LOGANATE	H23O10C16	Loganate	325.76, 331.00, 315.21, 221.32, 217.02, 161.12, 153.25, 143.25	375.12, 339.13, 329.08, 213.07, 169.08, 113.08	http://pmn.plantcyc.org/PLANT/NEW-IMAGE?type=COMPOUND&object=LOGANATE	Alkaloid	0.6976	1.59*
376.1516	17.59	C08747	C20H24O7	Euparotin	356.93, 345.19, 327.23, 195.27, 179.33, 165.29		http://www.kegg.jp/entry/C08747	Terpenoid	0.8548	1.08***
376.1516	15.3	C08747	C20H24O7	Ailanthone	356.93, 345.19, 327.23, 195.27, 179.33, 165.28		http://www.kegg.jp/entry/C08747	Terpenoid	0.7597	1.54**
402.1128	1.65	LMPK12120258	C24H18O6	8-p-coumaroyl-3,4-dihydro-5,7-dihydroxy-4-phenylcoumarin	382.76, 357.25, 355.29, 341.25, 303.18,258.20, 244.30, 216.71, 179.42		http://www.lipidmaps.org/data/LMSDRecord.php?LMID=LMPK12120258	Flavonoid	0.9061	1.55*
402.1519	14.96		C18H26O10	Benzyl alcohol beta-D-xylopyranosyl (1->6)-beta-D-glucopyranoside	382.92, 357.17, 340.62, 327.37, 309.25, 269.20, 179.25, 161.16		402.1525971	others	0.7948	1.34**
414.1277	11.45		C22H22O8	(-)-Podophyllotoxin	267.2,163.23		414.1314677	Phenylpropanoid	0.6938	1.5*
418.1623	20.74	C09435	C22H26O8	Euparotin acetate			http://www.kegg.jp/entry/C09435	Terpenoid	0.8904	1.28**
418.256	22.44		C21H38O8	Icariside C1			418.2566682		1.2522	1.45**

422.1714	11.99	LMPK12050184	C25H26O6	Lupinisoflavone G	277.3,217.4,319.27		http://www.lipidmaps.org/data/LMSDRecord.php?LMID=LMPK12050184	Flavonoid	0.9046	1.14*
429.1343	12.55		C24H19N3O5	Lycogarubin B			Knapsack		0.7934	1.22*
436.2667	18.81	LMST03020031	C25H40O4S	1alpha-hydroxy-24-methylsulfonyl-25,26,27-trinorvitamin D3 / 1alpha-hydroxy-24-methylsulfonyl-25,26,27-trinorcholecalciferol	391.06,375.25		http://www.lipidmaps.org/data/LMSDRecord.php?LMID=LMST03020031	Sterol lipids	1.0419	1.33*
438.261	22.86	LMPR0104350001	C24H38O7	(-)-Fusicoplagin A			http://www.lipidmaps.org/data/LMSDRecord.php?LMID=LMPR0104350001	Prenol lipids	0.3692	2.74*
440.2404	18.42		C24H32N4O4/C23H36O8	Spinanine A or Cryptoporic acid B			Knapsack		0.9718	1.84*
440.2766	23.56	LMGP10050002	C20H39O7P	PA(17:1(9Z)/0:0);1-(9Z-heptadecenoyl)-sn-glycero-3-phosphate			http://www.lipidmaps.org/data/LMSDRecord.php?LMID=LMGP10050002	Glycerophospholipids	0.3142	3.11*
446.1239	12.02	C05376	C22H22O10	Biochanin A-beta-D-glucoside	No MS		http://www.kegg.jp/entry/C05376	Flavonoid	0.784	1.34*
454.2769	21.15		C28H38O5	Isomeldenin/22,23-Dihydronimocinol			Knapsack		0.8697	1.69*
473.0857	1.49	C11175	C16H19N5O10S	S-(2,4-Dinitrophenyl)glutathione			http://www.kegg.jp/entry/C11175		1.584	1.58**
478.2769	16.48		C30H38O5	3-Geranyl-4-2',4',6'-tetrahydroxy-5prenyldihydrochalcone	No MS			Flavonoid	1.9126	1.38***
482.2175	21.88	Fusarium sporotrichiella var. poae	C24H34O10	3'-Hydroxy T-2 toxin	482.2151973	0.002302692			1.5211	1.44***
500.13	2.28	LMPK12020140	C25H24O11	Epigallocatechin 5,3',5'-trimethyl ether 3-O-gallate	438.8,341.2,400.8		http://www.lipidmaps.org/data/LMSDRecord.php?LMID=LMPK12020140	Flavonoid	0.9244	1.2*
520.1936	18.56	C17529, 71761	C26H32O11	(-)-Pinoresinol glucoside	501.23,357.28,267.28,179.18		http://www.genome.jp/dbget-bin/www_bget?cpd:C17529	Phenylpropanoid	0.6751	1.53**
522.2091	17.42	C08769	C26H34O11	Isobrucein A	329.29,341.27,358.87,383.08,393.04		http://www.genome.jp/dbget-bin/www_bget?cpd:C08769	Terpenoid	0.7964	1.46*
540.1623	25.61	C10548	C28H28O11	Cleistanthin A	No MS		http://www.genome.jp/dbget-bin/www_bget?cpd:C10548	Phenylpropanoid	0.2698	2.34
540.1658	16.29	C17781, 71901	C28H28O11	2"-o-p-Coumaroylaloesin	confusion		http://www.genome.jp/dbget-	Phenylpropanoid	0.7502	1.35

							bin/www_bget?cpd:C17781			
540.1844	16.39	67938	C25H32O13	Oleuropein	confusion		http://metlin.scripps.edu/metabo_info.php?molid=67938	Others	0.566	1.96
550.204	18.6	C10560	C27H34O12	Medioresinol 4'-O-beta-D-glucopyranoside			http://www.genome.jp/dbget-bin/www_bget?cpd:C10560	Phenylpropanoid	0.7558	1.39
564.1068	16.48		C25H24O15	Isorhamnetin 3-(6"-malonylglucoside)	473.19,443.18,383.26,353.18,503.17,545.18			Flavonoid	0.3717	2.53
580.2147	17.56	C10890	C28H36O13	(+)-Syringaresinol O-beta-D-glucoside	339.2,327.2,356.54,459.16	Flavonoid	http://www.kegg.jp/entry/C10890	Lignan	0.6818	1.75
584.2249	21.13	MG-PROTOPORPHYRIN	H30O4Mg1N4C34	Mg-protoporphyrin	369.17,357.15,535.11,354.19		http://pmn.plantcyc.org/PLANT/NEW-IMAGE?type=COMPOUND&object=MG-PROTOPORPHYRIN	Porphyrin	0.754	1.48***
592.2638	28.2	LMGP06050017	C27H45O12P	PI(18:4(6Z,9Z,12Z,15Z)/0:0)	no MS		http://www.lipidmaps.org/data/LMSDRecord.php?LMID=LMGP06050017	Glycerophospholipids	2.1605	2.16*
600.231	16.64	LMFA03120030	C29H41ClO11	12S-acetoxy-punaglandin 2	No MS	Plant defense signalling	http://www.lipidmaps.org/data/LMSDRecord.php?LMID=LMFA03120030	Fatty acyls	0.8635	1.48
600.2312	15.31	LMFA03120030	C29H41ClO11	12S-acetoxy-punaglandin 2	No MS		http://www.lipidmaps.org/data/LMSDRecord.php?LMID=LMFA03120030	Fatty acyls	0.7748	1.56
602.2352	18.82	LMPK12140101	C31H38O12	5,4'-Dihydroxy-6-C-prenylflavanone 4'-xylosyl-(1->2)-rhamnoside	No MS		http://www.lipidmaps.org/data/LMSDRecord.php?LMID=LMPK12140101	Flavonoid	0.8286	1.11
632.2457	20.31	C18154	C35H36MgN4O6	3-Hydroxyethylchlorophyllide a	No MS	Porphyrin and chlorophyll metabolism	http://www.kegg.jp/entry/C18154	cyclic tetrapyrrole	0.6422	1.57
642.1966	14.3	C09932	C32H34O14	Haemocorin	No MS		http://www.kegg.jp/entry/C09932	Aromatic hydrocarbon	0.8705	1.47
654.1786	19.4	LMPK12050397	C29H34O17	Iristectorigenin A 7-O-gentiobioside	329.19,314.10,299.21		http://www.lipidmaps.org/data/LMSDRecord.php?LMID=LMPK12050397	Flavonoid	0.8541	1.94
680.2277	15.34	LMPK12110838	C32H40O16	3-(3-Methylbutyl)tricetin 5-neohesperidoside	No MS		http://www.lipidmaps.org/data/LMSDRecord.php?LMID=LMPK12110838	Flavonoid	0.7831	1.54
726.2354	19.51	LMPK12140262	C33H42O18	Naringenin 7-O-(2",6"-di-O-alpha-rhamnopyranosyl)-beta-glucopyranoside	No MS		http://www.lipidmaps.org/data/LMSDRecord.php?LMID=LMPK12140262	Flavonoid	0.8826	1.43
742.2666	16.51	C10543	C34H46O18	Acanthoside D or (-)-	329.2,314.19,299.06		http://www.kegg.jp/entry/C10543	Flavonoid	0.8062	1.29

				Syringaresinol di-beta-D-glucoside						
800.2357	19.97	LMPK12110868	C35H44O21	Tricin 7-rutinoside-4'-glucoside	329.24,314.21,271.22		http://www.lipidmaps.org/data/LMSDRecord.php?LMID=LMPK12110868	Flavonoid	0.9262	1.56
862.2141	24.16	46869, LMPK12010102	C39H42O22	Cyanidin 3-[6-(6-p-hydroxybenzoylglucosyl)-2-xylosylgalactoside]	819.07,801.15,643.25,685.07,601.13		http://www.lipidmaps.org/data/LMSDRecord.php?LMID=LMPK12010102	Flavonoid	0.9635	1.75
862.2892	24.16	SIROHYDROCHLORIN	H38N4O16C42	Sirohydrochlorin	No MS	Chlorophyl metabolism	http://pmn.plantcyc.org/PLANT/NEW-IMAGE?type=COMPOUND&object=SIROHYDROCHLORIN	Tetrapyrole	0.9478	1.63

Appendix 4.1 continued **Fusarium head blight resistance related metabolites in the rachis (7dpi) wheat NIL with resistant *Fhb1* allele and absent in NIL-S following *F. graminearum* or mock inoculation**

Observed mass (Da)	**Retention time**	**Database ID**	**Molecular formula**	**Name**	**Observed fragments**	**Database fragments**	**URL**	**Chemical group**	**RM/SM**	**RP/RM**
164.0472	22.37	C00811	C9H8O3	P-coumarate	No MS	**(+ mode)147.04, 119.04, 91.05**	http://www.genome.jp/dbget-bin/www_bget?cpd:C00811	Phenylpropanoid	0.9997	0.9659
246.0498	27.16	C03274	C6H15O8P	Phosphatidyl glycerol	No MS		http://www.genome.jp/dbget-bin/www_bget?cpd:C03274	Glycerol	1.0108	0.9451
342.1306	8.51	C00761	C16H22O8	Coniferin	326.07, 308.92, 180.14, 162.15	180.14:Coniferyl alcohol, 162.15: Glucose-H2O	http://www.kegg.jp/entry/C00761	Phenylpropanoid	1.0127	0.9936
432.2265	28.11	LMGP10050023	C21H37O7P	PA(18:3(6Z,9Z,12Z)/0:0)	No MS		http://www.lipidmaps.org/data/LMSDRecord.php?LMID=LMGP10050023	Glycerophospholipids	#REF!	#REF!
453.2846	29.88	LMGP01050001	C21H44NO7P	PE(16:0/0:0)	255.32, 214.16, 196.20, 153.00	255.23: sn1 RCOO- ion, 214.05:Loss of sn1 acyl chain as ketene (RCH=C=O) from [M-H]-, 196.04: Neutral loss of sn1 RCOOH group from [M-H]-, 153.00: Glycerol-3-phosphate ion with loss of H2O, 140.01:Ethanolamine phosphate ion	http://www.lipidmaps.org/data/LMSDRecord.php?LMID=LMGP02050002	Glycerophospholipids	1.0505	1.0461
475.2844	28.16	C09248	C29H37N3O3	Tubulosine	475.12, 277.31, 196.36		http://www.kegg.jp/entry/C09248	Alkaloids	0.9983	0.9281
477.2529	29.03	C15694	C26H39NO5S	Epothilone C			http://www.kegg.jp/entry/C15694	Polyketides	0.9886	0.9279

479.3001	29.97	LMGP01050125	C23H46NO7P	PC(15:1(9Z)/0:0)	No MS		http://www.lipidmaps.org/data/LMSDRecord.php?LMID=LMGP01050125	Glycerophospholipids	0.9883	0.9168
503.3	28.25	LMGP02050022	C25H46NO7P	PE(20:3(8Z,11Z,14Z)/0:0)/LysoPE(0:0/20:3(11Z,14Z,17Z))	277.27,242.21		http://www.lipidmaps.org/data/LMSDRecord.php?LMID=LMGP02050022	Glycerophospholipids	0.9709	1.0023
505.3154	29.04	LMGP01050127	C25H48NO7P	PC(17:2(9Z,12Z)/0:0) or LysoPE(0:0/20:1(11Z))	471.49, 279.35, 242.20, 224.24, 167.99	242.08:Loss of sn1 acyl chain as ketene (RCH=C=O), CH3 and formate from precursor ion, 224.07:Glycerophosphocholine with loss of CH3 and H2O, 168.04:Phosphocholine with loss of CH3,	http://www.lipidmaps.org/data/LMSDRecord.php?LMID=LMGP01050127	Glycerophospholipids	1.0672	0.9318
507.3315	29.97	LMGP01050002	C25H50NO7P	PC(17:1(10Z)/0:0)	No MS		http://www.lipidmaps.org/data/LMSDRecord.php?LMID=LMGP01050002	Glycerophospholipids	1.0119	0.9057
508.3132	27.17	LMGP04050031	C25H51O9P	PG(19:0/0:0): 1-nonadecanoyl-glycero-3-phospho-(1'-sn-glycerol)	489.47, 415.22, 279.46, 245.07. 227.25, 153.14	245.04:Glycerophosphoglycerol ion, 227.03:Neutral loss of sn1 RCOOH group from [M-H]-, 153.00: Neutral loss of sn1 RCOOH group and glycerol from [M-H]-	http://www.lipidmaps.org/data/LMSDRecord.php?LMID=LMGP04050031	Glycerophospholipids	0.9692	1.0236
519.2594	29.53	LMGP03050017	C24H42NO9P	PS(18:3(6Z,9Z,12Z)/0:0)	No MS		http://www.lipidmaps.org/data/LMSDRecord.php?LMID=LMGP03050017	Glycerophospholipids	0.971	0.9791
555.3524	29.89	LMGP01050024	C25H52NO7P	PC(17:0/0:0);1-heptadecanoyl-sn-glycero-3-phosphocholine	480.32, 255.27, 224.07, 207.17	480.31: Loss of CH3 and formate from precursor ion, 255.23: sn1 RCOO- ion, 224.07:Glycerophosphocholine with loss of CH3 and H2O,	http://www.lipidmaps.org/data/LMSDRecord.php?LMID=LMGP01050024	Glycerophospholipids	0.9649	1.1201
559.2872	29.03	LMGP03050019	C25H48NO9P	PS(19:1(9Z)/0:0): 1-(9Z-nonadecenoyl)-glycero-3-phosphoserine	560.29, 514.11, 476.24, 279.46,			Glycerophospholipids	1.0645	0.9679
567.3523	29.97	LMGP03050026	C27H54NO9P	PS(21:0/0:0)	No MS		http://www.lipidmaps.org/data/LMSDRecord.php?LMID=LMGP03050026	Glycerophospholipids	1.0785	0.865

578.4295	27.55	LMGP10020002	C31H63O7P	PA(O-16:0/12:0)	546.83, 503.45, 277.48, 245.11, 193.41		http://www.lipidmaps.org/data/LMSDRecord.php?LMID=LMGP10020002	Glycerophospholipids	1.0646	0.9872
581.368	29.96	LMGP03050025	C28H56NO9P	PS(22:0/0:0)	506.40, 497.66, 281.40		http://www.lipidmaps.org/data/LMSDRecord.php?LMID=LMGP03050025	Glycerophospholipids	1.0749	0.8945
612.2979	18.36	JP004524	C24H60O6Si6	1,2,3,4,5,6-HEXA-O-TRIMETHELSILYL-MYO-INOSITOL; EI-B; MS	223.18,357.3,369.38,224.12		http://www.massbank.jp/jsp/FwdRecord.jsp?id=JP004524		0.9957	0.954
638.414	30.29	LMGP04010932	C32H63O10P	PG(14:0/12:0)	No MS		http://www.lipidmaps.org/data/LMSDRecord.php?LMID=LMGP04010932	Glycerophospholipids	0.85	1.1728
662.4139	29.95	LMGP04010920	C34H63O10P	PG(14:1(9Z)/14:1(9Z))	No MS		http://www.lipidmaps.org/data/LMSDRecord.php?LMID=LMGP04010920	Glycerophospholipids	0.9258	1.1298
722.4222	30.17	C08919	C39H62O12	Yamogenin 3-O-neohesperidoside	confusion		http://www.kegg.jp/entry/C08919	Terpenoid	0	0
755.5054	29.02	LMGP03020008	C39H76NO9P	PS(O-16:0/17:1(9Z)):1-hexadecyl-2-(9Z-heptadecenoyl)-glycero-3-phosphoserine	No MS			Glycerophospholipids	0.963	0.9906
976.5501	29.03	LMGP06010555	C51H87O13P	PI(20:2(11Z,14Z)/22:4(7Z,10Z,13Z,16Z)):1-(11Z,14Z-eicosadienoyl)-2-(7Z,10Z,13Z,16Z-docosatetraenoyl)-glycero-3-phospho-(1'-myo-inositol)	No MS		http://www.lipidmaps.org/data/LMSDRecord.php?LMID=LMGP06010555	Glycerophospholipids	#REF!	#REF!
990.5409	27.14	61311	C45H86O16P2	PIP(16:0/20:1(11Z)):Phosphatidylinositol Phosphate	971.95, 881.13, 743.94		http://metlin.scripps.edu/metabo_info.php?molid=61311	Glycerophospholipids	1.0346	0.9342

Appendix 5.1: Fusarium head blight resistance related metabolites in the rachis of wheat cultivars Sumai-3 and Roblin following *F. graminearum* or mock inoculation

Observed mass (Da)	Retention time	Database ID	Molecular formula	Name	Obsereved fragments	Database fragments	URL	Chemical group	RRC	RRI (*Tri5*$^{+}$)	RRI (*Tri5*$^{-}$)
74.0006	1.14		H1O3C2	Glyoxylate/Oxaloacetiec acid		45.03,55.02,43.02,41.04, 39.02	http://pmn.plantcyc.org/PLANT/NEW-IMAGE?type=COMPOUND&object=GLYOX	Carboxylate	0.86	1.40	2.05
103.0635	1.19	CPD-6141	H9N1O2C4	N-methyl-β-alanine	no		http://pmn.plantcyc.org/PLANT/NEW-IMAGE?type=COMPOUND&object=CPD-6141	Amino Acids and Derivatives	0.87	1.04	1.48
105.0427	1.41		H7O3N1C3	D-serine	no	74.02,56.01,42.03	http://pmn.plantcyc.org/PLANT/NEW-IMAGE?type=COMPOUND&object=D-SERINE	Amino Acids and Derivatives	1.74	0.46	0.65
116.011	1.14		H2C4O4	maleate	97.17, **71.08**, 59.26, 55.22	71.01(100%),84.98,44.99	http://pmn.plantcyc.org/PLANT/NEW-IMAGE?type=COMPOUND&object=MALEATE	Carboxylate	2.26	0.51	0.72
119.0583	1.4		H9N1C4O3	D-threonine or Homoserine	no	74.02,56.01	http://pmn.plantcyc.org/PLANT/NEW-IMAGE?type=COMPOUND&object=D-THREONINE	Amino Acids and Derivatives	0.48	1.62	1.04
132.0535	1.31		H8O3N2C4	L-asparagine	**113.11,114.14,95.18**,101.11, 83.38,85.23	41.99,58.0,70.0,72.0,95.0,113.0,114.0	http://pmn.plantcyc.org/PLANT/NEW-IMAGE?type=COMPOUND&object=ASN	Amino Acids and Derivatives	1.05	1.03	1.29
134.0215	1.15	C00149	C4H6O5	(S)-Malate	**115.05**, 103.37, 87.04, **75.17**,71.203	115.00,89.02,71.01(100%),72.99	http://www.kegg.jp/entry/C00149	Carboxylate	1.61	0.77	0.87
143.0582	1.16	C17357	C6H9NO3	2-Hydroxymethylclavam	**114.00**, **100.17**, **97.43,** 59.296	97.06,99.04,102.05,115.03	http://www.kegg.jp/entry/C17357	Others	1.71	1.05	0.86
146.0691	1.31			L-Glutamine	**145.22, 128.17, 127.14, 115.17, 109.20,** 101.14, 83.16, 74.23	84.0423, 87.009, 109.0399, 115.0054, 127.048, 128.0395, 144.8935, 145.0184	http://pmn.plantcyc.org/PLANT/NEW-IMAGE?type=COMPOUND&object=GLN	Amino Acids and Derivatives	0.45	1.78	1.28
147.0724	2.02		C4H9N3O3,	L-Albizziine	**146.23, 128.08,** 116.09, 110.22, **102.18, 101.53**, 84.51, 74.38, **57.17**	146.05, 128.05, 101.95, 100.93, 57.17	http://kanaya.naist.jp/knapsack_jsp/result.jsp?sname=formula&word=C4H9N3O3	Non-protein amino acid	2.18	0.96	0.85
155.0694	1.53	CPD-670		Histidine	no	72.01, 118.04, 136.06, 137.04, 154.06	http://pmn.plantcyc.org/PLANT/NEW-IMAGE?type=COMPOUND&object=HIS	Amino Acids and Derivatives	3.78	0.67	1.03
164.0836	16.78	CPD-6481	H12O2C10	eugenol	148.32, **145.45, 131.20**,133.16, 119.28, **91.24**	162.97, **144.88, 118.99**,75.00	http://pmn.plantcyc.org/PLANT/NEW-IMAGE?type=COMPOUND&object=CPD-6481	Phenols and Derivatives	0.90	1.29	1.77
178.0627	15.85		H10O3C10	coniferaldehyde	**177.20, 162.18, 159.14,** 145.16, 128.96, 95.22, 59.18	177.05, 162.03, 159.88, 133.02	http://pmn.plantcyc.org/PLANT/NEW-IMAGE?type=COMPOUND&object=CONIFERYL-ALDEHYDE	Phenylpropanoids	0.81	1.33	2.15
180.0632	16.43		H12C6O6	β-D-fructofuranose/ alpha D glucose	**179.11,** 165.26, 164.24, **161.24**, **125.12,** 159.18, 137.39, 117.21	179.05, 161.03, 143.03, 125.02, 99.00, 75.00,	http://pmn.plantcyc.org/PLANT/NEW-IMAGE?type=COMPOUND&object=BETA-D-FRUCTOSE	Carbohydrates and Carbohydrate Conjugates	0.88	1.43	1.81
185.9927	1.11		H4P1C3O7	2-phospho-D-glycerate			http://pmn.plantcyc.org/PLANT/NEW-IMAGE?type=COMPOUND&object=2	Carbohydrates and Carbohydrate	1.00	1.79	1.00

							-PG	Conjugates			
192.0632	1.31		H11O6C7	L-quinate	**191.37,** 173.13, 147.25, 129.19, **111.18, 85.33,**	191.06, 11.01, 87.11, 85.02	http://pmn.plantcyc.org/PLANT/NEW-IMAGE?type=COMPOUND&object=QUINATE	Carboxylate	0.57	1.54	1.98
195.0529	15.35		H9N1O4C9	dopaquinone	97.05,89.04,79.10,111.22,129.22,137.18,151.16,159.10,177.08,194.19	150.05, 121.02, 93.03, 74.02(doubt check in ms2t)	http://pmn.plantcyc.org/PLANT/NEW-IMAGE?type=COMPOUND&object=DOPAQUINONE	Quinone	0.47	1.10	4.57
204.0818	8.85	C00001396	C11H12N2O2	L-Tryptophan,	**203.35, 186.10, 159.17, 142.23, 116.25, 74.21**	203.08, 186.05, 159.09, 142.06, 116.05, 74.02	http://kanaya.naist.jp/knapsack_jsp/result.jsp?sname=formula&word=C11H12N2O2	Amino Acids and Derivatives	6.91	0.81	1.13
205.071	4.27	C02043	C11H11NO3	Indolelactate			http://www.kegg.jp/entry/C02043	Auxin	6.22	1.18	0.97
208.0578	1.21	C00002775	C11H12O4	Sinapaldehyde	**192.33, 175.10, 163.14,** 161.18, 1**47.20, 133.20, 129.22,** 109.11, 83.24	192.04, 175.03, 149.02, 147.04, 133.02, 129.03,	http://kanaya.naist.jp/knapsack_jsp/information.jsp?word=C00002775	Phenylpropanoids	2.42	0.16	0.76
210.0888	11.97		H14C11O4	sinapyl-alcohol	**194.21, 179.43, 151.11, 135.02**	209.04, 194.05, 193.04, 179.03, 151.03, 150.03, 135.04, 121.03,	http://pmn.plantcyc.org/PLANT/NEW-IMAGE?type=COMPOUND&object=SINAPYL-ALCOHOL	Phenylpropanoids	2.19	0.91	1.11
241.0734	17.93		H11N1O3C14	1,3-dihydroxy-N-methylacridone /Benzoylanthranilate		118.03, 105.03, 77.03, 71.99	http://pmn.plantcyc.org/PLANT/NEW-IMAGE?type=COMPOUND&object=13-DIHYDROXY-N-METHYLACRIDONE	Alkaloids	2.55	0.78	0.95
250.1282	14.86	C00002719	C13H18N2O3	N-Caffeoylputrescine	119.13,121.27,221.0,205.03, 176.18,152.32,164.15		http://kanaya.naist.jp/knapsack_jsp/information.jsp?word=C00002719	Phenylpropanoids	1.00	0.56	1.25
250.1412	12.74	C00015799	C18H18O	Juncunol	**230.95,** 219.39, **149.17, 137.60,** 128.21, **119.19**, 85.24	231.16, 149.91, 137.87, 135.86, 119.07, 99.002, 98.98,	http://kanaya.naist.jp/knapsack_jsp/result.jsp?sname=formula&word=C18H18O	Others	2.54	1.09	0.75
254.188	23.97	CPD-4746	H26O3C15	3-hydroxy-15-dihydrolubimin			http://pmn.plantcyc.org/PLANT/NEW-IMAGE?type=COMPOUND&object=CPD-4746	Fatty acids and conjugates	1.90	1.20	1.38
261.0426	13.16	CPD-3728	H10P1C9O6N1	O-phospho-L-tyrosine			http://pmn.plantcyc.org/PLANT/NEW-IMAGE?type=COMPOUND&object=CPD-3728	Amino Acids and Derivatives	0.35	1.51	1.50
262.0655	19.98	LMPK12130001	C17H10O3	Furano[2",3":6,7]aurone	**201.05**,229.38,242.83	201.02,127.04,141.01,196.99	http://www.lipidmaps.org/data/LMSDRecord.php?LMID=LMPK12130001	Phenylpropanoids	1.47	1.21	1.62
270.1097	13.47	C00029812	C13H18O6	Benzoyl beta D glucopyranoside			http://kanaya.naist.jp/knapsack_jsp/information.jsp?word=C00029812	Carboxylate	2.69	1.02	1.02
282.0945	1.2	CPD-13037	H18C10O9	(1,4)-β-xylobiose	281.24, 267.04, 263.26, 237.33, 213.10, 199.10, 170.83		http://pmn.plantcyc.org/PLANT/NEW-IMAGE?type=COMPOUND&object=CPD-13037	Carbohydrates and Carbohydrate Conjugates	2.74	0.79	1.24
283.0908	5.31		H13O5N5C10	Guanosine	**282.07,** 264.11, 255.00, **150.23, 132.96**	282.08, 164.05, 150.04, 133.01, 108.01	http://pmn.plantcyc.org/PLANT/NEW-IMAGE?type=COMPOUND&object=GUANOSINE	Nucleoside	2.24	1.35	1.59
289.0844	12.49	HMDB12266	C11H15NO8	N-Succinyl-L-amino-6-oxopimelate			http://www.hmdb.ca/metabolites/HMDB12266	Amino Acids and Derivatives	10.38	0.93	0.89

292.1529	15.99	CPD-12237	H21C14N4O3	4-coumaroyl-3-hydroxyagmatine	291.45, 274.06, 249.11, 247.25, 205.28, 171.22, 154.11, 127.20, 119.12, 109.01		http://pmn.plantcyc.org/PLANT/NEW-IMAGE?type=COMPOUND&object=CPD-12237	Phenylpropanoids	1.09	1.06	1.39
292.1594	15.98	CPD-9833	H20N2O1C19	Vellosimine	291.05, 274.09, 249.31, 232.11, 220.54, 203.16, 171.17, 154.16, 127.20, 119.08, 112.16, 93.23		http://pmn.plantcyc.org/PLANT/NEW-IMAGE?type=COMPOUND&object=CPD-9833	Alkaloids	0.47	0.95	1.34
300.1201	12.1	CPD-13354	H20C14O7	Salidroside	217.14, **299.07,** 284..42, 239.30, 195.43**, 179.27**, 143.25, 137.29, **119.26**	299.11, 179.05, 149.04, 119.01, 113.02, 101.02,	http://pmn.plantcyc.org/PLANT/NEW-IMAGE?type=COMPOUND&object=CPD-13354	Others	1.65	0.69	1.42
304.1204	25.01	C09130	C19H16N2O2	Ceceline	**116.05,186.11**,285.29,199.05,221.09,243.24,260.07,141.82	118.90,187.09,143.04	http://www.kegg.jp/entry/C09130	Others	5.33	0.56	0.68
306.0753	1.17	CPD-10411	H14O7C15	epigallocatechin	219.15,289.31,261.37,287.37,145.16	125.02,109.02,111.04,97.02,137.02,139.03	http://pmn.plantcyc.org/PLANT/NEW-IMAGE?type=COMPOUND&object=CPD-10411	Phenylpropanoids	1.04	0.34	1.34
312.12	11.52	C05855	C15H20O7	4-Hydroxycinnamyl alcohol 4-D-glucoside	**311.32, 293.97**, 293.29, 275.33, **253.40**, 241.18, 223.27, 201.28, **183.28,** 171.22	313.10, 297.07, 280.07, 295.06, 181.055, (positive ionization)	http://www.kegg.jp/entry/C05855	Phenylpropanoids	0.92	1.64	1.90
312.1411	3.65	C00002900	C19H20O4	4-prenyloxyreserveraol			http://kanaya.naist.jp/knapsack_jsp/information.jsp?word=C00002900	Stilbene	3.99	0.79	1.25
316.0786	1.46	PR040055	C16H12O7	Rhamnetin	297.10, 225.15, 217.18, 195.15, 179.10, 165.17, 153.09, 152.19, **109.10**	315.05, 300.02, 193.01, 165.04, 121.02, 109.02	http://www.genome.jp/dbget-bin/www_bget?cpd:C10176	Phenylpropanoids	0.38	1.89	1.71
316.094	27.45	C10204	C17H16O6	Cajanol /flavonoids((+)-Pisatin)	**315.38, 314.15**, 299.18, 297.26, 283.00, 257.34, 241.28, 185.05, 139.21	207.96,313.98,314.06,315.09	http://www.kegg.jp/entry/C10204	Phenylpropanoids	9.28	0.96	1.47
322.1628	16.77	LMFA13010043	C14H26O8	Butyl 3-O-beta-D-glucopyranosyl-butanoate	**302.80, 279.14, 261.05, 259.05, 239.22, 191.23, 179.02, 149.27, 134.23, 119.05**	86.09,114.94,120.08,177.05,261.11,302.14,261.11,259.1,239.06,191.08,179.05,149.05,134.05	http://www.lipidmaps.org/data/LMSDRecord.php?LMID=LMFA13010043	Fatty acids and conjugates	9.52	0.83	0.67
323.0997	14.83	C00007576	C15H17NO7	Indole-3-carboxylic acid beta-D-glucopyranosyl ester			http://kanaya.naist.jp/knapsack_jsp/information.jsp?word=C00007576	Others	4.67	0.87	1.43
326.0992	13.86	C04415	C15H18O8	Jacareubin	**307.52**, 281.28, 265.25, 235.24, 205.34, **187.16**, 163.20, **145.22**, **119.21**	119.09,145.04,147.07,185.16,191.0,307.09	http://kanaya.naist.jp/knapsack_jsp/information.jsp?word=C00002959	Phenylpropanoids	2.62	1.26	1.09
326.1147	20.9	C17474	C19H18O5	Methylophiopogonone B	**295.39**, 281.45, 265.02, 253.23, 237.12, **205.05**, 187.28, 163.09, 153.17, 145.16, 117.29	205.06,293.09,282.06,307.09,177.06	http://www.kegg.jp/entry/C17474	Phenylpropanoids	2.40	0.99	1.33
328.115	13.09	C09294	C15H20O8	Anisatin	312.16, 294.32, 285.08, 223.14, 179.19, 147.10, 119.23	224.76,165.05,246.93	http://www.kegg.jp/entry/C09294	Terpenoids	2.26	1.22	1.28

330.1459	17.55	C09173	C19H22O5	Podolide /Gibberlin A7	315.10, **314.16, 299.09, 193.31, 178.15**, 123.23	314.04,299.02,175.07,193.08,178.06,	http://www.kegg.jp/entry/C09173	Terpenoids	2.02	0.88	1.33
332.1253	18.21	LMPK12020146	C18H20O6	Catechin 5,7,3'-trimethyl ether	313.18, **283.20**, 274.37, 249.32, **209.67**, 195.20 **181.47**, 150.17, 130.26	182.06,210.07,266.05,271.09,284.06,285.06,299.09,301.07	http://www.lipidmaps.org/data/LMSDRecord.php?LMID=LMPK12020146	Phenylpropanoids	3.84	1.02	1.39
332.1827	17.75	C04655	C16H28O7	(2S,3S)-2-Hydroxytridecane-1,2,3-tricarboxylate			http://www.kegg.jp/entry/C04655	Fatty acids and conjugates	0.83	1.32	1.96
338.0694	1.51			alpha--N-carbomethoxyacettyl-D-4-chlorotryptophan				Others	18.26	0.50	1.04
340.1303	19.91	C00000997	C20H20O5	sophoraflavanone B	330.70, 324.18, 307.14, 294.25, 266.31, **179.24**, 123.15, **160.28**	177.07,178.06,160.06,173.07,219.08	http://kanaya.naist.jp/knapsack_jsp/information.jsp?word=C00000997	Phenylpropanoids	2.73	1.19	1.61
342.1089	1.44	C14472	C19H18O6	4',5,6,7-Tetramethoxyflavone	280.88, 193.11, 179.05, 161.08, 143.20, 119.03, 113.15	**161.02(35%)**,176.04,311	http://www.kegg.jp/entry/C14472	Phenylpropanoids	0.46	1.63	1.45
342.1305	10.77	CPD-1777	H22O8C16	coniferin	**340.99**, 297.33, 259.37, 243.16, **179.00**, 162.92	161.13,181.12,341.0,342.90	http://pmn.plantcyc.org/PLANT/NEW-IMAGE?type=COMPOUND&object=CPD-1777	Phenylpropanoids	1.77	0.44	0.95
344.0889	22.24	C00004649	C18H16O7	Quercetin 7,3',4'-trimethyl ether	**225.11,211.18**	202.9,225.86,342.1,211.1	http://kanaya.naist.jp/knapsack_jsp/information.jsp?word=C00004649	Phenylpropanoids	2.03	0.63	0.71
344.1462	16	CPD-82	H24O8C16	dihydroconiferyl alcohol glucoside	325.21, 307.23, 289.21, 267.41, **239.18**, **229.13**, 209.15, 185.31, 171.16,135.14	189.05,226.105,239.11, 269.103,285.16,	http://pmn.plantcyc.org/PLANT/NEW-IMAGE?type=COMPOUND&object=CPD-82	Phenylpropanoids	2.81	1.58	1.45
346.1254	4.19	C09771	C15H22O9	Aucubin			http://www.kegg.jp/entry/C09771	Terpenoids	1.79	1.12	1.52
352.1416	20.01	CPD-8935	H20O4N2C20	feruloylserotonin	336.18, 307.40, 278.19, 229.06, 201.00, 187.10, 161.11, 149.09, 134.95		http://pmn.plantcyc.org/PLANT/NEW-IMAGE?type=COMPOUND&object=CPD-8935	Phenylpropanoids	0.77	1.06	2.77
358.1255	13.97	C11654	C16H22O9	Tarennoside	342.01, 313.43, 297.17, 275.01, 235.26, 226.14, 195.15, **177.14**, 162.15, **119.08**,	117.03,145.02,146.03,177.05,178.05,339.10,356.20	http://www.kegg.jp/entry/C11654	Terpenoids	0.25	1.24	3.30
358.141	19.86	CPD-8905	H22O6C20	(+)-pinoresinol	343.25, 339.19, 327.26, 324.28, 275.25, 221.19, 203.14, 191.10, **163.06**, **151.03**, 123.20	151.04,164.00,101.02,121.03	http://pmn.plantcyc.org/PLANT/NEW-IMAGE?type=COMPOUND&object=CPD-8905	Phenylpropanoids	7.27	0.45	0.69
360.1564	19.52	CPD-8907	H24O6C20	(+)-lariciresinol			http://pmn.plantcyc.org/PLANT/NEW-IMAGE?type=COMPOUND&object=CPD-8907	Phenylpropanoids	1.57	0.79	1.30
365.1465	14.33	CPD-12621	H23O7N1C18	indole-3-butyryl-glucose	345.28, 322.30, 304.20, 281.65, 216.51, 179.18, **142.28**, **119.05**	141.97,121.99,95.97,137.98	http://pmn.plantcyc.org/PLANT/NEW-IMAGE?type=COMPOUND&object=CPD-12621	Auxin	1.24	1.11	1.31
368.1097	10.29	C02572	C17H20O9	5-O-Feruloylquinic acid	346.89, 331.37, 298.77, 279.15, 264.04, 193.14, 179.23, 148.91, 134.16	adduct peak	http://www.kegg.jp/entry/C02572	Phenylpropanoids	1.00	0.26	2.15

370.1408	19.86	C09831	C21H22O6	5'-Prenylhomoeriodictyol	**370.20**, **351.39**, **335.05**, 323.90, 299.16, 281.11, 256.99, 241.08, 223.16, 213.09, **176.94**, **150.97**, 138.84	137.06,148.05,177.05,176.04,213.14,225.07,240.08,257.18,333.07,351.11,370.18	http://www.kegg.jp/entry/C09831	Phenylpropanoids	4.51	1.48	1.84
372.1407	11.57	CPD-63	H24O9C17	syringin	355.15, 339.31, 249.21, 203.02, 175.20, 156.87		http://pmn.plantcyc.org/PLANT/NEW-IMAGE?type=COMPOUND&object=CPD-63	Phenylpropanoids	1.54	1.02	0.79
374.1202	11.02	C01957	C16H22O10	Secologanate	354.63, 329.02, 301.30, 251.14, 249.28, **211.14**, **193.18**, 178.06, 154.35, 115.56	193.06,211.06,373.11	http://www.kegg.jp/entry/C01957	Terpenoids	1.00	0.24	1.24
374.1357	19.34	HMDB33279	C20H22O7	Hydroxypinoresinol	**355.10,** 343.13, **325.15**, 313.08, 291.23, 275.27, 249.01, 231.19, 219.17, **203.11**, 193.25, 179.21, 161.16, 123.15	355.11,325.108,293.07,137.06,145.02,201.05	http://www.hmdb.ca/metabolites/HMDB33279	Phenylpropanoids	0.92	1.09	1.54
374.1559	15.98		H26O9C17	7-deoxyloganin	**356.22**, 325.16, 301.31, 291.24, 219.00, 193.33, **165.21**, 119.09	**357.18,**116.03,**168.06**,122.05,145.04,146.05,155.12,204.05,247.19	http://pmn.plantcyc.org/PLANT/NEW-IMAGE?type=COMPOUND&object=7-DEOXYLOGANIN	Terpenoids	0.05	8.08	14.50
376.1513	15.35	C08747	C20H24O7	Ailanthone	**327.21**,**195.15**,217.11,165.15,256.59,**302.50**,357.18,366.78	109.03,267.06,282.0,297.11,**327.12**,345.12, 345.15,375.10,198.93,304.77	http://www.kegg.jp/entry/C08747	Terpenoids	2.21	0.79	0.45
376.1515	17.44	C08747	C20H24O7	Ailanthone	**195.11,327.27,165.21,**179.28,345.47,360.24**,150.21**,123.32	149.02,150.03,164.04,165.06,195.06,231.06,297.11,327.12	http://www.kegg.jp/entry/C08747(http://kanaya.naist.jp/knapsack_jsp/information.jsp?word=C00010604)	Terpenoids	2.78	0.94	0.76
386.0978	10.67	C00002734	C20H18O8	Diferulic acid	351.13, 325.23, 305.26, 295.26, 281.26, 267.08, 249.19,	doubt(its there in ms2t)	http://kanaya.naist.jp/knapsack_jsp/information.jsp?word=C00002734	Phenylpropanoids	3.42	0.92	0.89
388.1148	14.03	LMPK12110945	C20H20O8	5-Hydroxy-7,2',3',4',5'-pentamethoxyflavone	351.13, 325.23, 295.26, 281.26, 267.08, 249.19, 239.11, 209.26, 174.21, 157.13, 115.03		http://www.lipidmaps.org/data/LMSDRecord.php?LMID=LMPK12110945	Phenylpropanoids	1.87	1.17	1.36
390.1514	11.21		H26O10C17	loganin			http://pmn.plantcyc.org/PLANT/NEW-IMAGE?type=COMPOUND&object=LOGANIN	Terpenoids	1.72	1.05	0.98
392.1095	10.78	CPD-13685	H19O9C19	2-naphthol 6'-O-malonylglucoside	317.16,299.23,329.24,179.32,243.21,257.17,287.30		http://pmn.plantcyc.org/PLANT/NEW-IMAGE?type=COMPOUND&object=CPD-13685	Phenols and Derivatives	1.47	1.02	1.30
392.2037	17.76	LMST03020008	C22H32O4S	(6RS)-22-oxo-23,24,25,26,27-pentanorvitamin D3 6,19-sulfur dioxide adduct / (6RS)-22-oxo-23,24,25,26,27-pentanorcholecalciferol 6,19-sulfur dioxide adduct			http://www.lipidmaps.org/data/LMSDRecord.php?LMID=LMST03020008	Sterol lipids	0.25	1.67	4.84

402.1485	1.4	LMPK12050212	C25H22O5	Ulexone B	341.26,177.27,219.05,296.77,**383.23**	383.116	http://www.lipidmaps.org/data/LMSDRecord.php?LMID=LMPK12050212	Phenylpropanoids	2.41	0.64	0.73
414.1278	11.12	C10874	C22H22O8	(-)-Podophyllotoxin	**249.19,**237.22,**251.19**,**223.15**,**207.32**,205.36	251.07,226.96,251.07,224.96,206.96,	http://www.genome.jp/dbget-bin/www_bget?C10874	Phenylpropanoids	0.27	1.11	2.59
420.1615	12.33	C11645	C18H28O11	Lamioside			http://www.kegg.jp/entry/C11645	Terpenoids	10.78	0.67	1.26
422.1712	11.71	LMPK12050184	C25H26O6	Lupinisoflavone G	277.21,377.31,319.05,338.75,361.05,398.66,179.26,194.97,209.02,225.24,259.19	in ms2t look	http://www.lipidmaps.org/data/LMSDRecord.php?LMID=LMPK12050184	Phenylpropanoids	0.18	2.62	5.35
426.1928	32.08	C00029293	C21H30O9	(+)-Abscisyl beta-D-glucopyranoside			http://kanaya.naist.jp/knapsack_jsp/information.jsp?mode=r&word=C00029293&key=0	Terpenoids	1.53	1.80	1.75
432.1047	17.77	CPD1F-461	H19C21O10	kaempferol-3-rhamnoside	**311.15**,**341.19**,**413.30**,353.28,371.20,383.18,395.21,149.21,165.39,187.23	117.0388 26 269.05,281.04,282.06,283.06,311.05,323.06,341.07,413.10	http://pmn.plantcyc.org/PLANT/NEW-IMAGE?type=COMPOUND&object=CPD1F-461	Phenylpropanoids	0.26	7.83	4.20
434.1567	19.48	C09401	C22H26O9	Eleganin	**223.1,224.17,208.1**,209.05,205.4,415.07,403.11,385.17,373.16	223.06,224.07,208.04,,163.04	http://www.kegg.jp/entry/C09401	Terpenoids	5.11	0.70	0.90
435.2152	20.68	89283	C25H29N3O4	Cadabicine			http://metlin.scripps.edu/metabo_info.php?molid=89283	Alkaloids	2.75	1.24	1.42
440.1131	15.98	C09105	C20H24O9S	Hallactone B			http://www.kegg.jp/entry/C09105	Terpenoids	2.02	0.60	0.97
456.1077	9.48	LMPK12020093	C23H20O10	Epicatechin 3-O-(3-O-methylgallate)			http://www.lipidmaps.org/data/LMSDRecord.php?LMID=LMPK12020093	Phenylpropanoids	2.59	0.41	0.69
458.1404	13.18	86818	C20H26O12	2'-(E)-Feruloyl-3-(arabinosylxylose), cis-p-Coumaric acid 4-[apiosyl-(1->2)-glucoside]			http://metlin.scripps.edu/metabo_info.php?molid=86818	Phenylpropanoids	1.84	0.74	0.82
462.1184	12.11	C05990	C22H22O11	Isoscoparine	**341.14,371.09,**433.15,443.04,**313.14**,299.11,273.11,343.23,425.18	341.06,371.109,313.08, 299.02,	http://www.kegg.jp/entry/C05990	Phenylpropanoids	2.62	0.83	0.86
472.157	14.52	86152	C21H28O12	b-D-fructosyl-a-D-(6-O-(E))-feruloylglucoside	162.18,163.21,160.78		http://metlin.scripps.edu/metabo_info.php?molid=86152	Carbohydrates and Carbohydrate Conjugates	4.12	0.78	0.93
474.1725	13.68	91362	C21H30O12	6-Feruloylglucose 2,3,4-trihydroxy-3-methylbutylglycoside	179.21,165.23,146.36,293.36,341.20,413.25,428.95,454.15,464.42,161.27,163.23,164.21		http://metlin.scripps.edu/metabo_info.php?molid=91362	Carbohydrates and Carbohydrate Conjugates	0.30	1.50	1.62
480.162	14.29	C08751	C23H28O11	Bruceine B	**317.11**,448.86,287.29,249.16,197.22,229.25,461.15	317.98,155.97,478.32	http://www.kegg.jp/entry/C08751	Terpenoids	8.07	0.25	0.63
488.2618	22.29	93385	C24H40O10	alpha-Ionol O-[arabinosyl-(1->6)-glucoside]			http://metlin.scripps.edu/metabo_info.php?molid=93385	Terpenoids	1.70	1.06	0.94

490.1673	14.53	88670	C21H30O13	Phloroacetophenone 6'-[xylosyl-(1->6)-glucoside]	252.06,235.54,233.15,207.21		http://metlin.scripps.edu/metabo_info.php?molid=88670	Carbohydrates and Carbohydrate Conjugates	0.92	1.27	1.17
490.1831	18.65	LMPK12140572	C25H30O10	5-Hydroxy-7,4'-dimethoxy-6,8-di-C-prenylflavanone 5-O-galactoside			http://www.lipidmaps.org/data/LMSDRecord.php?LMID=LMPK12140572	Phenylpropanoids	2.08	0.38	1.20
492.1258	20.74	64246	C23H25O12	Malvidin 3-O-glucoside	476.13,329.15,371.20,343.14,314.17,477.16	**329.06**(100%),328.05,**314.04,343.07**,491.11	http://metlin.scripps.edu/metabo_info.php?molid=64246	Phenylpropanoids	2.25	0.56	0.74
494.1775	13.44	C09783	C24H30O11	Harpagoside			http://www.kegg.jp/entry/C09783	Terpenoids	7.33	1.14	1.21
496.1204	15.48	96036	C22H24O13	4-Methyl-(-)-epigallocatechin 7-glucuronide	477.14,299.04,239.17,327.12,339.49,451.13		http://metlin.scripps.edu/metabo_info.php?molid=96036	Phenylpropanoids	0.60	0.89	1.27
508.1557	11.33	C00024026	C24H28O12	6-o-)p-coumaroyl)-procumbide			http://kanaya.naist.jp/knapsack_jsp/information.jsp?word=C00024026	Phenylpropanoids	3.46	1.17	1.09
520.1938	18.64	C00019165	C30H32O8	Formosanatin A	**357.22**,500.97,**339.21**,267.11,251.20,**179.17**,167.14,455.25	357.13,519.05,179.05,339.10	http://kanaya.naist.jp/knapsack_jsp/information.jsp?word=C00019165	Phenols and Derivatives	0.21	1.90	3.82
520.2496	15.32	95957	C24H40O12	3b,6a-Dihydroxy-alpha-ionol 9-[apiosyl-(1->6)-glucoside]			http://metlin.scripps.edu/metabo_info.php?molid=95957	Terpenoids	2.09	1.13	0.64
522.2086	17.92	C08769	C26H34O11	Isobrucein A	329.27,**358.94**,150.54,**153.06**,163.97,296.92,503.24,461.26	358.15,153.06,181.05,182.05	http://www.kegg.jp/entry/C08769	Terpenoids	8.11	0.90	1.17
540.1652	16.06	C10548	C28H28O11	Cleistanthin A	many fragments	85.02,303.05,304.05,449.11,611.16	http://www.kegg.jp/entry/C10548	Phenylpropanoids	0.76	0.73	1.78
550.1672	15.52	LMPK12120252	C26H30O13	Chalconaringenin 2'-rhamnosyl-(1->4)-xyloside	387.10,265.19,250.27,369.26,531.16,450.10,388.25**,191.06**,**205.14,206.12,207.30,223.06**	190.02,205.04,206.05,207.05,221.06,548.16	http://www.lipidmaps.org/data/LMSDRecord.php?LMID=LMPK12120252	Phenylpropanoids	1.00	2.51	2.45
552.1834	17.99	HMDB39910		cis-Reserverattrol-3,4-obeta glucoside	**506.93**,477.23,275.22,311.18,**389.26**,431.35,**193.1**	506.01,389.122,533.13,193.31	http://www.hmdb.ca/metabolites/HMDB39910	Stilbene	1.87	1.09	0.89
568.2136	15.21	93822	C27H36O13	Citrusin B	544.16, **525.11, 506.76, 473.33,** 405.02, **357.25, 345.04, 297.47**	567.20, 523.02, 505.19, 475.15, 357.14, 345.13, 297.13	http://metlin.scripps.edu/metabo_info.php?molid=93822	Phenols and Derivatives	1.05	1.15	1.49
578.168	12.53	C00004156	C27H30O14	Apigenin 7-o-rutinoside			http://kanaya.naist.jp/knapsack_jsp/information.jsp?word=C00004156	Phenylpropanoids	2.56	1.12	1.56
580.2146	17.67	C10890	C28H36O13	(+)-Syringaresinol O-beta-D-glucoside	561.40, **518.54, 387.29, 417.38,** 356.83, 339.19, 327.19,	579.22, 519.32, 417.15, 387.11, 181.04	http://www.kegg.jp/entry/C10890	Phenylpropanoids	0.32	1.55	3.98
580.2148	19.72	C10890	C28H36O13	(+)-Syringaresinol O-beta-D-glucoside	561.40, **518.54, 387.29, 417.38,** 356.83, 339.19, 327.19,	579.22, 519.32, 417.15, 387.11, 181.05	http://www.kegg.jp/entry/C10890	Phenylpropanoids	0.75	1.74	1.50
596.2234	21.98			Kadsulignan				Phenylpropanoids	1.37	1.24	1.35
614.2347	21.57	63936	C35H34MgN4O5	Chlorophyllide	594.98, 565.16, 417.21, 387.27, 357.25,		http://metlin.scripps.edu/metabo_info.php?molid=63936	Others	7.30	0.72	0.49

616.2155	18.64	86704	C38H32O8	Dimoracin	533.20,585.09,553.08,403.09,391.33,355.09,193.16	dfragments in ms2t but from pathogen(Kosinostatin)	http://metlin.scripps.edu/metabo_info.php?molid=86704	Phenols and Derivatives	1.00	1.08	1.70
624.2022	13.77	52107	C29H36O15	3,4\',6\'-Trihydroxy-4,2\'-dimethoxychalcone 4\'-O-rutinoside			http://metlin.scripps.edu/metabo_info.php?molid=52107	Phenylpropanoids	0.39	1.18	1.27
626.2182	17.03	LMPK12020157	C29H38O15	Pneumatopterin A	no		http://www.lipidmaps.org/data/LMSDRecord.php?LMID=LMPK12020157	Phenylpropanoids	10.74	0.57	1.21
638.2183	19.33	LMPK12140461	C30H38O15	4'-Hydroxy-5,7,2'-trimethoxyflavanone 4'-rhamnosyl-(1->6)-glucoside			http://www.lipidmaps.org/data/LMSDRecord.php?LMID=LMPK12140461	Phenylpropanoids	1.65	0.83	0.94
672.2069	15.06			(+)-pinoresinol 4-o-(6-ogalloyl)-bets-D-glucopyranoside	461.07,299.04,373.14,**491.13**,576.29	491.13,137.06,	http://kanaya.naist.jp/knapsack_jsp/information.jsp?word=C00049499	Phenylpropanoids	0.13	5.20	7.14
702.2173	15.14	93541	C34H38O16	Ramontoside	491.06,403.20,**329.15**,223.13,**241.09**,457.26,522.90,539.20,578.32	243.05,521.22,329.15	http://metlin.scripps.edu/metabo_info.php?molid=93541	Phenylpropanoids	0.87	0.31	2.20
712.2563	16.6	C00050612	C33H44O17	(+)-Medioresinol di-O-beta-glucopyranoside			http://kanaya.naist.jp/knapsack_jsp/information.jsp?word=C00050612	Phenylpropanoids	4.22	1.03	0.37
726.2339	19.57	LMPK12140262	C33H42O18	Naringenin 7-O-(2",6"-di-O-alpha-rhamnopyranosyl)-beta-glucopyranoside			http://www.lipidmaps.org/data/LMSDRecord.php?LMID=LMPK12140262	Phenylpropanoids	6.56	0.56	1.00
726.236	19.58	LMPK12140262	C33H42O18	Naringenin 7-O-(2",6"-di-O-alpha-rhamnopyranosyl)-beta-glucopyranoside			http://www.lipidmaps.org/data/LMSDRecord.php?LMID=LMPK12140262	Phenylpropanoids	4.91	1.51	1.74
730.2608	25.97	C00031413	C40H42O13	threo-carolignan E	369.21,532.05,587.28,681.16,711.08,605.14,339.19		http://kanaya.naist.jp/knapsack_jsp/information.jsp?word=C00031413	Phenylpropanoids	4.15	0.59	1.32
770.2024	20.99	LMPK12110272	C37H38O18	Isovitexin 2"-O-(6'"-feruloyl)glucoside			http://www.lipidmaps.org/data/LMSDRecord.php?LMID=LMPK12110272	Phenylpropanoids	4.62	0.77	0.75
772.1819	20	LMPK12110550	C36H36O19	Isoorientin 4'-O-glucoside-2"-O-(E)-caffeate	403.24,710.55,727.03,749.20,299.36,353.26,380.04,462.34,515.14		http://www.lipidmaps.org/data/LMSDRecord.php?LMID=LMPK12110550	Phenylpropanoids	4.91	1.54	1.58
862.2136	24.24	46869	C39H42O22	Cyanidin 3-[6-(6-p-hydroxybenzoylglucosyl)-2-xylosylgalactoside]	819.04,801.04,777.16,685.08,643.09,625.20,601.09,555.00,522.92,361.03		http://metlin.scripps.edu/metabo_info.php?molid=46869	Phenylpropanoids	1.79	0.85	0.83
884.2323	24.24	47158	C42H44O21	Salviamalvin	841.02,799.09,823.0,757.1,622.94,580.98,420.38,323.43		http://metlin.scripps.edu/metabo_info.php?molid=47158	Phenylpropanoids	1.97	0.25	0.85
934.2336	18.57	LMPK12110627	C42H46O24	Isoorientin 4'-O-glucoside-2"-(4-glucosylcaffeate)			http://www.lipidmaps.org/data/LMSDRecord.php?LMID=LMPK12110627	Phenylpropanoids	1.70	0.85	0.83